Dissertation

The role of sector coupling in the energy transition

Carried out to obtain the degree of

Doktor der Sozial- und Wirtschaftswissenschaften

submitted at the

Energy Economics Group

Faculty of Electrical Engineering and Information Technology

Technische Universität Wien

by

Jasmine Ramsebner

under the supervision of

Univ.Prof. Dipl.-Ing. Dr. Reinhard Haas

Technische Universität Wien

Reviewers and Examiners:

Dr. Johannes Reichl

Energieinstitut an der Johannes Kepler Universität Linz

Prof. Ing. Jaroslav Knápek, CSc.

Czech Technical University in Prague

Vienna, August 2022

Danksagung

Der Wunsch, einen Beitrag zur Eindämmung des Klimawandels und zur Erhaltung der Lebensgrundlage für diese und künftige Generationen zu leisten, hat mich zur Energy Economics Group an der TU Wien geführt. Mein besonderer Dank gilt Reinhard Haas, meinem Dissertationsbetreuer und ersten Ansprechpartner an der TU Wien, der mir einen Platz anbot, um Fachwissen in der Energiewirtschaft zu entwickeln und mich bei der Fertigstellung meiner Dissertation begleitet hat. Er hat mir immer größtes Vertrauen geschenkt und mir Verantwortung übertragen, mit der ich wachsen konnte. Ich danke Pedro Linares von der Universität Comillas, den ich hoffentlich eines Tages persönlich treffen werde, für die erfolgreiche Zusammenarbeit und den wertvollen Austausch im Zuge zweier wissenschaftlicher Veröffentlichungen. Außerdem möchte ich Johannes Reichl und Jarolsav Knápek für ihre Bemühungen als Gutachter und Prüfer dieser Dissertation danken.

Am EEG habe ich Kolleg:innen mit den gleichen Werten und Visionen kennengelernt, und Freunde, die bleiben werden. Gerne erinnere ich mich an die ersten Monate im Büro mit Eike in denen wir die Grundlagen der Energiewirtschaft erarbeitet haben. Als Kollege und Freund möchte ich Albert meinen besonderen Dank aussprechen. Während unser Büro für gute Laune und manchmal lautstarkes Mini-Basketball bekannt war, half Albert mir durch jegliche Frustration, die eine Dissertation mit sich bringt. Ich schätze ihn für seine Ehrlichkeit, Unterstützung und großartigen Sinn für Humor.

Meine tiefste Dankbarkeit und Liebe möchte ich meinen Eltern dafür ausdrücken, dass sie mir beigebracht haben, die Dinge auf meine Weise zu tun. Sie haben mich darin unterstützt, einfühlsam und selbstbewusst zu werden und daran zu glauben, dass ich alle meine Träume verwirklichen kann. Ich danke meinem Onkel Wolfgang, der diesen Doktortitel immer für mich im Sinn hatte, meiner Gota Ruth mit Familie und der Familie Humpeler, dass sie in Zeiten des Feierns ebenso wie in Zeiten, in denen ich ihre Unterstützung brauchte, da sind.

Inmitten all dieser Ereignisse trat Thorsten unerwartet in mein Leben, hat es mit Liebe, unglaublichem Verständnis für meine leidenschaftlichen Hobbies und manchmal auch die Arbeit, und vielen Abenteuern gefüllt und ist mein Gegenstück, das ich dringend brauchte. Seine bedingungslose Unterstützung überrascht mich hin und wieder. Mein Dank geht auch an Sabine, die mir das Gefühl gibt, immer willkommen und umsorgt zu sein. Schießlich schulde ich all meinen Freunden großen Dank, von denen mich viele seit dem Kindergarten, der Schule oder der Universität, begleiten. Sie haben meinen Weg und meine Interessen immer geschätzt und ich kann nur stolz und froh sein, dass ich immer auf sie zählen kann.

Acknowledgements

The desire to contribute to climate change mitigation and sustain a livelihood for this and future generations guided me to the energy economics group at TU Wien. I would like to express my gratitude to Reinhard Haas, my thesis supervisor and first contact at TU Vienna. Reinhard offered me a place to develop expertise in the field of energy economics and guided me towards completing my dissertation. He has always given me the greatest trust and responsibility, enabling me to gain experience and grow with the task. A special thanks to Pedro Linares from Comillas University, who I still hope to meet in person someday, for the valuable guidance and successful cooperation for two journal articles. I want to thank Johannes Reichl and Jarolsav Knápek for their effort as reviewers and examiners of this dissertation.

At the EEG, I met colleagues with the same values and visions, and friends who will last. I think back happily to the first months of sharing the office with Eike, where we elaborated on the basics of energy economics while having a splendid time. As a colleague and friend, I would like to express my special thanks to Albert. While our office was known for always being in a good mood and us sometimes loudly playing mini-basketball, Albert helped me through any frustration associated with a PhD thesis. I appreciate his honesty, support and great sense of humour.

I want to express my deepest gratitude and love to my parents for guiding me in doing things my way. They always supported me in growing empathetic and confident, believing in being capable of achieving any dream I have. I thank my uncle Wolfgang, who always had this PhD in mind for me, my godmother Ruth and family and the Humpeler family for being there in times of celebration and when I needed their support.

Amid all these happenings, Thorsten came into my life unexpectedly, filling it with love, unbelievable understanding for my passionate hobbies and sometimes work, many adventures and being the counterpart I desperately needed. His unconditional support surprises me now and then. My thanks also go to Sabine, who makes me always feel welcome and cared for.

Finally, I owe great thanks to my friends, many accompanying me since Kindergarten, school or close friendships that evolved during University. They always appreciated my way and my interests; I can only be proud and lucky that I can always count on them.

Abstract

The climate goals imposed by the Paris Agreement call for an energy transition in which the efficient use of large-scale, variable renewable energy (VRE) from wind and sun will be of great importance. The ongoing electrification brings about new electricity demand sources that must be managed. Sector Coupling (SC) describes using renewable power in all end-consumption sectors. The core objective of this thesis is an in-depth techno-economic analysis of successful VRE integration through SC in major CO_2 emitting end-consumption sectors: heating and cooling, transport and industry. This thesis mainly builds on four contributions, of which a review elaborates on the state of the art of sector coupling, and three articles answer specific research questions concerning i) the storage needs to achieve a strong correlation between hourly VRE profiles and temperature-dependent heating and cooling needs, ii) efficient management of increasing electricity demand for individual transport, and iii) renewable hydrogen production strategies for the industry. The first contribution presents a statistical analysis of the interrelations between weather-dependent variables and respective heating and cooling degree-days. Individual optimisation models compare load-management solutions for battery-electric vehicles (BEVs) and different electrolyser operation strategies. The results show that SC plays a major role in all three cases, and the applied methods provide valuable solutions: i) VRE can strongly correlate with heating and cooling degree-days on different time scales, ii) load-management solutions for BEV charging can reduce the required power-connection on-site by 62 % compared to uncontrolled charging, iii) and constant demand and just-in-time production achieve the lowest renewable hydrogen production cost. SC represents part of the solution in the energy transition, making renewable energy available to former fossil-fuel-based processes. The concept promotes local production, value creation, and independence from energy imports. Nevertheless, several challenges and uncertainties remain, which call for clear regulatory guidelines for renewable technologies to support decision-making and investments. Furthermore, historically grown market frameworks and energy grids must adapt for cross-sectoral integration to achieve the energy transition.

Kurzfassung

Die Pariser Klimaziele verlangen nach einer Energiewende, bei der die effiziente Nutzung variabler erneuerbarer Energie aus Wind und Sonne von großer Bedeutung sein wird. Die fortschreitende Elektrifizierung vieler Wirtschaftssektoren führt zu neuen Stromabnehmern, die optimal integriert werden müssen. Die Sektorkopplung beschreibt die Nutzung von erneuerbarem Strom in allen Endverbrauchssektoren. Das Hauptziel dieser Arbeit ist eine eingehende techno-ökonomische Analyse der Sektorkopplung in CO_2-intensiven Endverbrauchssektoren: Heizen und Kühlen, Verkehr und Industrie. Diese Arbeit basiert hauptsächlich auf vier wissenschaftlichen Veröffentlichungen, von denen sich ein Review Paper mit dem Stand der Technik in der Sektorkopplung befasst und sich drei Artikel mit spezifischen Forschungsfragen auseinandersetzen, wie mit i) dem Speicherbedarf, um eine starke Korrelation zwischen den stündlichen erneuerbaren Profilen und dem temperaturabhängigen Wärme- und Kältebedarf zu erreichen, ii) dem effizienten Management des steigenden Strombedarfs für den Individualverkehr und iii) Strategien zur Erzeugung von erneuerbarem Wasserstoff für die Industrie. Der erste Beitrag basiert auf einer statistischen Analyse der Zusammenhänge zwischen wetterabhängigen Variablen und den jeweiligen Heiz- und Kühlgradtagen. Individuelle Optimierungsmodelle vergleichen Lastmanagementlösungen für batterieelektrische Fahrzeuge und verschiedene Betriebsstrategien für die Elektrolyse von erneuerbarem Wasserstoff. Die Ergebnisse zeigen, dass Sektorkopplung in allen drei Fällen eine wichtige Rolle spielt und die angewandten Methoden wertvolle Lösungen bieten: i) erneuerbare Energie kann stark mit Heiz- und Kühlgradtagen auf verschiedenen Zeitskalen korrelieren, ii) Lastmanagementlösungen für das Laden von batterieelektrischen Fahrzeugen können die erforderliche Stromanschlussleistung vor Ort im Vergleich zu ungesteuertem Laden um 62 % reduzieren, iii) und konstante Nachfrage und ebenso konstante Produktion erzielen die niedrigsten Kosten für erneuerbaren Wasserstoff. Sektorkopplung ist ein Teil der Lösung in der Energiewende, um erneuerbare Energien für Prozesse bereitzustellen, die bislang auf fossilen Brennstoffen basierten. Das Konzept fördert die lokale Energieerzeugung und Wertschöpfung und die Unabhängigkeit von Energieimporten. Dennoch bleiben einige Herausforderungen und Unsicherheiten bestehen, die klare Richtlinien für erneuerbare Technologien erfordern, um Investitionsentscheidungen zu unterstützen. Darüber hinaus müssen die historisch gewachsenen Marktbedingungen und Energienetze für eine sektorübergreifende Integration angepasst werden, um die Energiewende zu erreichen.

Contents

Abbreviations

ALK	Alkaline
AUT	Austria
BEV	Battery electric vehicle
BOF	Basic oxygen furnace
C(C)HP	Combined cooling, heat and power
CCS	Carbon capture and storage
CDH/D	Cooling degree-hours/days
CH_4	Methane
CNG	Compressed natural gas
COP	Coefficient of performance
CP	Charging point
DC	Direct current
DH	District heating
DRI	Direct reduced iron
EB	Electric boiler
ESP	Spain
FCEVs	Fuel-cell electric vehicles
FLH	Full load hours
GHG	Greenhouse gas
H_2	Hydrogen
HBI	Hot briquetted iron
HDH/D	Heating degree-hours/days
HH	Household
HP	Heat pump
HRS	Hydrogen refuelling station
iDSM	Industrial demand side management
IESs	Integrated energy systems
IS	Infrastructure
JIT	Just in time
Kh	Kelvin hours
LCC	Low charging capacity
LCOE	Levelised cost of electricity
LCOH&S	Levelised cost of hydrogen and storage

LM	Load-management
MES	Multi-energy system
MILP	Mixed-integer linear program
NGR	Natural gas reforming
NEU	Northern Europe
NOx	Nitrogen oxide
P2G	Power-to-gas
P2H	Power-to-heat
P2L	Power-to-liquid
PEM	Proton-exchange membrane
PEV	Plug-in electric vehicle
PM	Particulate matter
PPA	Power purchase agreement
PV	Photovoltaics
RCP	Representative concentration pathways
RES	Renewable energy source
SC	Sector Coupling
SES	Smart energy system
ToU	Time-of-use
UC	Uncontrolled charging
V2G	Vehicle-to-grid
VRE	Variable renewable energy

1. Introduction

1.1. Motivation

The start of the industrial revolution around 1760 brought about many pioneering innovations that pushed living standards and created much-needed jobs and opportunities. At the same time, however, this upswing mainly relied on fossil resources that replaced mechanic with thermal energy and reduced the physical effort while improving efficiency and economic performance for the striving economies. In the last decades, with global economic growth, the debate on the long-term effect of emissions from fossil fuel burning on the environment has received more and more attention, and the damage of ignoring these aspects in economical market frameworks turns out to be severe. Global warming is happening noticeably and must be limited to a minimum in all ways. In 2015, therefore, 196 countries signed the Paris Agreement aiming to limit global warming to 2°C compared to pre-industrial times (United Nations, 2015). This agreement leads to ambitious national targets for all economic sectors to reduce greenhouse gas (GHG) emissions and substitute fossil fuels with renewables, supported by substantial efficiency improvements, potential avoidance of energy consumption and a change in market frameworks.

To achieve climate goals and the decarbonisation of all end-consumption sectors, specifically the efficient use of wind and solar power as large-scale, variable renewable energy sources (VRE), will be of great importance. However, the management of their intermittency imposes new challenges on the energy system (Ramsebner, Linares, et al., 2021b). The variability of these natural resources affects the energy system within a day and throughout the year's seasons. Excess electricity production can frequently occur, considering the known demand profiles. Especially in, for example, continental Europe during summer, high solar irradiance with low energy demand, or even in combination with high wind availability, may cause such a situation (Ramsebner, Haas, Ajanovic, et al., 2021). In winter, however, this region may experience a scarcity of renewable electricity generation with low solar irradiance and higher demand. In northern countries, by contrast, the dominance of wind power generation may lead to excess electricity generation, especially during winter (Ramsebner, Haas, Ajanovic, et al., 2021). As a simplified example of the seasonal variability of continental Europe, Figure 1 shows the monthly and especially the seasonal variability of renewable power generation in a scenario with run of river, wind and solar power for Austria. Figure 2 describes VRE generation on an exemplary summer day showing the amount of what may be identified as surplus generation from the peaks in solar irradiance during low electricity demand. Not all of this discrepancy may be balanced through short-term pumped hydro storage (Ramsebner, Haas, Ajanovic, et al., 2021). Questions emerge on how to manage these non-controllable sources, handle excess electricity generation, and use it efficiently in terms of economic, ecologic, and social welfare aspects.

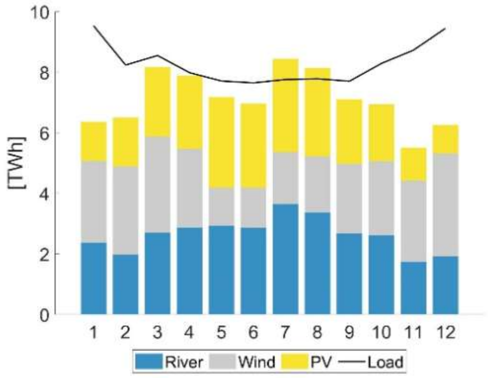

Figure 1 Monthly VRE electricity generation in a scenario for Austria (Ramsebner, Haas, Ajanovic, et al., 2021).

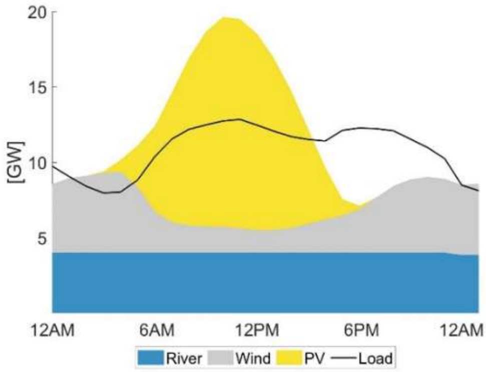

Figure 2 Exemplary summer day: surplus VRE electricity generation, Austria. (Ramsebner, Haas, Ajanovic, et al., 2021)

Apart from a supply side increase in the renewable energy share, the decarbonisation and ongoing electrification in all end-consumption sectors create new electricity demand sources. They consume the formerly identified electricity surplus. The electrification can be enabled either directly or through conversion technologies (e.g., power-to-gas) and requires a paradigm shift away from considering individual energy sectors (gas, electricity and heat), storage and demand towards a more integrated energy system (Iqbal, 2012; Ramsebner, Linares, et al., 2021b).

The concept of Sector Coupling (SC) or Sector Integration (SI) represents an approach to couple renewable electricity with the end-consumption sectors by electrifying transport, residential heating and cooling, and the industry. The concept was first mentioned during the energy transition in Germany. According to IRENA (2022), the energy transition is "a pathway toward the transformation of the global energy sector from fossil-based to zero-carbon by the second half of this century." This includes the reduction of energy-related carbon emissions, a process called decarbonisation, addressed by specific goals for climate change mitigation. The main pillars of the energy transition are the use of renewable energy and energy efficiency measures (IRENA, 2022). The EU has also attempted to promote investments into processes and activities that support the energy transition by providing clarity with a classification of sustainable projects, the EU taxonomy (EC, 2022). Any actions that contribute to renewable energy generation, enable other activities to mitigate climate change, such as the storage of renewable energy or represent a significant improvement to the industry standard in terms of efficiency and CO_2 emissions. In this respect, SC is the tool that links renewable energy with the demand sector that requires a transition. The EU taxonomy is an essential signal that provides guidance for investment decisions into renewable technologies.

SC supports establishing 100 % renewable energy systems by substituting fossil fuels with renewable electricity. Furthermore, the concept may add flexibility through transformation options from power to heat or gas that can be stored and distributed easier than electricity (Ramsebner, Haas, Ajanovic, et al., 2021; Schaber et al., 2013). Despite the growing attention to SC, however, the scope and main objectives vary broadly throughout the literature, and the term is often used inaccurately (Robinius, Otto, Syranidis, et al., 2017). Figure 3 provides an overview of the potential pathways of SC. While direct electrification is a possible SC approach, for example, in individual passenger transport, many processes rely on the conversion of electricity into gas or further into liquid fuels (power-to-gas/liquid (P2G/L)), into heat, known as power-to-heat (P2H), and storage in the respective form.

The role of SC in the energy transition and the opportunities and challenges concerning successful VRE integration with new demand sources differ among the end-consumption sectors. In this context, an interesting observation for the future electrification of heating and cooling is the impact of weather variables, such as wind speed and solar irradiance, on temperatures. Understanding these relationships reveals the potential of using solar and wind power to cover heating and cooling demand, for which different technologies would be applicable (Ramsebner, Linares, et al., 2021b). Another new electricity demand source through the energy transition concerns the electrification of individual passenger transport, which is characterised by dynamic growth and requires early investigation of appropriate system integration. Efficient load-management solutions control the charging processes and avoid additional demand peaks. As a result, SC may be implemented without an extensive distribution grid and electricity generation capacity expansion (Ramsebner et al., 2020). As already mentioned, SC also includes converting renewable electricity into gas to provide a feedstock and fuel for the decarbonisation of hard-to-abate sectors, such as industrial steel production. Companies already aim to transform the former coal-based production process into a renewable-hydrogen or electricity-based one. On-site renewable hydrogen production offers a non-regret option for upscaling production volumes to decrease the overall cost independently of distribution infrastructure. It is essential to compare different operation strategies and their characteristics, such as conversion efficiency, investment cost and market participation affecting hydrogen production cost, to make informed decisions and promote the successful VRE integration for industrial purposes.

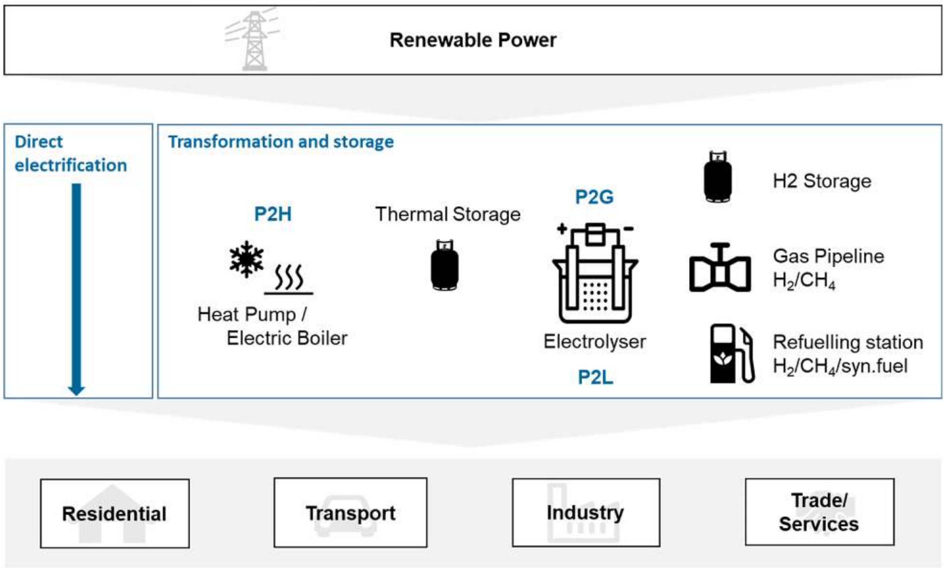

Figure 3 Overview of the main pathways of Sector Coupling in different end-consumption sectors

The energy transition depends on appropriate SC solutions to align VRE supply with demand in all end-consumption sectors. The efficient use of limited VRE capacities, load or demand side management, electricity grid expansion and the creation of flexibility through cross-sectoral integration are options to develop integrated renewable energy systems that may operate without fossil backup capacities. SC as a one-way path from power-to-X represents one part of this solution. However, the application of sector coupling remains challenging in historically built energy systems and market frameworks. The successful integration and broad application of renewable energy in new applications require new market frameworks and precise regulatory guidelines to develop attractive business models.

1.2. Research questions and objective

The core objective of this thesis is an in-depth techno-economic analysis of potential sector coupling applications to achieve the energy transition. This work evaluates the role of SC, potential new electricity demand sources, and the resulting challenges and required solutions for three different end-consumption sectors. After a critical review of the SC concept and its state-of-the-art provided by Ramsebner et al. (2021), three article contributions to international journals answer different research questions to fulfil the main objective. The research questions, hypothesis and individual contributions of this thesis to literature are as follows:

Research Question 1: *What is the estimated storage time required to cover the time discrepancy between hourly variable renewable energy and temperature-based heating and cooling profiles?*
Research Question 1 addresses the storage needs to achieve a strong timely correlation between the VRE source availability (wind and solar irradiance) and temperature-based heating and cooling demand. Given the relationships between meteorological phenomena such as wind and solar irradiance and temperatures, a certain correlation with temperature-dependent heating and cooling needs can be expected.

The contribution that answers this question applies a statistical analysis to estimate the storage requirements, considering up to monthly balancing, to cover the time discrepancy between VRE availability and the following change in temperature-based heating and cooling demand (Ramsebner, Linares, et al., 2021b). This contribution provides an understanding of the interrelations between weather variables and their potential for decarbonising the heating and cooling sector.

Research Question 2: *How can rising electricity demand in individual passenger transport be integrated into the energy system successfully to avoid any additional infrastructural costs for society and maintain user comfort?*
Research Question 2 concerns the implementation of SC in the transport sector. Increasing electricity demand through battery electric vehicles (BEVs) in the transport sector imposes challenges on the electricity infrastructure, specifically in densely populated areas. Therefore, intelligent load-management (LM) mechanisms and capable infrastructure are essential to control battery electric vehicle (BEV) charging processes.

The second contribution addresses this research question and provides an LM optimisation of large-scale residential BEV charging along BEV diffusion (Ramsebner et al., 2020). The results compare the required power connection with controlled or uncontrolled charging and are validated with data from a field test. This work clearly outlines the value of controlled charging and highlights further optimisation potential through more information and standardisation.

Research Question 3: *What is the most economic on-site renewable hydrogen production strategy for constant or variable demand, specifically considering load-dependent conversion efficiency?*
Research Question 3 refers to the optimal VRE integration for decarbonising energy-intensive industrial processes. However, direct electrification of operations is not always applicable and converting renewable electricity into gas can be a requirement. On-site production in so-called "hydrogen valleys" is associated with an opportunity to increase hydrogen production scales and decrease the cost in the long term.

The third contribution currently in the review process compares operation strategies for renewable hydrogen production in the industrial sector (Ramsebner et al., 2022). The applied model considers electricity sourced from the grid or directly from a renewable power plant to cover constant or variable demand. The arbitrage through electricity price optimisation is optimised against the potential load-dependent efficiency losses due to variable operation and respective capacity investment costs. The presented analyses provide the most economical renewable hydrogen production strategy under different parameters and elaborate on cost and market aspects.

1.3. Structure of the thesis

The remains of this thesis start with elaborating on the state of the art of Sector Coupling in Chapter 2 to establish knowledge of its background and critically reviews its role in variable renewable energy (VRE) integration and the remaining challenges. It outlines the pathways of sector coupling and for the decarbonisation of different end-consumption sectors as defined in energy economics: transport, industry, residential and trade/services. This review represents the basis for the work presented to answer the three research questions.

Chapter 3 addresses the storage requirements for using VRE for heating and cooling. Based on hourly wind speed, solar irradiance and temperature data, the correlation between VRE availability and heating and cooling degree-days is analysed in three different European regions Spain, Austria and Northern Europe. The contribution observes hourly correlation for daily, weekly and monthly time horizons and evaluates aggregated data assuming storage. An outlook on the impact of global warming on all three parameters provides insights into the change in heating and cooling needs and resource availability.

Chapter 4 elaborates how increasing electricity demand through BEV charging can be controlled to avoid the expansion of on-site power connection and distribution grid capacities. This work analyses load management approaches to minimise the impact on the distribution grid in densely populated areas while maintaining user comfort with an Austrian case study. The model sets up a multi-unit apartment with 106 households and modelled energy consumption per BEV based on an Austrian traffic survey. Uncontrolled and controlled charging are evaluated between 0-100 % BEV diffusion in the multi-unit apartment. The model results are validated with field test results in a facility of the same size with 51 BEV users (almost 50 % e-mobility share).

Chapter 5 investigates the most economical renewable hydrogen production strategy for the decarbonisation of the industrial sector. In two case studies for variable and constant demand, the costs of hydrogen production from the grid—based on electricity price optimisation and hydrogen storage or just-in-time production—and direct sourcing from a RES plant are compared.

Chapter 6 critically discusses the findings across the published research on the three different research questions, the chosen methodology's strengths and limitations, and the opportunities and risks of SC applications. Chapter 7 provides conclusions and recommendations for action and future research.

2. State of the art of sector coupling

As mentioned in the introduction to this thesis, SC plays a major role in the energy transition as a tool to apply renewable energy to a broad set of end-consumption sectors. Still, despite the growing attention to and research on SC applications, the scope and main objectives vary broadly throughout the literature, and the term is often used inaccurately (Robinius, Otto, Syranidis, et al., 2017). In order to provide a common understanding of the perspectives and remaining challenges of sector coupling, this work represents a critical review of enabling technologies and the use of this concept in renewable energy systems. This chapter is mainly based on a published article by Ramsebner et al. (2021).

2.1. Core objectives

The core objective of this contribution by Ramsebner et al. (2021) is to analyse the origin of the SC concept and its main purposes, as described in the present literature. It creates an understanding of how the sectors are defined within SC, followed by a review of SC definitions and available studies related to SC. In doing so, it provides a brief literature review of specific SC technologies (e.g., P2G or P2H) to understand the overall concept thoroughly. Finally, it aims to critically discuss the remaining challenges and value of SC for renewable energy systems.

2.2. Methodology

The methodology includes a thorough search for definitions of SC, starting with screening the interpretation of the sectors in this context, which is said to vary significantly, followed by a review of available research in this field. Our literature review considers the overall SC concept and its techno-economic requirements and challenges. It does not specifically focus on a detailed review of technological studies. At the same time, it adds a basic description of enabling technologies and potential SC applications, which we consider essential to understanding its techno-economic aspects.

First, publications in online libraries, such as Google Scholar and Science Direct, were screened. However, for the definition of SC and the sectors in this context, mainly German literature provided a solid basis that included reports and project results. Looking for available research on SC, the studies had to include the keyword "sector coupling" and focus on the use of renewable electricity. Therefore, our concept interpretation does not consider fossil fuels, biogas, biofuels, or excess heat.

The following reference count was identified as relevant for analysis:

1. Sector definition: 10
2. SC definition: 14
3. All results referring to SC on Science Direct: 361
4. Relevant SC research: 40

Throughout this paper, the authors,

1. provide a literature review on the definition of sectors and SC,
2. analyse available research on SC and the essential technologies mentioned in it,
3. describe enabling technologies required for the realisation of converting power for use in all end-consumption sectors,
4. investigate the role of SC in integrated, multi-energy systems (MESs),
5. provide a structured categorisation of SC applications for each end-consumption sector, a critical discussion of the findings, future techno-economic challenges, and assets of SC.

2.3. Literature review on the rise of the sector coupling concept

The principles of SC have already been known from the beginning of the 20th century. The first battery electric vehicle (BEV) produced in the US was demonstrated at the 1892 World's Fair in Chicago, Illinois (Warner, 2015). The developments in Europe, not only in electric bicycles and automobiles but also in public transport, disappeared in the middle of the 20th century. In the US, BEVs gained early market acceptance despite their short driving range and the speed limit of direct current (DC) motors to 32 km/h. Eventually, BEVs were defeated by the internal combustion engine of Henry Ford's low-priced Model T in 1908, the introduction of the automatic starter by Charles Kettering in 1911, and the US highway system expansion (Warner, 2015). Driven by the desire for an all-electric American home at the beginning of the 20th century, the residential sector experienced significant electrification using electric stoves, hot plates, washing and ironing machines, dishwashers, electric doorbells and a vast number of lightening devices (Foy & Schlereth, 1994). Robinius, Otto and Heuser, et al. (2017) found further early applications in energy generation, which applied the primary approach of SC: "Furthermore, while SC has always been practised, it has hitherto been in the context of fossil fuels such as kerosene, methane, oil or coal, rather than renewable energy sources (RES). For example, a combined heat and power plant that generates electricity would supply excess heat that would otherwise be wasted." In the 1980s and 1990s the so-called integrated energy systems (IES) were investigated aiming to integrate individual fossil fuel streams through new ways of distribution and conversion to reduce the environmental burden (Belyaev et al., 1987; Häfele & Nebojsa, 1983). The main idea included the decomposition of energy carriers into their elementary components to fulfil energy demand flexibly.

The authors, however, point out that today the focus lies in using renewable electricity in an increasing amount of end-consumption applications to increase the share of renewable energy in these sectors (assuming that the electricity supply is or can primarily be renewable). There are two options for electrification: adapting fossil-fuel-based processes for direct electrification or converting electricity into a more suitable or flexible fuel type. In this context, SC has become popular during the German energy transition (Schaber et al., 2013).

By investigating the integration of large-scale, variable wind power in future renewable energy systems, the first mention of this approach under the term SC was found in studies by Schaber et al. (2013), Schaber (2013) and later by Richts et al. (2015). In the course of the energy transition in 2017, several German ministries and international energy agencies developed thorough guidelines and information on SC (BMWi (2016), BMUB (2016a), BDEW (2017), IRENA et al. (2018)). Nevertheless, as often as the term "sector coupling" is used in energy policy debates today, it is not used clearly and uniformly (Scorza et al., 2018). One of the first scientific papers to specifically develop a more uniform interpretation of the concept was established by Robinius, Otto and Heuser, et al. (2017). Towards 2018, more peer-reviewed scientific papers were explicitly dedicated to SC, such as the work by Buttler and Spliethoff (2018) and Stadler and Sterner (2018). By 2019, the contributions to the concept were multiplied.

However, future research still needs to define SC uniformly and discuss critically which of its scopes are reasonable for future energy systems (Wietschel et al., 2018). There is still discussion about whether SC only includes renewable electricity or the coupling of conventional electricity generation may also be considered. Furthermore, the literature does not always agree on the question of whether biogas and biofuels, combined (cooling) heat and power (C(C)HP) plants and the use of excess heat are part of the concept. Additionally, the definition of the sectors referred to in SC widely differs throughout the literature depending on the research perspective, which may be technical or economical. The following sub-sections first provide an analysis of the interpretation of the sectors within SC and then continue with available definitions of SC. Once this basic understanding is established, a detailed literature review on SC and its common research focus is conducted.

2.3.1. Definition of sectors

For definitions of SC, 10 papers were detected, mainly represented by reports and project results, one position paper, one dissertation, and only two peer-reviewed papers (see Table 1). Our literature review reveals that the interpretation of the sectors differs widely across the field of SC research. Studies on SC often do not address the chosen interpretation of sectors and dive into the technical specifics very quickly (e.g., producing heat from renewable electricity for space heating).

Literature offers a broad spectrum of interpretations concerning the sectors, depending on the nature of research and whether it is technical, economic, and on macro or micro level. Robinius, Otto, Heuser, et al. (2017) aim to correct "inaccurate formulations" of how sectors are described in SC. They claim that heat supply is not a sector but an application, energy carrier, or service. Illumination in the household sector is another example. The authors thereby define sectors as industry, trade and commerce, residential/household, and transport, which is common in energy economics. These represent end-consumption sectors and are the source of energy demand. Figure 4 provides a simple overview of how the power sector is linked to the end-consumption sectors, using renewable electricity from wind and sun. The figure shows the possibilities for direct and indirect electrification. The latter can be achieved by applying power-to-heat (P2H) through heat pumps (HPs)—also applicable for cooling—or electric boilers (EBs). Another possibility is power-to-gas (P2G) through electrolysis, which converts power into hydrogen (H_2). With a CO_2 source, it can further be processed into methane (CH_4) or also methanol as a liquid fuel (see Section 2.4). Ausfelder et al. (2017) find that sectors in SC are often defined as heat, power, and mobility or even heat, power, and transportation (Richts et al., 2015). Wietschel et al. (2018) specifically define SC as applying renewable electricity in the transport, heat, and industry sector, according to BMWi (2016) and BMUB (2016a). However, BDEW (2017) interprets SC as the coupling of power, heat, and mobility to supply the end-consumption of the industry, residential, trade/services, and transport sector with renewable energy and emphasises a coupling of infrastructure as well as energy carriers for a more flexible supply.

Scorza et al. (2018) conclude that most research is based on a rough division into the power and consumption sectors: transport, industry, and buildings, which is mainly in line with the approach by Robinius, Otto and Heuser, et al. (2017). A "building" in this case includes the heating demands in residential/households and public buildings in services/trade. DVGW and VDE (2016) point out that SC has to be set up following specific goals and needs to fulfil the demand profiles of the residential, industrial, and trade/services sectors. Each sector prefers different technologies, and the various coupling elements enable system-friendly, macro-economic integration of the energy grids. The European Parliament (2018) addresses different perspectives of SC and differentiates between energy end-use sectors and the energy vectors or carriers (electricity, gas, and heat). Although they define end-use SC as the interaction between electricity supply and end-consumption sectors, cross-vector coupling involves the integration of different energy carriers, also known as vectors. They claim that "sector coupling involves the increased integration of energy end-use and supply sectors with one another" (EP, 2018).

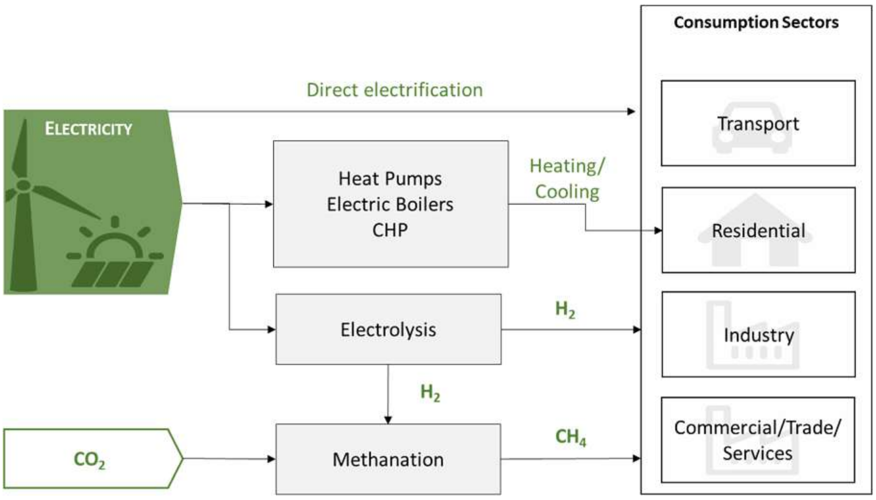

Figure 4 Sector coupling: pathways from the power to transport, residential, and industry sector (adapted from (Robinius, Otto, Heuser, et al., 2017)).

This strategy may thus improve the efficiency and flexibility of the energy system and add to its reliability. The European Parliament (2018) points out that a more integrated planning approach is needed in future renewable energy systems. Integration includes the supply side, with more flexible use of different energy carriers through the transformation of (surplus) electricity, and the cross-vector coupling on the demand side, for example, by using excess heat from power generation, conversion plants (electrolyser) or industrial processes for district heating (DH) (EP, 2018). The latter is not the focus of the SC interpretation in this paper. Nevertheless, the use of excess heat does substantially contribute to efficiency gains in future renewable energy systems and is investigated explicitly by research on multi, smart, and integrated energy systems ((Mathiesen et al., 2015), (Lund et al., 2012), (Lund H. et al., 2014)). The role of SC in multi-energy systems is discussed in Section 2.6.

Table 1 Interpretation of sectors in SC

Authors	*Interpretation of the sectors in literature*	*PR*
Schaber (2013)	Power, heat, hydrogen, and natural gas sector	
Schaber et al. (2013)	Power, heat, hydrogen, and natural gas sector	
Quaschning (2016)	Power, residential/heat, industry and transport as "sectors" with the distinction between households and heat describing only decentralised/centralised use	
BMUB (2016)	Define SC as the use of renewable electricity in the transport, heat, and industrial/services sectors	
BMWi (2016)	Define SC as the use of renewable electricity in the transport, heat, and industrial/services sectors	
Robinius, Otto, Heuser, et al. (2017)	Refer to the end-consumption sectors common in energy economics: industry, trade and commerce, residential/household, transport	X
BDEW (2017)	Coupling of power, heat, and mobility as a decarbonisation tool to enable flexible energy use across all end/consumption sectors: industry, residential, trade/services, and transport	
Ausfelder et al. (2017)	Identify that there are various interpretations of the sectors in SC. Their study is based on heat, power, and mobility	
Wietschel et al. (2018)	Differentiate sector, infrastructure, and technology perspectives on SC. Define SC as the use of renewable electricity in the transport, heat, and industrial/services sector but agree that classical consumption sectors in energy economics are households/residential, commercial/trade/services, industry, and transport	
Richts et al. (2015)	Refer to a coupling of electricity, heat, and transportation	X

PR… peer-reviewed

2.3.2. Definition of sector coupling

Definitions of SC range from limiting it to the one-way path from the power to another end-consumption sector, to including cross-energy-carrier integration, even with, for example, excess heat use and biomass energy. Essential interpretations of SC are summarised in Table 15 in Appendix A, starting with the broadest in scope and terminating with the strictest. Because some references provide a narrower and broader interpretation, they may be stated several times. Some authors agree that SC is about linking the power sector to the end-consumption sectors to fulfil this demand with renewable energy. However, others see it as a general integration of all the energy carriers and the respective infrastructure.

Although some papers strongly focus on using surplus energy from VRE to reduce, for example, curtailment needs, other definitions emphasise the decarbonisation potential of renewable power in the industry, heat, and transport sector. More definitions of SC were discovered in reports and position papers than in peer-reviewed scientific publications. Further, specific definitions of SC were found in 14 studies, mainly represented by reports and project results, one position paper, one dissertation, and only two peer-reviewed papers.

Ausfelder et al. (2017) attribute a very broad scope to SC with an integrated optimisation of the whole energy system by merging the power, mobility, and heat sector. Furthermore, they claim that in this concept, electricity, hydrogen, methane, and even energy produced from biomass and geothermal sources are used flexibly in all application forms. However, the authors define the use of power from large-scale VRE in the heat, industry, and transport sectors as a core objective of SC. The often cited BMWi (2016) adds that using power from VRE helps to promote the energy transition in other than the power sector and claims the application of "clean" power to reduce the share of fossil fuels in other sectors is called SC. BMWi (2016)**:** "With the integration of energy sectors (sector coupling), the power supply meets the demand for energy in households (heat and cooling) and transport (propulsion), as well as in industry and trade, commerce and services (heat, cooling and propulsion)." The strategy creates new demand in the power sector and may offer flexibility from the demand side for the inflexible power generation from VRE.

As a primary goal of SC, Wietschel et al. (2018) emphasise the importance of reducing GHG emissions, which puts VRE sources into the spotlight. They regard SC as the ongoing process of replacing fossil energy carriers with renewable electricity or other sustainable forms of energy, which also includes the use of excess heat. The authors further suggest the interaction between classic consumption sectors such as residential, trade/services, industry, and transport through the integration of their infrastructure. BDEW (2017) published 10 theses on SC where they define SC as follows: "The energy-technical and energy-economic integration of electricity, heat, mobility, and industrial processes, as well as their infrastructures with the aim of decarbonisation and simultaneous flexibilisation of energy use in industry, households, commerce/trade/services, and transport under the premises of economic efficiency, sustainability, and security of supply." IRENA et al. (2018) claim, that "the concept of sector coupling encompasses co-production, combined use, conversion, and substitution of different energy supply and demand forms - electricity, heat, and fuels."

Richts et al. (2015) also interpret SC as an integral approach to successfully reducing GHG emissions and defined it as an overall integration or coupling of electricity, heat, and transportation using technologies based on renewable electricity. BMWi (2016) regard SC as a requirement to promote the decarbonisation of all sectors effectively and economically. In combination with classic energy efficiency measures and direct heat generation through other RES (biomass and solar thermal energy), SC supports reducing GHG emissions. Scorza et al. (2018) offer one narrow and one very broad interpretation of SC. The narrow definition refers to the use of power in consumption sectors or applications in which it currently has little or no meaning (e.g., the electrification of transport instead of traditional fossil fuels or indirectly via P2G for FCEVs). The definition can be even narrower if only surplus power generation from VRE is considered. Noussan (2018) provides a similarly strict interpretation, "Sector coupling includes different applications that have the common goal of transforming the power excess into other forms of energy, e.g., power-to-heat, power-to-liquids, or power-to-gas." In the broader definition, Scorza et al. (2018) claim that SC may refer to integrating or coupling all sectors to increase the flexibility of the overall energy system operation. The concept may support the security and economic performance of the energy supply. VRE surplus generation might result in large-scale curtailment, lowering the value of VRE output and reducing investment attractiveness. VRE electricity needs to receive new demand from more end-use and supply sectors to maintain its value. Considering SC as a large-scale and economically attractive solution for using temporary excess electricity from VRE, Schaber (2013) focuses on applying renewable electricity in the heat sector or generating H_2 through electrolysis.

Olczak and Piebalgs (2018) show that SC leads to new links between energy carriers and infrastructure by, for example, using surplus power from renewables and transforming it into gas, such as hydrogen (H_2) or methane (CH_4), liquid fuels, or heat. Through these technologies, demand from all end-consumption sectors becomes relevant for energy supply from the power sector, offering sinks for peak power generation from VRE.

2.3.3. Research on sector coupling

The available research on SC ranges from a focus on policies, and overall system perspective to techno-economic aspects, modelling, and specific technical analyses (see Table 16 in Appendix A). Between 2014 and 2017, research on SC and its holistic view of end-consumption sectors has been scarce in peer-reviewed journals and instead covered the isolated view of technologies. Relevant literature has been increasing substantially since 2018. So far, in 2020, more peer-reviewed studies on SC have been published than in the two years before. Papers that focus on a specific sector mainly investigate the field of residential heating or transport. A few publications analyse SC in the industry or the commercial/trade/services sector. Studies on P2H and P2G technologies are dominant, whereas P2L and direct electrification from VRE are addressed less often. The work considered relevant for this paper mainly focuses on the European area and provides numerous analyses for Germany. Studies without a geographic focus usually represent general, techno-economic research, for example, the state of the art of P2G or P2H or its potential in future energy systems.

There is numerous research available on the techno-economic aspects of SC, such as the use of renewable electricity for heating (Arabzadeh et al., 2020; Bellocchi et al., 2020; Brown et al., 2018; Felten, 2020; Jimenez-Navarro et al., 2020; Richts et al., 2015; Schaber, 2013; Schaber et al., 2013; Schill & Zerrahn, 2020; Stadler & Sterner, 2018; Zhu et al., 2020). Others focus on the transport sector (Arabzadeh et al., 2020; Bellocchi et al., 2020; Brown et al., 2018; Lester et al., 2020; Sterchele et al., 2020) and even the commercial/trade/services sector (Brown et al., 2018; Jimenez-Navarro et al., 2020; Zhu et al., 2020).

Several papers specialise in the enabling technologies for SC without a significant economic perspective and focus on the transport sector (Robinius, Otto, Heuser, et al., 2017; Schemme et al., 2017), heating in the residential sector (Bloess et al., 2018; Buffa et al., 2019; Witkowski et al., 2020), and industry (Posdziech et al., 2019). Technical papers sometimes do not analyse a specific sector but apply a system perspective or focus on the transformation technologies (Ausfelder et al., 2017; Hidalgo & Martín-Marroquín, 2020; Quaschning, 2016).

Although policy strategies are rarely covered in the context of SC, work is available covering the geographical area of Europe, Germany, and the UK (Cambini et al., 2020; Frank et al., 2020). We assume that the complexity of the whole SC dimension leads to the fact that modelling is not addressed excessively or focuses on one sector in which the majority includes transport and residential heating (Bloess et al., 2018; Burandt et al., 2019; Jambagi et al., 2015; Pavičević et al., 2020; Robinius, Otto, Syranidis, et al., 2017).

Jambagi et al. (2015) and Witkowski et al. (2020) analyse SC as one tool within integrated MESs. Section 2.6 is dedicated explicitly to SC from an integrated/smart energy system perspective. This approach integrates the electricity, gas, and heating infrastructure and includes the flexible use of possible energy generation and storage means. Therefore, it also requires SC and the enabling technologies described in Section 2.4 for renewable energy use and flexible transformation.

2.4. Enabling technologies for sector coupling

According to current research, P2X technologies will be inevitable to decarbonise various end-use applications, such as industrial process heat, chemical production, international air, or maritime transport. Many of these processes cannot be powered by electricity directly but depend on specific chemical conditions that can only be provided by a material energy source, such as gas and liquid fuel. P2X technologies compete with direct electrification in many energy-consuming processes. These, for example, include railway and long-distance truck transport or low-temperature heating. For private vehicles, local truck transport, and short-term flexibility within the electricity system, however, P2X transformation technologies are only competitive under certain conditions. Transformation processes from electricity into, for example, gas or fuel ideally are operated at times of excess electricity generation during which electricity prices are low (IRENA et al., 2018). Matthes (2018) point out that if full decarbonisation and 100 % supply from renewables shall be achieved, more powerful battery storage systems and P2G options for seasonal storage and sector integration will play a crucial role. These applications require intensive research to become mature technologies in the next two decades.

As an example of drive types in transport, Figure 5 shows that direct electrification through BEVs represents the most efficient overall resource use in mobility. Indirect electrification via liquid diesel fuels results in an overall efficiency Well-to-Wheel of only about 20 %, and hydrogen fuel cell electric vehicles (FCEV) provide about 33 % efficiency (Transport&Environment, 2020). Fuel provision and the transformation into motion are much more efficient through direct electrification in a BEV, which achieves an overall efficiency of almost 80 %. Any conversion toward renewable gas or liquid fuels will cause substantial efficiency losses. Still, on some occasions, they might be required to enable timely decarbonisation of hard-to-abate processes such as the industrial steel, cement or chemicals sector or heavy-duty transit transport.

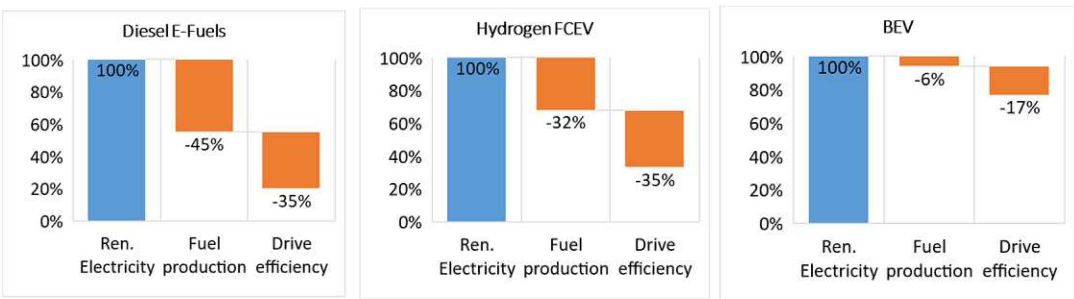

Figure 5 Efficiency of different electricity-based drive options (Transport&Environment, 2020); Renewable (Ren.)

2.4.1. Direct electrification

One potential application of SC refers to the direct electrification of processes. Formerly fossil-fuel-based applications and technologies may be adapted to be powered by electricity. Some currently directly electrified processes have already used electricity a long time ago. The mid-to-long-term goal nowadays, however, has to be using renewable electricity. Common examples include switching from traditional vehicles with combustion engines powered by fossil fuels to BEVs. Although usually direct electrification is not defined as a transformation process similar to P2G, etc., Wietschel et al. (2015) define e-mobility as power-to-move. Moreover, industrial processes often have vast direct electrification potential. Steel production can, for example, be transformed using an electricity-based electric arc furnace instead of a coal-fired blast furnace and a basic oxygen furnace (BOF) (see Section 2.5.3). Direct electrification is also an option for smaller-scale residential heating and cooling (see Section 2.5.2).

2.4.2. Power-to-gas/liquids

Not only is the importance of integrating large-scale renewable electricity generation mentioned frequently in the literature, but also the importance of integrating the gas sector. The existing gas infrastructure may already enable large-scale distribution and storage of renewable energy (BMUB, 2016a; DVGW, 2020; DVGW & VDE, 2016)). Water electrolysis converts power into gas—an electrochemical process that splits water into hydrogen (H_2) and oxygen (O_2) (IEA, 2019). H_2 is an energy carrier with a high energy density or energy-to-weight ratio, three times higher than that of gasoline or diesel, and low storage cost ((Schiebahn et al., 2015), (Lewandowska-Bernat and Desideri, 2018)). This renewable gas is not only a promising alternative for diesel and gasoline in the transport sector but is also used in various industrial applications, such as ammonia synthesis, fertiliser production, glass, and fibre production, etc. (Lewandowska-Bernat and Desideri, 2018).

Today, three-quarters of H_2 demands are produced from natural gas, followed by coal (IEA, 2019). Water electrolysis today accounts for less than 0.1 % of dedicated H_2 production globally; however, it is expected to rise substantially with an increasing share of renewable electricity. Electrolysers currently operate between 60 % and 81 % efficiency, depending on the technology type and load factor. H_2 may be processed to methane using renewable H_2 and a CO_2 source and even into liquid, synthetic fuels with similar characteristics to diesel or gasoline, such as methanol. CO_2 as a required input for methanation may either be produced from organic matter, for example, biomass, from fossil power plants, industrial processes, or captured from the air (Schiebahn et al., 2015). While hydrogen may be fed into the natural gas grid only at a particular share—depending on local technical characteristics—methane can function as a direct substitute.

The liquefaction process is usually defined as P2L (DEA, 2017). However, some authors even specifically name it power-to-fuel (Robinius, Otto, Heuser, et al., 2017; Schemme et al., 2017). Ridjan et al. (2016) reviewed the difference between synthetic fuels and electro-fuels, finding that the first does not directly indicate the type of resource or production process used. The authors suggest using electro-fuels if a large amount of electricity is included in the production process, as is the case for hydrogen or methanol production via electrolysis. We will refer to electro-fuels for gaseous or liquid fuels generated from P2G or P2L.

2.4.3. Power-to-heat

The transformation of power into heat can be realised using HPs and EBs either on a central level for DH purposes or on a decentralised level directly at the consumption location. For small applications, even direct electric heating is possible. The flexible heating and cooling generation from renewable electricity is gaining importance in future renewable energy systems (Bloess et al., 2018). Currently, at least in Denmark, a decrease in taxes on electricity use for these technologies is improving economic performance (Nielsen et al., 2016). HPs are known to be more efficient compared with EBs. HPs transform heat from a low-temperature heat source (e.g., ammonia, air, seawater, industrial waste heat, etc.) to a higher temperature-level output heat (DEA, 2016) and can also function the other way around for cooling. There are so-called "compression HPs"—powered by electricity or combustion engines consuming fuel or biogas—and "absorption HPs"—driven by steam, hot water, or flue gas. They can be used in industrial processes, individual space heating/cooling, or DH. Compression HPs achieve a seasonal performance factor or average coefficient of performance (COP) of 3–5 times the utilised electricity input (DEA, 2016).

Nielsen et al. (2016) claim that EBs, in contrast, are easier to implement from a financial perspective because of lower investment costs and more flexible operation without any start-up cost or constraints . They use electricity to generate hot water or steam, similarly to oil or gas boilers (DEA, 2016). EBs operate at an average COP of 1 and are primarily implemented for ancillary services owing to their systemic benefits promoting wind energy utilisation and efficient heat source use. EBs are using electrical resistance for 1–2 MW; for example, a standard hot-water heater or electrode boilers for larger applications of more than a few MW directly connected to the high voltage grid (DEA, 2016).

The technologies described above enable various pathways for using renewable power to achieve the decarbonisation of the energy system. Figure 6 and Figure 7 illustrate the principles of SC from a technological perspective. In Figure 6, the authors call direct electrification of transport using BEVs power-to-move, sometimes referred to as power-to-mobility or power-to-transport. Figure 7 outlines the integration of the energy carriers, namely, electricity, gas, and heat, as well as their cross-sectorial utilisation and energy storage options. Because the original figure by Stadler and Sterner (2018) focused on integrating energy carriers, the end-consumption sectors (transport, industry, and residential) were added as final demand sources.

Supply sector	**Potential application of renewable electricity after transformation**	Transformation 1 Energy carrier	Transformation 2 For end-use	End Use
Renewable electricity	Power-to-heat	-	Heat pump Electric boiler CHP plant	Space heat Process heat
	Power-to-gas	Gas (H_2/CH_4)	Combustion	Space heat Process heat Industrial products Transport
	Power-to-liquid	1. Gas (H_2/CH_4) 2. Liquefaction	Combustion	Space heat Process heat Industrial products Transport
	Direct electrification			Space heat
	Power-to-move/mobility/transport		*Electrolyte*	*Transport*

Figure 6 Sector coupling transformation pathways from a technical perspective (adapted from Wietschel et al. (2018)).

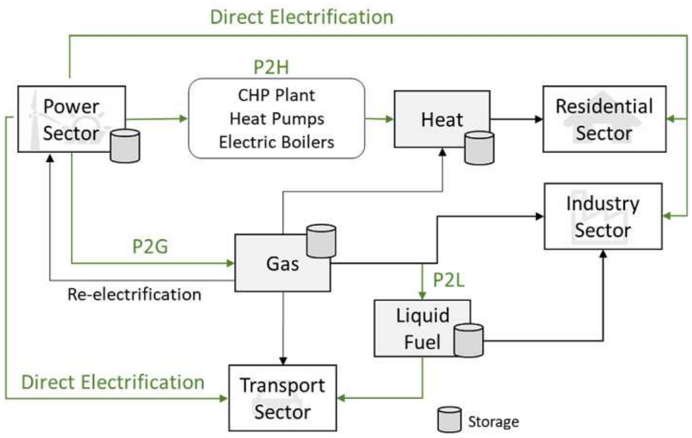

Figure 7 Power-to-X technologies and cross-sectorial energy storage for sector coupling (adapted from Stadler and Sterner (2018))

2.5. Sector coupling applications

2.5.1. Sector coupling in the transport sector

Traditionally, the transport sector, including road and rail transport, aviation and maritime shipping, was mainly based on crude-oil-derived liquid fuels (Robinius, Otto, Heuser, et al., 2017). Figure 8 shows the potential pathways of direct and indirect electrification of transport. For individual passenger transport, electricity may be used in BEVs or H_2-powered FCEVs for decarbonisation (Lund H. et al., 2014). Direct electrification via BEVs is efficiently applicable in passenger cars. International air and sea freight transport would require much higher battery capacity, which results in too much weight and energy consumption for efficient operation. For freight transport by road, BEVs currently enter the market in the smaller but also large truck classes. Research is also being conducted on overhead line trucks for the larger weight classes. H_2 has long been promoted as a potential transport fuel for cars, trucks, and trains (IEA, 2019). There are various application options for renewable gas in different forms, either as H_2, methane, or blends in conventional internal combustion engines (DEA, 2017).

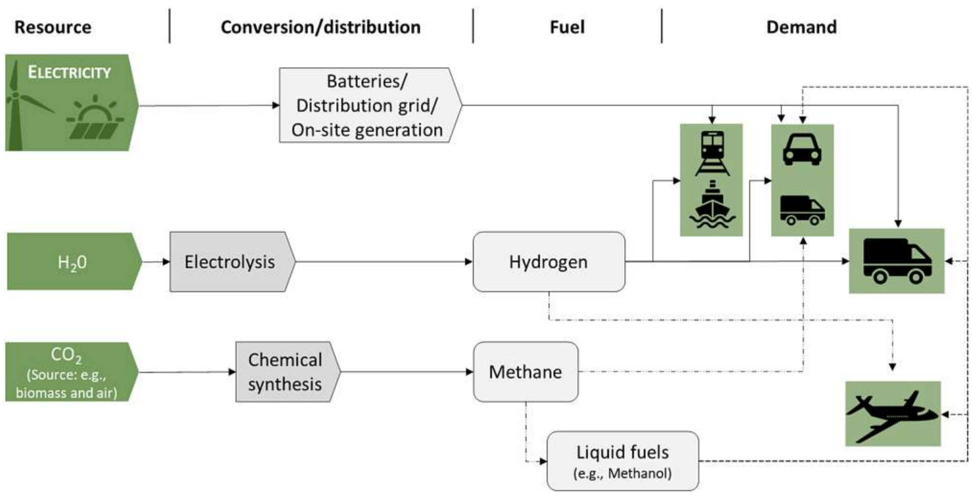

Figure 8 Renewable power use for common modes of transportation (adapted from Lund H. et al. (2014)).

Hydrogen produced from renewable electricity or biomass instead of fossil fuels has a much better climate balance than conventional vehicles (Schemme et al., 2017). FCEVs convert H_2 into electrical energy and represent a dynamic buffer for load management, using H_2 as a link between the power and the transport sector. While large parts of rail transport are driven by electricity, regions with no electricity lines could use fuel-cell-powered trains (Alstom Group, 2020b; Schreiner and Fleischhacker, 2018). The Coradia iLint, the first hydrogen-fuel-cell train of its kind in the world, shown in Figure 9, was developed by Alstom (Alstom Group, 2020b).

The hydrogen train performs similarly to traditional regional trains at low noise and zero emissions with up to 140 km/h of speed. The Coradia iLint has a range of approximately 1,000 km—the same as an equivalent-size diesel multiple unit (Alstom Group, 2020b). Furthermore, in maritime transport, electric shipping is already considered, apart from fuel-cell-powered vessels (IRENA, 2015). Using biofuels is being investigated but remains challenging concerning storage on board and the resulting corrosion and bio fouling. Biofuels are not considered SC in our interpretation and are therefore not included for maritime transport in Figure 8.

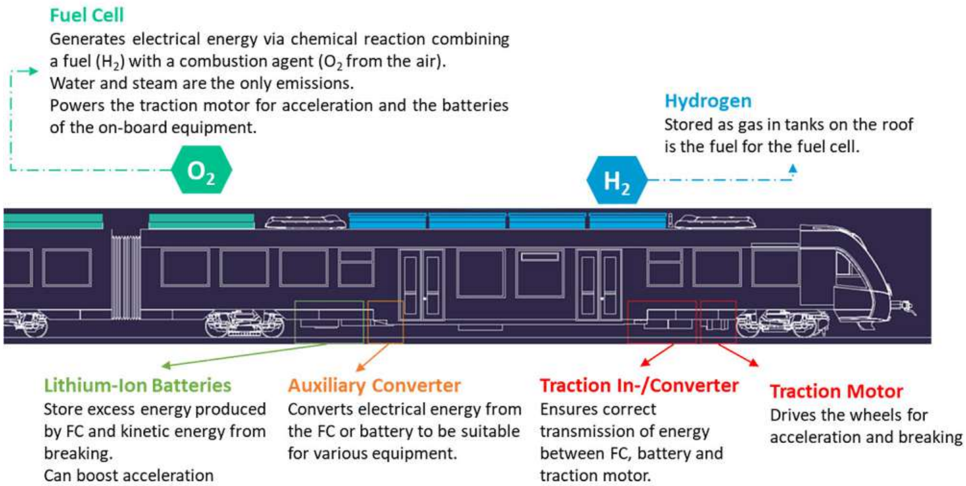

Figure 9 Coradia iLint—the world's first hydrogen-powered train. Fuel cell (FC) (adapted from (Alstom Group, 2020a))

Of course, liquid electro-fuels with similar specifications as diesel or kerosene are also an option and are, together with H_2, the only realistic decarbonisation approach for maritime and air transport. However, large-scale and low-cost CO_2 sources will be required for production—for example, from biomass—representing a challenge in an increasingly decarbonised energy system (Robinius, Otto, Heuser, et al., 2017). The qualification of an electro-fuel as a future transport fuel depends on its technical suitability to be used in existing systems and combustion technologies and the economic competitiveness with conventional fuels (Schemme et al., 2017).

2.5.2. Sector coupling in the residential sector

Achieving the decarbonisation of the residential sector mainly focuses on the area of heating. The power conversion into heat and cold can be achieved on a centralised level—from a spatial or infrastructural perspective—close to the power generation plant or on a decentralised level near the customer location. Bloess et al. (2018) provide a comprehensive overview of the potential applications of using P2H as a technology to offer an alternative to fossil fuel heating (see Figure 10). Direct electric heating, HPs or EBs can be applied on a decentralised level. The decentralised P2H network can also include a private BEV or a rooftop PV system with battery storage to provide flexibility. On a centralised level, renewable electricity may be fed into the central electricity grid, used in centralised HPs or EBs, or fed into the DH system. The authors also include power generation from thermal plants, which may be reduced or operated through renewable gas instead of natural gas in the long term (Bloess et al., 2018). A critical role concerning renewable DH is assigned to existing CHP plants, which may be enhanced through HPs and heat storage for efficient VRE integration (DEA, 2017).

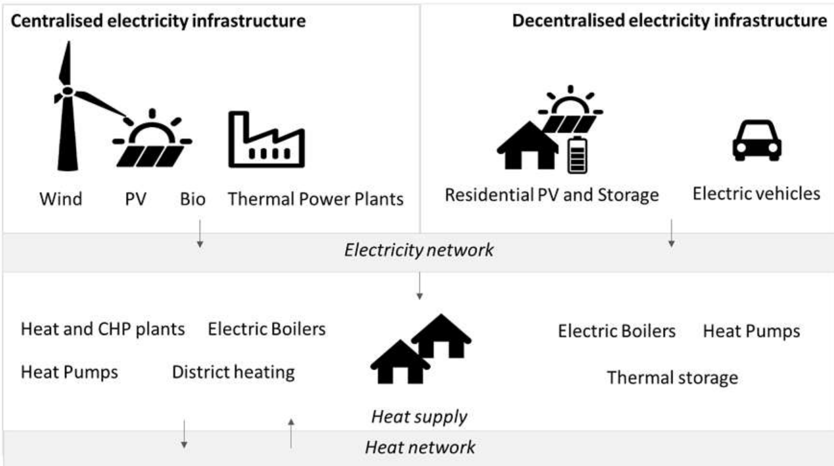

Figure 10 Power-to-heat (P2H) technologies on central and decentralised level, adapted from Bloess et al. (2018).

Generally, the literature on heating and cooling in future renewable energy systems primarily focuses on extended DH and using HPs and EBs. These technologies are far more efficient than renewable hydrogen, which is produced at about 75 % efficiency, followed by further efficiency losses in heat production. Decarbonising existing buildings, often equipped with decentralised gas boilers, requires extensive refurbishment. Nevertheless, an increasing amount of processes in other end-consumption sectors (e.g., transport and industry) may be able to use renewable hydrogen instead of, for example, liquid fuels, and long-term storage is most promising with P2G. Consequently, the gas infrastructure remains an essential asset in future energy systems.

DH has experienced vast development from its first application until now. From coal-powered steam generation in 1880 and CHP plants in the 20th century, it advanced toward heat generation from biomass and large-scale solar systems. Modern DH now uses large-scale renewable electricity (Lund H. et al., 2014). Temperature levels also decreased substantially compared with the start of DH applications, leading to higher efficiency and parallel operation of district cooling. DH development is essential for MESs to levy synergies between all three types of infrastructure, namely, the electricity, thermal, and gas grid. Such a development may be supported by the more flexible operation of CHP plants, which may be achieved by the following three steps (Mathiesen and Lund, 2009):

1. Active regulation of CHP plants by use of thermal heat storage: The heat generation of CHP stations should not only depend on heat demand but should also adapt to produce less gas-powered electricity during the high availability of renewables (DEA, 2017). Therefore, heat storage capacity can add flexibility to decouple heat generation from demand (Lund et al., 2014).
2. Using EBs and HPs in CHP systems: Enables heat generation from excess renewable electricity (Lund et al., 2014). Renewable energy integration is again supported by thermal storage for a more flexible generation independent of demand.
3. Bypass of turbines: At low electricity prices because of high renewable electricity availability, a bypass for electricity enables a CHP plant to only produce heat from VRE at the efficiency of a heating-only boiler (DEA, 2017).

There is already one successful example of a future energy plant with the Skagen CHP plant located in the northern part of Denmark, which has been in operation for several years (Lund et al., 2012). This CHP plant includes three gas engines (CHP 1–3) and is supplemented with a waste incineration boiler, an EB, and contribution from industrial surplus heat. It plays an active role in grid stabilisation and regulating power tasks and promotes the integration of substantial amounts of wind power in the electricity and heat supply, leading to the decarbonisation of these sectors. Heat generation with the EB is conducted at low electricity prices, and the CHP plant generates heat at high electricity prices (see Figure 11).

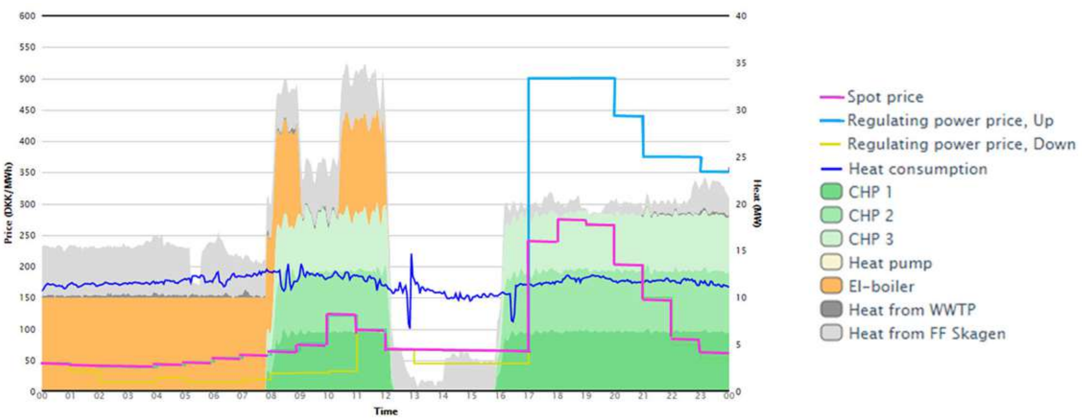

Figure 11 Flexible operation of Skagen CHP plant, equipped with heat pump and electric boiler on March 18th, 2020 (EMD International (2020)).

Additionally, waste heat is used continuously. Thus, with heat generation mostly exceeding heat demand, the thermal storage is built-up on that day. Only recently, Skagen CHP plant invested in a large-scale HP, which reduced fossil-fuel heat generation and replaced the EB most of the time because of its high COP.

2.5.3. Sector coupling in the industrial sector

The industrial sector requires reliable electricity availability for manufacturing processes and usually uses fossil fuels to power motors or produce H_2 for industrial chemicals. Many of these types of energy consumption may be decarbonised through SC. However, generating fuels that fit into the existing infrastructure and are suitable for standard combustion engines or can replace fossil-fuel-based components of chemical products is a challenge. Thus far, manufacturing has largely been neglected regarding decarbonisation action. In the US, however, the industrial sector is responsible for one-third of the total energy consumption, of which manufacturing activities make up the most significant part (Zhong et al., 2017). Onsite renewable energy generation systems would allow the manufacturer to mitigate the disturbances of the utility grid and improve reliability, affordability, resilience, and security of energy supply. Additionally, these decentralised, renewable power systems will decarbonise the industrial sector and reduce the pressure on electricity transmission and distribution systems (Zhong et al., 2017).

Besides the energy to run machines in manufacturing, the chemical industry has substantial demand for H_2, which is included in most industrial chemicals, such as ammonia for fertiliser production and methanol for various solvents (IEA, 2019). The chemical sector is responsible for the second greatest demand for H_2 for ammonia and the third biggest demand for producing methanol at 31 and 12 Mt H_2/a, respectively. Including further minor applications of H_2, the chemical sector causes 40 % of total H_2 demand in pure and mixed forms. Until 2030, H_2 demand in chemical production, especially ammonia and methanol, is expected to increase from 44 to 57 Mt/a and remains an important material (IEA, 2019). Furthermore, producing steel from iron ore in a direct reduction process represents the fourth-largest single source of H_2 demand today (4 Mt H_2/a) (IEA, 2019). Steel demand is expected to increase by 6 % by 2030. One ton of crude steel results in around 1.4 tons of direct CO_2 emissions. Less CO_2-intensive processes are currently being developed and can be divided into the following two categories:

- "CO_2 avoidance" pathways: Through low-carbon sources of energy, usually using H_2;
- "CO_2 management" pathways: Recovery and management of CO_2 in traditional fossil-fuel-based routes, usually via carbon capture, utilisation, and storage.

Herrmann et al. (2014) developed their vision of a "factory of the future" (see Figure 12). They point out that future manufacturing needs to address all three dimensions of sustainability, namely, economy, ecology, and society. The environmental impact has to be reduced by aiming at a zero-emission concept or even a positive effect on society, improving the quality of air and water, providing renewable energy, and acting as storage for surplus energy to maintain or even improve profitability. This is the only way to achieve an appropriate degree of sustainability in manufacturing, which preserves resources for future generations. As seen in Figure 12, the factory of the future shall integrate energy flows across the industry, households, and urban infrastructure as well as provide renewable power from, for example, a rooftop PV system. This approach shall enable SC for transport and manufacturing processes or renewable H_2 production (Herrmann et al., 2014). The most famous prototype of such a factory has been realised within an eco-industrial park in Kalundborg, Denmark.

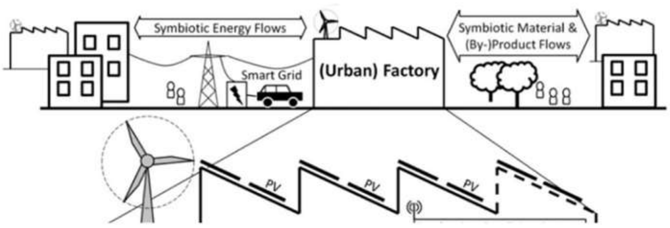

Sector Coupling Aspect:
- On-site renewable electricity generation
- Use for production processes
- Provision of this electricity to community for BEV charging or households
- Use of renewable electricity on site
- Methanation using surrounding carbon sources from waste and local emissions

Figure 12 Sector coupling aspects in holistic factories of the future (adapted from Herrmann et al. (2014)).

As an exemplary project, voestalpine strives for a continuous increase in the use of renewable electricity and renewable H_2 in their steel production process, allowing the Group to reduce its CO_2 emissions by over 80 % by 2050. Figure 13 shows this restructured production process in which renewable electricity and hydrogen can replace all the coal input. The formerly used coal-powered blast furnace and BOF are eliminated and substituted by a hydrogen-powered direct reduction plant and an electric arc furnace. Such a change in the production process, however, highly depends on the availability of renewable electricity at commercially realistic prices to stay competitive.

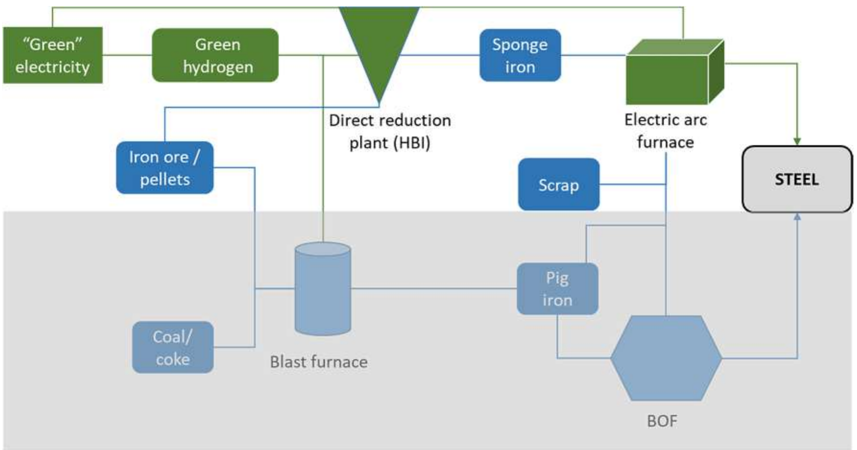

Figure 13 Restructured steel production process powered by renewable energy (adapted from voestalpine (2020)).

2.6. The role of sector coupling in multi-energy systems

Thus far, the SC concept has been discussed as a measure to integrate renewable electricity into a broad range of applications in different energy end-consumption sectors, enabled by transformation technologies and an adaption of traditional processes. Apart from a link between the power and other sectors, integrating different energy carriers and grids for electricity, gas, and heat is also gaining attention. The interactions between these energy carriers are essential to provide flexibility and handle renewable resources efficiently. These concepts can be found in the literature under several terms, such as multi-energy system, integrated energy system, or smart energy system (SES) (Connolly et al., 2016; Lund H. et al., 2014; Witkowski et al., 2020).

The common isolated view of energy grids is changing, and hybrid or integrated multi-energy systems are gaining importance with increasing VRE input (Ramsebner, Haas, Auer, et al., 2021). Geidl et al. (2007) claim that the traditionally grown energy grids are not ready for the new requirements. Considering existing frameworks is a barrier when modelling this new view of optimal renewable energy systems. Mancarella (2014) understand MES as the optimal interaction of systems and energy carriers on different levels, for example, geographically within a district, city or region (Ramsebner, Haas, Auer, et al., 2021).

Lund H. et al. (2014) define an integrated energy system enhanced by new technologies and infrastructure as smart energy system. However, the "smart" in SESs does not explicitly indicate many intelligent technologies but implies a radical shift in the understanding of energy system infrastructure. The authors also point out that the combination of smart electricity, thermal, and gas networks is a benefit for individuals and the whole energy system. SESs are considered an option to efficiently use a larger share of VRE sources in future energy systems by using new types of flexibility and integrating the infrastructure of smart or bi-directional electricity, smart gas, and smart thermal grids (Lund H. et al., 2014). The smart electricity grid connects the flexible electricity demand of HPs and EBs and the VRE sources. The smart thermal grid enables the integration of electricity and heating and cooling and provides flexibility through thermal energy storage. Finally, the smart gas grid connects electricity, heating and cooling, and transport by considering renewable gas generation through electrolysis (Lund et al., 2017). Modelling such MESs for a time in the future is highly complex. According to Arent et al. (2021), the interconnectivity of energy supply and demand sources is the value and challenge of hybrid energy systems.

Also, the successful realisation of such system change via sector integration depends on technologies, interfaces, supportive regulatory frameworks and market design (Raux-Defossez et al., 2018). Once again, establishing such a new approach to the existing environment results in several challenges, such as complicated interdependencies between energy systems on technical, economic and market perspectives; a lack of commercial tools to operate them; isolated market structures and high operational and management complexity through the different energy grids managed together (Abeysekera, 2016). Furthermore, substantial investments must be made in distribution grid expansion and installing new renewable power and transformation plants such as electrolysers. However, Haas et al. (2021) conclude that the current framework for financing grid infrastructure and renewable technologies is not always setting the right incentives. This is specifically true for applications where the technology has not yet been decided and imposes uncertainty on investors. As a result, pilot plants need to generate a specific volume to decrease the prices of new technologies, e.g. from grid operators to guarantee supply security in renewable energy systems (Ramsebner, Haas, Auer, et al., 2021). While (Geidl et al., 2007) suggest designing everything newly, the risk of stranded investment favours the adjustment of existing infrastructure, e.g. for the distribution of renewable hydrogen or methane.

The ongoing indirect or direct electrification of formerly fossil-fuel-based processes will result in a tighter connection between the relevant end-consumption sectors and the electricity sector (Mancarella, 2014). The more prominent share of electricity in a renewable system may substantially change the role of traditional energy grids, such as gas and heat, and the share between grid and non-grid-related energy consumption. An increase in distributed solar, solar-thermal PV or heat pump systems, for example, increases non-grid-related energy consumption with a specific share of own electricity consumption on site. These renewable energy technologies also represent competition for the gas grid, which distributed 41 % of the grid-related energy in 2015 (Ramsebner, Haas, Auer, et al., 2021). Still, the storage characteristics of gas will be the key to the seasonal balancing of renewable availability. They will remain a significant energy carrier in the future in terms of flexibility and security of supply.

Hybrid energy systems can flexibly handle multiple inputs and supply energy as multiple outputs (Arent et al., 2021). To optimise all energy streams, intelligent communication technology (ICT) is essential in the form of a hybrid demand-control system to achieve environmental and economic benefits (see Figure 14). Real-time data is collected and evaluated through sensors and communication technology for optimal decision-making and forecasting (Masera et al., 2018).

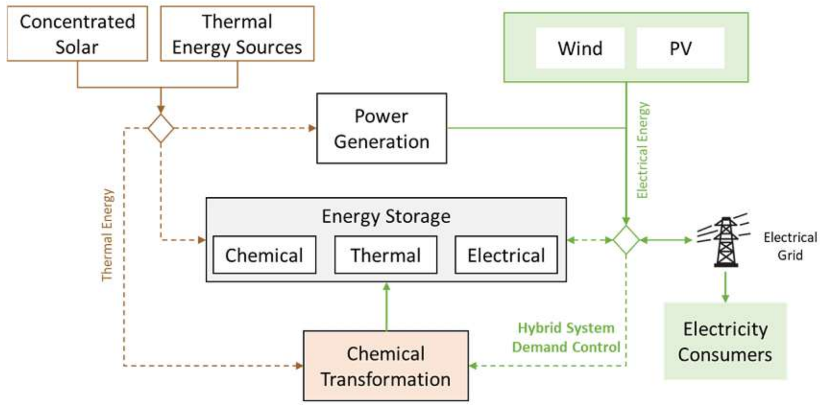

Figure 14 Integration of the electricity and thermal energy flows in a hybrid energy system ((Ramsebner, Haas, Auer, et al., 2021), adapted from (Masera et al., 2018))

Nevertheless, MESs and efficient VRE integration rely on the basic P2X transformation technologies for renewable electricity. Therefore, SC does not only represent an independent system but can also support fully integrated MESs. Witkowski et al. (2020) specifically analyse the ability of SC to provide flexibility in the form of renewable heat or gas.

Figure 15 shows that the input and conversion processes related to SC, marked in blue, are at the heart of such a multi-energy system or SES. They initiate electricity use and transformation into any suitable energy carrier for more flexibility. The transport, residential, and industry sectors demand mobility, electricity, and heating and cooling. Therefore, the SC concept is essential to the future 100 % renewable energy systems. Hybrid energy systems require a successful link between formerly separated infrastructure through ICT and data-based action and prediction (Ramsebner, Haas, Auer, et al., 2021).

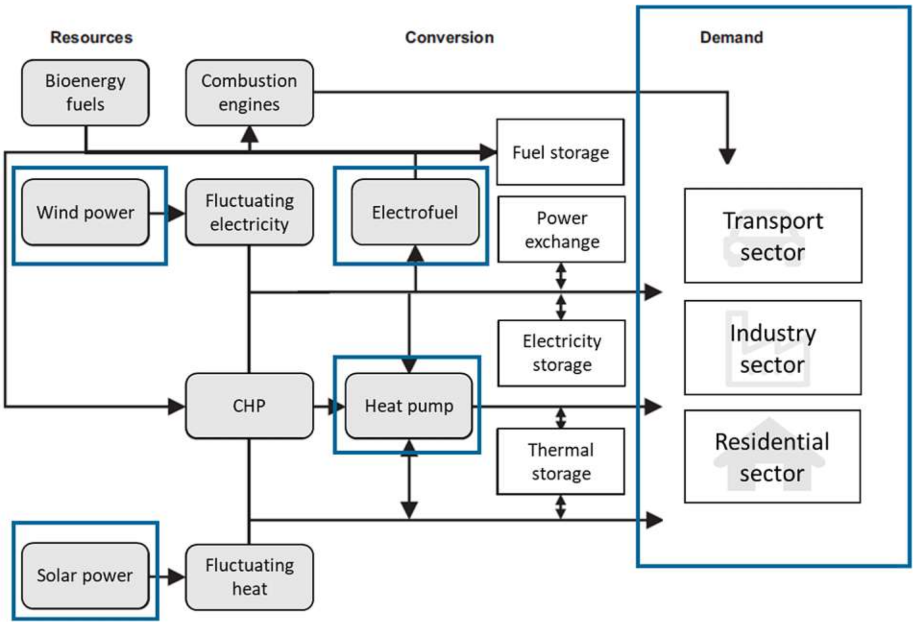

Figure 15 The role of sector coupling in a future Smart Energy System (adapted from Connolly et al. (2016)).

2.7. Discussion of findings

The current Section provides a summary and critical discussion of the literature review conducted in this paper. First, an interpretation of the sectors in SC is suggested, followed by a structured categorisation of the SC concept from our findings in Section 2.3. Finally, the remaining challenges of SC technologies and their value for future renewable energy systems are discussed.

2.7.1. Definition of sectors

Our work proves that the interpretation of SC is multiplied, and the concept understanding varies with the sector definition. The differences in the sector definitions originate from research perspectives and depend on the field of application, either engineering or energy economics. Although Wietschel et al. (2018) use a technical approach in defining the sectors as transport, heat, and industry, Robinius, Otto, Heuser et al. (2017) refer to sectors as transport, residential/household, industry, and trade/commerce. The latter is common in energy economics, while heat or gas do not represent a sector but an energy carrier or service. BDEW (2017), however, regards SC as the coupling of power, heat, and mobility to supply the end-consumption sectors, namely, industry, residential, trade/services, and transport, with renewable energy and used two approaches to the sector definition. Further, BMWi, (2016) mentions SC as the coupling of the heating sector and speaks of a coupling of the residential sector, not specifically following one approach.

A requirement for future renewable energy systems is the determination of new demand sources for renewable electricity by substituting fossil energy. The final goal is fulfilling the demand of end-consumption in industry, transport and residential homes. In contrast, the processes in these end-consumption sectors can be adapted to be powered by another form of energy carrier. A definition of end-consumption sectors, as in Robinius, Otto, Heuser, et al. (2017), provides a technology-neutral approach and allows for a broader range of solutions, independently of the energy carrier applied (electricity, gas, or heat). To avoid thinking based on the existing infrastructure and trying to establish a new design of future energy systems, specifically supply, represents one crucial paradigm shift attempted through the energy hub by Geidl et al. (2007). We, therefore, suggest using the common sector definition in energy economics for techno-economic research on SC. More specifically, in technological research, it is evident that the perspective may focus on transforming power into a specific energy carrier. This would largely meet the approach by the European Parliament (2018), differentiating so-called end-use SC and integrating energy carriers as a cross-vector coupling, which is explained in Section 2.3.1.

2.7.2. Sector coupling: categorisation from an own perspective

As our introduction indicates, SC lacks a consistent definition and is often interpreted misleadingly. Drawing conclusions from our literature review in Section 2.3, this section aims at a comprehensive overview of the potential pathways of SC and the enabling transformation technologies in Figure 16. A detailed categorisation per sector is provided in Table 17 in Appendix A. Renewable electricity may be used directly or through transformation into heating (P2H) or cooling, gas (P2G), or liquid (P2L) in the end-consumption sectors, namely, residential, transport, industry, and commercial/trade/services. We strongly suggest avoiding additional terms, such as power-to-move or power-to-fuel, which imply all potential technologies for fuel generation or movement, and are not specific enough. While the first term summarises all types of transport electrification, the latter summarises different fuels and should be categorised more specifically as P2G or P2L to follow the known structure. Excess electricity may also be used in flexible CHP plants equipped with HPs, as described in Section 2.5.2. The re-electrification of H_2 in times of little availability of renewable electricity sources via CHP plants or gas turbines is possible, although at substantial efficiency losses.

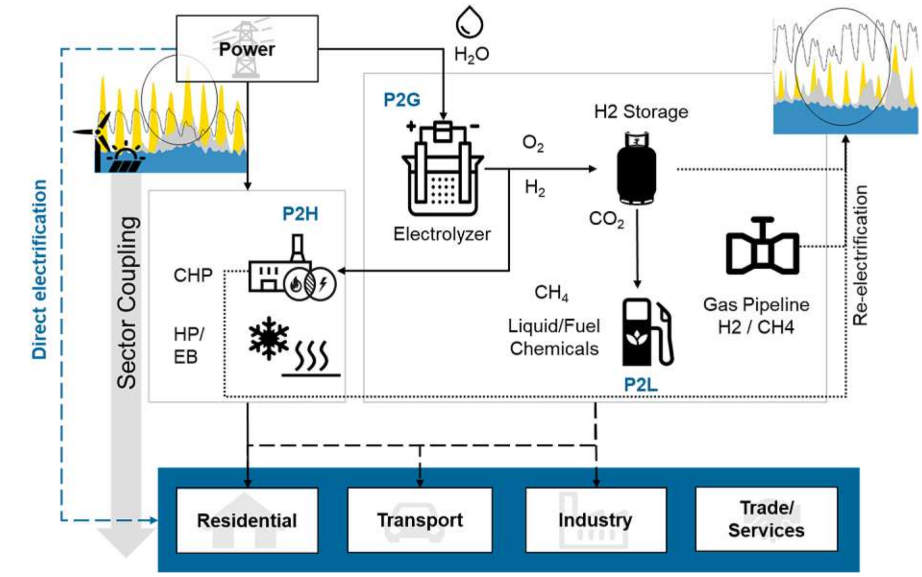

Figure 16 Comprehensive high-level overview of SC pathways from a technological view.

Figure 17 describes direct (electricity flow) and indirect electrification (chemical energy flow) pathways mainly for transport and heating. Apart from grid-dependent electricity use, a decentralised PV system can directly electrify transport using a BEV or indirectly electrify heat using a decentralised HP. H_2 or methane may also be stored long-term in chemical storage or fed into the natural gas grid.

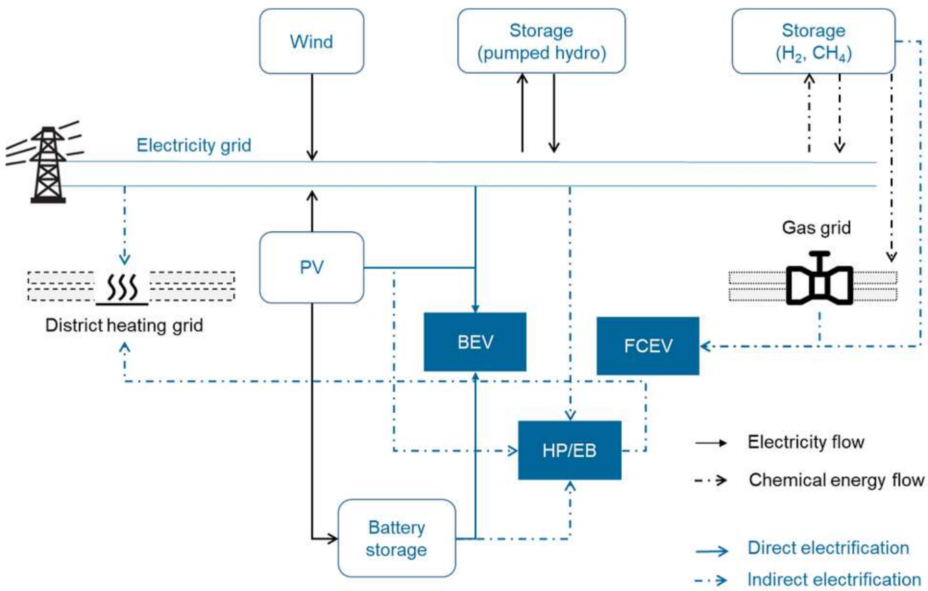

Figure 17 Direct and indirect electrification of transport and heating, heat pump (HP), electric boiler (EB), battery electric vehicle (BEV), fuel-cell electric vehicle (FCEV), photovoltaic (PV).

Table 17 in Appendix A categorises SC applications for each sector as direct and indirect electrification and centralised (C) and decentralised (D) SC. The categorisation is conducted based on the proximity to the consumer and the scale of generation or conversion. SC can be performed on a large scale, centralised level or on a smaller-scale decentralised level, with the transformation or use taking place closer to the end customer. For example, while large-scale P2H from the electricity grid via central EBs is regarded as central SC with indirect electrification, using decentralised EBs or HPs is defined as decentralised SC (Bloess et al., 2018).

One matter often discussed is whether further renewable or waste energy sources, such as biofuels and excess heat, are part of the SC concept. Section 2.3 outlines that the new rise of SC was triggered by the increasing share of VRE electricity generation along with the energy transition. Based on this observation and supporting statements in various literature, we claim that SC mainly originates in the efficient integration of VRE (BMWi, 2016; Robinius, Otto, Heuser, et al., 2017; Schaber et al., 2013; Scorza et al., 2018). Consequently, we do not consider renewable energy that does not include electricity as the primary input, such as waste heat or biofuels, as the central aspect of the SC concept but state it as alternative options in our summary in Table 17 of Appendix A. Even if we agree that, for example, the use of excess heat from power generation or industrial processes is essential to increase energy system efficiency, we suggest addressing it within the area of MESs and regard it as out of scope in SC (Lund H. et al., 2014; Ma et al., 2018; Mancarella, 2014; Marnay and Lai, 2012).

2.7.3. The challenges and value of sector coupling

An increasing share of electricity from VRE sources requires an energy system with more flexible consumption, distribution, and storage. In contrast, VRE sources represent an excellent chance to decarbonise the end-consumption sectors and are essential to reaching climate goals. IRENA (2018) considers P2G the most promising transformation technology that enables SC in various ways. Thanks to the large capacity of gas pipelines in Europe, even low blending shares of H_2 would lead to the absorption of substantial quantities of VRE. Renewable gas may replace fossil fuels in many end-use applications while fully utilising existing infrastructure. Olczak and Piebalgs (2018) are convinced that SC will exploit the rising share of electricity by distributing and storing it after a transformation into H_2 and synthetic methane.

While P2G seems promising for various end-consumption sectors and as a large-scale storage technology, the importance of all potential transformation technologies together needs to be emphasised. The development of transformation technologies faces multiple uncertainties, such as electricity prices and competition through transmission grid expansion. However, its economic feasibility remains challenging with a few full load hours if considered to operate only at times of excess electricity generation. Environmental effects of operation processes need to be internalised in new market frameworks to set the right incentives. To promote the economic feasibility of renewable transformation processes, transformation plants need to be regarded as producers/transformers and not as consumers when sourcing from the electricity grid and markets need to handle gas, electricity and heat flexibly.

Low electricity prices may promote direct electrification within the existing market environment instead of P2G or P2H, whenever possible. Brown et al. (2018) detect SC and transmission grid expansion as competing concepts concerning renewable energy integration. In their study, many scenarios favour expanding transmission network capacity, specifically in the North and Baltic seas. They also find that direct electrification of individual transport is more efficient without the losses of P2G and P2L (Brown et al., 2018). Furthermore, beyond sector coupling, the electricity grid competes with the traditional gas and heating grids, whose role may change. Nevertheless, P2G provides flexibility and long-term storage to renewable energy systems. We interpret these results as a suggestion to implement transmission network expansion and SC to integrate renewable energy efficiently.

Robinius et al. (2018) compare the cost efficiency of P2G and transmission grid expansion and conclude that investment in the latter is currently more cost-effective. Achieving a certain amount of flexibility through transmission network expansion only costs 30 % of the same capacity implementation of an electrolyser; however, they do not consider an income from selling the hydrogen at a competitive price. Hörsch and Brown (2017), in contrast, argue against a substantial cost benefit of transmission grid expansion compared with P2X technologies. They conclude that an almost fully renewable energy system without grid expansion is only about 20 % more expensive. They assume the cost-benefit to be even smaller if investment in line volume was included to avoid the public rejecting a growing amount of new lines. Robinius et al. (2018) later acknowledged that their results highly depended on the regional situation and scenario assumptions. Decreasing capital investment costs and an expected decrease in wholesale electricity prices may eventually support the economic feasibility of P2G, at least for seasonal storage (Robinius et al., 2018). This argument stands against the likely trend of using low-cost renewable electricity directly, reducing the need for P2G. Other transformation technologies also face uncertainties in the long term. For example, the importance of P2H may change along with the consequences of global warming, whereas, simultaneously, requirements for cooling may increase. This uncertainty asks for an appropriate design of DH using lower temperatures that allow efficient heating and cooling in the same network.

Additionally, further research is required in interface technologies for integrating new and more distributed demand sources, e.g. BEVs, heat pumps etc., in currently isolated energy grids. The future energy grid planning on the national and international level does not yet follow integrated system modelling but instead happens uncoordinatedly. This uncertainty also harms decision-making regarding the right technology for producers. Flexibility, furthermore, needs to be integrated into market structures and classified as a service instead of an energy consumer to avoid consumption-based energy fees. Eventually, the large amounts of data gathered and evaluated in such integrated energy systems impose a technical challenge. Still, they may also change demand behaviour and increase control and awareness by consumers. Pfeiffer et al. (2021) found that residential consumers do accept a substantial amount of demand-side flexibility or optimisation of their demand and potential on-site energy production if rewarded appropriately.

Despite all these risks, some arguments justify the continuous investment into SC technologies and appropriate infrastructure. First, with the path towards CO_2 neutrality in Europe, direct or indirect use of large-scale renewable electricity remains a requirement in many cases. The flexible transformation between energy carriers provides a basis for efficiently managing renewable energy systems. This can be realised partly within the SC concept. Second, Novak (2017) explains the value of energy carriers based on the amount of exergy, defined as the net energy provided. Renewable energy from wind and solar power is pure exergy with zero variable fuel cost. Therefore, it needs to be used most efficiently without being wasted. Third, because of the increasing share of electricity generation from wind and PV, the demand for seasonal renewable storage, for example, in the form of H_2, is growing. These arguments only make sense if the input electricity for SC is produced from renewable sources and does not include grey electricity from coal, oil, or gas.

Nevertheless, hybrid solutions may be necessary to develop the required technologies in the long term before a sufficient VRE capacity is available. Another important aspect is the political risk related to the dependency on oil and gas extracting countries. Historically, severe crises have been caused by a lack of alternatives through national energy provision, such as the oil crisis in 1973. SC represents an option to fulfil former fossil-based fuel demand with renewable hydrogen, methane, and liquid electro-fuels. Because the electricity market does not currently provide the incentives to install P2G capacities, a possible solution is an initiation within the regulatory framework of national TSOs and DSOs. With the capital investment largely being refunded to these regulated institutions, they could install electrolyser capacity at a low cost and auction it to power plant operators for excess VRE feed-in. Renewable hydrogen may be stored or support the decarbonisation of the end-consumption sectors (Robinius et al., 2018). Such projects have already been initiated to develop the technology towards maturity, establish economic feasibility, and guarantee the security of supply. One example is the hydrogen valley in the northern Netherlands, where emission-free hydrogen will become cost-competitive throughout the upcoming decade (Foresight Climate and Energy, 2019). The generation scale is the measure to reduce the cost, thereby achieving energy expertise and using the available pipeline infrastructure. The project aims at generating 3–4 GW of wind energy for hydrogen production until 2030, which could be extended to 10 GW up to 2040. 800,000 t of renewable hydrogen could avoid 7 Mt of CO_2 emissions in 2040 (Foresight Climate and Energy, 2019).

2.8. Conclusions

The basic idea to couple different sectors and energy carriers has already been applied previously for the electrification of transport and residential homes and by coupling conventional thermal power plants for efficiency gains. During the past decade, the SC approach emerged to handle the increasing share of VRE power generation, implemented for climate protection. The definitions of SC in the available literature range from exclusively using excess renewable electricity to a cross-energy-carrier integration with excess heat and biomass energy. Our literature review concludes that the concept is rooted in the increasing share of VRE in the overall energy system (see Section 2.3). Therefore, we suggest considering SC as a concept to promote the integration of large-scale renewable electricity by increasing its direct or indirect application through transformation into a suitable energy carrier, such as heat, gas, and liquids. Consequently, we do not consider renewable energy, which does not include electricity as the primary input, such as waste heat or biofuels, as a central aspect of the SC concept but instead associate it with MESs. SC as a sub-system may thus allow for a more specific analysis of technologies for power transformation with slightly less complexity than fully integrated energy systems. SC can be applied on a centralised level with large-scale electricity generation and conversion or closer to the demand location on a decentralised level. In this analysis, all end-consumption sectors are thoroughly categorised in Section 2.7.2. Concerning the sectors considered in SC, the approach common in energy economics (transport, residential, industry, and trade/services) is found suitable for analyses regarding the techno-economic and system perspective because these represent the final demand (see 2.7.1). For specific technological research such as P2G, however, a focus on the energy carriers—such as electricity, heat, and gas—may be helpful.

Apart from already highly developed renewable energy systems, as in the Northern European countries such as Norway, the economic feasibility of P2H and especially of P2G and P2L continues to include uncertainty in many regions of the world. The developments also depend on unpredictable future global demand and supply situations and climate change roadmaps. P2G faces substantial competition from transmission grid expansion and direct electrification with minimal efficiency losses (see Section 2.7.3). There are various trade-offs to consider, and predicting system-wide effects is highly challenging. After all, direct electrification is not possible for all processes, and the transport sector will rely on electro-fuels for larger vehicles.

Furthermore, a certain amount of P2G will be required to enable the efficient management of renewable energy systems. Currently, P2G projects are initiated within the regulative environment of TSOs and DSOs, which are interested in the long-term security of supply in renewable energy systems and receive refunds for the capital investment cost. The SC concept can only fulfil its role in the energy transition with sufficient renewable energy capacity installed. Additionally, the market and price coupling of commodities such as electricity, heat, methane, hydrogen, and others is essential for the development of SC from a technological and economic perspective. Such an adjusted market structure enables more choices between fuels and a more flexible substitution of energy carriers. This will guarantee higher price stability and lower price risks owing to greater interdependencies.

SC and its enabling technologies still face challenges in the long-term future; however, the path toward renewable energy systems is inevitable, and the climate goals need to be met. The use of large-scale renewable electricity in many applications will be required and can partly be realised with SC. Nevertheless, the research gap in system-wide effects of SC and the competition between different technologies and solutions needs to be closed soon.

3. Estimating the simultaneity of variable renewable supply and heating and cooling demand patterns in Europe

Variable renewable energy from wind and solar power represents an essential alternative to fossil fuels in the energy transition. The patterns of and interrelation between these weather-dependent variables must be understood to match supply with demand successfully. Given the relationships between meteorological phenomena such as wind and solar irradiance and temperatures, a specific correlation with temperature-dependent heating and cooling needs can be expected. This work analyses the storage required to cover the time discrepancy between hourly temperature and VRE profiles and is based on a published article by Ramsebner et al. (2021).

3.1. State of the art

Engeland et al. (2017) emphasise that renewable electricity supply and demand largely depend on the variability of climate aspects such as temperature, wind speed, solar irradiance and others. The world's northern regions are known for successfully using wind energy, and the rougher northern climates cause substantial heating demand. Southern countries, by contrast, build on the vast availability of solar irradiance, which is expected to correlate often with significant cooling needs during the day (Bremen, 2010). A broad set of literature studies the patterns and behaviour of these weather variables and renewable energy sources. While Emeis (2018) provides meteorological insight into wind speed characteristics, solar irradiance is known to have a strong daily pattern related to sunrise and sunset (Iqbal, 2012). Influencing factors on the level of solar irradiance include cloudiness or other characteristics of the atmosphere, such as air pollution. Its short-term variability has been investigated globally (Vindel & Polo, 2014) and in different geographical regions, among others, for Chile (Castillejo-Cuberos & Escobar, 2020) and northern Europe (Tomson & Tamm, 2006). According to Kiviluoma et al. (2016), wind speed depends on turbulent eddies in the short term and pressure changes with weather patterns in the long term. Dai & Deser (1999) find a strong diurnal (daily) wind speed cycle over land areas which peaks at dawn, while nearby oceanic regions peak in the early evenings (Cabello & Orza, 2010). Wooten (2011) observes that wind speed and pressure both rely on temperature differences. The complementarity between wind speed and solar irradiance has been proven on a global scale (Widén et al., 2015), for Sweden (Widén, 2011), Britain (Bett & Thornton, 2016) and the Iberian Peninsula (Jerez et al., 2013), to define an optimal mix for energy generation.

However, the relationship between solar irradiance or wind speed and climate or temperature seems complex, specifically in the case of wind speed. A study on circulation types and British weather revealed that the direction of airflows determines the temperature consequences (Lamb, 1950; O'Hare & Sweeney, 1993). In the British Isles, winds from the west or south lead to mild winters, whereas airflows from the east and north result in cold periods. In summer, air from the south and east creates warm and from the west and north cold temperatures. Despite the apparent interaction between solar irradiance and temperature, there is a lack of research in energy economics.

The literature frequently studied the historical interaction between temperature and European electricity consumption. Most investigations have a geographical focus since weather data differs across the globe. Pardo et al. (2002) developed a model to forecast daily electricity demand from heating- and cooling degree days (HDD and CDD). Further research confirms the impact of weather patterns—specifically temperature—and seasonality on demand (Bessec & Fouquau, 2008) for the UK (Hekkenberg et al., 2009), the US (Le Comte & Warren, 1981; Sailor & Muñoz, 1997), Hong Kong (Lam, 1998; Lam et al., 2008), Saudi Arabia (Al-Zayer & Al-Ibrahim, 1996), Bangkok (Wangpattarapong et al., 2008) and Serbia (Jovanović et al., 2015). Other investigations detect a significant impact of mean daily air temperatures on the energy demand in office buildings (Eto, 1988) or households (Hart & de Dear, 2004; Quayle & Diaz, 1980). These conclusions could optimise energy system planning and avoid electricity system breakdowns.

The aspect of covering electricity demand, which also covers heating and cooling needs, with renewable energy has mainly been studied considering wind speed. Bell et al. (2015) investigate the correlation between wind speed and electricity load for Australia without storage and find that both increase during the morning and evening hours, which is confirmed by further research (Coughlin et al., 2014; Coughlin & Eto, 2010; Sinden, 2007). After analysing wind power variability in the Nordic countries (Holttinen, 2005), Holttinen et al. (2013) studied the impact of wind power variability on the electricity load along different integration levels using historic data from 2009-2011. While Leahy & Foley (2012) focus on cold periods in Ireland, which often coincide with low winds and a lack of potential wind energy supply, wind speed and overall electricity demand in New Zealand correlate on a monthly time scale (Suomalainen et al., 2015). Ueckerdt et al. (2015) focus on the impact of wind and solar variability on the residual load and conclude that high shares of PV power over-production are a challenge, while the effects of increasing wind energy shares are less severe.

However, techno-economic research on the correlation between renewable energy sources and their known impact on temperatures in the context of heating and cooling needs is scarce. Coker et al. (2013) analyse the variability of wind, solar and tidal resources while, however, the analysis of their relationship with demand lacks implications on future energy system requirements. In this respect, the authors' main conclusion is that solar irradiance shows the most direct correlation with electricity demand, diminished by its unavailability overnight and an even more significant monthly variability than wind speed.

Recently, climate change effects are increasingly being investigated, specifically on the supply side for solar irradiance and wind speed (Pašičko et al., 2012; Schaeffer et al., 2012; Tobin et al., 2015, 2018; Wild et al., 2009). While in China, a decreasing trend in sunshine hours between 1960-2009 can be explained by the air pollution index (Y. Wang et al., 2012), the same trend on the Canadian Prairie is caused by a climate-change-related increase in cloudiness (Cutforth & Judiesch, 2007). Western Europe is characterised by an increase in solar irradiance in winter, and the Iberian Peninsula experiences negative trends in summer and positive trends in March (Sanchez-Lorenzo et al., 2007, 2008). However, a proven phenomenon is a global decadal variability of stronger and weaker solar irradiance, referred to as dimming and brightening (Cutforth & Judiesch, 2007; Stanhill & Cohen, 2001; Wild, 2009; Wild et al., 2005). Furthermore, it is important to note that higher temperatures may also affect solar panel efficiency (Wilbanks et al., 2008; Wild et al., 2015). Several pieces of literature found a decreasing trend in wind speed (Breslow & Sailor, 2002; Santos et al., 2015), accounting for -0.014 m/s globally (Watson, 2014), apart from coastal sites, which experience increases. However, Tobin et al. (2015) observe an increase in wind power potential for most of Europe, apart from Mediterranean areas and northern Europe. Wind power potential in Northern Europe could benefit from decreased icing frequency and sea ice (Pryor & Barthelmie, 2010).

Several studies also consider the impact of climate change on the demand side. Totschnig et al. (2017) find that cooling demand peaks strongly impact residual load and suggest ambitious initiatives in building insulation and passive cooling solutions. This relationship has also been evaluated in Europe (Larsen et al., 2020; Silva et al., 2020), the US (Sailor, 2001), Australia (Ahmed et al., 2012), Brazil (Trotter et al., 2016) and China (Fan et al., 2019). Most detected increased cooling and decreased heating demand caused by climate warming, whereas the effects seem to be more significant in southern compared to northern Europe. Dowling (2013) and Girardi et al. (2020) provide work including the impact on both the demand and the supply side. Nevertheless, many aspects of the relationship between natural resources and heating and cooling needs remain untouched and require more detailed investigation.

While existing work mainly analyses the relationships between VRE and temperatures, HDD/CDD and electricity demand or wind speed and electricity demand, a literature gap has been identified in the correlation between wind speed and solar irradiance and temperature-related energy demand (HDD and CDD). There is a lack of such investigation historically and considering climate change effects. It is, however, necessary in smart energy systems to understand the characteristics of natural resources and their relationship with temperature and consequent heating and cooling demand, to estimate timing discrepancies and balancing requirements.

3.2. Core Objectives

This paper by Ramsebner et al. (2021) aims to prove the hypothesis of a positive correlation between the patterns of solar irradiance and cooling degree hours (CDH) and wind speed and heating degree hours (HDH). It estimates the timing discrepancy between wind speed or solar irradiance and a consequent temperature change, which causes storage requirements. Nevertheless, the relationship between solar irradiance, which is available with a repetitive daily pattern throughout the year, and HDH could be interesting and will be analysed.

This work aims at providing policy recommendations for smart energy systems. It analyses the correlation between the supply sources, wind speed and solar irradiance—in their purity without limiting the energy supply to a specific technology or related constraints in the electricity system—and HDH and CDH to estimate the storage needs to match supply with demand successfully. Our analysis is conducted for different climate regions in Europe (Austria, Spain and northern Europe), historically in different time-resolution, and into the future. Since this work is based on weather variables, implications for actual energy demand rely on additional parameters: energy efficiency measures on building insulation, comfort in more extended periods of heat and cold, and the progressive integration of the energy system.

3.3. Methodology

The first part of this study analyses the historical characteristics of and correlation between primitive weather variables (wind speed and global horizontal irradiance) and hourly dependent weather variables derived from the temperature (HDH and CDH). The study is carried out for three different European climate regions Austria, Spain and northern Europe. The correlation coefficient is analysed between the weather variables per location in each climate region, referred to as "self-correlation". Additionally, the relationship between locations is investigated to derive a potential value of external natural energy supply via the energy grid. The correlation coefficient is analysed based on two approaches outlined in Section 3.3.4 and considers different time periods and data aggregation to evaluate the storage requirements. The relevant historical weather data is provided on hourly resolution between 2005 and 2016 and consists of the following (*PVGIS - European Commission*, 2020):

- Temperature at 2 m in °C,
- Wind speed at 10 m in m/s
- Global horizontal irradiance in W/m²

Finally, we investigate the impact of climate change on weather variables and correlation based on daily CMIP5 weather data projected between 2020 and 2100 (see Section 3.3.5).

3.3.1. Selection of case study locations

The case study areas have been defined as Spain, Austria and northern Europe (Sweden and Norway) to cover different European climate regions. For each of these regions, six locations were selected with the main objective to cover a broad range of solar irradiance and wind speed levels in each country, evaluated by the historic mean solar irradiance and wind speed between 2008 and 2017 provided by the global solar and wind atlas (*Global Solar Atlas*, 2020; *Global Wind Atlas*, 2020). An additional requirement was to cover inland and coastal regions and focus on cities with larger populations. The selections are not based on covering potential power supply or specific densely populated demand locations.

1. Spain

Three selected Spanish locations are inland, and three represent coastal locations (see Figure 18). Figure 19 lists the chosen sites for Spain coloured in their solar irradiance level, and Figure 20 shows the historic mean wind speed level.

Figure 18 Selected locations in Spain

No	Location	Province
1	A Coruña	Galicia
2	Barcelona	Catalunya
3	Burgos	Castilla y Leon
4	Madrid	Madrid
5	Tomelloso	Castilla la mancha
6	Vitoria-Gasteiz	Pais Vasco

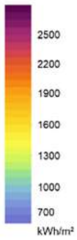

Figure 19 Mean historical solar irradiance level of the locations in Spain (Source: (*Global Solar Atlas*, 2020))

No	Location	Province
1	A Coruña	Galicia
2	Barcelona	Catalunya
3	Burgos	Castilla y Leon
4	Madrid	Madrid
5	Tomelloso	Castilla la mancha
6	Vitoria-Gasteiz	Pais Vasco

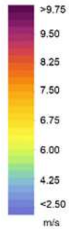

Figure 20 Mean historical wind speed level of the locations in Spain (Source: (*Global Wind Atlas*, 2020))

A Coruña, located at the coast northwest of the country, shows relatively low solar irradiance and high average wind speed. Tomelloso has the highest solar irradiance, followed by Madrid in central Spain. They both experience low to very-low wind speed levels, respectively. Burgos and Barcelona are characterised by medium to high solar irradiance, with very high and shallow wind speeds, respectively.

2. Austria

The six locations selected in Austria are distributed across all directions of the country (see Figure 21). The selection aims to avoid locations at high elevations that would not be relevant for the CDH analysis—herein manipulating the average result for Austria—and provide little potential for using local wind power. Figure 22 lists the Austrian locations coloured in their solar irradiance level, and Figure 23 shows their wind speed level.

Figure 21 Selected locations in Austria

Due to its central location, Austria does not specifically feature high solar irradiance levels apart from Klagenfurt in the south and Nickelsdorf in the southwest. The wind map looks more diverse, where these two locations show shallow and high wind speed, respectively.

Bregenz, located far west of the country, is also characterised by low wind speed, compared to Vienna and Gmünd in the east, which show higher values.

No	Location	Province
1	Bregenz	Vorarlberg
2	Gmünd	Lower Austria
3	Klagenfurt	Carinthia
4	Nickelsdorf	Burgenland
5	Ried i. Innkreis	Upper Austria
6	Vienna	Vienna

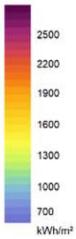

Figure 22 Mean historical solar irradiance level of the locations in Austria (Source: (*Global Solar Atlas*, 2020))

No	Location	Province
1	Bregenz	Vorarlberg
2	Gmünd	Lower Austria
3	Klagenfurt	Carinthia
4	Nickelsdorf	Burgenland
5	Ried i. Innkreis	Upper Austria
6	Vienna	Vienna

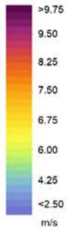

Figure 23 Mean historical wind speed level of the locations in Austria (Source: (*Global Wind Atlas*, 2020))

3. Northern Europe

Since cooling demand is hardly relevant in northern Europe, as becomes clear from the descriptions in Section 3.3.3, only the relationship between wind speed and solar irradiance with HDH was considered. The six selected locations are situated in Norway and Sweden (see Figure 24). Figure 25 lists the locations coloured in their solar irradiance level, and Figure 26 indicates the wind speed level. The wind speed level in Bodø is the highest, followed by Gothenburg and Stockholm. Wind speed levels in Kiruna, Trondheim and Oslo are rather low.

Figure 24 Selected locations in northern Europe

No	Location	Country
1	Bodo	Norway
2	Oslo	Norway
3	Trondheim	Norway
4	Gothenburg	Sweden
5	Kiruna	Sweden
6	Stockholm	Sweden

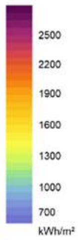

Figure 25 Mean historical solar irradiance level of the locations in northern Europe (Source: (*Global Solar Atlas*, 2020))

No	Location	Country
1	Bodo	Norway
2	Oslo	Norway
3	Trondheim	Norway
4	Gothenburg	Sweden
5	Kiruna	Sweden
6	Stockholm	Sweden

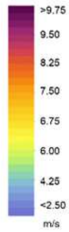

Figure 26 Mean historical wind speed level of the locations in northern Europe (Source: (*Global Wind Atlas*, 2020))

3.3.2. Heating and cooling degree hours

This work uses temperature-based estimations of heating and cooling needs and does not consider energy technologies, carriers or cross-sectoral interdependencies. In our historical analysis, heating and cooling needs are derived from outdoor temperatures on an hourly basis, referred to as HDH and CDH. The projected future data to analyse climate change is provided at a daily resolution, from which HDD and CDD can be derived. HDH and CDH describe the extent of heating and cooling needs in Kelvin hours (Kh), which occur below or above a certain temperature threshold or reference temperature. They measure the difference between the outside reference temperature and the desired room temperature.

The reference temperatures for heating and cooling are defined according to a general climatological approach as described in Eq. (1) and Eq. (2). Heating is expected to be desired at or below 15°C outside temperature (reference temperature T^h) and the desired room temperature $T^{\mathrm{h}}_{\mathrm{room}}$ is defined as 18°C (eurostat, 2020).

$$T^h = 15°C$$

$$T^{\mathrm{h}}_{\mathrm{room}} = 18°C$$

$$T_i \leq T^h : HDH = (T^h_{room} - T_i) \qquad (1)$$

$$T_i > T^h : HDH = 0 \qquad (2)$$

If, for example, the air temperature at time step i (T_i) is 12°C, the HDH index accounts for 6 Kh (18°C-12°C). If the air temperature is 17°C and lies above the heating threshold of 15°C, the HDH index is 0 Kh. HDH, therefore, rise with decreasing temperatures.

The reference temperature for cooling is set to 24°C outside temperature (T^c) and the desired room temperature T^c_{room} to 21°C (eurostat, 2020). Cooling degree hours occur if the air temperature is above 24°C (see Eq. (3) and Eq. (4))

$T^c = 24°C$

$T^c_{room} = 21°C$

$$T_i \geq T^c : CDH = (T_i - T^h_{room}) \quad (3)$$

$$T_i < T^c : CDH = 0 \quad (4)$$

If, for example, the current air temperature (T_i) is 28°C, the CDH index amounts to 7 Kh (28°C-21°C). If the air temperature is 21°C and lies below the cooling threshold of 24°C, in that hour the CDH index is 0 Kh. CDH, therefore, rise with rising temperatures.

3.3.3. Weather variable characteristics per climate region

Figure 27 and Figure 28 present the historical monthly average wind speed and solar irradiance for Spain (ESP), Austria (AUT) and northern Europe (NEU) across all locations and years between 2008 and 2017 based on the data described at the beginning of this section. While the monthly wind speed in northern Europe peaks in December and January and decreases continuously towards July, Austria and Spain both experience a minor decline in wind speed in winter between December and February. Solar irradiance shows the same pattern in all three regions, with Spain experiencing the highest level followed by Austria and finally northern Europe. Remarkably, Austria and northern Europe achieved the same average solar irradiance in June despite the spatial difference.

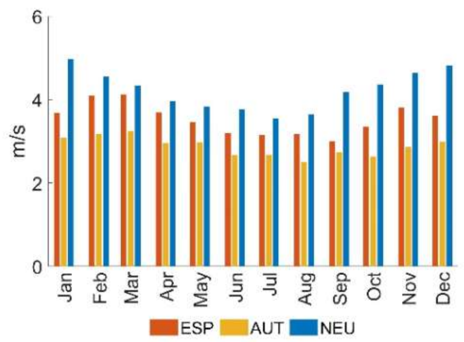

Figure 27 Monthly average wind speed for each region

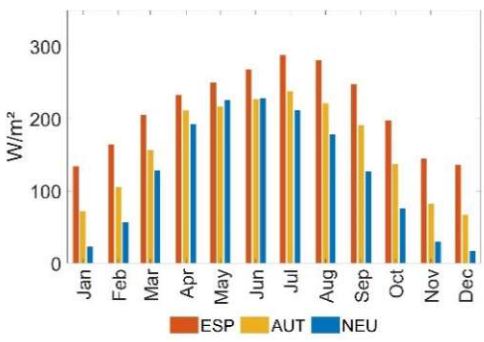

Figure 28 Monthly average solar irradiance per area

The average CDD and HDD for one location per region are presented in Figure 29. Madrid in the most southern region analysed in this study, shows a comparatively high number of CDD between May and September, with a peak in July and August at around 5.8Kd. Since the country still tends to have cold winters, heating demand and the amount of HDD are significant from October to May, with a peak between December and February. Located in central Europe, Vienna in Austria shows a small amount of CDD between May and September, with a peak in July of 3.1Kd. The colder winters lead to frequent and high heating needs. The HDD are significant from September to May, peaking from December to February with almost 19.9Kd.

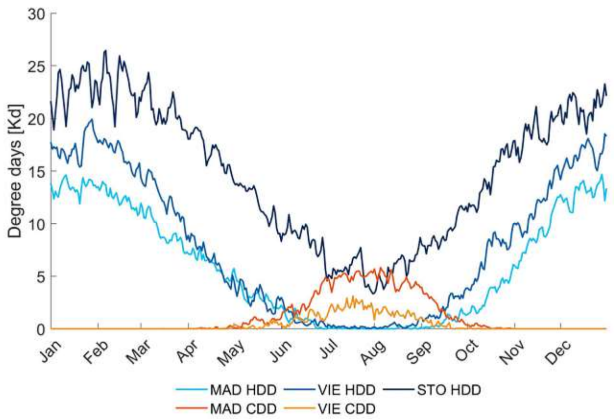

Figure 29 Historical average HDD and CDD for Madrid, Vienna and Stockholm

Table 2 additionally provides an overview of the historical average, maximum and minimum yearly amount of heating and cooling degree hours. The northern European countries only experience an insignificant amount of CDD between June and August. This leads us to the conclusion that an analysis of its correlation with solar irradiance can be neglected. The cold climate, however, results in substantial HDD. HDD occur all the year through, reaching a maximum between December and February at 26.5Kd (see Figure 29).

Table 2 Annual heating and cooling degree hours per region

	CDH/a			HDH/a		
	Average	**Max**	**Min**	**Average**	**Max**	**Min**
SPAIN	10.272	21.225	661	63.132	74.05	50.31
AUSTRIA	5.691	7.699	2.905	70.241	79.121	65.296
NORTHERN EUROPE	182	620	3	91.309	99.433	84.324

3.3.4. Correlation coefficient: research approaches and interpretation

This study analyses the correlation coefficient between solar irradiance and CDH, wind speed and HDH and solar irradiance and HDH, concluding with positive or negative correlation and flexibility needs. The correlation coefficient (ρ) is calculated between the primitive variables (wind speed and solar irradiance) (V_p) and the derived weather variables (V_d) CDH and HDH for the six locations across the available weather data for twelve years. Finally, an average correlation is built per location across the twelve years. The correlation results are evaluated after Pearson (Evans, 1996), as illustrated in Table 3.

Table 3 Assessment of the correlation coefficient "ρ" after Pearson (Evans, 1996)

ρ	INTERPRETATION
< 0.19	Very weak
0. 20-0.39	Weak
0. 40-0.59	Moderate
0. 60-0.79	Strong
0. 80-1.00	Very strong

This paper differentiates between the relevant seasons concerning heating and cooling demand to achieve a most comprehensive view of the correlations. The seasons are defined based on a standard for the northern hemisphere, as described in Table 4.

Table 4 Meteorological seasons

PERIOD	SEASON
Mar 1st – May 31st	Spring
Jun 1st – Aug 31st	Summer
Sep 1st – Nov 31st	Autumn
Dec 1st – Feb 29th	Winter

Usually, the impact of the primitive variable—solar irradiance or wind speed—on the temperature and consequently the derived variable—CDH and HDH—takes some time. The presented main analysis already accounts for the time discrepancy between the primitive and derived variable and assumes storage to that extent. There is, for example, a time lag between the increase of solar irradiance and its impact on temperature—and consequently, CDH. However, a similar phenomenon can be observed between solar irradiance or wind speed and

HDH, if to a different extent. The variable x describes the number of hours that the derived variable (*Vd*), for example, CDH, lags behind the primitive variable (*Vp*) solar irradiance at any point in time (*t*) (see Figure 30). In other words, *Vp* needs to be moved backwards by x hours from t to match *Vd*. The best estimate of the time lag is determined by defining x in a way to maximise the overall correlation coefficient (ρ), representing the best possible overlay of the primitive and derived weather variables. Our analysis focuses on a time lag of up to 24 hours. The time lag in each relationship between a renewable source and HDD or CDD is calculated as an average that remains constant over time. The fact that the time discrepancy may differ throughout the seasons is neglected.

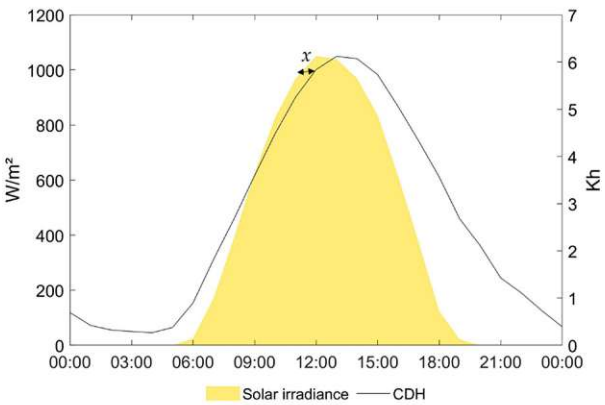

Figure 30 Exemplary day describing the time lag (x) between solar irradiance and cooling degree hours

Our work applies two approaches, focusing on hourly data adjusted by the time lag between the supply source and the temperature change. While approach 1 determines the hourly correlation for different time periods, approach 2 investigates the correlation assuming daily, weekly, and monthly storage by aggregating the data. The two approaches provide valuable insights concerning the hourly fit of the supply and demand pattern and show how the aggregated amounts of supply coincide with demand.

Approach 1 (A1) determines the hourly correlation adjusted by the lag for hourly, daily and weekly time periods in a season (see Eq. (5)). For example, if the hourly correlation is calculated per day for the summer season (n=2208 hours), 90 correlation results are received (2208/24). Next, the average for the season across this time interval, e.g. the number of days or weeks (i), is created. If most daily correlations are weak, according to Pearson described in Table 3 (< 0.4), this average result will be weak too. If the daily correlations are moderate (0. 40-0.59) or vary significantly, the average result for the daily time period will be moderate. A strong average correlation (>0.6) for the daily time periods implies continuously high daily correlation results. This approach describes the hourly fit of the supply and demand pattern and analyses if storage is required to achieve a better match. A negative correlation would imply, for example, high solar irradiance at times of low cooling needs. The potential solar energy would therefore need higher storage amounts to match demand.

$$\rho_{Vp,\,Vd} = \frac{1}{i}\ \sum_{t=1}^{n} \frac{cov(Vp_{t+x}\ Vd_t)}{\sigma_{Vp_{t+x}}\ \sigma_{Vd_t}} \tag{5}$$

σ .... *standard deviation*
Vd .... *derived variable (CDH, HDH) [Kh]*
Vp .... *primitive variable (wind speed [m/s], solar irradiance [W/m²])*

Approach 2 (A2) investigates the value of storage based on daily or weekly aggregated weather data (Vp_{A2}, Vd_{A2}) in a specific season or the monthly aggregated data across the whole year, as described in (Eq. (6) and (7)). The total amount of the primitive and derived variables are compared—for the number of hours of a day, week or month (h) in the respective season—to see if higher heating or cooling demands coincide with higher natural resource availability (see Eq. (8)). If the correlation is strong (>0.6), storage for the considered time period is of value.

$$Vp_{A2} = \sum_{h=1}^{n} Vp_{t+x} \tag{6}$$

$$Vd_{A2} = \sum_{h=1}^{n} Vd_t \tag{7}$$

$$\rho_{Vp_{A2},\,Vd_{A2}} = \frac{1}{i}\ \sum_{h=1}^{n} \frac{cov(Vp_{A2}\ Vd_{A2})}{\sigma_{Vp_{A2}}\ \sigma_{Vd_{A2}}} \tag{8}$$

Vd_{A2} .... *aggregated derived variable (CDH, HDH) [Kh]*
Vp_{A2} .... *aggregated primitive variable (wind speed [m/s], solar irradiance [W/m²])*

Another important investigation is the seasonality of the correlation coefficient, which is calculated hourly for monthly time periods based on approach 1. This analysis enables conclusions on the relationship between the hourly weather variables and heating and cooling demand each month.

3.3.5. Climate change effect: data and evaluation

The assessment of climate change effects on the weather variables and the consequences for future correlation coefficients is based on projected CMIP5 weather data between 2020 and 2100 (EC, 2021a). The model EC-EARTH provides future projections considering the representative concentration pathways (RCP) assuming different radiative forcing levels between 2.6 and 8.5 (Moss et al., 2010). Our research is based on a middle path applying the RCP4.5 of the CMIP5 data. This is provided in daily resolution within certain latitude and longitude boundaries for one location per climate region: Madrid, Vienna and Stockholm.

A 5-year trend towards 2100 is compared with the situation in 2020 to evaluate the development of weather variables. The relative per cent development is presented for temperatures, solar irradiance, wind speed, and CDD and HDD in Section 3.4.2. In the next step, the absolute correlation coefficients are calculated for the future based on this daily data and analysed concerning the changes observed in the weather variables.

3.4. Results

This section provides a detailed analysis of the correlation coefficients in the locations per climate region according to the approaches described in the methodology. Finally, the climate change effect on the weather variables and the impact on the correlation coefficients is described.

3.4.1. Correlation results

The analysis for Spain and Austria starts with the relationship between solar irradiance and CDH—which is not relevant for northern Europe—followed by wind speed and HDH and solar irradiance and HDH. A detailed graph shows the results for both approaches (see Section 3.3.4) with the locations numbered 1-6 according to the assignment in Section 3.3.1. Additionally, the interrelation between the different locations is evaluated to consider spatial exchange and investigate the value of the energy networks.

In all three regions, the time lag between solar irradiance and CDH accounts for 2 hours, which describes the time solar irradiance takes to change the temperature. The lag between wind speed and HDH amounts to 14 hours and between solar irradiance and HDH to 16 hours, which leads to an overly of the noon peak of solar irradiance with the early morning HDH peaks.

3.4.1.1. Correlation between CDH and solar irradiance

1. Spain

CDH in Spain, as was shown in an example for Madrid in Section 3.3.3, mainly occur from July to September, while solar irradiance peaks from June to August (see Section 3.3.3). With the adjustment of the weather data by the time lag of 2 hours, as discussed in Section 3.3.4, the correlation coefficient can be increased in all seasons relevant for CDH—summer, spring and autumn—by 15-52 %.

Analysing the hourly correlation for different periods according to A1, in A Coruña (1), Burgos (3) and Vitoria Gasteiz (6), the results in the summer season increase with the considered period from day to season (see Figure 31). Daily and weekly patterns of hourly data match less than the hourly pattern of the whole summer season. The other locations Barcelona (2), Madrid (4) and Tomelloso (5) show decreasing results with increasing periods and a better daily than weekly or seasonal hourly fit. In Madrid and Tomelloso, the daily correlation is very strong, with an average coefficient in summer above 0.80, followed by Barcelona with a strong correlation of 0.63. Calculating the solar irradiance and CDH correlation with daily and weekly storage for the summer season and monthly storage across the whole year (A2) and comparing it to the hourly correlation for the summer season (A1) also suggests a strong hourly fit.

Regarding daily or weekly storage (A2), weekly total solar irradiance and CDH, all locations apart from A Coruna (1) achieve a moderate correlation above 0.4. In autumn, the hourly fit is very weak for all periods (A1), but weekly aggregated data results in a moderate to very strong correlation. The monthly solar irradiance throughout the year correlates strongly with CDH in most locations, exceeding 0.60 in all locations but A Coruña (1). This leads to the conclusion that for CDH to be covered by solar power in summer, 2-hourly to daily storage is sufficient. At the same time, weekly storage might be required for cooling needs in autumn and spring, which may be relevant in Spain, specifically with rising temperatures in the future.

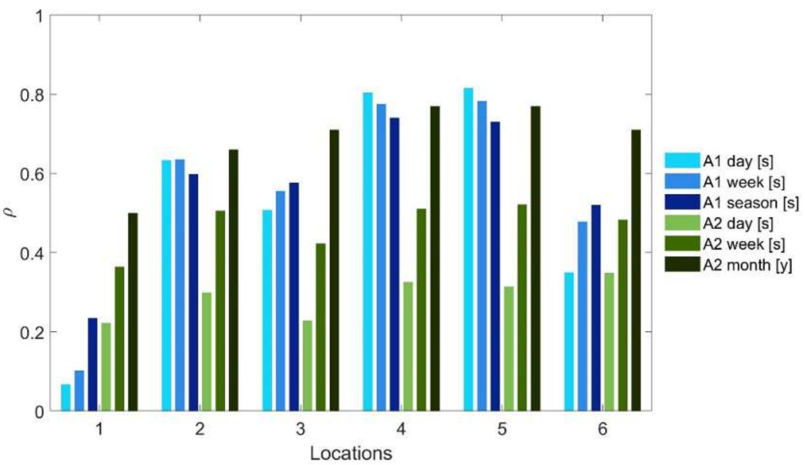

Figure 31 Spain: Solar irradiance and CDH correlation coefficient (ϱ) in summer season [s] applying approach 1 (A1) and approach 2 (A2) for the locations 1-6 as described in Section 3.3.1 (monthly correlation across the whole year [y])

Table 5 describes the CDH and solar irradiance relationships between the locations in summer on an hourly basis adjusted by the lag. The correlation between the locations indicates the potential of the external energy supply to achieve a stronger correlation than the local self-correlation. Burgos would benefit from a connection with the solar energy supply from Vitoria Gasteiz (6) and reach a coefficient of 0.63 compared to its self-correlation of 0.58. However, the value of exchange through the energy grid is low in all cases.

Table 5 Hourly solar irradiance and CDH correlation between locations in Spain (top numbers 1-6 refer to locations as numbered on the left)

No.	Location		CDH 1	2	3	4	5	6
1	A Coruña	Solar irradiance	$\boxed{0.23}$	0.48	0.48	0.69	0.69	0.35
2	Barcelona		0.20	$\boxed{0.60}$	0.58	0.71	0.70	0.47
3	Burgos		0.21	0.57	$\boxed{0.58}$	0.76	0.75	0.45
4	Madrid		0.19	0.57	0.55	$\boxed{0.74}$	0.74	0.43
5	Tomelloso		0.20	0.57	0.55	0.73	$\boxed{0.73}$	0.43
6	Vitoria Gasteiz		0.22	0.56	0.63	0.74	0.73	$\boxed{0.52}$

2. Austria

In Austria, the cooling demand mainly occurs during July and August and is much lower than in Spain due to the lower temperature level. Accounting for the 2-hour time lag between solar irradiance and CDH, an improvement of the correlation results in the summer season of around 30 % can be achieved. In contrast to Spain, for the hourly CDH and solar irradiance correlation for different periods (A1) in the summer season, all selected locations in Austria show a similar pattern increasing with the length of the period from day to season (see Figure 32).

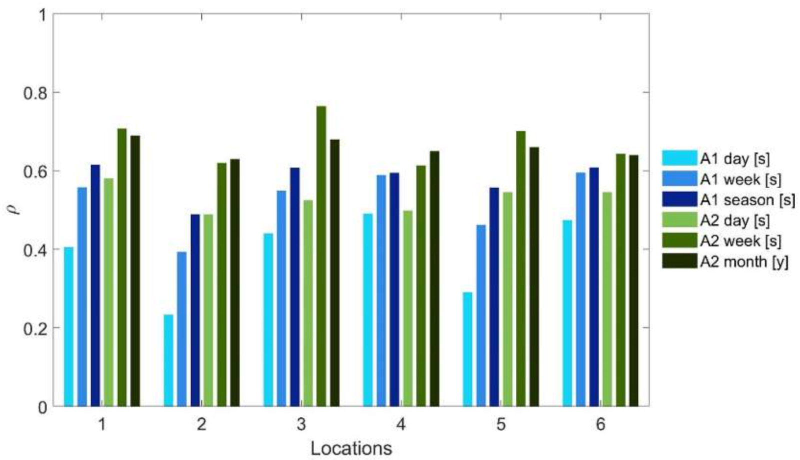

Figure 32 Austria: Solar irradiance and CDH correlation coefficient (ϱ) in summer season [s] applying approach 1 (A1) and approach 2 (A2) for the locations 1-6 as described in Section 3.3.1 (monthly correlation across the whole year [y])

Bregenz (1), Klagenfurt (3), Nickelsdorf (4) and Vienna (6) achieve strong results above 0.60 on a seasonal basis. This means that the hourly solar irradiance pattern during summer matches CDH better than the weekly or daily one. Nickelsdorf (4), with relatively high solar irradiance, reaches the highest result for the daily period at 0.50, closely followed by Vienna (6).

In Austria, weekly storage (A2) achieves a strong correlation between CDH and solar irradiance in summer in all locations, reaching a coefficient of above 0.70 in Klagenfurt (3) in the south of the country, followed by Bregenz (1) in the far west and Ried i. Innkreis (5). Monthly total solar irradiance gain correlates well with CDH across the whole year. Concerning the relationships between locations, the self-correlation in the framed cells in Table 6 is usually higher than allowing for external solar energy supply. Even if there are strong relationships between the CDH in Bregenz (1), Klagenfurt (3), and Vienna (6), with the solar irradiance of other locations, improvements are limited.

Table 6 Hourly solar irradiance and CDH correlation between locations in Austria (top numbers 1-6 refer to locations as numbered on the left)

			CDH					
No	**Location**		**1**	**2**	**3**	**4**	**5**	**6**
1	Bregenz	Solar irradiance	0.62	0.38	0.50	0.46	0.48	0.49
2	Gmünd		0.58	0.49	0.59	0.58	0.55	0.62
3	Klagenfurt		0.57	0.44	0.61	0.58	0.51	0.59
4	Nickelsdorf		0.53	0.45	0.59	0.59	0.49	0.60
5	Ried i. Innkreis		0.61	0.47	0.58	0.55	0.56	0.59
6	Vienna		0.55	0.46	0.58	0.59	0.52	0.61

3. Region Comparison

Figure 33 describes the solar irradiance and CDH correlation results in summer as an average across all locations. The average hourly solar irradiance and CDH correlation in Spain (ESP) does not improve significantly by considering longer periods (A1) than a day. However, for some locations, it would, as described earlier in this section. In Austria (AUT), by contrast, an increase was visible for all locations implying that daily patterns match less than the weekly and seasonal ones.

While in Spain, the hourly correlation is already moderate to strong on all time scales (A1), in Austria, weekly storage (A2) achieves the strongest correlation with 0.68. This suggests a stronger hourly relationship in the south than in central Europe. Regarding autumn and spring with lower cooling needs and lower solar irradiance levels, both countries' results improve towards weekly aggregation or storage, implying high storage needs for daily balancing.

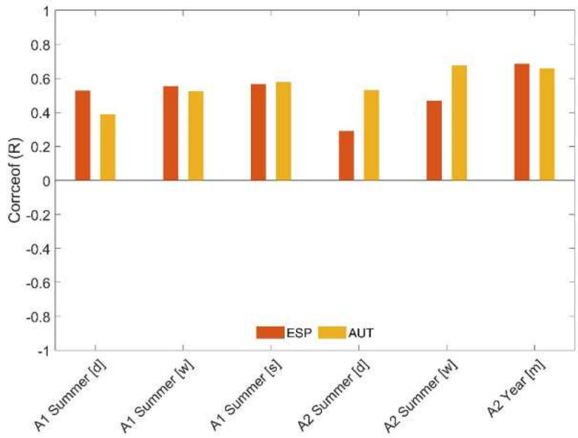

Figure 33 Hourly solar irradiance and CDH correlation coefficient (ϱ) per climate region for different time-periods (day [d], week [w], season [s], month [m]) applying approach 1 (A1) and approach 2 (A2)

Figure 34 describes the seasonality of the correlation based on the hourly correlation for monthly periods. CDH and solar irradiance patterns match best during the main cooling season from June to August, which is convenient. With increasing solar irradiance and cooling needs towards summer, the average hourly correlation also rises to a strong level in July at 0.62 in Spain and 0.64 in Austria.

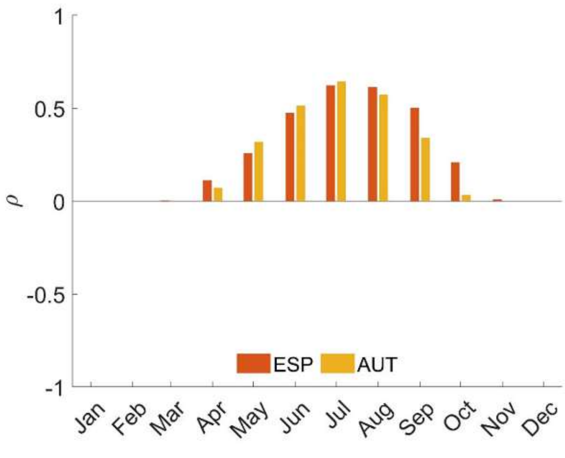

Figure 34 Seasonality: Hourly solar irradiance and CDH coefficient (ϱ) per month (A1)

3.4.1.2. Correlation between HDH and wind speed

1. Spain

In Madrid, HDH peak between December and February, while wind speed is high in November and reaches its highest average level in February and March, after a minor interruption in December and January (see Section 3.3.3). The hourly correlation between wind speed and HDH (A1) in the winter season shows a similar pattern in all locations with a weak (around 0.2) positive result on a daily basis, decreasing further towards longer time periods (see Figure 35). Increasing wind speed does not necessarily cause lower temperatures and heating needs immediately. It can even be observed that winds often bring about warmer temperatures, as explained in our literature review in Section 3.1.

Data aggregation assuming daily and weekly storage (A2) results in a negative correlation in almost all locations (around -0.2), implying that the amount of wind speed does not match the heating needs. In spring and autumn, seasons in which HDH still occur even in this southern European region (see 3.3.3), daily and weekly storage achieve moderate results below 0.52 in Burgos (3) and Vitoria Gasteiz (6) with very high wind speed levels and also Barcelona (2). Wind speed and HDH only reach solid, moderate relationships with monthly storage across the year (0.56 in Vitoria Gasteiz (6), followed by Barcelona (2) and Burgos (3) with 0.51). The correlation between locations also shows no substantial improvement. The results remain weak, and the benefit of the energy network is, in this case, limited.

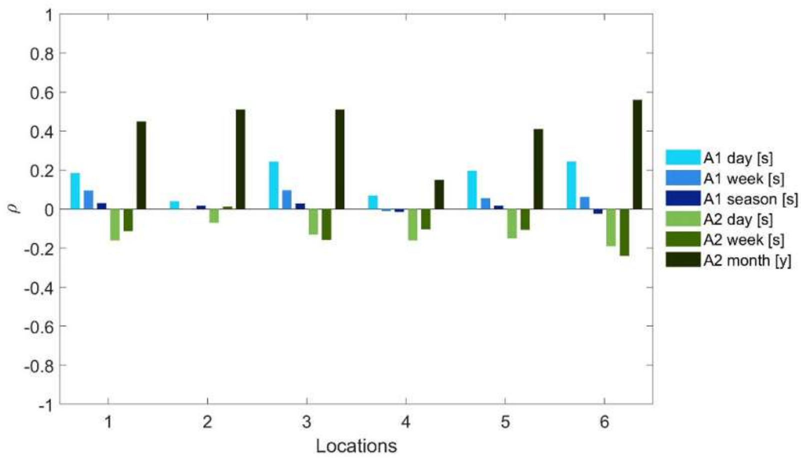

Figure 35 Spain: Wind speed and HDH correlation coefficient (ϱ) in winter season [s] applying approach 1 (A1) and approach 2 (A2) for the locations 1-6 as described in Section 3.3.1 (monthly correlation across the whole year [y])

2. Austria

The correlation between wind speed and HDH on an hourly basis in Austria is similar to that of Spain. Again, wind speed and HDH during winter do not correlate significantly at daily time periods and are even negative on a weekly and seasonal basis. An extension of the time period in almost all locations leads to an even lower correlation. The best fit of lag-adjusted hourly wind speed and HDH according to A1 in winter occurs on a daily basis (see Figure 36). In spring and autumn, all the same, the correlation is weak. Daily and weekly storage (A2) does not achieve a positive fit between supply and demand. Only monthly data aggregation throughout the year achieves moderate results in Gmünd (2) and Ried i. Innkreis (5).

Spatial integration hardly improves the results. Only the HDH in Bregenz (1) correlate slightly better with the potential wind power supply from Klagenfurt (3) and HDH of Ried i. Innkreis (5) with the wind supply in Klagenfurt (3), Nickelsdorf (4) and Vienna (6). Still, spatial integration has little benefit.

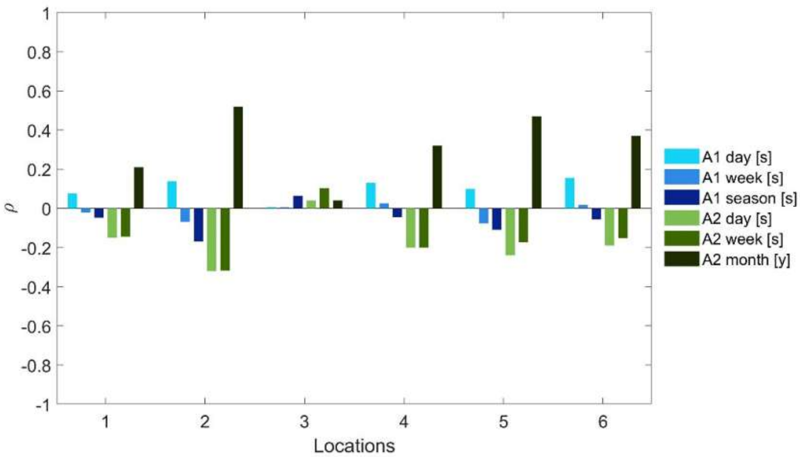

Figure 36 Austria: Wind speed and HDH correlation coefficient (ϱ) in winter season [s] applying approach 1 (A1) and approach 2 (A2) for the locations 1-6 as described in Section 3.3.1 (monthly correlation across the whole year [y])

3. NEU

The HDH and wind speed correlation without accounting for the 16-hour time lag in northern Europe is even more negative than in Spain and Austria. Also, after an adjustment for the lag, northern Europe shows the least significant results on a daily basis (see Figure 37). The negative weekly and seasonal relationships of hourly data (A1) are stronger than in central and southern Europe. Since in the winter season, no positive relationship between HDH and wind speed can be achieved irrespectively of the regarded time-period, storage will also be required in this region to match supply and demand.

Assuming daily and weekly storage of potential power from wind speed (A2) does not achieve a positive correlation with heating needs in winter. This means that the wind speed in the respective time-period does not match the heating needs. Only the monthly amounts of wind speed throughout the year correlate with heating needs. In the north, the summer season is also a relevant heating period with cold temperatures. Here weekly storage leads to a moderate correlation in two Swedish locations, Kiruna (5) and Stockholm (6).

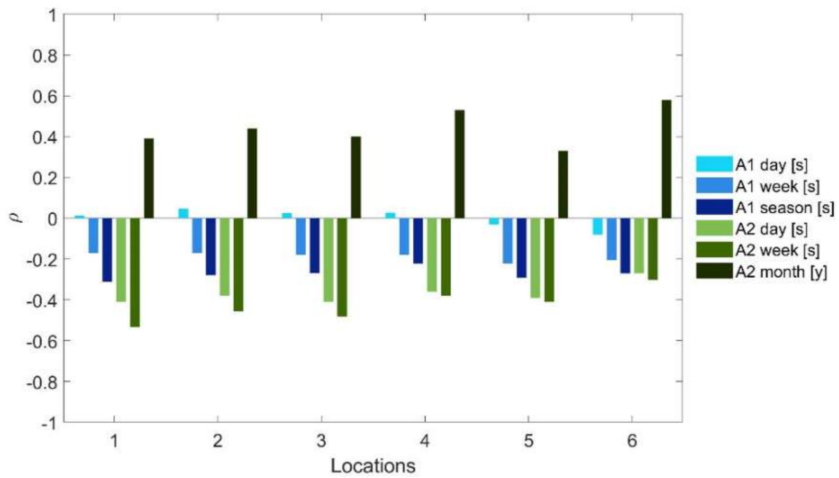

Figure 37 Northern Europe: Wind speed and HDH correlation coefficient (ϱ) in winter season [s] applying approach 1 (A1) and approach 2 (A2) for the locations 1-6 as described in Section 3.3.1 (monthly correlation across the whole year [y])

Summer represents the season with the most vivid results on an hourly basis concerning the correlation between the locations (see Table 7).

Table 7 Hourly wind speed and HDH correlation between locations in northern Europe (top numbers 1-6 refer to locations as numbered on the left)

			HDH					
No	**Location**		**1**	**2**	**3**	**4**	**5**	**6**
1	Bodø	Wind speed	0.27	0.22	0.35	0.14	0.27	0.08
2	Oslo		0.32	0.28	0.34	0.23	0.27	0.10
3	Trondheim		0.18	0.14	0.26	0.08	0.21	0.08
4	Gothenburg		0.24	0.18	0.26	0.17	0.26	0.12
5	Kiruna		0.22	0.21	0.20	0.18	0.37	0.30
6	Stockholm		0.11	0.09	0.08	0.10	0.25	0.33

The most significant improvement from the local self-correlation with the external supply of wind speed can be reached within Norway between Bodø (1) and Trondheim (3). An interaction, therefore, could be valuable. A potential exchange via the energy grid does not have a significant benefit for all other locations.

4. Region Comparison

Figure 38 shows that the correlation between HDH and wind speed is insignificant to negative in winter irrespectively of the chosen approach or time period in all three climate regions throughout the year. Only monthly storage leads to a moderate positive correlation. Weekly amounts of HDH and wind speed in northern Europe almost reach a strong negative relationship (A2). These results show the need for monthly to seasonal storage to match power from wind speed with heating needs.

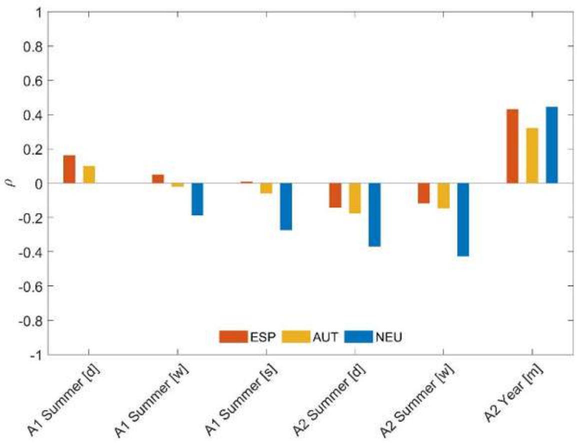

Figure 38 Hourly wind speed and HDH correlation coefficient (ρ) per climate region for different time-periods (day [d], week [w], season [s], month [m]) applying approach 1 (A1) and approach 2 (A2)

The hourly wind speed and HDH correlation in Spain is moderate during the spring season and negative to insignificant during the winter season when the heating demand is most relevant (see Figure 39). In Austria, the correlation in winter is negative between November and January. The strongest season in Austria is again spring. In northern Europe, the seasonal pattern of the hourly correlation between HDH and wind speed is extremer. In this region, hourly HDH and wind speed correlate negatively from October until March. Paired with strong heating needs in northern Europe, this implies substantial storage requirements to cover demand with wind power.

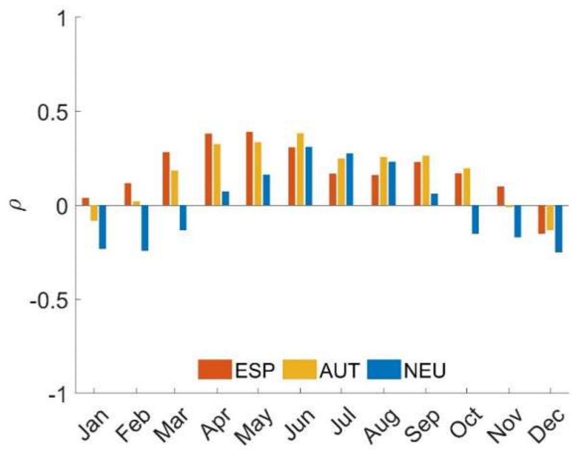

Figure 39 Seasonality: Hourly wind speed and HDH correlation coefficient (ϱ) per month (A1)

3.4.1.3. Correlation between HDH and solar irradiance

1. Spain

The hourly relationship is strongly negative without adjusting the weather data by the time lag of 16 hours between HDH and solar irradiance. This seems logical since temperature usually increases with solar irradiance. Spain reveals the strongest positive results after the time discrepancy is removed, and the solar irradiance peak at noon matches the highest heating needs in the early mornings.

The investigation of the hourly solar irradiance and HDH correlation (A1) during different time periods in the winter season shows strong levels on a daily basis right above 0.60 in Barcelona (2), Madrid (4) and Tomelloso (5), while for the week and season they remain moderate. Nevertheless, the relation to heating needs is more promising than wind speed (see Figure 40). The stronger results for the daily than for the weekly and seasonal time period imply a good daily fit of the solar irradiance and HDH pattern and a weaker relationship across longer time periods. The spring season also achieves positive results.

Daily and, even more so, weekly storage of solar irradiance (A2) leads to insignificant correlations in winter and stronger negative correlations in spring and autumn. It can be concluded that the HDH and solar irradiance patterns in winter match quite well if balanced to the extent of the time lag of 16 hours. It is not surprising, though, that the monthly solar irradiance correlates with HDH on a strong negative level throughout the year and reaches very strong levels below -0.8.

A connection between locations cannot significantly improve the local self-correlation between solar irradiance and HDH. Therefore, spatial integration via the distribution grid has little benefit.

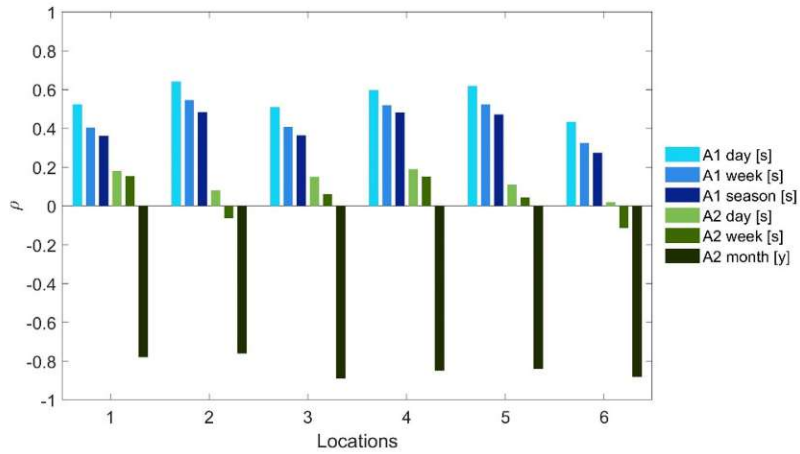

Figure 40 Spain: Solar irradiance and HDH correlation coefficient (ϱ) in winter season [s] applying approach 1 (A1) and approach 2 (A2) for the locations 1-6 as described in Section 3.3.1 (monthly correlation across the whole year [y])

2. Austria

For daily time periods (Figure 41), the lag adjusted hourly solar irradiance and wind speed correlation (A1) in the winter season is moderate in Bregenz (1), Klagenfurt (3) and Nickelsdorf (4). The daily patterns of hourly solar irradiance and HDH match better than the weekly ones or those of the whole season.

Daily and weekly aggregated solar irradiance and HDH (A2) correlate negatively in most cases since higher heating needs usually come with lower solar irradiance. Spring and autumn show more extreme results with hardly any positive correlation on an hourly basis and a strong negative correlation with aggregated data. Throughout the year, monthly solar irradiance and HDH correlate on a strong negative basis in all locations. Like in Spain, hourly HDH and solar irradiance patterns in Austria match best on a daily basis (A1) after adjustment for the time lag. The analysis of the HDH and solar irradiance correlations for winter between the locations does not show any benefit through interaction between the locations.

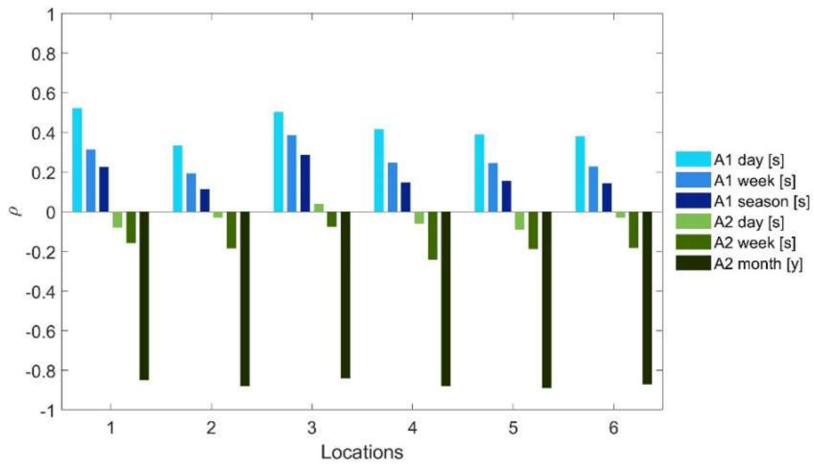

Figure 41 Austria: Solar irradiance and HDH correlation coefficient (ϱ) in winter season [s] applying approach 1 (A1) and approach 2 (A2) for the locations 1-6 as described in Section 3.3.1 (monthly correlation across the whole year [y])

3. NEU

The hourly correlation between solar irradiance and HDH (A1) is much lower in northern than central and southern Europe for all time periods. This can be explained by the low solar irradiance level and higher temperature-dependent heating demand. However, the difference between the time periods in the winter season is similar, with stronger results for the daily than for the weekly and seasonal time period (see Figure 42).

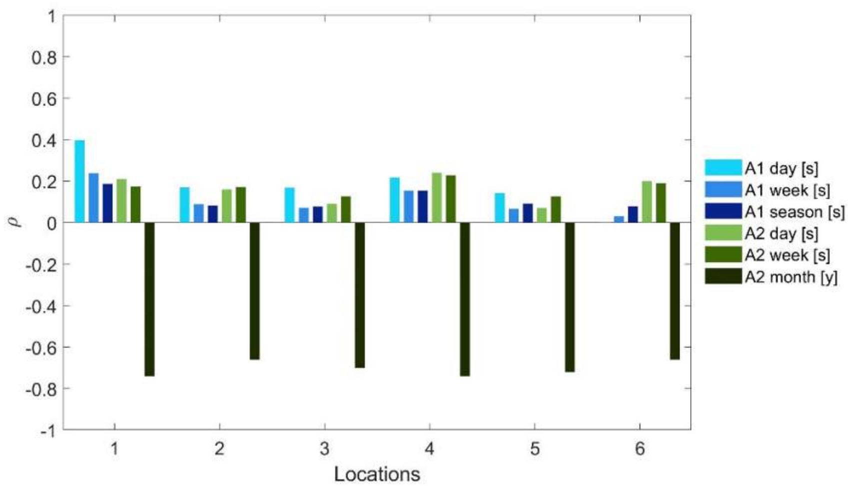

Figure 42 Northern Europe: Solar irradiance and HDH correlation coefficient (ϱ) in winter season [s] applying approach 1 (A1) and approach 2 (A2) for the locations 1-6 as described in Section 3.3.1 (monthly correlation across the whole year [y])

In contrast to the other European regions, daily and weekly storage (A2) leads to weak positive results. Nevertheless, monthly storage again shows the expected strong negative correlation between heating needs and solar irradiance throughout the year. Eventually, using solar energy for heating needs seems less feasible in northern Europe than in the south.

Kiruna (5) in the north of Sweden benefits the most from an external supply of wind energy from Bodø (1) and Trondheim (3) in northern and central Norway but also Gothenburg (4) in the far south of Sweden (see Table 8). The exchange with Gothenburg would require long-distance transmission and only accounts for a moderate correlation. All relationships are at most moderate; therefore, the value of spatial integration is interpreted to be low.

Table 8 Hourly solar irradiance and HDH correlation between locations during the summer season in northern Europe (top numbers 1-6 refer to locations as numbered on the left)

			HDH					
No	**Location**		**1**	**2**	**3**	**4**	**5**	**6**
1	Bodø	**Solar irradiance**	0.46	0.22	0.33	0.48	0.48	0.32
2	Oslo		0.37	0.16	0.28	0.38	0.41	0.27
3	Trondheim		0.46	0.25	0.33	0.45	0.48	0.34
4	Gothenburg		0.45	0.19	0.31	0.43	0.45	0.28
5	Kiruna		0.40	0.17	0.26	0.42	0.39	0.29
6	Stockholm		0.42	0.20	0.30	0.40	0.35	0.14

4. Region Comparison

According to Figure 43, the lag-adjusted hourly solar irradiance and HDH correlation is moderate on a daily basis in Spain and Austria, weak in northern Europe, and decreases towards longer time periods in all regions (A1). This means either that the weekly and seasonal correlation are characterised by stronger variability, leading to a lower average result, or the correlation is weak throughout. In Spain, hourly solar irradiance and HDH fit best, while in Austria and specifically northern Europe, more flexibility on all time scales is required. In northern Europe, daily and weekly storage (A2) lead to a fit of the demand and supply patterns, which is similar to the hourly correlation per day (A1 winter [d]). In Austria and Spain, the daily and weekly totals assuming storage do not (A2) match as much. Monthly solar irradiance and HDH show a strong negative correlation, as described earlier.

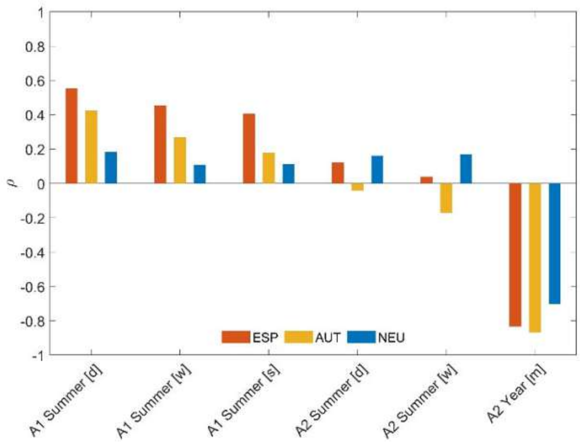

Figure 43 Hourly solar irradiance and HDH correlation coefficient (ϱ) per climate region for different time-periods (day [d], week [w], season [s], month [m]) applying approach 1 (A1) and approach 2 (A2)

The seasonality of the hourly correlation between HDH and solar irradiance shows moderate positive results throughout the year (see Figure 44). This indicates that solar power requires less storage for winter to cover HDH than wind power. The correlation is lower in Austria and NEU than in Spain, but all three regions show a very similar pattern, with the highest results in April and a dip in July and August. During the winter months, the correlation is relatively weak.

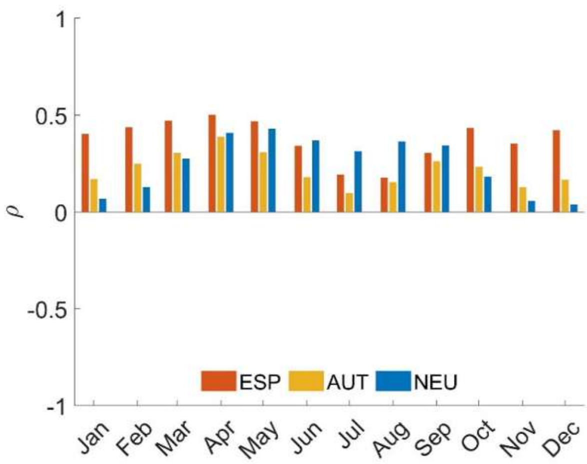

Figure 44 Seasonality: Hourly wind speed and HDH correlation coefficient (ϱ) per month (A1)

3.4.2. Climate change effect

3.4.2.1. Impact on the weather variables

This section analyses the climate change effect concerning the weather variables and their relationships using projected weather data by CMIP5 for the scenario RCP 4.5 (see Section 3.3.5). The analysis is carried out for one exemplary location per area: Madrid, Vienna and Stockholm. This section first analyses the overall development of the weather variables with a 5-year trend. Since the data only provides daily temporal resolution, we will talk of heating and cooling degree-days in the following (HDD and CDD). The second part evaluates the correlation coefficients from 2020 to 2100.

Figure 45 describes the relative change in the mean temperature towards 2100 compared to 2020. For all three areas, a clear increasing trend can be observed. In Madrid, the projected CMIP5 weather data estimates an increase in the mean temperature of more than 10 % until 2100. Additionally, the maximum temperature rises by 8 % in the last third of the 21st century. This is specifically concerning because of Madrid's overall high temperature level, compared to Vienna, which experiences a similar relative development. The long-term trend also shows a significant mean and maximum temperature increase in Stockholm of about 5 % each towards 2100. The minimum temperature level rises most remarkably (5-6 fold) in Madrid, while Vienna and Stockholm experience a rise of about 45 %.

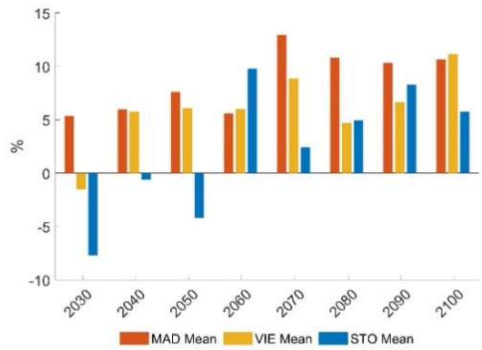

Figure 45 Relative change in mean temperature compared to 2020

As described in the introduction, solar irradiance is subject to decadal brightening and dimming, which may explain the less obvious development of solar irradiance from decade to decade. The long-term trend, shown in the relative change of the mean solar irradiance compared to 2020, however, indicates an increasing trend, at least for Madrid (see Figure 46). In Vienna and Stockholm, the development of solar irradiance seems to be rather variable and often lower compared to 2020. Madrid and Vienna show several time periods with higher mean wind speed compared to 2020, as described in Figure 47. Furthermore, a slow but steady increase can be observed in the maximum wind speed in Stockholm.

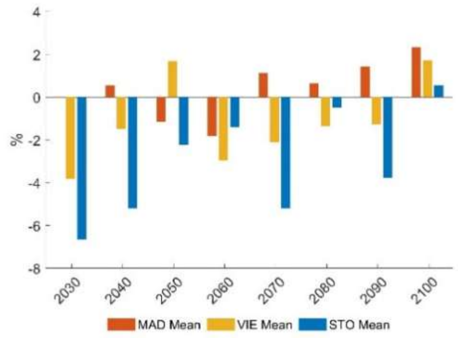

Figure 46 Relative change in mean solar irradiance compared to 2020

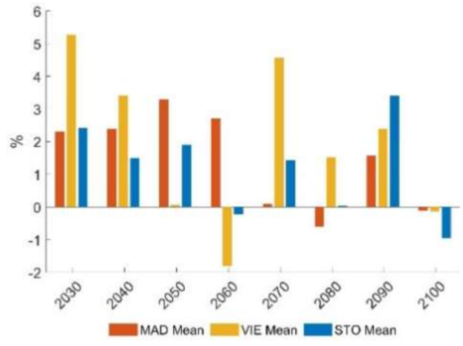

Figure 47 Relative change in mean wind speed compared to 2020

The trend in the HDD towards 2100 shows the expected significant decrease, with the biggest relative change compared to 2020 in Madrid of almost 20 %, followed by Vienna at about 10 % (see Figure 48). In the long term, cooling is only expected to be relevant for Vienna and Madrid. The increase in the mean CDD toward 2100 is substantial at both locations, with about 180 % and 250 %, respectively, compared to 2020 (see Figure 49). The maximum CDD increases by around 45 %.

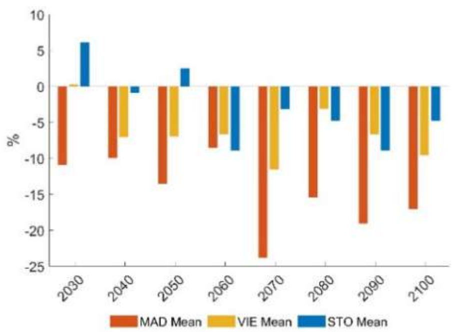

Figure 48 Relative change in mean HDD compared to 2020

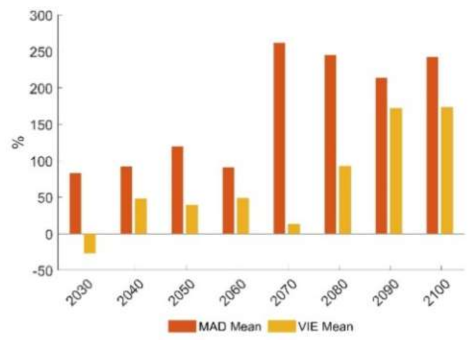

Figure 49 Relative change in mean CDD change compared to 2020

3.4.2.2. Impact on the correlation coefficients

In the following, the absolute correlation coefficients with projected data between 2020 and 2100 are analysed for the selected location per climate region: Madrid, Vienna and Stockholm.

With the daily resolution for the projected weather data, the results are not directly comparable with the more detailed hourly resolution of the historical correlation analysis. The herein conducted analysis of daily data assumes daily storage. Nevertheless, the development of the correlation coefficients smoothed across ten-year periods shows various trends caused by the climate change effects described earlier up to 2100. The correlation coefficient between CDD and solar irradiance in Madrid and Vienna for the expected weather data between 2020 and 2100 is illustrated for the summer season in Figure 50.

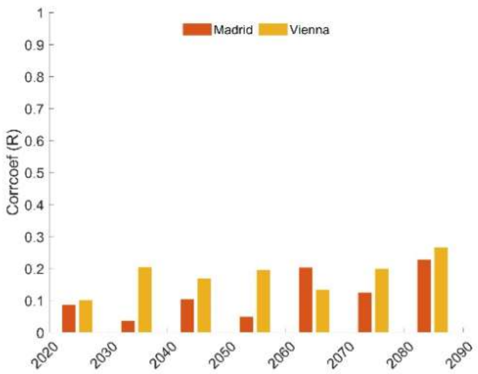

Figure 50 Projected average CDD and solar irradiance correlation in summer based on daily data (2020-2100)

As was described in Section 3.4.2, the mean temperature is expected to rise significantly in Vienna and Spain for the considered RCP4.5 projections. At the same time, mean solar irradiance tends to increase slightly at these two locations. This also explains the increase in the correlation between CDD and SR, with a higher amount of relevant cooling days by exceeding the cooling temperature of 24°C more frequently. The increase seems slightly more evident in Vienna, possibly due to the lower overall temperature level. In contrast, the cooling needs have already been frequent in Madrid historically. A critical development towards 2100 is an extension of cooling needs into September as an extension of the summer, which is again more relevant in Madrid.

While the development of wind speed did not show any real trend, HDD are expected to decrease remarkably at all three locations and most significantly in Spain. This reduces the negative correlation between weekly aggregated HDD and wind speed (see Figure 51). Figure 52 shows the correlation between daily HDD and solar irradiance in winter, which presents a slightly decreasing trend. With HDD falling and solar irradiance increasing, their patterns match less in the future. The correlation between HDD and solar irradiance is expected to decrease in winter significantly in all three locations.

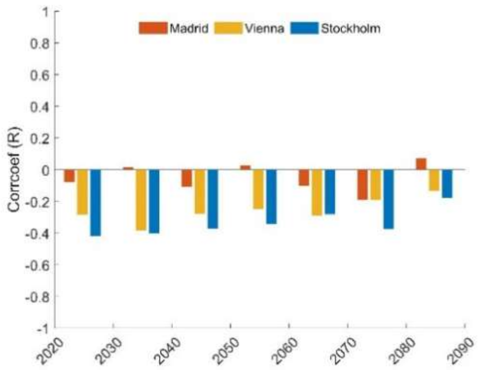

Figure 51 Projected average HDD and wind speed correlation in winter based on weekly aggregated data (2020-2100)

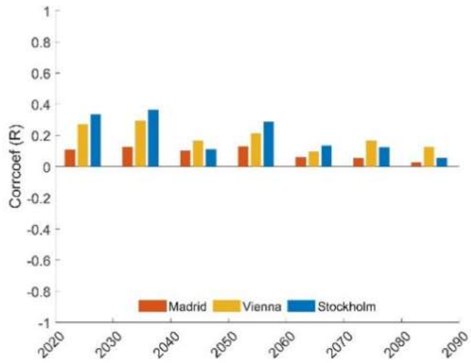

Figure 52 Projected average HDD and solar irradiance correlation in winter based on daily data (2020-2100)

In central and specifically in southern Europe, climate change shifts the focus from HDD towards CDD, which means that in winter, less energy will be required to supply heating needs. Higher building standards will even support this. In summer, however, where renewable energy from the sun is conveniently available and correlates directly with the temperature increase, cooling needs can be supplied without significant storage needs. The temperature-dependent cooling needs will increase substantially with the mean and maximum temperatures.

3.4.2.3. Discussion

The steepest increase in the mean and maximum temperatures is expected in Madrid. At the same time, solar irradiance is expected to increase. This would lead to higher solar resource availability to cover higher cooling needs in southern Europe, which is favourable. An increase in the maximum temperature with an already high level, as in Madrid, can also harm the efficiency of PV power systems, as described in Section 3.1 (Wilbanks et al., 2008). This would require an increase in the installed capacity for the same output. In Austria, temperatures are also expected to increase, while no apparent trend is visible for solar irradiance. A measure to avoid the direct representation of warmer temperatures in the energy demand for cooling is the improvement of building standards in the form of insulation and similar efforts to prevent buildings from heating up, such as shading through trees, which also provides cooling outside the building. Especially for the warming temperatures in Madrid, with an increasing amount of days surpassing the cooling temperature of 24°C, this approach could be one solution to limit and adapt to the increase in CDD in the long term. The correlation between solar irradiance and CDD increases, specifically in Madrid, from 0.2 to almost 0.3. The results are still low given the rough daily time resolution. Vienna experiences the highest impact on this relationship, from 0.1 to nearly 0.3.

The projected increase in the minimum temperature could lead to an increased potential for wind power generation in northern Europe, which is often subject to icing in very cold temperatures, as described in Section 3.1 (Pryor & Barthelmie, 2010). This is favourable to meet a growing amount of the still substantial heating needs with a renewable power source. In Madrid, HDD are expected to decrease the most, followed by Vienna, while the cooling needs increase substantially in both regions at about 200 %, leading to higher cooling needs. An expected decrease in the energy needs for heating through climate change will even be exaggerated by an improvement in building standards, which lowers the heating threshold due to better building insulation. The correlation between HDD and wind speed tends to decrease slightly, similarly in all three cities with a decrease in cold days below the heating temperature of 12°C.

3.5. Conclusions

This work was conducted to address the correlation between natural energy sources (wind speed and solar irradiance) and—motivated by their interrelations with climate—temperature-derived heating and cooling needs, not only historically but also for future projections. It aims at proving the hypothesis that there is an apparent relationship between solar irradiance and wind speed and temperature-related heating and cooling needs. The results emphasise the importance of considering differences in climate regions when analysing the relationship between VRE and energy demand. The correlations were analysed in three very different climates: Spain in southern Europe, Austria in central Europe and Norway and Sweden in northern Europe.

Our results confirm that the hourly correlation between solar irradiance and CDH as a consequence of rising temperatures is moderate to strong on a daily basis in Austria and Spain, reaching a strong coefficient of 0.8 in summer in some locations in Spain. So far, the correlation between solar irradiance and heating needs has hardly been investigated but reveals substantial value in renewable energy systems. After accounting for the time lag between the morning peak of heating needs due to a temperature decrease and the solar irradiance peak at noon, Spain and Austria achieve moderate (0.40-0.59) results in winter. However, the relationship between wind speed and temperature-derived heating needs turns out to be more complex, specifically in winter—the strongest heating period. The analysis does not show an obvious correlation. Only monthly aggregated wind speed and HDH data across the year match moderately in Spain (0.41-0.56) and northern Europe (0.39-0.58). Our correlation results show that a potential distribution of wind speed or solar irradiance among the locations via the energy grid has limited value apart from some cases in northern Europe. Understanding these relationships provides a basis for appropriate planning and forecasting in smart energy systems, intending to use large-scale renewable energy sources, which naturally cause temperature changes, most efficiently for heating and cooling needs.

With the analysis of the climate projections provided in daily resolution and development of the correlations into the future, the time period for storing wind and solar power can be assessed. Madrid is expected to experience the strongest mean temperature increase (almost 10 %) towards 2100, accompanied by growing solar irradiance. A decrease in the yearly HDD and an even more substantial increase in CDD can be estimated in all three climate regions, most substantially in Madrid (-20 % HDD and +100 % CDD), followed by Vienna and Stockholm. The increase in CDD, through temperatures exceeding the cooling threshold more frequently, causes an increase in the correlation with solar irradiance. At the same time, the correlation between solar irradiance and HDD is expected to decrease in all regions. From a supply side, the decreasing temperatures in northern Europe might lead to less icing and reduce its negative impact on wind power efficiency.

This study is based on the mere natural resources and temperature-derived heating and cooling needs. An investigation of consequent energy demand needs to consider efficiency gains, potential intensifications of the energy need through, e.g. very long heat periods in summer, and PV system efficiency losses caused by very high temperatures. Smart energy systems, therefore, should embrace the positive correlation between solar irradiance and CDH and account for at least monthly storage of potential wind power to use VRE for heating and cooling efficiently. The results also show that the role of different SC applications may change throughout the decades with changing renewable availability and demand characteristics due to temperature and climate changes.

4. Efficient load management in multi-apartment buildings

The transport sector is among the top emitters of CO_2 in Europe (EC, 2021b) and is often regarded as a slow mover concerning the energy transition. Apart from avoiding the use of transportation or shifting to more environmentally friendly options, the decarbonisation of the remaining vehicles is essential. As outlined in Section 2.4, SC through direct electrification of BEVs represents the most efficient opportunity for individual passenger cars. The rising electricity demand, however, must be controlled to avoid extensive grid capacity expansion and save costs. The following work, referring to a published article by Ramsebner et al. (2020), investigates the impact of load management approaches on overall power connection requirements with an optimisation model validated by measured field test data.

4.1. State of the art

Reasons for the growing interest in e-mobility include the increasing awareness for climate change, as well as the obligation of car manufacturers to reduce the CO_2 emissions of their fleets by 2030 (EP&EC, 2019). One of the most significant keys to success associated with this development is the provision of appropriate charging infrastructure (IS) (Spöttle et al., 2018). Since BEV charging currently remains primarily connected to single homes with private charging stations or charging at public stations, large-scale load management (LM) applications are still not commonly applicable. Major questions include where charging can take place (e.g., private and public charging, charging at work, etc.), at which charging speed and capacity, and how the potential temporal distribution of this load behaves. The successful management of BEV charging demand is related directly to the economic aspects of charging IS installations and distribution grid performance and expansion requirements.

Many projects have already been conducted for public fast charging, single-family buildings, and small company applications. Hall & Lutsey (2017) provide a global best practice overview, and IEA/Nordic Energy Research (2018) describes the Nordic BEV outlook. Different projects evaluate BEV charging IS in Denmark (CleanTechnica, 2018; European Commission DG-ENER, 2021) and Germany (Netze BW GmbH, 2019). Nevertheless, our literature review reveals that research on large-scale charging IS with optimal load management (LM) in residential buildings remains scarce. Efficient LM is also referred to as smart charging in the literature, defined as an adaption of the BEV charging cycle to both the restrictions of the distribution grid and the needs of BEV users (IRENA, 2019). IRENA (2019) claims that smart BEV charging enables peak shaving, network congestion management, and reduced grid capacity investments. Various studies cover the electricity demand profiles of BEVs and potential peak increases. Van Vliet et al. (2011) discover the adverse effects of uncontrolled BEV charging on the distribution grid and find that with a BEV diffusion of 30 %, the Dutch peak electricity demand would grow by 7 %, and the household (HH) or overall building peak demand by 54 %. Several studies observe the benefit of off-peak charging, in which the base load is increased while the national peak load remains untouched.

While Van Vliet et al. (2011) highlight the benefit of off-peak charging for the energy use cost and CO_2 emissions of BEVs, Bitar & Xu (2016) suggest a price that decreases with the deadline granted by the user for the completion of the charging process. Limmer & Rodemann (2019) highlight the cost aspects of peak charging at public stations. They argue that although the majority of public charging stations for BEVs are presently uncontrolled, controlled charging should offer a price that decreases with the latest deadline the user allows for charging to increase the availability of the BEV at the station. From our perspective, however, this pricing scheme requires an appropriate interface for the user and would lead to parking lots being blocked for a considerable amount of time. This scheme, therefore, is designated for applications with an assigned parking lot.

Several studies on LM for BEV charging address pricing mechanisms to limit negative effects on the distribution grid. Some suggest a time-of-use (ToU) pricing mechanism that incentivises off-peak charging with a lower charging price (Hu et al., 2016; Yi et al., 2020). New peaks, however, may still arise if too much charging power is pushed into off-peak times. Therefore, so-called dynamic load-based pricing is a potential solution in which charging power decreases with the amount of BEVs charged at a time (Bitar & Xu, 2016; Hu et al., 2016). Dynamic pricing, while the BEV is already plugged in, represents high price uncertainty and would need to be based on a forecast of charging demand. It has to be kept in mind that such an LM or restrictions on charging power can also be implemented top-down from the control station across the charging points to guarantee distribution grid performance. On the other hand, Yan et al. (2020) find that traffic jams and weather forecasting can enhance the operation of LM. Temperatures affect battery performance and heating and cooling demands, while the traffic conditions influence the electricity consumption of driving.

Recently, many studies have been published concerning the impact of e-mobility on the distribution grid, power quality, and power generation capacities. Crozier et al. (2020) observe that controlled charging significantly benefits Great Britain's electricity network. It can reduce expansion requirements for electricity generation capacities and investment into the distribution network. Das et al. (2020) focus on the grid integration of BEV charging IS. In contrast, Khalid et al. (2019) emphasise the power quality aspects of the utility grid, and Brinkel et al. (2020) analysed the need for grid reinforcement because of growing e-mobility. The benefits of controlled charging have also been discussed within the context of smart grids and smart cities, where optimal charging scheduling is carried out to improve grid system operation, voltage, and efficiency (Y. Luo et al., 2016; Monteiro et al., 2019). Another paper developed an optimised charging framework using knowledge of the upcoming trip schedule of the BEVs (Usman et al., 2016). However, such detailed information is difficult to obtain.

Using the BEV battery to switch flexibly between charging and providing energy to the power grid has been analysed from various perspectives throughout the last decade. Some focus on the potential of vehicle-to-grid (V2G) for BEV integration into smart grids (Hariri et al., 2019; Tan et al., 2016) and its impact on the grid in general (Aguilar-Dominguez et al., 2020). From a user perspective, V2G sometimes is regarded as the potential missing link for the acceptance of BEVs as a cost-effective support policy. C. Chen et al. (2020), for example, explain that in Nordic countries, V2G capability—apart from charging time—is a technical aspect that improves BEV adoption. Sortomme & El-Sharkawi (2011) study optimal charging strategies for V2G application. Various studies, however, analyse the techno-economic feasibility of V2G (Gough et al., 2017; Kempton & Tomić, 2005; Mullan et al., 2012) and find that, economically, this strategy may only be feasible in specific scenarios which highly depend on the battery degradation costs related to V2G cycling. Noel et al. (2020) and Parsons et al. (2014) investigate the willingness to pay for V2G applications and conclude that V2G is only relevant in countries with higher overall education or knowledge of the technology.

Furthermore, the concept needs to provide a financial incentive for the user to be successful. While Habib et al. (2015) studied the impact of V2G technology and charging strategies on the distribution network, the parker project represented a field test of V2G infrastructure and found that V2G can be commercialised by providing frequency containment reserves (Peter, Bach Andersen et al., 2019). Rezania (2013) even conclude in a study on Austria that, from an electricity system point of view, the participation of BEVs can hardly be competitive in the frequency reserve market. The competition from other providers with technological and cost advantages, such as heat pumps and pumped hydro, is too strong, and the battery degradation cost limits the potential economic benefit. Some recent studies also investigate the ability of LM to reduce greenhouse gas (GHG) emissions and promote VRE integration. Apart from the cost and emission optimisation of BEV charging by Brinkel et al. (2020), Tu et al. (2020) optimise BEV charging to minimise the emissions from electricity consumption. Additionally, (Dixon et al., 2020) set up a BEV charging schedule that minimises carbon intensity and seeks to absorb otherwise curtailed renewable electricity. Their method achieves an average 25 % reduction of the CO_2/km compared to uncontrolled charging from Great Britain's grid.

Nevertheless, despite this technique's great potential, little work is available that focuses specifically on private BEV charging IS and the potential of large-scale LM in multi-apartment buildings. Lopez-Behar et al. (2019) claim that in many cities, most residents live in multi-apartment buildings not yet equipped with proper BEV charging IS. Simulation results based on real-world driving data by D. Wang et al. (2017) show that home charging can meet the energy demands of most BEVs under average conditions. Kim (2019) analyses residential BEV charging behaviour. Additionally, Yi et al. (2020) optimise BEV charging via charging behaviour models based on a real-world data set of a Nissan Leaf during weekdays, measured from thousands of charging points over several years. The authors find that BEV charging occurs together with distribution grid peak loads. Five scenarios with varying BEV penetrations are simulated to show the difference between uncontrolled and controlled charging. Each scenario includes 100,000 households and considers BEV penetrations between 10 % and 90 %. Jang et al. (2020) eventually optimise residential BEV charging to avoid peak loads and minimise the charging cost for the user, and Khalkhali & Hosseinian (2020) investigate a residential smart parking lot to control grid performance.

4.2. Core objectives

This work by Ramsebner et al. (2020) results from the Austrian research project "URCHARGE", which aims to extend currently available LM functionalities for large-scale private charging IS at the technical, economic, and customer levels (Klima- und Energiefonds, 2022; LINZ AG, 2021). From a technical perspective, URCHARGE aims to substantially enhance LM functionalities from static management across a maximum of 15 sub-stations to the dynamic control of more than 150 charging points, including improved data gathering and analysis, appropriate billing functionalities, and efficiency improvements. This is one of the few projects globally currently investigating private charging IS on such a large scale. Three projects in the US—in San Diego (Sandag, 2019), Los Angeles (Balmin et al., 2012) and Columbus - Ohio (Smart Columbus, 2018)—and one in Germany (Netze BW GmbH, 2021) aim at higher availability of BEV charging points in multi-unit dwellings.

The main objective of this paper is to evaluate the potential LM approaches for BEV diffusion to avoid an increase in existing household electricity demand peaks in multi-apartment buildings and thus substantial long-term, system-wide capacity investments and operational costs. While the 6-month field test within URCHARGE tested LM for 51 BEVs representing

50 % e-mobility in this area, our model provides a framework to analyse the impact on electricity demand profiles up to 100 % e-mobility. The situation of uncontrolled charging is compared to the results with LM approaches, and the environmental effects of substituting conventional cars with BEVs and their electricity consumption are illustrated. Another important goal of this analysis is to define the minimum charging capacity required for each BEV (kW/CP) as an indicator for cost-efficient sizing. Once the power connection assigned to the area is exceeded by the household plus BEV electricity demand, substantial costs occur to reinforce the power cables or buy additional power capacity from the grid operator. Our contribution mainly benefits from being embedded in a holistic research project for Austria, and our model results are verified by experience from the project's field test in Section 4.5.2.

4.3. Methodology

First, a yearly household (HH) load profile for a residential area with 106 HHs is defined to analyse the impact of different LM approaches on the building's electricity demand. The BEV charging demands and availability times at home or at public charging points depend on the trip's start time and length and are determined in a modelling approach by Hiesl et al. (2021) based on an Austrian traffic survey. The methodology is briefly outlined in Section 4.3.2. Our model coordinates BEV charging in the home network according to the constraints for each charging scenario (Section 4.3.4). The results allow assessing the impact of LM on large-scale BEV charging on electricity demand peaks and valleys. The model parameters largely reflect the common technical standards on battery capacity, charging speed, and efficiency for private stations.

On the one hand, our model analysis is subject to simplifications from more detailed, real-world technical functionalities to enable more generally applicable conclusions. On the other hand, it can conduct additional analyses that were not tested throughout the URCHARGE field test to conclude on the impact of e-mobility toward 100 % BEV diffusion. Simplifications to the model include the operation of the LM optimisation model under full information of BEV electricity consumption and the trip start times across one year, as well as the assumption of one uniform battery size and uniform technical characteristics for all BEVs. Furthermore, the model operates under the knowledge of the battery's state of charge, which is currently not the case in an authentic setting. A detailed description of the differences between the modelled and field test environment and verification of the model results with the field test are provided in Section 4.5.2. The model does not cover any load flows of the distribution grid or V2G approaches but instead focuses on an analysis of potential LM approaches to reduce the impact of e-mobility on the overall building load.

4.3.1. Household electricity demand

For our analysis, the electricity demand profile throughout the day is essential. Of course, demand may vary with parameters such as the HH size and the habitants' ages and types of profession. Furthermore, the HH electricity demand profile is subject to changes due to increasing electrification. However, this study only considers the relative impact of e-mobility on existing building electricity demand and no future HH demand scenarios.

To determine the aggregate HH electricity demand that largely resembles the field test site's 106 HHs, two weeks of data were measured on-site at the respective building's power connection. An alternative yearly dataset from a similar project was used to achieve a realistic yearly profile for our model. This alternative yearly dataset was extrapolated to the demand level during the measured two weeks at the URCHARGE demo site, such that the average electricity demand during the same two-week time periods matched. Eventually, the patterns were similar, and the adapted yearly data was considered feasible for our study. The two weeks of measured URCHARGE HH electricity demand and the aligned yearly data are shown in Figure 53.

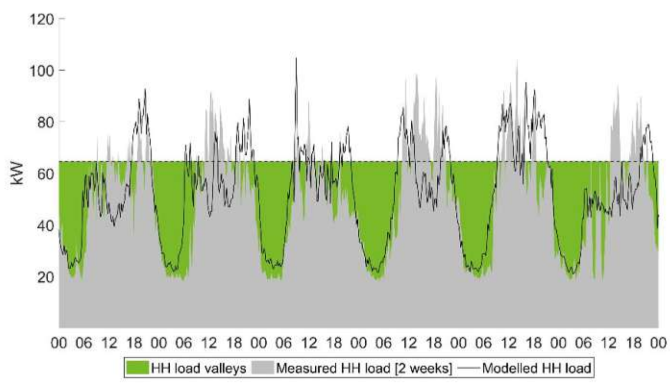

Figure 53 Measured household load in the residential area of the URCHARGE project (2 weeks data) and the aligned common yearly household load profiles with peaks and valleys.

For further analysis, a threshold to differentiate the HH load valleys and peaks was defined using the 70th percentile (Q_{70}) also illustrated in Figure 53. This parameter represents the threshold that 70 % of all HH load values lie below, which accounts for 64.5 kW and allows for a plausible differentiation between noon and evening electricity demand peaks and off-peak times. Then, the LM approaches mostly aim to minimise the impact on the peaks or shift BEV charging demands in the HH load valleys. The detailed approaches for LM are described in Section 4.3.4. The impact of e-mobility on the existing building electricity demand and the effectiveness of LM approaches were evaluated according to the specific indicators determined to be appropriate, as described in Table 9. P^h_{max} represents the maximum demand peak (see Eq. (9)), P^h_{min} the minimum of the demand profile (see Eq. (10)), P^h_{peak} the sum of all electricity demand exceeding (see Eq.(11)) and P^h_{base} below the Q_{70} threshold in the household load valleys (see Eq. (12)).

$$P^h_{max} = max\ P_{con_{(1-T)}} \tag{9}$$

$$P^h_{min} = min\ P_{con_{(1-T)}} \tag{10}$$

$$P^h_{peak} = \sum_{t=1}^{T} P_{con_t} > Q_{70} \tag{11}$$

$$P^h_{base} = \sum_{t=1}^{T} P_{con_t} < Q_{70} \tag{12}$$

Table 9 Important result parameters (see Figure 2).

Parameter	***Description***
Maximum demand (P^h_{max})	Annual maximum electricity demand [kW]
Minimum demand (P^h_{min})	Annual minimum electricity demand [kW]
Peak demand volume (P^h_{peak})	Electricity demand volume exceeding Q_{70} [kWh]
Base demand volume (P^h_{base})	Electricity demand volume beneath Q_{70} [kWh]

4.3.2. BEV driving profiles

The driving profiles defined in Hiesl et al. (2021) represent common BEV charging demands and are a static input to the optimisation model. Eight typical driving purposes with the relevant distribution of common distances, electricity consumption, and potential start times were applied to determine when and with which energy demand each BEV returns to the private charging point (BMVIT, 2016). The modelled energy consumption meets the traffic survey results for Austrian cities (excluding Vienna), with an average yearly distance travelled by each driver of 12.237 km/a.

BEV consumption is modelled as an interpolation between 15 kWh/100 km in summer and 17 kWh/100 km in winter due to the additional power consumption for heating and the temperature sensitivity of the batteries (AAA, 2019). Due to computing performance, the model calculates the distribution of BEV charging availability for 10 different BEV profiles. Assuming one parking lot for each HH, these charging profiles are extrapolated to the number of BEVs for specific percentages of BEV diffusion according to Table 10.

Table 10 Number of BEVs in the modelled multi-apartment building for BEV diffusion.

No. of BEVs	11	32	53	80	106
BEV Diffusion	10 %	30 %	50 %	75 %	100 %

4.3.3. Optimisation model

The BEV charging demand is controlled within a charging network, including one central control or master station, thereby coordinating charging for each private sub-station in the area (see Figure 54).

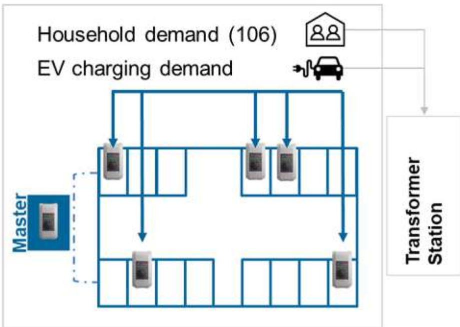

Figure 54 Private charging network: The master station controls all sub-stations

The maximum charging power of private stations is defined as 3.7 kW, whereas public charging stations operate at 22 kW. 3-phase charging is not examined, with which a vehicle can charge at a speed of 11 kW (3 × 3.7) at home, but only 1-phase charging. The battery capacity of the individual passenger BEVs is set to 40 kWh. This work does not aim at modelling a specific vehicle model. The current battery state of charge (SOC) is determined according to Eq. (13) by the state at the end of the former time step plus the energy currently consumed (discharged) (P_{DC}) or charged (P_{Ch}).

$$SOC_t = SOC_{t-1} + P_{Ch(t)} - P_{DC(t)} \tag{13}$$

Our model optimises private charging in 15 min time-steps based on the full information of the yearly BEV power consumption, potential charging times, and HH load and is established as a linear optimisation model. The objective function generally aims to minimise the costs of BEV charging (c^{ch}) depending on the cost (c) per consumed charging power (p) at the home (h) and public (p) charging point in each time step (t) and across the number of vehicles (n) (see Eq. (14)). The different the LM approaches then request specific objectives for their optimisation (see Section 4.3.4). The BEV demand is a static input to this LM model from Hiesl et al. (2021). It depends on the distance travelled for each driving purpose and the respective electricity consumption (see Section 4.3.2). The charging consumption is derived from the net battery charging power (p_{ch}), the charging efficiency (η_{ch}) and the vehicle availability matrix (a^h) at the public (p) or home (h) charging point (see Eq. (15)). The vehicle availability matrix (0/1) in each time step at the home or public charging point as a static input to the model is derived by Hiesl et al. (2021) and determined from journey start times, path lengths, and consequent end times. Overall, charging should primarily be carried out within the private, controlled network, while public charging should only occur at urgent times.

$$\min_{\substack{\{p_t^p,\ p_t^h\} \\ \{c_t^p, c_t^h\}}} \sum_{k=1}^{T} \sum_{i=1}^{n} c_t^{ch}(p_{t'}, c_t) \tag{14}$$

$$p_t^{h/p} = p_{ch_t}^{h/p}\, \eta_{ch}\, a_t^{h/p} \tag{15}$$

This objective function derives the optimal allocation of charging power across all time steps to fulfil the BEV demands within the constraints for each BEV charging scenario described in Section 4.3.4. This function aims at recharging the BEV before the next journey starts. The reality this far does not provide any information on the upcoming consumption of the BEV. Nevertheless, modelling with full yearly information offers valuable insights into the benefits of exact customer information.

4.3.4. Charging strategies

The BEV charging strategies represent different approaches toward charging power control by the master station top–down across all charging points (see Figure 3). An uncontrolled charging scenario, without any control measure, is used as a reference. This represents the start of charging once the BEV is plugged in at the home station. Then, these results are compared to the expected improvements with two LM approaches aimed at a specific distribution of BEV electricity demand. For all charging approaches, it is assumed that the BEVs are plugged in and available for charging while parked at home.

The following BEV charging approaches are being analysed:

1. Uncontrolled charging (UC)

As a reference scenario, there are no LM measures applied. Charging demand occurs at the point of return to the parking space and is fulfilled at maximum power and the cost for charging (c_t^h) is constant.

2. Low charging capacity (LCC) LM approach

The LCC approach refers to slow charging at very low charging power for each BEV to avoid excessive peaks in charging demand. Charging is operated at a high simultaneity rate. In contrast to uncontrolled charging, specifically the peak power consumption (P_{CP}^h) across all vehicles as described in Eq. (34) shall be minimised (see Eq. (33)).

$$\min P_{CP}^h \tag{16}$$

$$P_{CP}^h = \max \sum_{i=1}^{n} P_t^h \tag{17}$$

3. Time-of-use (ToU) LM approach

With the ToU approach, the master station shifts BEV charging power from the HH load peaks into the valleys, as described in Figure 2. The HH load peaks are defined as any value exceeding the Q_{70} threshold (see Section 4.4.1).

As important indicators of the impact of different charging strategies on the distribution of charging power and the length of charging processes, the simultaneity factor, the average charging power, and the charging time ratio are analysed. These factors are also compared to the results of the project field test in Section 4.5.2. The underlying price structure for this LM optimisation is described in Figure 55.

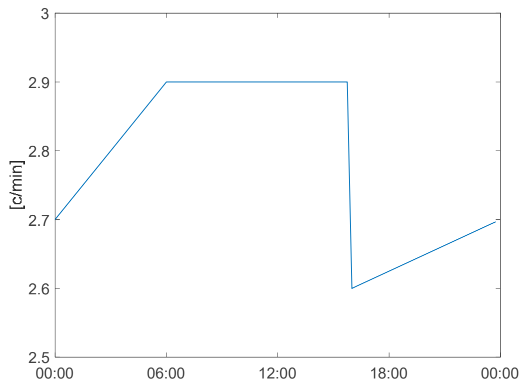

Figure 55 Time of Use tariff to avoid household load peaks [c/min]

1. Simultaneity factor

The simultaneity factor describes the average amount of vehicles charging at the same time across the whole year. Therefore, LM approaches that promote longer charging time periods result in a higher factor of simultaneously charging BEVs.

2. Charging time ratio

This indicator relates the time a vehicle is charged to when it is parked. This factor is expected to be much higher for the LM scenarios ToU and LCC than for the uncontrolled approach, leading to shorter charging periods at higher charging power.

3. Average and maximum charging power

The average charging power refers to the average power consumed by the BEV during active charging. Furthermore, the maximum charging power is analysed to reveal the charging load peak, which indicates the speed at which charging is processed. It is assumed that uncontrolled charging, which does not promote the management of charging power, will lead to a higher average charging power than the ToU or LCC approach.

4.3.5. Minimum charging capacity

The cost for charging capacity for the whole area is subject to step fixed costs, which increase substantially once the regional power connection capacity needs to be expanded. We, therefore, evaluate the minimum charging capacity (P^h_{CPmin}) required to fulfil BEV demand exploiting load shifting to a maximum. This analysis uses the objective function described in Eq. *(22)* to minimise the charging capacity that needs to be installed for the charging network across all vehicles. The highest 5 % of charging power consumed was removed to eliminate outliers in the BEV electricity demand from rare, very high BEV electricity consumption due to few long-distance trips. Then, this aggregated capacity is divided by the amount of charging points or vehicles (n) to arrive at the desired indicator kW/CP (see Eq. (35)). This indicator represents the minimum charging power for each BEV required to fulfil the demand throughout the year.

$$P^h_{CPmin} = \frac{\max \sum_{i=1}^{n} P^h_t}{n} \text{ [kW/CP]} \tag{18}$$

Two modelling approaches representing different levels of information are applied: yearly optimisation with full information and daily rolling optimisation. For the daily approach, a higher required minimum capacity is expected due to the inability to balance charging over more than one day.

4.3.6. Environmental impact of e-mobility

The environmental impact of e-mobility in the considered residential area is evaluated based on the following aspects:

1. Savings in GHG emissions from the substitution of fossil-fuel-powered vehicles with BEVs

The savings in CO_2-eq, particulate matter (PM), and nitrogen oxide (NOx) are analysed through the continuous substitution of conventional vehicles using diesel- or petrol-powered internal combustion engines with BEVs across the whole life cycle—from vehicle and battery construction to energy provision and driving. This is based on the average yearly km travelled by each car from our model results and the Austrian data on specific emissions for each type of fuel (UBA, 2018). Scenarios on the future development of individual transport, such as a shift to public transportation or bicycles along with the energy transition or an increase in BEV use resulting from a rebound effect due to driving without regret of air pollution, are not included. The emissions are based on current measures and will likely decrease further in the future for conventional and battery-powered vehicles. The CO_2-eq emissions are 178 g/km for diesel and 225 g/km for petrol-powered vehicles. However, diesel includes much higher amounts of NOx, with 0.385 g/km, compared to petrol with 0.162 g/km. PM emissions are 0.021 g/km and 0.024 g/km for diesel and petrol, respectively. The Austrian shares of diesel and petrol vehicles from the stock of 2019 are applied, whose diesel share of 56 % is much higher than the European average (Statistics Austria, 2019).

According to the Austrian climate goals, by 2030, national electricity generation must be 100 % renewable (BMNT, 2018; Oesterreichs Energie, 2019). For our scenario of 10 % BEV diffusion, which represents the status in 2020, we, therefore, use the specific emissions of the current Austrian electricity mix represented in the UBA scenario "BEV(Aut-Mix)" (UBA, 2018). Between 30 % and 100 % BEV diffusion, representing the situation from 2030 onwards, the electricity consumed is assumed to be almost fully renewable with specific emissions, as in the UBA "BEV(UZ-46-Mix)" scenario (UBA, 2018).

2. Impact of LM on the environmental aspect of the electricity mix consumed for charging

Based on the correlation between the Austrian fossil electricity generation (p_{foss}) from coal and gas (ENTSO-E, 2022) and the BEV charging power consumption (p_{ch}) from the model, the potential effect on the environmental aspect of electricity consumption is evaluated according to Eq. (19).

$$r_{foss} = \frac{Cov_{p_{ch}, p_{foss}}}{\sigma_{p_{ch}}, \sigma_{p_{foss}}} \tag{19}$$

3. Environmental impact of e-mobility and LM on potential grid expansion

From the resulting impact of uncontrolled and controlled charging on the maximum and peak demand and the importance of the minimum charging capacity, conclusions on the consequences for grid expansion and its environmental effects are derived.

4.4. Results

The modelling results in this section are structured as follows. Section 4.4.1 describes the existing HH electricity demand as a basis for evaluating the impact of e-mobility on the building load. Sections 4.4.2 and 4.4.3 show the effects of BEV charging with uncontrolled charging and applying the LM approaches (LCC and ToU). Section 4.4.4 addresses the minimum charging capacity that must be available for each BEV. Generally, throughout the diffusion of e-mobility up to 100 %, it was observed that the model mainly uses the private charging network. In comparison, public charging only fulfils up to 3 % of the yearly demand. Therefore, we conclude that the sufficient availability of efficient private charging IS reduces the need for fast charging options, at least for common daily business.

4.4.1. Household electricity demand characteristics

The HH electricity demand is the basis for our analysis of the impact of increasing BEV diffusion and has a duration curve, as shown in Figure 56. The total yearly demand accounts for 487 MWh, and the profile shows the characteristics outlined in Table 11. While the LM approaches aim to minimise any increase in the building's maximum and peak volume demand through e-mobility, a successful shift into the HH load valley will increase the minimum and base volume demand (see Figure 53). This will result in a more balanced daily building demand profile with less variability. On the one hand, this can mean greater predictability and stability in the building load profile for the distribution grid. On the other hand, the increasing electrification of a growing number of applications could result in additional or new peaks.

However, the HH load valleys largely coincide with national electricity demand valleys. Therefore, a BEV load shift to these times may avoid the expansion requirements for the distribution grid and electricity generation capacities for a reasonable amount of time. The material production, infrastructure implementation, land use associated with installing power plants and cables, and disposal entail substantial environmental and economic impacts.

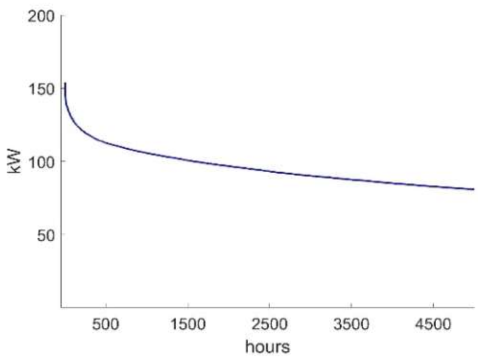

Figure 56 Duration curve for household electricity demands.

Table 11 Household load characteristics.

Parameter	*Result*
Maximum demand (P^h_{max})	153.8
Minimum demand (P^h_{min})	19.2
Peak demand volume (P^h_{peak})	49.2
Base demand volume (P^h_{base})	437.6

4.4.2. Uncontrolled charging characteristics

As explained in the introduction, charging without any load control mechanism increases electricity demand peaks, showing a strong correlation between the electricity demand for BEV charging and that for the HHs. Without any LM approach, most BEV users return home during the evenings and immediately plug in their vehicle for charging. Figure 57 shows the impact of BEV charging on electricity demands without control for an exemplary day, along with the diffusion of e-mobility. In this uncontrolled scenario, only 50 % of all vehicles charge simultaneously (simultaneity factor); on average, the vehicles only charge 9 % of the time they are parked (charging time ratio). The latter proves the short time period during which charging is completed, which implies high charging power in the uncontrolled scenario. The average charging power consumed per BEV is 0.40 kW, and the maximum charging power consumed accounts for 1.80 kW.

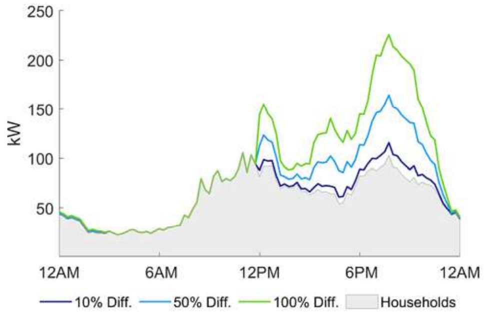

Figure 57 Charging profiles and household electricity demands without control (UC).

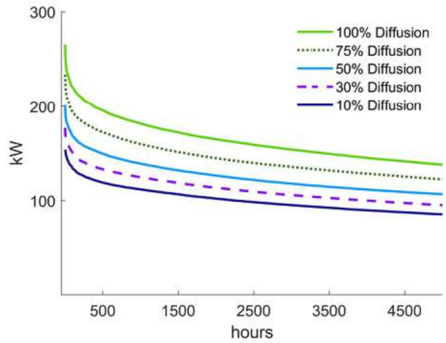

Figure 58 Duration curve with uncontrolled charging (UC).

The impact of uncontrolled BEV charging on the electricity demand peaks becomes even more visible in the duration curve shown in Figure 58, where the total building electricity demand (BEV charging plus HHs) is ranked from the highest to the lowest for the highest 4,500 h in a year. This curve reveals a remarkable increase in the building's maximum and peak volume demand along with growing e-mobility. Toward 100 % BEV diffusion, the maximum electricity demand increases by 72 %, from 153.8 kW without e-mobility to 265.2 kW, and the peak volume demand grows almost four-fold. This increase in peak electricity demand may have severe consequences for the distribution grid and capacity investment in the area. The minimum electricity demand remains untouched since charging coincides with higher HH electricity demand. The base volume demand increases only by 20 % up to 100 % BEV diffusion. Therefore, the next section outlines the advantages of the defined LM approaches.

4.4.3. Load management scenarios

LM can significantly influence the characteristics and distribution of the BEV electricity demand profile. Suppose the BEVs are available for charging for a sufficient amount of time. In that case, the charging demand can successfully be shifted away from the HH load peaks into the valleys, as indicated in Figure 53. The results of the two LM approaches are also compared to uncontrolled charging. A more detailed quantitative discussion of all charging strategies is provided in Section 4.5.1.

Figure 59 shows the results for the LCC approach, whose slow charging speed leads to a greater BEV load distribution over time compared to uncontrolled charging. In this scenario, on average, 86 % of all vehicles charge simultaneously, and the vehicles charge 16 % of the time they are parked. This represents long charging times and great simultaneity, though at substantially reduced charging power. The charging times still correlate with the evening HH load peaks. Nevertheless, the extreme peaks in the evening times experienced with uncontrolled charging are reduced substantially with the limitations on overall charging capacity. The duration curve of the building electricity demand in Figure 60 reveals a much smaller peak increase throughout BEV diffusion with a steadier distribution of BEV charging power than uncontrolled charging.

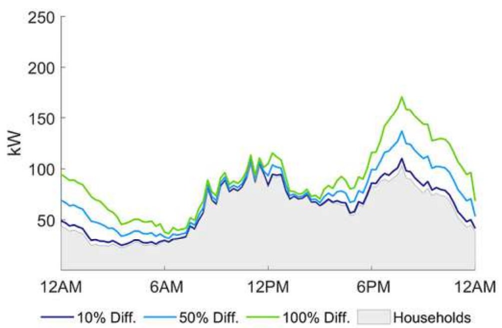

Figure 59 Household load and charging profile applying a low charging capacity (LCC).

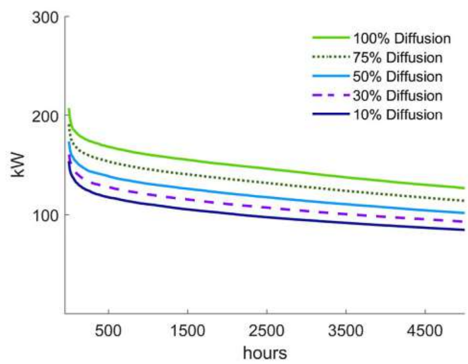

Figure 60 Duration curve applying a low charging capacity (LCC).

The ToU approach achieves the best results in shifting the charging demand away from the HH load peaks (see Figure 61). On average, 81 % of all vehicles charge simultaneously, which is a bit less than with the LCC approach, and again the vehicles charge 15 % of the time they are parked. For both LM approaches, the average charging power consumed per BEV is cut down to 0.24 kW; this is only half that with uncontrolled charging, and the maximum charging power consumed only accounts for 0.67 kW. This proves the greater distribution of BEV charging power with the LM approaches. The duration curve in Figure 62 illustrates the capability of this approach to minimise the impact of e-mobility on electricity demand peaks in the building. Here, an increase of only 4 % was observed in the yearly maximum demand under the full diffusion of BEVs.

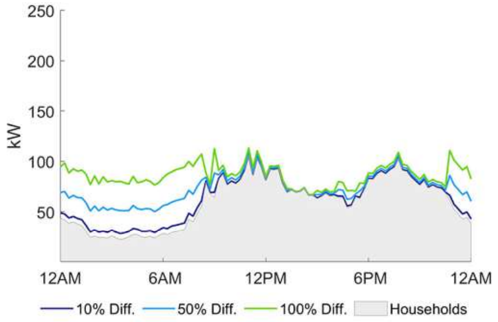

Figure 61 Household load and charging profile applying the time-of-use (ToU) approach.

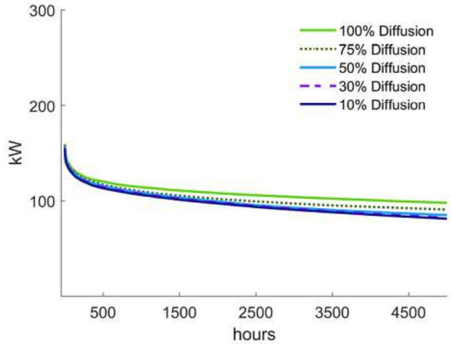

Figure 62 Duration curve applying the ToU approach.

4.4.4. Minimum charging capacity

First, using the approach described in Section 4.3.5, the minimum charging capacity for each BEV is calculated by applying yearly optimisation with full information. The yearly information of charging demand allows for a very efficient dimensioning of charging capacity. A minimum charging capacity of only 0.44 kW/CP must be available. However, charging mainly occurs at home, and public stations cover only 4 % of the BEV power demand. Figure 63 depicts the resulting distribution of BEV charging demand, which largely relies on the availability of BEVs over time.

If daily rolling optimisation is applied, charging can only be carried out based on the information available for one day, without any knowledge of later demand. In our model, less information leads to a substantially higher minimum charging capacity of 1.30 kW/CP. This capacity can result in higher costs for IS implementation. Hence, even foresight into the next day could help provide more flexible charging and integrate important aspects into the LM process, such as a positive weather forecast leading to longer weekend trips or an alignment of charging with renewable power availability. The efficient sizing of charging capacity reduces the risks and costs associated with exceeding the available regional power connection and thus guarantees a fair price to the final user for private charging.

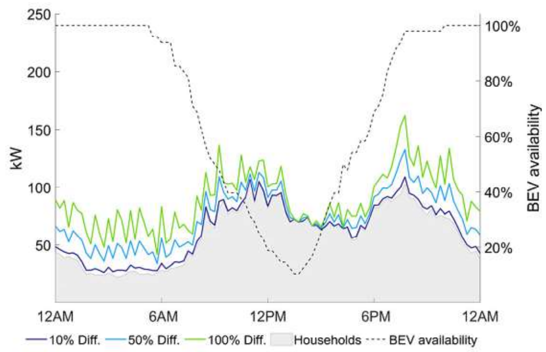

Figure 63 BEV charging demand at the home station under minimum charging capacity.

4.5. Discussion

In this section, the modelling results are discussed, and the environmental implications of e-mobility and the advantages of LM are evaluated in detail.

4.5.1. Impact of LM on BEV charging profiles

Here, the development of each parameter defined in Table 9 for BEV diffusion under the different charging strategies (UC, LCC, and ToU) is discussed. The results are compared to those without e-mobility (see the HH load characteristics in Section 4.4.1). In general, the simultaneity of charging, which indicates how many BEVs charge simultaneously, increases from 9 % under uncontrolled charging to 16 % under both LM approaches. Between uncontrolled charging and the LCC approach, the charging time ratio increases from 50 % to 86 %. Both factors indicate the ability of LM to achieve longer charging periods at lower charging power.

Figure 64 shows that while uncontrolled charging (UC) leads to a rise in the detected yearly maximum electricity demand up to 100 % BEV diffusion of 72 %, reaching 265 kW, a restriction in the charging capacity with the LCC approach already achieves some reductions. With the LCC approach, the maximum demand reaches 207 kW with the full diffusion of BEVs—an increase of 35 %—but it hardly increases until 50 % BEV diffusion. The ToU approach almost manages to keep the electricity demand below the existing HH maximum demand, which only increases by 4 % with full BEV diffusion. This way, e-mobility has hardly any impact on the yearly maximum demand.

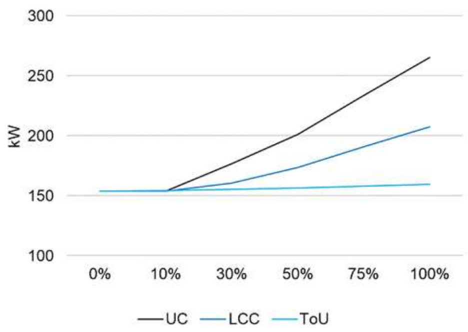

Figure 64 Development of the building's maximum demand.

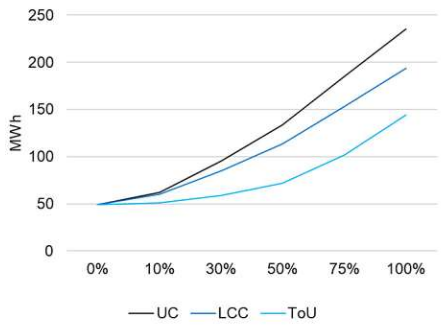

Figure 65 Development of the building's peak volume demand.

The peak volume demand, which represents the sum of the demand above the Q_{70} threshold, rises exponentially for all charging strategies between 50 % and 100 % BEV diffusion (see Figure 65). The uncontrolled scenario leads to a yearly peak volume of 236 MWh up to full BEV diffusion—a fourfold rise compared to no e-mobility. While the LCC still results in a threefold increase up to 193 kWh, the ToU approach achieves a successful shift in BEV charging demand away from the HH load peaks, resulting in a twofold increase in peak volume demand.

Compared to uncontrolled charging, where BEV charging coincides with a higher HH electricity demand, the LCC approach operates at a slower charging speed, leading to an extension of charging times into the load valleys. The most successful load shift into the valleys is achieved by the ToU approach, which is based on this exact objective (see Figure 66). While the demand-minimum does not change through e-mobility in the uncontrolled charging scenario, it increases by 7.5 % with the ToU approach. Similar developments can be observed for the base volume demand below the Q_{70} threshold (see Figure 67). With uncontrolled charging increasing the base volume demand by 20 % toward full BEV diffusion, the LCC approach already leads to an increase of 42 %. The aim of the ToU approach to avoid HH load peaks and shift the demand into the base volume represents the most successful load shifting measure. As a result, the base volume demand increases substantially under this LM strategy up to 551 kWh—a 74 % increase compared to no e-mobility.

Suppose the value of a ToU approach is compared to the situation under uncontrolled charging between 10 % and 100 % BEV diffusion. In that case, a 10–40 % reduction in the maximum demand and a 17–39 % reduction in the peak volume demand were discovered. Toward full BEV diffusion, the minimum demand rises by 56 % with the ToU approach, and the base volume demand increases by 18 % compared to uncontrolled charging, resulting from effective load shifting away from existing HH peaks into valleys. These results represent a substantial reduction in the maximum and peak volume demands caused by e-mobility. Therefore, they could have a significant value related to the sufficiency of the local power connection, distribution grid performance, and the prevention of IS expansion requirements.

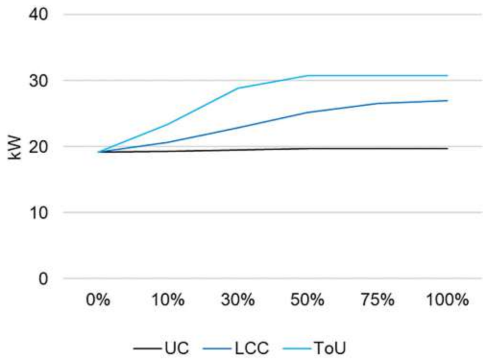

Figure 66 Development of the building's minimum demand

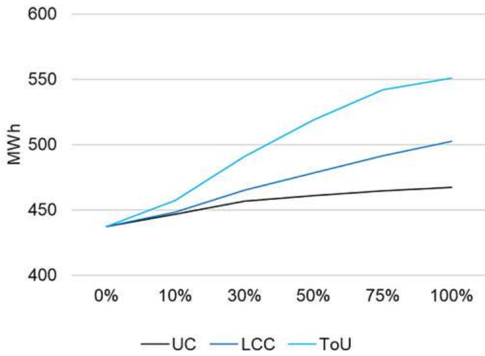

Figure 67 Development of the building's base volume demand

This highlights the importance of LM for the further development of charging solutions. At the same time, fears of the impact of e-mobility on these aspects or scepticism about the sufficient availability of charging points in nearby public or, ideally, private environments is often a reason not to switch from conventional cars to this more environmentally friendly alternative. Therefore, communicating the benefit of LM may help legitimate such solutions in urban, multi-apartment buildings—a decision that needs to be made by the facility owner—and also promote the acceptance of e-mobility among potential users. Thus, overall, the availability of solutions for large-scale charging IS may contribute to the goal of zero-emission mobility.

4.5.2. Verification with the field test results

The field test of the URCHARGE project tested extensions of the LM algorithm over 6 months in a residential area with 50 % e-mobility, where 27 CPs were controlled with LM and 24 were uncontrolled. The project mainly included BEVs of the type Renault Zoe, a few Nissan Leaf, and two Tesla models. Mode 3 charging points with Type 2 chargers were used. Additionally, the customer perspective was analysed with surveys and interviews among the participants. In this real environment, the basic LM approach, enhanced by specific technical functionalities, involves control over the charging capacity across all or single charging stations to avoid exceeding the building's available power connection. Therefore, the charging processes of single vehicles are only interrupted or postponed when the current defined capacity is reached. This largely represents the LCC approach of our model (see Section 4.4.4).

However, the modelled environment cannot fully depict the reality of the relevant technical functionalities. The main differences are described in Table 18 in Appendix B.

The average distance travelled during the field test by the project participants extrapolated to one year would be 11.100 km, slightly below the average of big cities in Austria (except Vienna) of 12.237 km/a (BMVIT, 2016). The customer perspective analysis within the project, carried out through surveys, revealed that this result could be due to the Covid-19 restrictions on daily driving for purposes such as work, visits, and leisure. On the other hand, few have increased their driving to avoid crowds in public transport. The monitoring shows that with an increasing experience, the user reduces the frequency of charging at the private station due to increasing knowledge of the BEV's charging requirements. The average user plugs in every fourth day for about 14 h. The overall charging time ratio related to the total plug-in time in the field test is 50 %, whereas the plug-in to parked time ratio is about 45 %. This results in a charging time ratio related to the parking time of 22.5 %. Our model has an average charging to plug-in time ratio of 9% with uncontrolled and 15 % with ToU charging, which can be explained by the fact that the BEVs are always assumed to be plugged in when parked (100 %). In our model, sometimes, all BEVs are charging at the same time. However, on average, the uncontrolled scenario leads to 50 % of simultaneous charging, and the LCC approach leads to 86 %. The project's field test showed significantly lower simultaneity and charging time. At maximum, 12 BEVs were plugged in at the same time, representing 44 % of all BEVs, and a maximum of 11 BEVs were charging simultaneously (41 %). The average results were 24 % and only 12 %, respectively.

Of course, this is a major difference from our model parameters in which all BEVs are assumed to be available and plugged in at the charging point at any time while parked at home. The average energy consumed during each charging session and BEV is 22 kWh. The plug-in times typically range between 5 and 7 pm and plug-out times between 6 and 7 am. This fact supports the assumption of high flexibility due to long charging periods in private networks. Public charging is used very rarely.

Despite the assumptions in the modelled environment, the conclusions from the field test support the findings in this study. To test the capabilities of the LM functions and the minimum required charging capacity to guarantee the fulfilment of the BEV charging demand, during the field test, the available charging capacity was reduced several times from 35 kW for 27 CPs (1.3 kW/CP) down to 25 kW (0.9 kW/CP). Therefore, the required charging capacity across all CPs could be reduced below the expected level of about 1 kW/CP, and critical situations concerning the power connection capacity would not occur. This matches our analysis in Section 4.4.4 of the minimum charging capacity, which can significantly affect the cost of charging infrastructure.

Figure 68 shows the BEV charging power with an overall initial charging capacity of 35 kW together with the number of cars currently plugged in. In this exemplary period, 31 kW were reached once in the evening, resulting in a significant impact of e-mobility on the overall building load. On the other hand, Figure 69 shows the situation with a reduced overall charging capacity down to 25 kW, which results in longer charging periods and significantly limits the electricity demand peaks. Furthermore, the dependence on the availability of BEVs plugged in at the charging station, which only accounted for 45 % of the parking time in this project, becomes more important under this situation since charging operates much slower. The project experience also revealed that a higher share of plug-in times would improve LM efficiency. In the first week, with 1.3 kW/CP of charging capacity, the building's electricity demand maximum (HH + BEV) increased almost twofold due to e-mobility. Later, with a reduction down to 0.9 kW/CP, the LM successfully operated below this threshold, which reduced this surge.

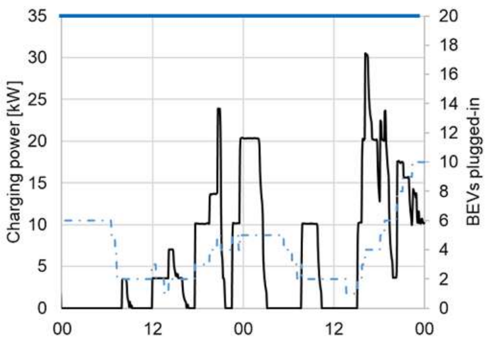

Figure 68 Load management with a maximum charging capacity of 35 kW (1.3 kW/CP).

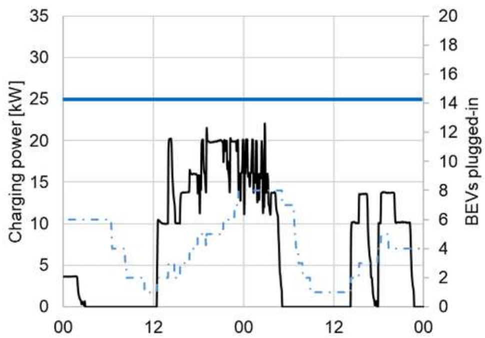

Figure 69 Load management with a maximum charging capacity of 25 kW (0.9 kW/CP).

The users hardly recognised any reduction in charging performance under a reduced capacity. From the field test, it can be expected that LM will enable the coordination of 100 % e-mobility in the residential area with sufficient comfort for the users and without any impact on the distribution grid capacity. As calculated in Section 4.4.4, our model determined a minimum charging capacity of 0.44 kW/CP under a scenario with full information and 1.3 kW/CP with a daily rolling approach, roughly matching the threshold identified in the field test. The capacity gains achieved by the phase-dependent charging currently being developed and tested, as explained in line 6 of Table 18, will lead to more efficient LM.

4.5.3. Economic aspects of LM

The modelling results and the field test data for the new LM functionalities reveal that controlled charging reduces the average grid connection capacity per charging point from about 3.5 kW with uncontrolled charging to about 1-1.3 kW in a managed situation. As a result, the impact on the distribution grid is reduced, and demand peaks and building power connection expansion can be avoided. Figure 70 describes different cases and the resulting overall power connection (PC) required from 0-200 coordinated charging points. Uncontrolled charging w/o LM from the model applied in this work results in PC up to 700 kW for 200 CPs (3.5 kW/CP).

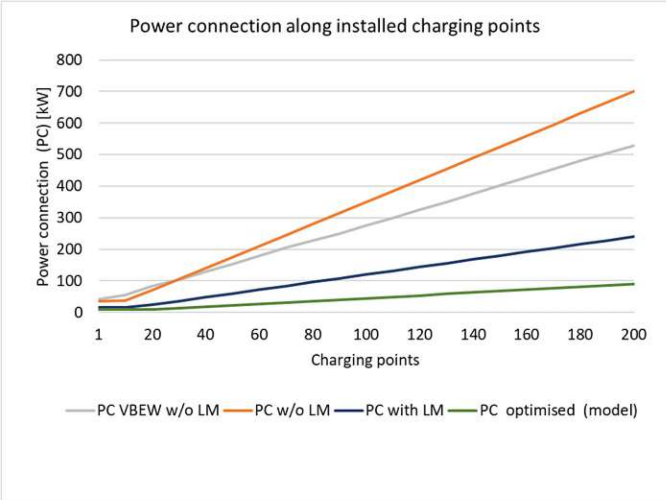

Figure 70 Grid connection capacity up to 200 charging points

The measured PC by VBEW (2019) in an uncontrolled scenario increases up to 520 kW for 200 CPs. LM in the URCHARGE field test reduces the PC to 240 kW for 200 CPs (1.2 kW/CP), and the ideal model environment with full information and yearly optimisation achieves a further decrease to 88 kW (0.44 kW/CP). The optimal model result describes a situation with known charging demand and battery SOC. The gap toward the field test results can only be closed through accurate demand forecasting, e.g. by machine learning, access to the battery state of charge, further standardisation of the vehicles' charging behaviour and incentives for plug-in discipline to provide sufficient flexibility.

4.5.4. Environmental aspects of e-mobility and advantages of LM

All the considerations for minimisation of the capacity requirements have environmental and economic aspects. This section discusses the environmental effects of e-mobility, as well as the advantages of LM and efficient charging capacity sizing.

1. Savings in GHG emissions from the substitution of conventional vehicles with BEVs

In the considered residential area, e-mobility accounts for an increase in the yearly electricity consumption of 13 % with a 30 % BEV share and 43 % with full BEV diffusion, as shown in Figure 71. The development of the yearly CO_2-eq and NOx emissions, as well as particulate matter (PM), through the substitution of conventional cars with BEVs, is shown in Figure 72. All conventional cars in the residential area, considering an Austrian mix of diesel- and petrol-powered engines, emit 268 tCO_2-eq/a. By 2030, Austria aims at a BEV share of 30 %, representing a substitution of 32 conventional cars with BEVs in the residential area.

This would result in 26 % savings in yearly CO_2-eq emissions, accounting for 12 tCO_2-eq and 21 % NOx savings by 2030. However, according to the (UBA, 2018), during their life cycles, BEVs emit more PM than diesel- or petrol-powered combustion engines due to the emissions caused during vehicle and battery construction. This would lead to a 4 % increase in PM emissions for 30 % BEV diffusion. The overall 2030 goal in Austria is a 36 % reduction of CO_2 emissions in transport (BMNT, 2018). Under the aim of increasing public transportation use and decarbonisation and the planned diffusion of BEVs, this goal may be realistic.

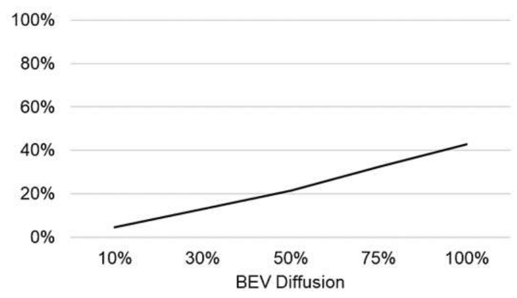

Figure 71 Increase in yearly building electricity demand through e-mobility.

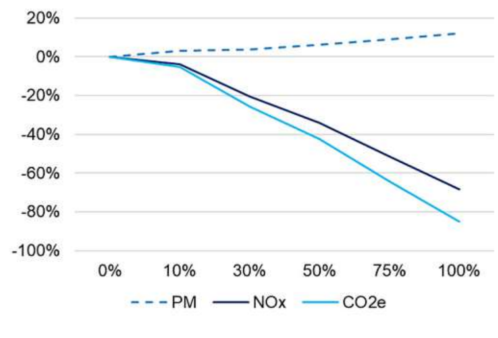

Figure 72 Expected yearly emission development through e-mobility.

2. Impact of LM on the environmental aspects of the electricity mix consumed for charging

Our model provides evidence of the negative environmental impact of electricity demand increases concerning the electricity mix consumed at least from the correlation coefficient between BEV charging and fossil electricity generation (r_{foss}). Whereas uncontrolled charging shows a very weak positive correlation with 0.10 according to Pearson, the ToU approach results in a weak negative correlation of −0.24. It, therefore, seems to increase the use of renewable energy sources (Evans, 1996). Furthermore, an analysis of the Austrian national electricity demand and the amount of national fossil power generation (coal and gas) in 2019 revealed a strong positive correlation between the two of 0.65. Additionally, an average HH load profile shows a moderate correlation with the overall national load profile of 0.49. Therefore, an increase in the building's electricity demand peaks due to e-mobility, as with uncontrolled charging, leads to a negative environmental impact on the electricity mix consumed. LM can control the distribution of charging power to reduce the consumption of fossil fuel electricity generation during demand peaks.

3. Environmental impact of e-mobility and LM on potential grid expansion

The electricity demand profile of BEVs has a widespread impact on the cost and environmental effects related to the required capacity of power connection, the distribution grid, and even electricity generation capacities. A reduction in electricity demand peaks through LM can guarantee the sufficiency of existing distribution grid capacities and thereby prevent the need for expansion investments (van Vliet et al., 2011). Additionally, short-term peaks, apart from the described impacts on the electricity mix and use of flexible fossil power plants, would affect the installed electricity generation capacities. A greater distribution of the overall electricity demand would yield a flatter demand profile and avoid the significant investment costs and associated resource consumption, land use, and emissions from component production.

4.6. Conclusions

The modelling results prove that uncontrolled charging promotes the correlation between BEV electricity demand and HH load peaks. This situation results in a negative impact of growing e-mobility on distribution grid performance and the environmental aspect of the electricity mix consumed while charging. LM is an important solution to control BEV charging demands and reduce this impact to enable successful SC via the direct electrification of BEVs. Under full information, with between 10 % and 100 % BEV diffusion, an off-peak time of use

(ToU) approach can reduce the building's maximum electricity demand between 10 % and 40 % compared to uncontrolled charging. The peak volume demand—the sum of the demand exceeding a certain threshold—can be reduced between 17 % and 39 %. This is partly achieved by a time shift of charging into valleys, a reduction in the charging power consumed, and an associated increase in the charging time periods. As a result, the electricity demand is shifted away from the HH load peaks into the load valleys and increases the former demand minimum. This may result in a modification of known building electricity demand profiles. On the one hand, these profiles could become more even due to the filled valleys. On the other hand, increasing the electrification of a growing amount of applications could result in additional (or new) peaks in the future. While the ToU approach avoids more extreme electricity demand peaks at noon and the evening and represents the most favourable strategy from a grid perspective, it also establishes a negative correlation with fossil fuel based electricity in Austria. From an environmental perspective, charging all available vehicles at noon to exploit the solar electricity generation peak could be another desirable strategy. More investigation on the optimal coordination of VRE availability and charging LM is recommended in the future, also on a regional level, e.g. in energy communities with local renewable electricity generation.

Our study reveals the value of information on user behaviour and BEV energy consumption for LM efficiency. This study calculated the minimum size of the charging capacity required to fulfil the BEV electricity demands in a private charging network. In a yearly optimisation model with full information and assuming that parked BEVs are always plugged in, the minimum charging capacity is 0.44 kW/CP. Less information in a daily rolling optimisation leads to an almost threefold capacity requirement of about 1.3 kW/CP. The URCHARGE field test reveals that the average user plugs in for charging only every fourth day, reducing the flexibility of LM in a real environment. Nevertheless, the charging capacity in the field test was decreased to 0.9 kW/CP, cutting the demand peaks and reducing the impact on the distribution grid. It was decided that 1.3 kW/CP would be sufficient to provide some buffer capacity to guarantee BEV charging with LM. Uncontrolled charging, by contrast, would require more than 3.5 kW/CP, causing substantial investment into local grid capacity connections and the distribution grid.

This study highlights the benefit of using more information to provide longer foresight and flexibility with higher predictability for upcoming BEV charging demands. An electricity provider can collect users' behavioural information and charging preferences via a mobile app. Currently, because the battery state of charge remains unknown to the master station, electricity providers could assign pre-defined charging profiles to single charging points aligned with the user's preferences communicated via an app (charging deadlines, day/night charging, etc.). Efficient LM and charging capacity sizing also have significant positive environmental effects. While 100 % e-mobility increases yearly electricity demands in the residential area by 43 %, the substitution of fossil-fuel-powered vehicles results in substantial reductions in CO_2-eq and NOx emissions over a vehicle's lifecycle. Interestingly, off-peak charging can achieve a negative correlation between fossil fuel electricity generation and BEV electricity consumption, promoting renewable energy sources. Without an increase in peak demand through e-mobility and efficiently sized private charging capacity, not only could the expansion of the distribution grid and power generation capacities be avoided, but the emissions associated with the electricity mix consumed could also be controlled.

In general, our work proves the ability of LM in multi-apartment buildings to solve most of the common challenges associated with distribution grid performance throughout growing BEV diffusion. Implementing this controlled, large-scale, and private charging IS offers vast economic, technical, and environmental advantages compared to more isolated and uncontrolled solutions. First, a private charging network provides substantial advantages to LM due to the high availability of the BEVs at the charging station and the lower time-criticality of charging. Secondly, LM avoids an increase in electricity demand peaks and thus prevents distribution grid expansion and the use of thermal power generation. As a result, the total cost of BEV charging and the environmental impacts can be managed. In the future, for the benefit of the whole energy system in terms of costs and environmental effects, regulatory and market frameworks need to be established to promote the implementation of a charging IS that applies controlled, joint solutions rather than isolated, fast charging options. LM could be enhanced by research on forecasting the relevant parameters, such as weather and traffic conditions, and the optimal integration of renewable energy. Eventually, BEV charging needs to be integrated into an overall system perspective. These are the next steps for future research and development.

5. An economic evaluation of renewable hydrogen generation strategies for the industrial sector

Whereas many applications can be adapted to the direct use of renewable electricity, several processes in the industrial sector will rely on hydrogen as an energy carrier or feedstock, making the industry a hard-to-abate sector concerning GHG reduction. SC through power-to-X technologies enables the conversion of large-scale renewable electricity (wind and solar power) into renewable hydrogen. On-site hydrogen production is often regarded as a low-risk approach to increasing production scales independently of distribution infrastructure. The electrolyser operation options affect the load-dependent electrolyser efficiency and the renewable hydrogen cost. Such strategies have mainly been undiscovered and are compared in this chapter based on a contribution by Ramsebner et al. (2022) that was still under review at the time of completing this thesis.

5.1. State of the art

Renewable gas may provide long-term renewable energy storage and, more critically, an energy source or feedstock for many industrial processes that cannot be electrified directly (Rissman et al., 2020). It, therefore, may represent an essential element for decarbonising CO_2-intensive processes through sector coupling, which allows more flexible use of renewable electricity in all end-consumption sectors (Ramsebner, Haas, Ajanovic, et al., 2021; Tang et al., 2021). Some relevant industrial processes already heavily rely on hydrogen as an input, such as oil refining or ammonia production, with an expected growing trend in the coming years (IEA, 2019). However, so far, 96 % of hydrogen is mainly produced from fossil fuels (natural gas 48 %, fossil oil 30 %, coal 18 %), causing a substantial amount of CO_2 emissions (830 Mt CO_2/a in the industrial sector (Tang et al., 2021)). Renewable hydrogen, produced through water electrolysis, is a promising alternative to decarbonise these processes.

In addition, renewable hydrogen can supply high-temperature heat to other industrial processes (Gerres, Chaves Ávila, et al., 2019; Rissman et al., 2020). For example, in the steel industry, several projects consider replacing the coke-driven blast furnace with an electric arc furnace and the direct reduction of iron ore by renewable hydrogen (H_2) in a direct reduction plant described in Section 2.5.3 (Tlili et al., 2020). The large-scale introduction of renewable hydrogen in the industry will depend on its cost competitiveness, not only with natural gas but also with other low-carbon alternatives (such as biogas or blue hydrogen). Currently, the cost of renewable H_2 production mainly depends on the electrolyser investment cost, the cost of electricity consumption, and the system efficiency, and usually accounts for about 2.5–6 $/kg or 76-181 $/MWh H_2 (Rissman et al., 2020). Natural gas, for example, had an average market price in Europe of 24 $/MWh in 2019 (IEA, 2022). A continuous cost reduction for renewable H_2 needs to be promoted by supportive policies to achieve market penetration (Gerres et al., 2019; Linares et al., 2008; Neuhoff et al., 2019, 2020, 2021).

Several studies, such as Bristowe & Smallbone (2021), Frischmuth & Härtel (2022) and Weidner et al. (2018), have assessed the potential H_2 cost reduction with upscaling of capacities in a central European context. Brändle et al. (2020) estimate the global H_2 production development and supply cost from renewables and natural gas until 2050. Their results show that a substantial cost decrease could drive renewable H_2 towards competitiveness. The authors expect a hydrogen cost decrease for PV and wind connected electrolysis from about 4.0 $/kg in 2020 down to 1.8 $/kg in 2050 in a not too optimistic scenario. Hydrogen production from Qatar or Russia-sourced natural gas is expected to reach 0.4-0.6 $/kg for pyrolysis and 0.95-1.2 $/kg for natural gas reforming (NGR) with carbon capture and storage (CCS) in 2025. If a gas price of 40 $/MWh is assumed this could increase up to about 2.8-3.2 $/kg for pyrolysis or NGR with CCS.

However, these studies mainly focus on large-scale, grid-connected electrolysers. While this centralised production benefits from high production volumes and the pooling of many varying demand profiles, it also relies on an appropriate hydrogen transport and distribution infrastructure. For example, a *Hydrogen Backbone* could be built in Europe using existing and new dedicated H_2 pipelines (A. Wang et al., 2020). An alternative option, which would prove to be more robust in the early stages, would be to produce hydrogen locally in what is termed "hydrogen valleys" or industrial hubs (Tu et al., 2021). This decentralised H_2 production may be beneficial due to the elimination of distribution infrastructure requirements and associated costs as well as the possibility to optimise electricity consumption according to specific demand situations. On the other hand, it poses several challenges, such as coupling H_2 production with industrial demand or optimising the cost of electricity supply, which in turn will affect the cost of the hydrogen produced. Although Matute et al. (2019) observe that a large part of the renewable hydrogen cost depends on the cost of electricity, the potential need for hydrogen storage, the definition of the capacity of the electrolyser and the operation regime will also influence the final cost of the hydrogen delivered to industry to a large extent.

When it comes to the electricity source, Schlund & Theile (2021) define three possibilities of electricity procurement that are applicable. A direct connection with a renewable power plant, an additional link to the public grid for risk management and supply balancing purposes, and a purely grid-connected electrolyser. Sourcing from the grid is convenient due to constant electricity availability, allowing for several H_2 deployment strategies. However, the electricity consumption from the grid requires certification of the consumed amount as renewable electricity, and grid fees need to be considered unless regulations exempt H_2 production plants from paying them. Sourcing electricity from a dedicated renewable power plant would avoid these fees but implies substantial supply variability for the electrolyser and low flexibility in H_2 production (El-Emam & Özcan, 2019). According to Gahleitner (2013), balancing the supply variability requires additional battery storage to match demand reliably. This investment, of course, increases the total cost of H_2 production.

Suppose a high capacity utilisation of the electrolyser is achieved, meaning high full load hours. In that case, the capacity cost per MWh is lower, and electricity consumption becomes the larger share of the levelised cost of hydrogen (LCOH). This significant part of the renewable hydrogen cost is increasingly exposed to market price variability (Machhammer et al., 2016; Schlund & Theile, 2021). However, full load operation requires a constant hydrogen demand or substantial storage capacities, which are not necessarily feasible for industrial hubs. In these cases, hydrogen may be produced according to demand requirements (just-in-time, JIT) or optimising the cost of electricity (which would, in turn, require storing the electricity purchased or the hydrogen[1] produced to fit demand). In both cases, the variable operation of the electrolyser means that the actual conversion efficiencies may be affected. As a result, the capacity optimisation of the electrolyser is not trivial and subject to uncertainty.

5.1.1. Hydrogen supply in the industry

Scientific literature already covers many aspects of renewable H_2 production and its competitiveness with conventional H_2 from the present to the long-term future. Jacobasch et al. (2021) evaluate the long-term economic aspects of low-carbon steelmaking in an industrial context. They name similar studies by Abdul Quader et al. (2016), Fischedick et al. (2014), Joas et al. (2019), and Otto et al. (2017), mainly focusing on the technological development for and competitiveness of renewable steelmaking processes.

[1] For H_2 storage, Gahleitner (2013) finds that the best option is pressure tanks, characterised by low cost and high capacities without the necessity of spending cost and losing efficiency through compression.

Several studies analyse the suitability and cost of different electricity input sources for centralised H_2 production: hydro, PV, wind power plants, or the grid. Mohammadi & Mehrpooya (2018) find that hydropower achieves low production costs, but wind and solar energy are available more widely and support increased H_2 production. Timmerberg et al. (2020) consider a combined wind and photovoltaic (PV) system without grid connection as well as gas combined cycle power plants. The cost of electricity is defined as the LCOE and is input to the model as a constant value. Bhandari & Shah (2021) analyse the cost of decentralised H_2 production in Germany for a set of refuelling stations with a PV power plant as an electricity source. They consider a grid-connected PV power system in which the grid functions as a buffer at times of low solar PV availability. Additionally, an isolated system with additional battery storage to balance electricity feed-in to the electrolyser is analysed. The refuelling station demand already functions as a sort of storage, balancing the PV system's variable electricity supply. Due to the electricity supply from a dedicated plant, there is no electricity price optimisation possible.

Gorre et al. (2020) optimise H_2 storage and methanation capacity by evaluating three different electricity sources to use otherwise curtailed renewable electricity: a PV power plant, grid electricity and a wind power plant. They aim to optimise H_2 storage and methanation capacities to minimise levelised synthetic natural gas production costs. Bertuccioli et al. (2014) point out that the electricity market price variability is a promising characteristic for optimising electricity consumption. Low electricity prices usually coincide with low demand or large amounts of renewable feed-in. In Austria, the hourly correlation in 2018 between wind and PV power feed-in and electricity prices accounted for -0.28. Therefore, optimising industrial processes according to electricity prices seems to be a feasible balancing method. A broad range of work focuses on centralised applications of H_2 production optimisation according to electricity prices. However, such optimisation can only be carried out with a continuous electricity supply from the grid. The economic performance is much more uncertain if the RES plant's variable input needs to be balanced through additional battery storage.

Larscheid et al. (2018) optimise a grid-connected electrolyser for H_2 revenue maximisation and use it for grid congestion management. Fragiacomo & Genovese (2020) allow the P2G plant to receive electricity from local RES plants and the public grid while considering H_2 feed-in into the gas grid and supply for the transport sector. In their study, the authors also apply a power purchase agreement within a range of 50-100 €/MWh for electricity from renewable power plants and the electricity grid cost for grid consumption. They state that the potential of PPAs[2] lies in hedging against market fluctuations.

As may be seen, most studies have focused on large-scale, centralised production of H_2, assuming a constant demand for hydrogen. However, decentralised, on-site production of H_2 is also an interesting possibility, mainly to avoid the upgrading or new construction of hydrogen transport infrastructure. On-site production, or production limited to "hydrogen valleys", has been proposed by Agora Energiewende et al. (2021) as a non-regret, robust way of starting the deployment of this technology and achieving higher production scales to decrease the cost.

There are, however, few investigations into decentralised supply strategies to fulfil local industrial demand. On the decentralised H_2 production level, research offers a selection on the potential of industrial demand side management (iDSM) concerning industrial electricity consumption. DSM requires a shift of production schedules according to electricity prices. These approaches are electricity focused and do not consider storage due to its cost. Arnold & Janssen (2016) define the electrolysis of ammonia as a suitable process for electricity DSM. In a study investigating the potential of iDSM for electricity markets in Germany, Paulus & Borggrefe (2011) identify that electric arc furnaces in steel manufacturing could provide a significant positive reserve capacity by decreasing demand when the electricity system falls short of capacity. Castro et al. (2013) investigate the economic potential of iDSM according to fluctuating energy prices. They find that large-scale, energy-intensive processes may play an important role. Chen et al. (2021) confirm the potential of industrial load shifting.

Apart from the price-based approach where customers respond to the electricity price by exploiting low-priced periods and avoiding production in high-priced periods, Castro et al. (2013) describe an incentive-based program. In that case, electricity can be bought at a lower price if the electricity consumption is contracted ahead of time and the agreed consumption curve is followed as closely as possible. Such an approach can be compared to a power purchase agreement. Often the location of the industrial plant does not allow for a direct connection to a renewable power plant. For spatial decoupling, sourcing from the grid with later certification of renewable electricity is a solution.

Potential demand-side load shifting could provide additional flexibility to decentralised H_2 production and electricity price optimisation. However, Arnold & Janssen (2016) find that the

[2] Power purchase agreements define the delivery of a specific amount of renewable electricity, in this case from a dedicated renewable power plant at a defined price, still with the option to source this amount from the grid and enable certification of green electricity at continuous supply. PPAs furthermore act as a funding support towards investors.

industry players' willingness to participate in DSM is low due to adverse effects on the industrial process. iDSM is an electricity-focused approach that does not allow for the benefit of storage due to the cost. Electricity price optimisation for H_2 production in the industrial sector may harm the production performance but could still represent a cost-competitive scenario.

5.1.2. Electrolyser efficiency and operating range

Current commercially relevant technologies for electrolysis are alkaline (ALK) and proton exchange membrane (PEM) electrolysers. While the ALK electrolyser has already reached technology readiness level 9, the PEM electrolyser has not yet achieved this level for larger capacities (Wulf et al., 2018). The ALK technology is based on a liquid electrolyte to achieve electrochemical reactions, while the PEM electrolyser uses a solid polymer electrolyte conducting positive ions such as protons (Caparrós Mancera et al., 2019). The ALK electrolyser convinces with its maturity, lower investment cost and a higher lifetime of the stack, and has downsides in the longer time response and longer cold start time. The PEM electrolyser has benefits in dynamic operation and partial load performance facing variable operation and disadvantages such as the stack's lower lifetime, the need for platinum group metals and a backlog of maturity (Matute et al., 2019; Wulf et al., 2018). The ALK electrolyser can operate down to 20 % of its installed capacity. The lowest operating range of a PEM electrolyser lies between 0-10 % due to a higher current density achieved with the PEM technology and the solid electrolyte (Caparrós Mancera et al., 2019; Pascuzzi et al., 2016a; Tom Smolinka et al., 2010).

Several references estimate the theoretical maximum conversion efficiency of ALK and PEM electrolysers under different conditions (see Table 12). Experiments with relatively small PV-connected systems, as described by Zini & Tartarini (2009), reveal an efficiency of 62 % for a 5 kW ALK electrolyser and 70 % for a PEM electrolyser. Pascuzzi et al. (2016) analysed a 2.5 kW ALK electrolyser, achieving a maximum energy efficiency of 67 %. Since this study assumes rather large electrolysers for industrial use, maximum efficiency of 70 % is considered appropriate. Tom Smolinka et al. (2010) point out that the electrolyser efficiency increases to a maximum at a specific size of about 100 Nm^3/h. Assuming a higher heating value of hydrogen of 3.54 kWh/m^3 and a conversion efficiency of about 65 %, this represents a 0.5 MW electrolyser (Kopp et al., 2017). The authors claim that this maximum can represent about 85 % system efficiency. Nguyen et al. (2019) assume one average efficiency each for the ALK (62 %) and PEM (64 %) electrolyser irrespective of the implemented size. Kopp et al. (2017) analyse a 6 MW PEM electrolyser and observe a maximum conversion efficiency of 64 %.

Due to its characteristics, the PEM electrolyser provides better performance in the case of electricity price optimisation, implying variable electricity feed-in. It may be worth the additional cost, while the ALK electrolyser is favourable for continuous operation ranges with higher load factors.

Table 12 Theoretical efficiency of PEM and alkaline electrolysers

Reference	ALK	PEM
Zini & Tartarini (2009)	62 %	70 %
Pascuzzi et al. (2016)	67 %	
Tom Smolinka et al. (2010)	85 %	
Nguyen et al. (2019)	62 %	64 %
Kopp et al. (2017)		64 %

Nevertheless, load changes affect temperature and pressure levels and may negatively affect the actual conversion efficiency (Tjarks et al., 2016; Wulf et al., 2018). Specifically, loads below 30 % lead to a much higher energy demand per kWh of hydrogen produced (Bourasseau & Guinot, 2015; Wulf et al., 2018). After a complete shutdown of the electrolyser, the ramp-up causes substantial efficiency losses and takes up to several tens of minutes (Bourasseau & Guinot, 2015). The actual efficiency may, therefore, differ from the theoretical maximum efficiency in Table 12, depending on the load factor. The actual efficiency is a significant aspect modelled in this work and described in Section 5.3.3.1, determining the economic performance of the H_2 production strategies and technology decisions to a large extent.

5.1.3. Techno-economic characteristics

5.1.3.1. Electrolyser investment cost

Available research includes a broad range of estimations for the investment cost per kW electrolyser capacity, especially for short-term development. Figure 73 shows the investment costs gathered from literature for alkaline and PEM electrolysers between 2020 and 2050. For 2020, different types of literature estimated costs for alkaline electrolysers between 370 €/kW in the most optimistic case and 2,600 €/kW in the most pessimistic one. Currently, this is the more established technology, while PEM electrolysers are more expensive, leading to cost estimates between 700 €/kW and 3,700 €/kW in 2020. Long-term projections are characterised by higher uncertainty, but the development towards substantial cost decreases due to technological learning and increasing production volumes is taken for granted. Unfortunately, such long-term projections are scarce in the literature. The investment cost ranges between

250 €/kW in the optimistic case and 800 €/kW or 1,600 €/kW in the pessimistic case for alkaline and PEM electrolysers, respectively.

The CAPEX usually include stack or actual fuel cell cost, the balance of plant (BoP)—including additional electronic equipment apart from the main stack such as sensors, compressors, pumps etc.—and the power supply unit (Matute et al., 2019). In this study, the indirect investment cost is added based on Matute et al. (2019), according to Appendix C. In an analysis by Nguyen et al. (2019), direct and indirect investment cost makes up 28.4 % of the LCOH. The direct cost for the electrolyser represents about 15 % of the LCOH and 55 % of the total investment cost. Nguyen et al. (2019) provide a detailed analysis of the investment cost decrease with increasing electrolyser capacities. Above an installed capacity of 10 MW, the cost seems to stagnate for ALK electrolysers, and the decline visibly slows down for the PEM technology.

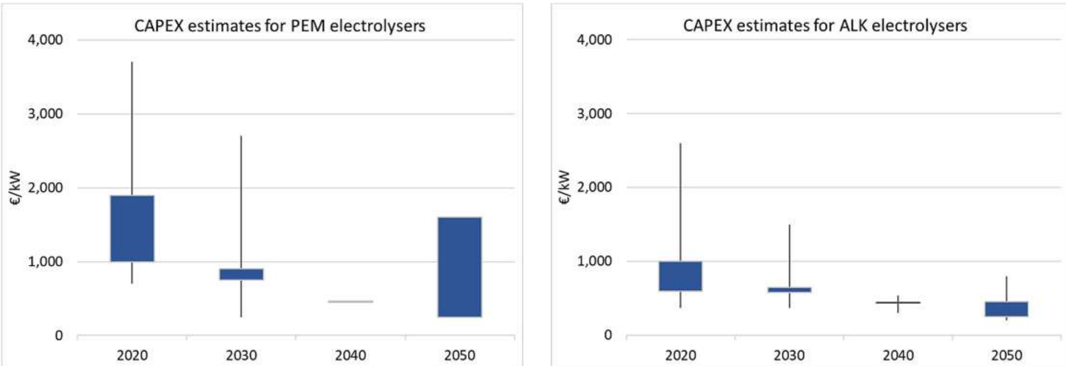

Figure 73 Literature review on PEM electrolyser investment cost (l) and ALK electrolyser investment cost (r) [€/kW]; (Sources: (Bertuccioli et al., 2014; Bhandari & Shah, 2021; Brändle et al., 2020; Brynolf et al., 2018; European Commission (EC), 2020; Gorre et al., 2020; International Energy Agency (IEA), 2019; Machhammer et al., 2016; Mansilla et al., 2012; Parkinson et al., 2019; Tlili et al., 2019, 2020))

5.1.3.2. Electricity prices

Renewable electricity prices are a significant driver of renewable hydrogen production costs. A vast amount of research is available on the expected development of electricity market prices with increasing renewable feed-in. The feed-in of renewables with a negligible marginal cost usually leads to a decrease in the electricity price. However, it needs to be considered that variable renewables need backup or storage, which will set prices based on the merit order approach. With increasing CO_2 prices, spot market prices may therefore increase during the operation of fossil backup capacities and develop a more attractive environment for the sale of renewables on the market and the value of renewables (Hartner, 2016). Furthermore, current turbulence in energy markets shows that global political and health risks causing uncertainties and scarcity can cause significant price increases. Higher electricity market prices, however, will also increase the cost of grid-connected hydrogen production.

If an electrolyser is operated to minimise electricity consumption cost, it will produce hydrogen at low spot market prices, usually implying high renewable feed-in. A more continuous operation cannot account for such aspects. Nevertheless, with a specific renewable electricity contract, a yearly amount of renewable electricity could be sourced decoupled from the time of consumption. A power purchase agreement can provide a basis that even allows for the definition of a fixed electricity price. Additionally, PPAs are considered an alternative support option for renewable power plants for investors. This could be an opportunity to achieve a lower price for electricity consumption. At the same time, market volatility risk can be reduced, the certification of the renewable electricity consumed simplified, and storage avoided.

5.1.3.3. Storage cost

Few references exist on the cost of tank storage for hydrogen, primarily providing cost as €/kg of hydrogen storage capacity. Gorre et al. (2020), for example, assume 490 €/kg hydrogen storage capacity. Since 1 kg of non-pressurised hydrogen corresponds to about 33 kWh, this equals 15 €/kWh, representing the high-cost case (see Figure 74).

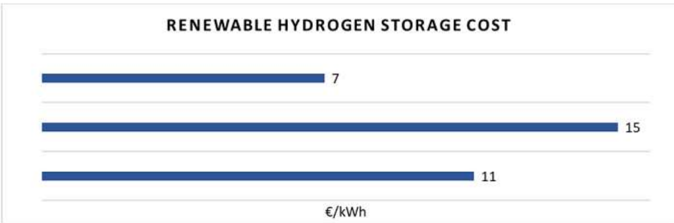

Figure 74 Cost for hydrogen tank storage capacity (Gorre et al., 2020; Tlili et al., 2020)

5.1.3.4. Hydrogen production cost

The analysis of H_2 cost also shows a denser landscape of estimations for the short-term horizon until 2030 than towards 2050 (see Figure 75). Driven by the broad range of scenarios on electrolyser investment cost, H_2 production cost ranges between 36 €/MWh and 220 €/MWh, or 1.3 and 7.3 €/kg, short term. Long-term, with fewer studies available, the production cost range decreases and arrives at 63-88 €/MWh.

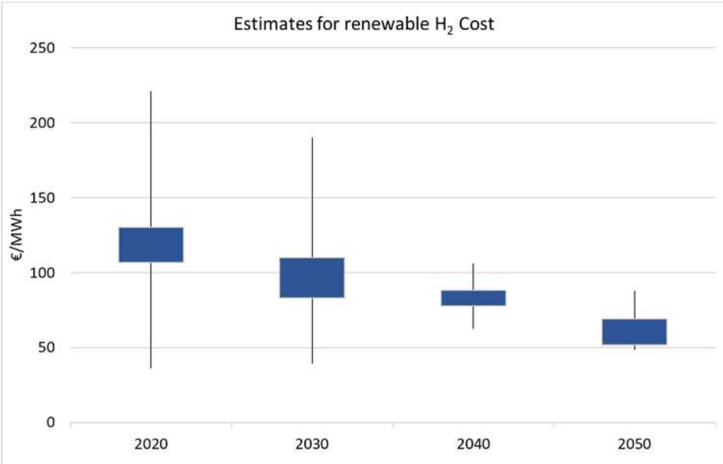

Figure 75 Renewable hydrogen cost estimates from literature (Sources: (Bertuccioli et al., 2014; Bhandari & Shah, 2021; Brändle et al., 2020; Brynolf et al., 2018; European Commission (EC), 2020; Gorre et al., 2020; International Energy Agency (IEA), 2019; Machhammer et al., 2016; Mansilla et al., 2012; Parkinson et al., 2019; Tlili et al., 2019, 2020))

5.2. Core objectives

This contribution assesses the different technical configurations and strategies that may be used to provide renewable hydrogen for the industry by looking at different on-site operation strategies and storage and electrolyser configurations and the implications that these may have for the cost of producing hydrogen in industrial hubs. While the importance and potential of a deep decarbonisation of the industrial sector is evident, the knowledge among companies, analysts and policymakers lags behind the ambitions and specific goals for decarbonisation of other end-consumption sectors such as transport and heating (Bataille, Fischedick et al., 2014b; Loftus et al., 2015)

The cost implications of the following configurations shall be assessed: just-in-time (JIT) production, electricity price optimisation plus storage, and RES island configurations. Two different types of industrial hubs are considered: variable demand, representing a hydrogen valley, and a full-load, constant demand case, which can represent either a constant demand industrial facility or a centralised production scenario. Furthermore, the performance of two electrolyser technologies is compared, alkaline (ALK) and proton-exchange membrane (PEM), given their different efficiencies under variable operation. The cost assessment for these options has not yet been undertaken in the literature but may contribute to making better decisions in deploying renewable hydrogen in industrial hubs.

5.3. Methodology

Depending on the investment cost for the electrolyser and storage capacity as well as the electricity price, the different H_2 supply strategies are compared based on their economic performance, defined by the lowest LCOH. The strategies are compared based on two hypotheses about hydrogen demand. One would be a constant demand, either because of a fixed industrial production (such as a steel production facility) or by the aggregation at the system level (hence a centralised production of hydrogen). The second alternative would be a more variable demand, probably corresponding to a hydrogen valley with a variety of industries demanding hydrogen, and is represented here by the Spanish current industrial high-temperature heat demand. For comparability reasons, both alternatives have normalised to the same yearly H_2 demand and optimised against the Austrian electricity market price in 2019. Exemplary four weeks of hydrogen demand in both cases are shown in Figure 76. Since exemplary demand profiles of total sectors or the industry are used as the main driver of the supply strategy comparison, this work does not represent a feasibility study on the installed plant capacities. The main result is derived from comparing the strategies for the same H_2 demand and electricity price variability.

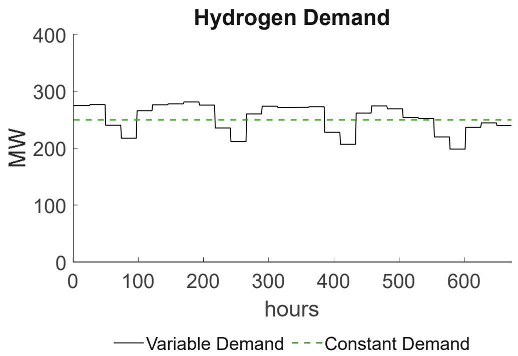

Figure 76 Exemplary 4-week hourly hydrogen demand (continuous and variable case)

The base scenario includes electrolyser CAPEX of 1,500 €/kW and hydrogen storage cost of 15 €/kWh derived from the literature in Section 5.1.3.1. The critical investigation, however, is not the exact overall cost but the difference between the H_2 production strategies based on the same cost parameters. A sensitivity analysis in Section 5.4.3 provides insights into the impact of CAPEX on the strategy comparison.

5.3.1. Hydrogen generation process

Figure 77 describes the H_2 generation process assumed in our research. The electrolyser sources renewable electricity from the grid or a dedicated RES plant to split water (H_2O) into H_2 and oxygen (O_2). The scenarios compare Austrian and Spanish renewable feed-in. H_2 can either directly cover demand or be stored in tanks intermediately.

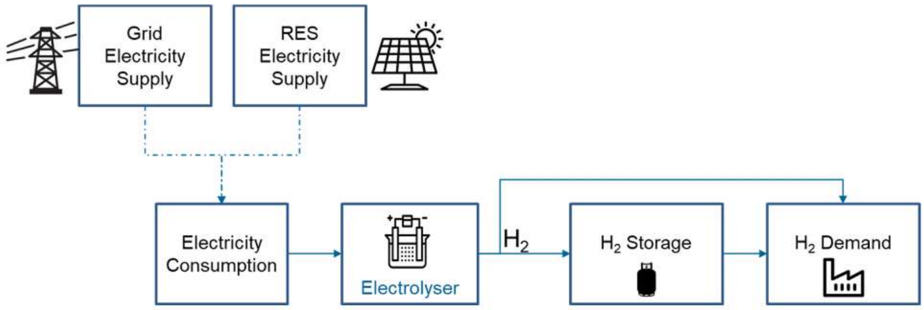

Figure 77 Hydrogen Production process

5.3.2. Hydrogen supply strategies

Grid connected electrolyser:

a) **Electricity price optimisation**: The electrolyser consumes electricity at times of low electricity prices. Hydrogen is stored after transformation to balance against demand. An advantage of this approach is the possibility to exploit low and avoid high electricity prices through hydrogen storage. This approach may require greater electrolyser and storage capacity to increase electricity consumption at low prices but minimises electricity cost. Nevertheless, substantial variability of the electrolyser could reduce actual H_2 production efficiency, and the storage cost must not offset the benefit of price optimisation.

b) **Just in time sourcing:** H_2 is produced JIT and electricity is sourced according to demand. Just-in-time production does not consider any hydrogen storage facility. Depending on the hydrogen demand characteristics, production variability may be negligible. With JIT H_2 production, electricity consumption cost is subject to the electricity price variations.

Island solution – electrolyser connected to a dedicated RES power plant:

This scenario presents the direct connection of the electrolyser to a dedicated wind or PV power plant without any grid support. Electricity supply and H_2 demand are only balanced through hydrogen storage.

The cost of electricity is evaluated based on an average LCOE. Fraunhofer ISE (2021) arrive at an LCOE for isolated PV of about 30 €/MWh and for wind at a minimum of 40 €/MWh. According to IEA (2020) and IRENA (2021), based on an exchange rate of 1/1.2 USD/EUR in 2021, large-scale PV power has an LCOE of about 15-30 €/MWh and wind of 25-37 €/MWh. In this scenario, the electrolyser optimisation depends on the RES availability and storage is used to balance against demand. The RES capacity in the model is minimised to fulfil hydrogen demand.

5.3.3. Optimisation model and data

5.3.3.1. Faraday efficiency

As described in Section 5.1.2, the actual efficiency of an electrolyser can be lower than the theoretical maximum efficiency at lower loads. Therefore, the model aims to consider this dynamic actual efficiency. The Faraday efficiency (η_{fa}) in Eq. (20) describes the share of the actual efficiency (η_{ac}) based on the theoretical maximum efficiency (η_{th}) and decreases with a declining load factor (r_h) (Pascuzzi et al., 2016a).

$$\eta_{fa}(r_h) = \frac{\eta_{ac}}{\eta_{th}} \tag{20}$$

The load factor (r_h) represents the share of electricity consumption (P_{con}^{el}) on installed electrolyser capacity (P_{Ely}^{el}) and is described in Eq. (21). The maximum electricity input defines the electrolyser capacity.

$$r_h = \frac{P_{con}^{ele}}{P_{Ely}^{el}} \tag{21}$$

The Faraday efficiency is different for the PEM and the ALK electrolyser, with the first performing better at lower loads. This work will compare the hydrogen supply strategies with both technologies and their respective efficiencies.

a. PEM electrolyser

The Faraday efficiency of PEM electrolysers remains more stable at lower load factors than that of ALK electrolysers (Tijani & Rahim, 2016; Yodwong et al., 2020). Assuming that the maximum current density of 200 mA.cm^{-2} in both studies represents a load factor of one, the Faraday efficiency evolves according to Figure 78. This relationship can be modelled with one single curve. The theoretical efficiency is defined as 70 %. The faradic efficiency is therefore 100 % once the effective efficiency reaches the theoretical maximum of 70 %.

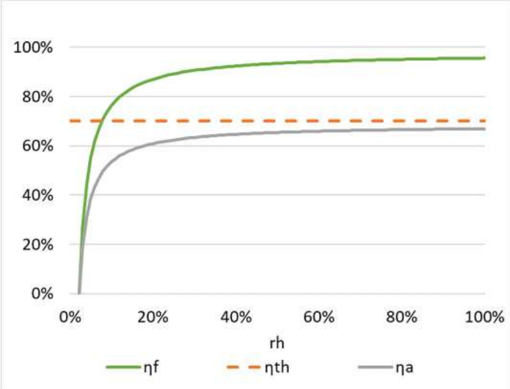

Figure 78 Faraday efficiency of a PEM electrolyser (Tijani & Rahim, 2016; Yodwong et al., 2020); actual efficiency (η_{ac}), theoretical efficiency(η_{th}), Faraday efficiency(η_{fa})

The actual efficiency is calculated as additional losses at certain load factors. This is the reason for the initial optimisation of the electrolyser capacity on which the load factor depends. The absolute additional loss can be modelled as a linear function in which a specific utilisation rate causes a certain absolute additional efficiency loss in MWh (see Figure 79). Due to the relatively low losses at low loads with a PEM electrolyser, the **absolute** losses increase with higher utilisation. Nevertheless, the relative loss compared to the electricity consumption decreases as expected (see Figure 80). This curve indicates the loss that leads to decreased Faraday efficiency at lower loads in Figure 78.

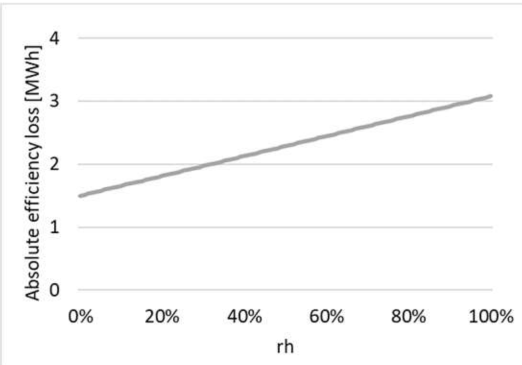

Figure 79 Absolute additional hourly efficiency loss at a particular load factor (for an exemplary PEM electrolyser capacity of 100 MW)

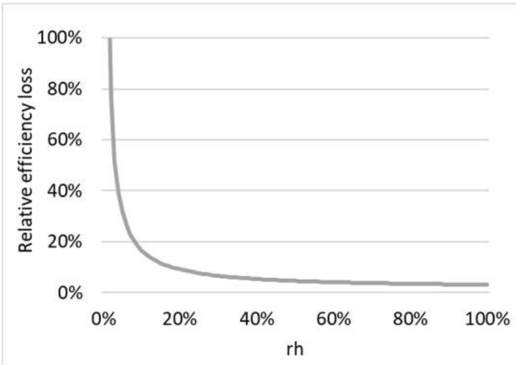

Figure 80 Additional efficiency loss at a particular load factor related to the electricity consumption (for an exemplary PEM electrolyser capacity of 100 MW)

b. ALK electrolyser

Pascuzzi et al. (2016) provide a detailed analysis of the actual efficiency of an ALK electrolyser and measured data on the faradic efficiency. Figure 81 shows the theoretical and the observed actual and faradic efficiency relative to the electrolyser load factor. Since a stop of the electrolyser and a cold restart comes at substantial efficiency losses, also zero operation leads to losses of 0.25 % of installed capacity in the model. Mohanpurkar et al. (2017) provide a similar analysis of the decreasing effective efficiency with decreasing loads.

Replicating the observations from Pascuzzi et al. (2016) across the whole load factor range from 0-1 requires two modelled curves with differing gradients for loads below and above the factor 0.36 (see Figure 82). JIT production, however, only causes a minimum load factor of 0.39 with variable demand in the hydrogen valley case study. In that case, the blue curve is sufficient, and no MILP model is required to switch between the two curves based on the load factor.

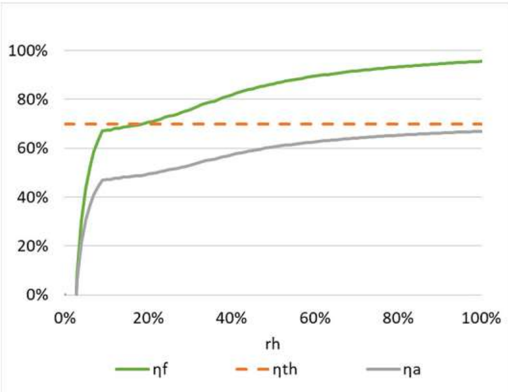

Figure 81 Faraday efficiency of an alkaline electrolyser (Pascuzzi et al., 2016a)

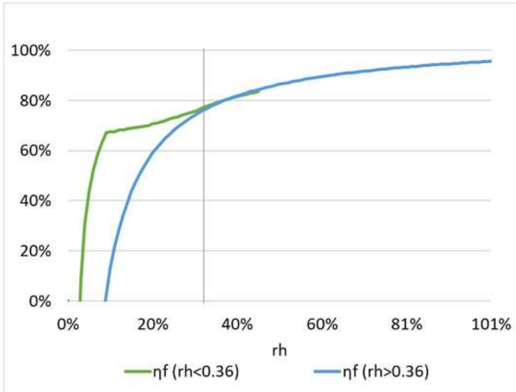

Figure 82 Replication of the Faraday efficiency for an ALK electrolyser based on the load factor

To match the overall Faraday efficiency for ALK electrolysers, the additional loss is also modelled by two functions in which a specific utilisation rate causes a certain absolute additional efficiency loss in MWh Figure 83 shows the two curves and compared to the PEM efficiency losses shown earlier. The function ALK1 is approximated manually and modelled with integers to achieve the desired Faraday-efficiency curve. Function ALK2 represents a linear function that can be input to the model. The absolute losses at very low loads are substantial with the ALK technology and must increase even with increasing electrolyser utilisation. The relative efficiency losses, however, decrease with increasing loads (see Figure 84)

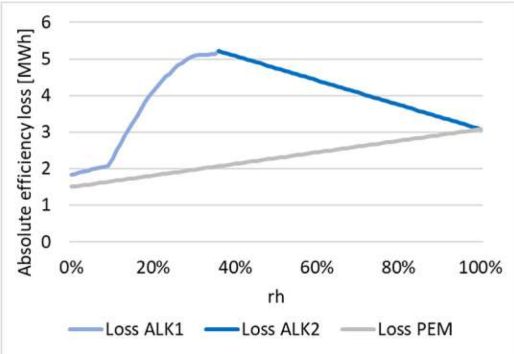

Figure 83 Absolute additional efficiency loss at a particular load factor (for an exemplary ALK electrolyser capacity of 100 MW) compared to the PEM electrolyser

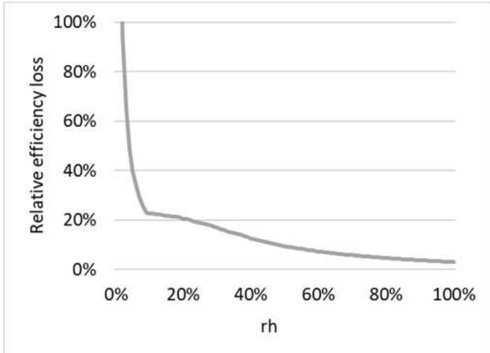

Figure 84 Additional efficiency loss at a particular load factor related to the electricity consumption (for an exemplary ALK electrolyser capacity of 100 MW)

5.3.3.2. Optimisation model

The optimisation model aims to minimise the levelised cost of hydrogen and potential storage (LCOH&S) depending on investment cost, the variable cost for electricity consumption, and the Faraday efficiency. The interdependency of the Faraday efficiency with the load factor based on the installed capacity always leads to a non-linear optimisation. Therefore, the optimisation model is set up as a two-stage optimisation similar to Luo et al. (2020) (see Figure 85). Determining the electrolyser capacity in the first step enables consideration of a dynamic Faraday efficiency depending on the load factor in the second step.

The first iteration optimises the electrolyser capacity by minimising the LCOH&S, including CAPEX (€/kW installed capacity), the electricity spot market price, an estimated overall efficiency, plus additional cost for taxes and electricity fees, and storage cost. This specific electrolyser capacity is then equally used for the respective strategy for ALK and PEM electrolysers. The optimisation is based on grid or RES electricity supply. The available electricity supply is, therefore, a constraint. In the case of just-in-time production, the electrolyser capacity (P_{ely}^{el}) is designed to match the maximum hydrogen demand ($P_{con}^{H_2}$). The Faraday efficiency is first estimated based on the expected load factor range in the chosen production strategy and can only be calculated precisely in the second step. The resulting installed capacity will differ for variable and continuous H_2 demand.

$$P_{ely}^{el} = \frac{max(P_{con}^{H_2})}{\eta_{th}\,\eta_{fa(r_h)}} \qquad (22)$$

The second iteration determines the LCOH using the electrolyser capacity from step one as a constraint and considering efficiency losses depending on the load factor according to Section 5.3.3.1. The model aims at minimising the LCOH&S for the respective operation strategy. This is achieved in two steps: the optimisation of the electrolyser—and in the island case, the renewable capacity—followed by the electrolyser and hydrogen storage operation. More details about the model can be found in Appendix C.

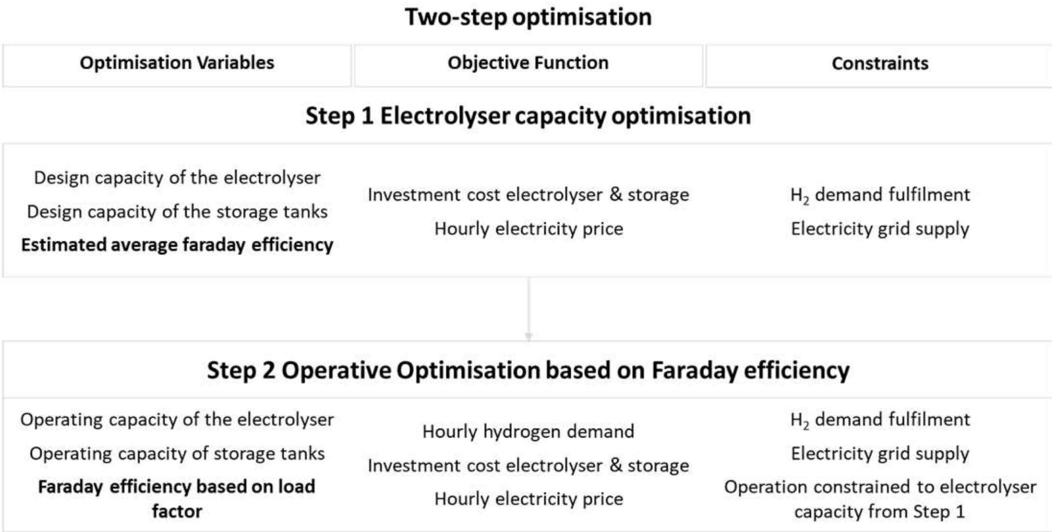

Figure 85 Two-step optimisation framework

5.4. Results

First, the base scenario is presented, assuming an electrolyser investment cost of 1,500 €/kW and a medium storage cost of 15 €/kWh. These results are outlined for the different supply strategies described in Section 5.3.2 in two parts: variable demand in a hydrogen valley and constant demand in centralised or facility-specific H_2 production. The operation strategies include a PEM electrolyser directly connected to a PV or wind power plant in Austria or Spain, a grid-connected PEM or ALK electrolyser with electricity price optimisation, and JIT production exposed to the Austrian electricity price of 2019. The consequent actual efficiencies described in the methodology were considered for each case.

Only PEM electrolysers were considered for electricity feed-in from a renewable power plant. The highly variable electricity feed-in and the consequent losses during low loads do not make the ALK electrolyser a feasible technology. Even with the more flexible technology, a certain amount of electricity storage had to be implemented with the PV and wind power plant to cover the losses due to the supply variability. In the grid-connected scenarios, an equal investment cost was assumed for the ALK and PEM electrolyser for comparability reasons. In reality, however, the ALK electrolyser is currently available at a lower cost than the PEM technology due to its maturity. This situation is expected to remain until 2040 (see Section 5.1.3.1). After a more detailed discussion of the results for the variable and constant demand alternatives, a sensitivity analysis considers a broader range of scenarios in terms of investment cost and the effect on hydrogen production cost.

5.4.1. Base scenario

5.4.1.1. Constant demand

Constant demand is similar to centralised bulk H_2 production through demand pooling. Figure 86 describes the resulting renewable hydrogen production cost per MWh ordered from highest to lowest. For better visibility of the low-cost scenarios, the higher-cost scenarios have been compressed between 150 and 500 €/MWh. The results show that direct electricity feed-in from a dedicated PV power plant results in up to five-fold hydrogen production cost per MWh compared to a grid-connected case based on 2019 spot market prices. The latter leads to an H_2 cost of 107.5 €/MWh with price optimisation and 105 €/MWh producing JIT. PV power generation is characterised by long periods of zero availability, requiring daily ramp down and restart of the electrolyser causing substantial efficiency losses and additional capacity needs along the supply chain from RES supply to hydrogen storage. In addition, and to minimise these efficiency losses, the model installed electricity storage of 17 % of the PV capacity to cover hydrogen demand, proving the findings by Gahleitner (2013) mentioned in Section 5.1. The RES and battery storage capacity were minimised to fulfil hydrogen demand. The primary balancing tool is hydrogen storage.

The Spanish hourly wind generation profile of 2019 is characterised by a lower variance and higher mean availability. Spanish wind availability hardly requires any battery storage and seems to provide a more stable electricity supply to achieve costs closer to a grid-connected case. With the Austrian wind profile, however, the size of the electricity storage installed by the model is 22 % of the RES capacity. Figure 87 shows the required RES capacity to fulfil demand from a PV or wind power plant with the Spanish or Austrian renewable profile. Since the presented case studies are characterised by national or sector-wide H_2 demand and our goal is not to aim for a feasibility study, capacities are related to the scenario with the largest installed capacity—the so-called reference capacity—which represents 100 %. This refers to the Austrian PV-powered case for RES capacity, while the other RES-powered scenarios operate at 60-40 % of this reference capacity.

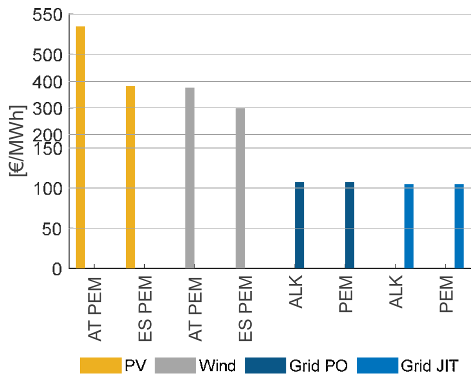

Figure 86 Renewable hydrogen production cost with constant demand; price optimisation (PO), Just in Time (JIT); Austrian renewable profile (AT), Spanish renewable profile (ES)

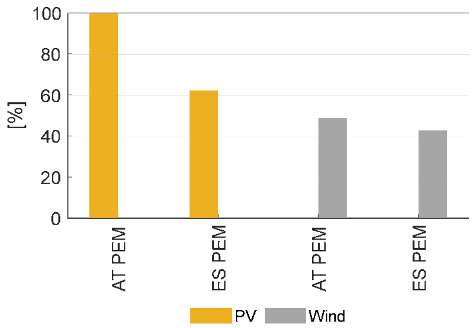

Figure 87 Relative RES capacity with constant demand; Austrian renewable profile (AT), Spanish renewable profile (ES)

The cost of electricity from RES plants is considered as a fixed LCOE from the literature and does not vary according to the optimal PV or wind power capacity. PV capacity needs to be between 17-30 % and wind capacity about 7 % higher than electrolyser capacity to fulfil demand. Nevertheless, even the most promising RES case with a Spanish wind power profile leads to a 178 % higher cost (299.0 €/MWh H_2) than a grid-connected JIT scenario. The lower costs for electricity consumption from the PV or wind power plant with an LCOE of 26 €/MWh and 36 €/MWh compared to the average Austrian electricity market price in 2019 of about 40 €/MWh cannot fully compensate for the additional capacity investment required.

The electrolyser capacity for each production strategy relative to the largest installed reference capacity is described in Figure 88. Electrolyser capacity also needs to be higher for renewable electricity feed-in than with constant grid supply. The reference capacity refers to Austria's PV-connected case characterised by high supply variability. With wind power, electrolyser capacity can be reduced to about 50 %, and in the grid-connected case, only 20 % of the reference capacity is still required. The full load hours account for about 2,000 with RES feed-in, while more than 8,600 can be reached in a grid-connected JIT scenario.

In this work, intermittent electricity feed-in or consumption is mainly compensated by hydrogen storage. The hydrogen storage capacity for each production strategy is presented relative to the largest installed capacity in Figure 89. It is substantially higher for the renewable electricity feed-in than for the grid-connected scenario. The highest hydrogen storage capacities are required for PV-connected electrolysis in Austria, marking the reference capacity at 100 %. The characteristics of Spanish PV or Austrian wind power reduce the capacity needs to about 70 % and Spanish wind power to 45 %.

The grid-connected production strategies only require 0.18 % of the reference capacity. A deeper analysis of the grid-connected scenarios indicates that the lowest hydrogen production cost can be achieved with JIT production. In this case, full operation throughout the year with full load hours of almost 8,700 can be achieved, representing full utilisation of the electrolyser capacity investment. Exposure to the electricity market price does not harm these effects that maximise the Faraday efficiency while refraining from storage.

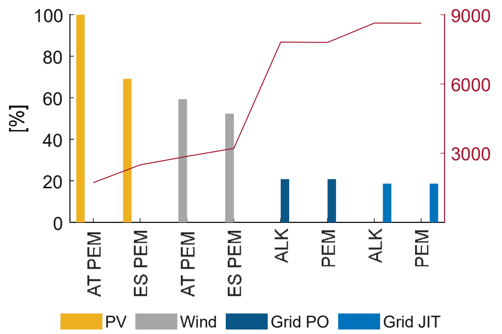

Figure 88 Relative electrolyser capacity and FLH with constant demand; price optimisation (PO), Just in Time (JIT), Austrian renewable profile (AT), Spanish renewable profile (ES)

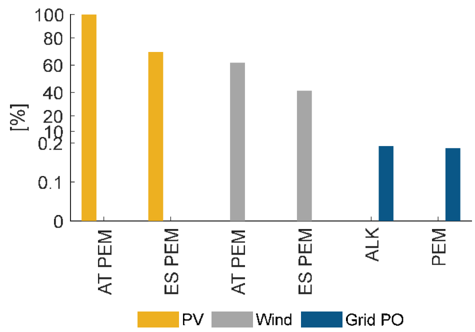

Figure 89 Relative hydrogen storage capacity with constant demand; price optimisation (PO), Austrian renewable profile (AT), Spanish renewable profile (ES)

5.4.1.2. Variable demand

Variable hydrogen demand can be more realistic in a situation of decentralised H_2 production for a specific industry or group of industries characterised by variable operation. Figure 90 describes the renewable hydrogen production cost per MWh for each strategy ordered from highest to lowest. The results have again been compressed between 150 and 500 €/MWh to improve visibility. The hydrogen production cost from a dedicated PV power plant of 525.7 €/MWh is almost 4.8 times higher than with a grid-connected electricity price optimisation based on the 2019 spot market price (109.7 €/MWh). Electricity storage of 17 % of PV capacity was required to cover hydrogen demand. If electricity is sourced directly from a wind power plant, the electricity storage needs to increase to 30 % of the installed wind capacity when the Austrian renewable profile is used. The Spanish wind availability hardly requires any battery storage (only 2 % of RES capacity). It seems to provide a more stable electricity supply to achieve costs closer to a grid-connected case.

Figure 91 shows the required RES capacity to fulfil demand from a PV or wind power plant with the Spanish or Austrian renewable profile. The results are very similar to the constant demand case. The capacities are again related to the largest installed capacity—the so-called reference capacity—which represents 100 %. This refers to the Austrian PV-powered case, while the other RES-powered scenarios operate at 60-40 % of this reference capacity. With variable demand, direct electricity sourcing from a wind power plant in Spain still causes a 159 % higher cost (283.6 €/MWh H_2) than in a grid-connected scenario. PV capacity needs to be between 17-30 % and wind capacity about 7 % higher than the electrolyser capacity to fulfil demand.

The electrolyser capacity for each production strategy relative to the most extensive installed reference capacity in Figure 92 shows the difference between scenarios with renewable electricity feed-in and constant grid supply. The reference capacity is represented by Austria's PV-connected case, whereas grid-connection reduces capacity requirements to about 21 %. It is, however, interesting that H_2 production with a JIT approach is slightly more expensive than electricity price optimisation, according to Figure 90, despite featuring a marginally lower electrolyser capacity and higher full load hours. Hence, electricity price optimisation successfully reduces the cost of electricity consumption to achieve a lower overall LCOH&S. This is even true irrespective of the chosen electrolyser technology. With variable hydrogen demand, full load hours of a maximum of 7,490 can be achieved through JIT production.

The hydrogen storage capacity for each production strategy relative to the largest installed capacity is described in Figure 93. PV-connected electrolysis in Austria requires the highest hydrogen storage capacities, followed by Spanish PV or Austrian wind power feed-in and Spanish wind connection, not differing much from the constant demand case with about 70 % and 45 %, respectively. The grid-connected production strategies only require 0.19 % of the reference capacity.

A closer look at the grid-connected scenarios reveals that based on the electricity price of 2019, the lowest hydrogen production cost can be achieved through electricity price optimisation. The cost decrease through arbitrage on electricity consumption exceeds the additional investment into electrolyser and storage capacities. Nevertheless, the benefit is almost negligible, with a 0.9 or 1.3 €/MWh cost decrease for the PEM and ALK technology representing 0.8-1.2 %.

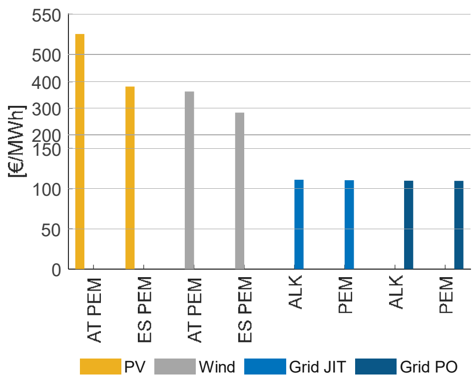

Figure 90 Renewable hydrogen production cost with variable demand for different operation strategies; price optimisation (PO), Just in Time (JIT), Austrian renewable profile (AT), Spanish renewable profile (ES)

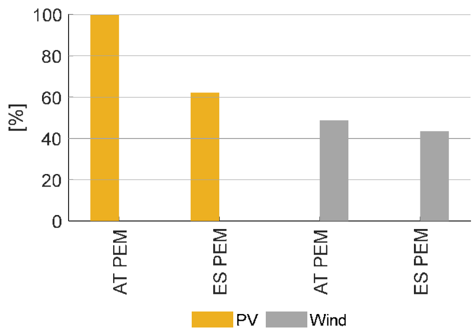

Figure 91 Relative RES capacity with variable demand for different operation strategies; Austrian renewable profile (AT), Spanish renewable profile (ES)

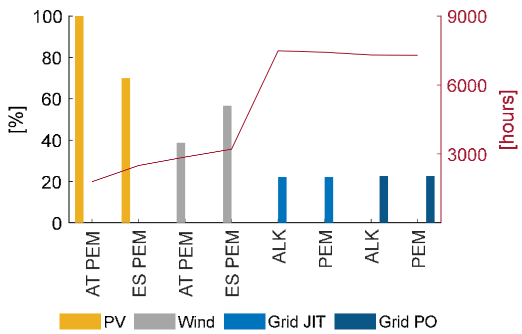

Figure 92 Relative electrolyser capacity and FLH with variable demand for different operation strategies; *price optimisation (PO), Just in Time (JIT), Austrian renewable profile (AT), Spanish renewable profile (ES)*

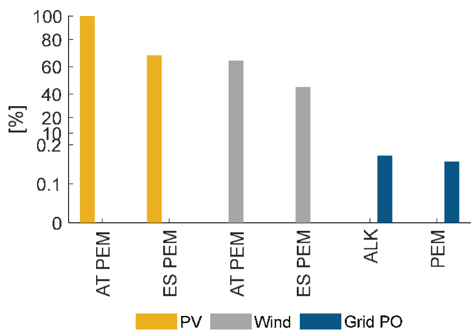

Figure 93 Hydrogen storage capacity with variable demand for different operation strategies; *price optimisation (PO), Austrian renewable profile (AT), Spanish renewable profile (ES)*

5.4.2. Discussion on the base scenario

In general, constant hydrogen demand allows for a lower hydrogen production cost than variable demand due to the more efficient use of the capacity of the electrolyser (see Figure 88 and Figure 92 in Section 5.4.1.2). If demand is more variable, electricity price optimisation and storage achieve lower costs than JIT production. The PEM technology usually leads to lower hydrogen production costs than the ALK electrolyser—due to better performance at lower loads—when assuming the same electrolyser investment costs. However, since the ALK technology is more mature and currently cheaper, and electrolyser investment cost represents a significant cost aspect of hydrogen production, the ALK electrolyser has an economic advantage for grid-connected scenarios.

In RES-connected scenarios, the renewable electricity profile is the primary cost driver. For example, while using PV power is more expensive with the Austrian PV profile than the Spanish one—a logical conclusion due to the climate characteristics (see (Ramsebner, Linares, et al., 2021a))—the results do not differ much between constant and variable demand.

With grid connection, JIT is 5.4 % and electricity price optimisation 2.1 % more expensive than in a constant demand situation with about 111.0 € and 109.7 €, respectively. Electrolyser capacity requirements shown in Figure 92 are higher with variable demand: about 7 % for price optimisation and 16 % for JIT production. Since, with JIT production, the electrolyser capacity needs to correspond to maximum demand, variable hydrogen demand does not enable full utilisation, which causes lower full load hours, leading to a higher cost per MWh (Figure 92). It is interesting to see that with variable hydrogen demand, JIT production becomes more expensive than electricity price optimisation (see Figure 90) even if the full load hours, as described in Figure 92, are higher in a JIT approach (7,450) compared to price optimisation (7,300). In this case, electricity price arbitrage is sufficient to decrease hydrogen production costs. In the constant demand case, JIT achieved full load hours of more than 8,600 - driving the low-cost result. Variable demand leads to slightly higher H_2 storage capacity needs than constant demand in grid-connected scenarios. Therefore, the hydrogen storage capacity cost, according to Figure 93, also seems to be a minor cost driver.

Apart from the cost aspect, the decision on a specific H_2 generation strategy may also have a certain impact on the overall energy system if H_2 production becomes a significant part of electricity demand. Sourcing electricity directly from the electricity grid, on the one hand, imposes specific grid infrastructure requirements to guarantee stability with the connection of an additional consumer. On the other hand, optimisation based on electricity prices is a form of demand response that can help manage better the whole power system.

5.4.3. Sensitivity analysis

Electricity cost

Exposure to market prices entails risks, such as mid- to long-term price increases. The average Austrian electricity market price of 2019 used in the scenarios accounted for 40.2 €/MWh (APG, 2022b) plus a grid access tariff of 1.2 €/MWh. The electricity directly sourced from the PV power plant costs 26 €/MWh and from the wind power plant 36 €/MWh, without any additional connection cost. However, the results revealed cheaper H_2 production with grid-connected strategies than RES-based electrolysis because of the impact of variable operation on electrolyser efficiency. The current market situation, with an average electricity price in Austria that surged to 109 €/MWh in 2021 and even reached 207 €/MWh at the end of May 2022 (APG, 2022b), would, however, support the competitiveness of direct sourcing from a renewable plant instead of being exposed to the market price.

Lifting the 2019 spot market price to an average electricity price of 150 €/MWh would result in hydrogen production costs of 267 €/MWh with JIT production in the constant demand base scenario. This would almost make the wind power-connected scenario competitive, which, at least in Spain, could be achieved with a reasonably low RES capacity effort at 283 €/MWh for variable demand (see Figure 86). An average electricity market price of 250 €/MWh would lead to a hydrogen production cost of 414 €/MWh with JIT production. In this situation, even a dedicated PV power plant in Spain would become cost-competitive with the grid-connected case at 380 €/MWh.

Power purchase agreements might be a favourable solution for risk minimisation that combines both stable electricity supply and fixed price**s**. Since the results for grid-connected JIT operation are very promising in this study, a favourable PPA could lead to a further H_2 cost reduction. As a result, JIT could become more convenient and economically feasible in the variable demand case than electricity price optimisation. With this solution, renewable electricity generation can be decoupled from demand through the electricity grid. If a favourable PPA price can be agreed upon for the upcoming years, potential market price increases can be avoided, and H_2 production costs can be further decreased.

Demand access fee

A demand access fee for grid-connected electrolyser could deteriorate the economic performance compared to direct renewable feed-in. This cost for the maximum power capacity sourced from the grid has been exempt for electrolyser operation since it represents a significant financial barrier to variable operation.

Impact of electrolyser and storage investment cost on LCOH&S

Reduced electrolyser investment cost enables more vigorous exploitation of the electricity price variability with higher electricity consumption ranges. Paired with low hydrogen storage cost, this effect is even more substantial. In the base case, for constant demand, JIT is cheaper than electricity price optimisation. However, electricity price optimisation could be cheaper than JIT production once the electrolyser investment cost falls below 500 €/kW. Under this assumption, the cost impact of larger electrolyser capacities is lower, and arbitrage can be exploited to a greater extent with larger production ranges. Storage costs below 15 €/kWh can further support this. However, such a significant price decrease is only expected to be likely after 2040 (see Section 5.1.3.1). Above 500 €/kW electrolyser capacity cost, JIT production is the cheapest H_2 generation approach for constant demand. For variable demand, JIT is more expensive than electricity price optimisation for all scenarios, with storage costs between 2-24 €/kWh and electrolyser investment costs between 250 €/kW and 3,000 €/kW.

Figure 94 and Figure 95 show an exemplary optimisation week with low or high investment costs. In the low-cost scenario, the optimal electrolyser capacity is more significant, and hydrogen production varies more to exploit electricity prices. In the scenario with higher investment cost, however, the production range is reduced to minimise the investment cost share in the LCOH&S. Maximum electricity consumption, which is limited by the electrolyser capacity, is reduced by about 50 % in the high compared to the low-cost scenario.

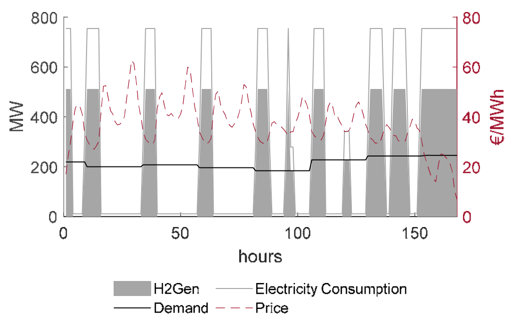

Figure 94 Exemplary week electricity price optimisation at 250 €/kW electrolyser investment cost and low storage cost

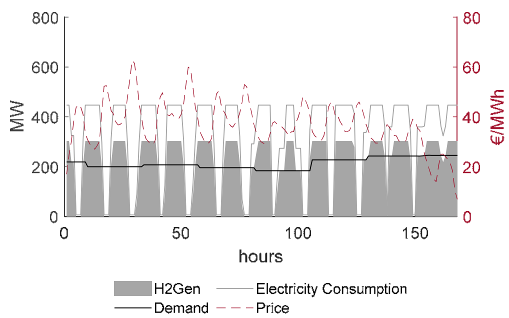

Figure 95 Exemplary week electricity price optimisation at 3,000 €/kW electrolyser investment cost and high storage cos

Additional analyses reveal that the electrolyser investment cost makes up a much larger part of the cost per MWh than the storage cost. The electrolyser capacity cost, therefore, has a major impact on the operation configuration. As described in Figure 96, related to the yearly demand, the impact of storage on the cost per MWh of hydrogen demand is minimal and, within the assumptions of this work, accounts for less than 2 % of the hydrogen LCOH&S. Not every hydrogen unit is stored, but part of it is directly used. Electrolyser investment costs, however, are a primary driver of hydrogen cost. This raises the question of why storage is not used more extensively to exploit electricity variability more and reduce hydrogen production costs. The reason is that such an increase in operation variability would also require even higher electrolyser capacities installed. This additional cost cannot offset the benefits of arbitrage.

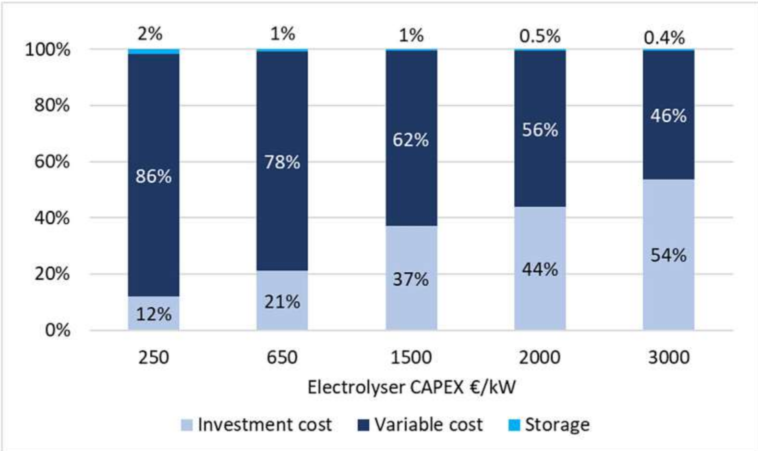

Figure 96 Electricity and investment cost share of hydrogen production cost for constant demand

Up to 2,000 €/kW electrolyser investment cost, the variable cost based on electricity consumption makes up the largest share of hydrogen production cost. At 250 €/kW, the investment cost only makes up 12 % of the overall hydrogen production cost despite the higher installed capacity for arbitrage reasons. At the same storage capacity cost in the base case of 15 €/kWh, 83 % lower electrolyser investment cost achieves only 5 % lower electricity consumption cost per MWh due to higher arbitrage exploitation. In comparison, the investment cost per MWh decreases by 77 %. Figure 96 shows that at an electrolyser investment cost of 250 €/kW, variable cost, including electricity cost plus additional fees and water consumption, makes up 86% of overall hydrogen production cost. This share decreases to only 46 % with an electrolyser investment cost of 3,000 €/kW. In the base case, this study reveals an electricity consumption cost share of 62 %, which corresponds with findings in the literature.

5.5. Conclusions

Renewable hydrogen is expected to play a major role in decarbonising the industrial sector as feedstock and fuel to many processes and products. On-site production, or production limited to "hydrogen valleys", has been proposed by Agora Energiewende et al. (2021) as a non-regret, robust way of starting the deployment of this technology and achieving higher production scales to decrease the cost. There are several options for on-site production, directly from a renewable power plant or the grid, which have been analysed in this work based on two different electrolyser technologies. Due to the different applied electrolyte components leading to different current densities, the PEM technology achieves a higher actual efficiency at lower loads than the more mature ALK electrolyser. These characteristics are modelled in detail for optimisation.

In a situation with grid connection—assuming the same investment cost for comparability reasons—hydrogen production cost with the ALK technology is slightly higher than with a PEM electrolyser. However, since the ALK technology is more mature and usually cheaper, it has a major economic advantage for grid-connected scenarios. The PEM electrolyser may catch up in terms of investment cost, although it needs to handle its current shorter stack lifetime and the need for platinum group metals.

In a grid-connected scenario, constant demand representing centralised bulk production always allows for cheaper hydrogen production by optimising electrolyser operation. In this case, electricity price optimisation does not provide economic benefits unless the electrolyser investment cost decreases or price profiles change significantly. Grid-connected JIT production achieves the lowest renewable hydrogen cost with constant hydrogen demand. In this case, maximising asset utilisation with more than 8,600 full load hours leads to a cost-optimal solution. Power purchase agreements would also be helpful in reducing the cost of the electricity sourced from the grid while ensuring its renewable character.

If hydrogen demand is variable, then electricity price optimisation and storage can be used to achieve lower costs. These results are valid under the assumption of no demand access fee applied for the maximum power sourced from the grid. They may be intensified with higher electricity price spreads through higher renewable shares. Electricity price optimisation also becomes a demand response tool to help manage the system. It is also interesting to note that the cost difference between the variable and constant demand alternatives is just 2 %. This small difference may not justify efforts to aggregate demands or to focus only on constant demand industrial facilities.

However, cost differences are much larger when comparing grid-connected and island configurations. According to the presented results, wind power feed-in is 2.5 and PV power connection up to 5-fold more expensive than a grid-connected scenario for hydrogen production based on the Austrian electricity market price 2019. The intermittency of renewable resources leads to substantial electrolyser and storage capacity requirements and huge variability, harming actual operation efficiency. The RES profiles drive hydrogen production cost and capacity requirements more than the hydrogen demand profile. Wind power seems to be more favourable than PV in terms of availability. Based on the findings and in line with the available literature, the ALK electrolyser is not recommended for direct renewable electricity feed-in due to the supply variability causing substantial performance losses.

An electrolyser's isolated RES connection may only become competitive if electricity market prices skyrocket, as currently observed. With the current average Austrian electricity price reaching 207 €/MWh by the end of May 2022, even the Spanish PV power could almost compete in the presented base scenario. Additionally, a mid-to-long-term expected decrease in electrolyser investment cost would also support the economic performance of direct renewable electricity feed-in. However, these results are subject to the existence or not of demand charges imposed on electrolysers, which is currently being discussed in several countries.

Hence, our results show that, although renewable hydrogen production in grid-connected configurations is more competitive in normal circumstances, this is subject to several uncertainties, such as the evolution in the cost and efficiency of electrolysers, or the regulation of the power system. Including these uncertainties in the analysis to produce more robust investment decisions would be a natural next step in this research.

6. Synthesis of results and discussion

This chapter discusses the findings concerning the research questions raised in Section 1.2 and outlines the strengths and limitations of the methodology applied to answer each of them. Section 6.1 describes the findings referring to the research questions. Section 6.2 provides a deeper insight into the strengths and limitations of the chosen modelling approaches. Section 6.3 elaborates on the opportunities and potential barriers to SC in the energy transition and the use of VRE in former fossil fuel-based sectors. Section 6.4 provides a short statement of the highlights of the presented work.

6.1. Findings referring to the research questions

This thesis' primary objective is an in-depth techno-economic analysis of potential sector coupling applications and their role in the energy transition. Three contributions provide insights into specific SC applications in the heating and cooling- transport- and the industrial sector and answer the underlying research questions raised in Section 1.2. The current chapter outlines the key findings.

For **Research Question 1:** *"What is the estimated storage time required to cover the time discrepancy between hourly variable renewable energy and temperature-based heating and cooling profiles?"* Chapter 3 of this thesis concludes that solar irradiance has the potential to cover cooling or heating needs directly without storage. There is a strong correlation between the hourly solar irradiance pattern and the temperature-based cooling needs profile in Austria and Spain. However, wind speed and heating needs only correlate on a monthly aggregated level, implying storage needs in all three climate regions—also in northern Europe. Unexpectedly, solar irradiance and heating demand patterns also correlate significantly during winter.

An analysis of the impact of climate change on temperatures reveals that cooling needs increase substantially in all regions while heating degree-days decrease. The temperature increase seems to be more severe in Spain, an already warmer southern country. These changes, such as long summer heat periods, will significantly influence future energy demand for heating and cooling. Furthermore, changes in solar irradiance and wind speed occurrence are expected. The projected increase of the minimum temperature in winter could, for example, also lead to an increased potential for wind power generation in northern Europe. This region is often exposed to very cold temperatures leading to icing of wind turbines, as described in Section 3.1 (Pryor & Barthelmie, 2010). The detected correlation of renewables with heating and cooling degree-days provides recommendations for SC. Additionally, demand needs to decrease further to support the energy transition through efficient heating and cooling, building insulation and shading.

Many aspects of **Research Question 2**: *"How can rising electricity demand in individual passenger transport be integrated into the energy system successfully to avoid any additional infrastructural costs for society and maintain user comfort?"* can be answered by the findings in Chapter 4. The results show that controlled charging can decrease the required power connection by about 63 % to an average of 1.3 kW/charging point (CP) compared to uncontrolled charging, which requires 3.5 kW/CP. These results describe how intelligent solutions can avoid intensified electricity demand peaks through BEV charging. Urban, densely populated areas where many BEVs are charged represent an ideal environment for LM to distribute substantial charging power across long parking times overnight.

The user comfort is maintained, and—depending on the vehicle characteristics—the charging process of all BEVs usually is completed in the morning. A typical daily travel distance of BEVs is about 30 km. With an expected energy consumption of 0.17 kWh/km, only about 5 kWh usually need to be charged daily. Power connection needs are relatively low, with simultaneity of about 40 % (BEVs plugging in simultaneously) and additional load-management (LM). One LM approach in the model aims to shift charging loads away from existing household load peaks. The LM algorithm applied to the infrastructure tested in the field test can technically also react to the current grid performance or household electricity demand. Consequently, LM is essential for the energy transition since it saves the distribution grid from additional pressure from BEV demand peaks, avoids the cost of extensive building power connection expansion and guarantees household and BEV electricity demand.

Research Question 3: "*What is the most economic on-site renewable hydrogen production strategy for constant or variable demand, specifically considering load-dependent conversion efficiency?*" is addressed in Chapter 5. The investigations consider constant and variable hydrogen demand and include grid-connected electrolysis based on Austrian electricity market prices of 2019 or a direct link to a RES power plant. The model results reveal that, for constant demand, just-in-time (JIT) production has a major advantage with almost full utilisation of the installed capacities. This can only be achieved through grid-connected electrolysers to guarantee electricity supply to produce H_2 according to demand. In that case, applying the more mature ALK electrolyser, characterised by higher maturity and lower cost than the PEM technology, is recommended and can further reduce the cost compared to other more variable operation strategies.

Once hydrogen demand is variable, JIT production can no longer achieve as high full load hours since electrolyser capacity needs to match the maximum hydrogen demand. In this case, electricity price optimisation with a PEM electrolyser and hydrogen storage could be a viable option. Nevertheless, if the cost advantage of an ALK electrolyser is considered for a more stable JIT production, this more mature technology could achieve cheaper H_2 production. Due to the variability and relatively high electrolyser and storage requirements, direct wind or PV power feed-in is not competitive with grid-connected electrolysis considering 2019 electricity prices. The current almost 5-fold average grid price increase compared to 2019, however, closes the gap between grid-connected and RES-based approaches, which have been evaluated with their LCOE.

6.2. Strengths and limitations of the methodology applied

As frequently pointed out in this thesis, the methodology applied to the herein presented SC applications does have strengths but also several limitations concerning the assumptions made and putting the concept into practice. Table 13 provides a summary of the aspects described in this section.

Table 13 Strengths and limitations of the applied methodology and modelling

	Strengths	Limitations
Sector Coupling	• Reduced complexity of SC concept • Detailed view on specific transformation processes	• No full consideration of feasibility concerning plant and grid capacities • Dependent on renewable capacity expansion
Estimating storage	• Understand interrelations between renewable sources and temperature-dependent heating and cooling needs • Impact of climate change on supply and demand	• Based on weather variables without investigation of energy demand and supply • Selected locations not based on hot spots for renewable energy plants
Load-Management	• Results from 0-100 % BEV diffusion • Validation of model results with field test data	• Set of 50 users extrapolated from 8 different driving profiles • Difference between information in modelling environment and reality
Renewable Hydrogen	• Replication of the electrolyser's actual efficiency at specific load factors • Comparison of on-site production technologies independent of H_2 distribution infrastructure	• No feasibility study concerning the demand volume of the cases • Comparison of different technologies at the same investment cost/kW

Since this thesis investigates three SC applications in different end-consumption sectors, each situation and applied model has different strengths and limitations, apart from the overall strengths and weaknesses of the SC concept. In the following, Section 6.2.1 describes the strengths of each approach for the SC applications and Section 6.2.2 the limitations of the chosen modelling concept.

6.2.1. Strengths of the methodology applied to evaluate the role of SC in the energy transition

Decarbonising all end-consumption sectors will rely on large-scale, infinite renewable resources such as wind and solar power. In the energy transition context, considering one-way power-to-X pathways based on the SC concept described in Chapter 2 may reduce complexity. The process initiates with an electricity source, which needs to be adapted to the process needs if no direct electrification is possible within a reasonable time. The SC concept allows a detailed view of a specific conversion process, its requirements and economic potential regarding operation strategies, market integration and efficiency. This approach enables a simplified view of specific energy streams within renewable energy systems.

The analysis of hourly VRE patterns and their correlation with temperature-based heating and cooling degree-hours in Chapter 3 describes important relationships for renewable energy systems and helps to understand their requirements. The work includes a statistical analysis of the correlation coefficient on an hourly basis and by aggregating the data to longer time periods, assuming storage. Without aiming to fulfil a certain energy demand with a certain energy supply, the hourly availability of wind speed and solar irradiance is compared with temperature profiles and consequently determined heating and cooling needs. In some specific cases, aggregating daily, weekly or monthly amounts of solar irradiance or wind speed and demand by assuming storage will achieve better results. This approach, therefore, allows for an estimation of storage time periods required to match VRE with temperature profiles without being restricted to a specific renewable heating or cooling technology. The data gathered also allows for an estimation of future developments in terms of temperature increases or VRE availability and the impact of climate change on the respective correlations. The investigation provides an understanding of the interrelationships between weather-based renewable electricity sources and temperature changes, deriving conclusions on a correlation with heating and cooling needs.

The modelling approach for evaluating load management in multi-apartment buildings applied in Chapter 4 is described explicitly by Hiesl et al. (2021). Different driving profiles derived by Hiesl et al. (2021) from an Austrian traffic survey by BMVIT (2016) establish a realistic portfolio of leave and return times from the charging point (CP) at the private parking spot and define energy demand based on a specific driving distance. The model was set up to achieve Austria's average yearly driving distance. This quarter-hourly dataset of driving profiles can function as input to further analysis and, together with the results, has been verified with real field test results from the underlying project providing plug-in and charging data under LM for 5 months. The LM approaches are optimised throughout the year but also with a daily rolling horizon, representing a more realistic scenario. The model includes household and BEV electricity demand for the building and may show results from 0-100 % BEV diffusion. The average power connection required per CP with this rolling approach matches the findings from the field test with 50 % BEV diffusion, which also reached the average Austrian driving range broken down to this time period. The model, the underlying driving profiles, energy demand, and the chosen LM approaches are, thus, valid and provide a basis for decision-making in similar applications for large-scale charging. The difference between the power connection achieved in the perfect modelling environment with full information and the results from the field test provides further potential for LM improvements. By forecasting electricity demand and driving profiles, upcoming charging processes can be managed based on more information.

Furthermore, standardising vehicle behaviour and knowledge of the battery state of charge would improve LM efficiency and forecasting accuracy. The presented approach offers a tool for controlled low-cost slow charging in urban areas without causing extensive grid capacity expansion and the related social cost. LM is an enabler of successful e-mobility integration into the energy system. In general, considering on-site production technologies, which do not depend on transportation of H_2 and appropriate infrastructure, is a gap in the literature that requires attention. The strength of the methodology applied to the economic evaluation of on-site renewable hydrogen generation strategies presented in Chapter 5 lies in the exact replication of the actual conversion efficiency. The efficiency differs with the load factor based on the observations by Pascuzzi et al. (2016) for the ALK technology and by Tijani & Rahim (2016) and Yodwong et al. (2020) for PEM electrolysis. The load factor depends on the applied operation strategy with either constant or variable electricity feed-in. The model proves, for example, that ALK electrolysers, due to their high efficiency losses at very low loads, are not suitable for the operation under direct feed-in from PV or wind power plants. The investigations address two different hydrogen demand patterns. A grid connection or a direct link to a RES plant with two renewable profiles is considered from the supply side. For constant and variable demand, different production strategies lead to the lowest cost of renewable decentral hydrogen production. The chosen methodology and results offer insights into the impact of investment cost and variable energy prices on hydrogen production cost and discuss additional aspects of the strategies. The investigation of on-site production or production limited to "hydrogen valleys" represents an opportunity to increase production scales and decrease the cost in the long term. Additionally, various market participation levels are possible depending on the operation strategy applied, leading to a different impact on the capacity requirements and resulting investment and energy cost.

6.2.2. Limitations concerning the approach and modelling

Limiting the scope of work to a one-way path from power-to-X without modelling the overall system integration, as indicated in Chapter 2, often is criticised as inaccurate. Efficient VRE integration demands flexible interaction between formerly isolated gas, heat and power grids and systems. Additionally, grid capacity and other parameters must be considered to evaluate the feasibility of certain electrification processes. However, the work presented in this thesis focuses on a techno-economic perspective without specifically analysing all technical aspects such as grid characteristics, which would require a more electro-technical approach. Furthermore, the SC concept and the overall energy transition depend on successfully expanding renewable capacities. Renewable energy systems will highly rely on large-scale solar PV and wind electricity and the timely installation of sufficient capacity to enable its use by additional demand sources in various end-consumption sectors.

Limitations to estimating storage needs from a correlation between hourly renewable energy and temperature patterns, as presented in Chapter 3, concern using mere weather variables. This work analyses the correlation between wind speed, solar irradiance, and HDH and CDH as temperature-based heating and cooling needs. Implications for actual energy demand need consideration of additional parameters, such as energy efficiency measures on building insulation, comfort during longer periods of heat and cold, and impacts of other energy demand sectors with progressive energy system integration. The selected locations do not represent high wind or PV power potential or demand hubs. The choice was oriented toward covering a broad set of historical average solar irradiance and wind speed levels, directions across the country, inland and coastal locations, and choosing main capitals. Another limitation is the focus on a subset of locations, which may not exactly represent the energy systems' characteristics. The identified time lag between solar irradiance or wind speed and CHD or HDH is based on an average calculation across all locations. No significant difference was detected for different locations in our analysis of wind speed or solar irradiance patterns and the heating and cooling needs patterns based on temperature. Concerning the significance level of the individual correlation results, almost all p-values for the data set of six locations and twelve-year time series were below the significance level (α) of 0.05, indicating significant correlations. Irrespective of single insignificant results in the series across twelve years, however, average correlations have been built to provide one result for each location, as explained in Section 3.3.4.

A limitation to the BEV load-management model in Chapter 4 relates to the portfolio of driving profiles for 50 virtual users, which is extrapolated from only eight different profiles. The variety had to be reduced due to substantial calculation times resulting from 35040 time-steps on a quarter-hourly basis considering several parameters (Hiesl et al., 2021). Additionally, the settings in the LM model differ from reality in the way that the BEVs are always plugged-in when parked at their private charging station. After a few weeks in the field test, users tended to plug in about every four days. This behaviour compresses the energy demand for the upcoming charging session and limits load-management flexibility.

Furthermore, the model knows the battery state of charge, which is currently not valid for the load-management controller in an authentic setting due to missing vehicle standards. Nevertheless, the daily rolling optimisation results match the findings in reality very well. The discrepancy between the average power connection per charging point achieved in the yearly optimisation model under full information and reality provides insights into potential improvements and further efficiency gains.

The methodology to evaluate different operation strategies for renewable hydrogen production described in Chapter 5 is limited concerning some cost aspects. The estimation of electrolyser investment cost is based on a literature review, and additional indirect cost is considered with 60 % of investment cost according to findings by (Matute et al., 2019). However, the practical implementation of an electrolyser may include higher costs depending on regional circumstances, such as land rent, additional technical installations or project management, etc. The objective of this contribution, however, does not depend on the exact estimation of the cost per kW of electrolyser capacity but focuses on comparing different operation strategies based on the same cost parameters.

Another limitation is the deliberate avoidance of presenting explicitly installed capacity sizes for fictive case studies. The operation strategies' differences are rather described relative to a reference scenario representing the highest installation at 100 %. There is, consequently, no investment cost degression with increasing electrolyser capacity considered. The presented approach is expected to address rather large-scale operations, and the sensitivity analysis provides different scenarios. Above a cost of 250 €/kW electrolyser capacity, the optimal electrolyser size does not differ significantly from that implemented with JIT. Therefore, the comparison of strategies is expected to be valid. For transparency reasons, the same investment cost per kW is assumed for the ALK and PEM electrolyser. Still, the ALK electrolyser represents the more mature, cheaper technology. The potential effect of this cost difference is outlined in the results. No demand access charge is considered, which is usually imposed on the maximum electricity load sourced from the grid. This charge would eliminate any variable electrolyser operation. Furthermore, no stack replacement cost is considered, which can have an impact if evaluated against the differing full load hours between just-in-time and RES-based operation. Additionally, the cost of electricity directly sourced from a renewable power plant is estimated by a common LCOE from literature without making our own calculations since this does not represent the main contribution of this work.

6.3. Opportunities and potential risks concerning the practical achievement of SC concepts

6.3.1. Opportunities of SC concepts

The opportunities through SC in the energy transition are as manifold as potential risks to a successful implementation and appear on many levels from environmental to economic aspects, including risk mitigation, efficiency and welfare aspects (see Table 14). In the following, the first aspects of the individual contributions are highlighted, complemented by an elaboration concerning VRE use for the energy transition. Solar irradiance and wind are sources that occur in nature, distributed across the globe, without additional material, human or financial effort, compared to, e.g. biomass, which requires additional treatments or transportation to the plant sites. Solar panels and wind turbines enable the use of these natural resources at a large scale most efficiently for electricity production. This renewable electricity can be a major chance to decarbonise the energy system by coupling the power to other end-consumption sectors directly or indirectly by applying conversion processes.

First of all, the natural effect of sun and wind on temperatures, though complex at times, can act as a perfect energy source to supply heating and cooling. The analysis provided in Chapter 3 explains the correlation between the weather-dependent variables and estimates storage needs to match supply and demand. To integrate rising electricity demand from BEV charging smoothly, LM provides an opportunity to control charging on a large scale without causing extensive grid capacity expansion and social costs. LM is a significant enabler of successful system integration of e-mobility and other new electricity demand sources. Concerning the decarbonisation of industrial purposes, on-site renewable hydrogen production can represent a non-regret option for the upscaling of production volumes to decrease the overall cost.

Depending on the electrolyser operation strategies, different attention is given to electricity price optimisation, investment cost and grid-connection characteristics. Despite the currently high cost, a direct connection of the electrolyser with a RES plant enables the direct use of renewable electricity and avoids stressing limited grid infrastructure. Grid-connected electricity price optimisation, by contrast, is based on reactions to market signals and could lead to favourable load shifting from a system perspective.

Table 14 Opportunities and risks to the practical implementation of SC

Opportunities	Risks
• Insourcing: Local VRE production and value creation • Building local technical expertise • Decarbonisation of all end-consumption sectors • Risk mitigation concerning foreign resources • Flexibilisation through industrial H_2 hubs • Storage of large-scale renewable electricity in heat and gas infrastructure • Digitalisation and automation knowhow • Improved data gathering and analysis • Efficiency gains	• Change of RES characteristics • Economic feasibility of transformation processes at low full load hours • New global dependencies • Uncertainty due to high research and development dynamics, undecided technologies and missing regulations • Inappropriate market structures for integrated energy systems • Consumer charges for transformation plants • System complexity • Security of supply is at risk if challenges are not addressed appropriately

Despite their intermitted character, renewable energy sources offer an opportunity for local energy production and value creation. By substituting former fossil fuels—imported from other countries across long distances—with locally produced renewable energy, energy production is insourced and creates wealth locally. Investments that formerly streamed into foreign countries can create value and build expertise in the own region, create jobs, build infrastructure and provide flexibility within the local energy systems. As a result, the dependency of the regional security of supply on imports from usually few foreign, partly politically unstable countries and on limited and environmentally harming fossil resources can be vastly reduced. For example, the electrification of transport substitutes imported fossil fuels with mainly locally produced renewable electricity. Additionally, this change promotes the development of load-management equipment and charging infrastructure, which local companies can provide with the available technical know-how or can be created locally. Such a situation may simultaneously lead to increased cooperation between countries and regions to exchange know-how and resources.

Through the integration of different sectors also beyond SC, for example, as multi-energy systems, industrial hubs around Europe can provide flexibility to energy systems and decarbonise industrial processes. Renewable hydrogen that will be required for many industrial applications could be produced at industrial sites and either used on site or fed into the gas grid and sold to other sectors, such as transport or energy suppliers. This could represent a future business model to leverage additional income from the decarbonisation of industrial processes.

Coupling the power to other end-consumption sectors, also enabled by the transformation into gas and heat, provides flexibility to renewable energy systems through more appropriate storage options than large-scale electricity storage and reduces electricity grid expansion needs. The potential use of electricity in other forms of energy enables the decarbonisation of many end-consumption sectors but requires new market frameworks and business models. A more integrated view of energy infrastructure electricity, gas and heat will be a prerequisite for successfully implementing the SC concept.

The efficient handling of sectoral integration for the energy transition will require additional effort concerning digital interfaces with the energy grids and data gathering and analysis. An increasing number of actors, such as transformation plants (P2G) and decentral renewable energy prosumagers in the form of households and companies and industries, add complexity to the energy system. At the same time, these additional steering requirements can turn into an opportunity to create a higher level of information that may result in partly automated control as well as informed, transparent decisions for short-term management as well as long-term planning. The accurate forecasting of VRE availability and its use for heating and cooling can be enhanced and optimally integrated by appropriate digital interfaces. Load-management for BEV charging can also be improved through more information and standardisation and operate intelligently and automated if equipped with control algorithms. Electricity-price-based operation of renewable hydrogen production also allows for so-called industrial demand side management (iDSM) since operation reacts to market signals.

6.3.2. Risks associated to SC concepts

As is true for all changes in large systems, implementing SC in renewable energy systems and the energy transition face several success risks. This is mainly based on the requirement to change historically grown systems to new goals and an increasing amount of actors with very different characteristics that the formerly known approach cannot address. First, the urgently required conversion technologies, such as P2G, are still struggling with their efficiency in representing a solution that can easily be applied. The losses through transformation currently call for a minimal application in hard-to-abate sectors or for the security of supply in the electricity sector. Specifically, if electrolysis is only carried out to source so-called "excess electricity", only few FLHs can be achieved, reducing the capacity utilisation. As a result, rather continuous, grid-connected electrolysis may provide a solution for a cost decrease.

The independence from imports through locally produced renewable energy is an opportunity. At the same time, however, the local characteristics do not always support the extensive installation of massive wind and PV capacities, or the availability faces extreme seasonal variability. Given the efficiency of P2G, local renewable electricity potential may not always be sufficient to cover the renewable gas demand, e.g. for large industrial sectors and energy production, to guarantee the security of supply. Therefore, dependency on renewable hydrogen from countries with substantial solar PV potential or off-shore wind capacities may develop towards a fully renewable energy system. Decisions concerning creating stable business relationships and risk management require major attention.

Furthermore, in the current energy transition state, it is often undecided, which will be the most appropriate technology. Energy production, transport and industry still develop alternatives dynamically, and the required energy carrier may change throughout the upcoming years and often depends on regulatory guidelines. This uncertainty can slow down investment decisions. Not only the developments in technology but also market frameworks and related regulations have a major impact on SC approaches' economic feasibility and competitiveness. As mentioned in Chapter 2, the current combination of market frameworks and infrastructure is not ready for the requirements of a renewable energy system. Often fees on the consumption of electricity are imposed on the operation of, e.g. P2G plants. If P2G shall become a measure for flexibility and decarbonisation, these plants must not be regarded and charged as consumers but as energy producers. Additionally, as described in Chapter 5, decision access fees may currently be charged on the maximum power consumed. The goal is to avoid variable demand sourcing, which also harms the flexible operation of SC conversion plants and their participation in the market based on electricity prices or the reaction to market signals.

New supply and demand sources to the electricity system impose pressure on the distribution grid. Therefore, other enablers of SC are appropriate grid expansion and load- and demand-side management solutions. Chapter 4 investigates load-management for BEV charging to avoid distribution grid expansion. Without the extensive implementation of such intelligent, digital solutions and effective and efficient handling of the complexity in renewable energy systems, a more dominant dependency on electricity and new flexibility needs will be impossible. Therefore, the current way of integrating new electricity demand sources into the energy system is not appropriate for a smooth energy transition, and challenges remain in creating hybrid, integrated energy systems. If the new requirements cannot be met, the security of supply may be at risk, or fossil backup capacities will remain part of the energy system.

6.3.3. Impact of the current market situation on SC applications

The dependence of many countries on natural gas currently causes turbulences in energy markets, leaving natural gas and electricity prices skyrocketing since mid-2021 (see Figure 97 and Figure 98). A situation that has multiple impacts on the attractiveness of different renewable and conversion technologies and can significantly affect the development of the SC applications that are analysed in the three contributions of this thesis in Chapters 3, 4 and 5.

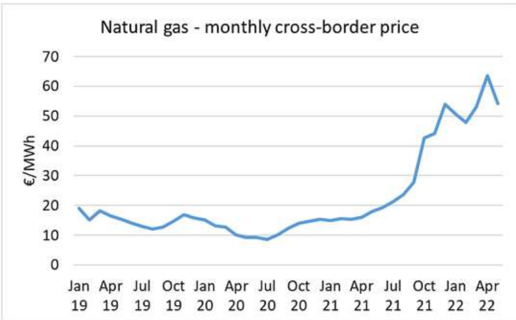

Figure 97 Monthly cross-border price for natural gas (BAFA, 2022)

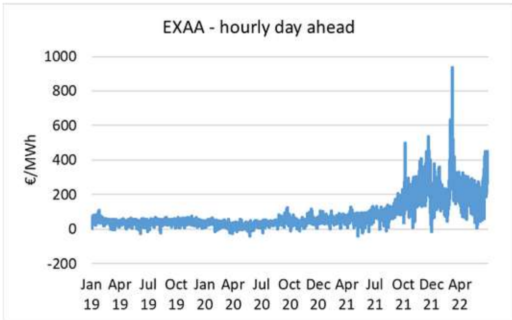

Figure 98 Hourly EXAA day ahead price for electricity (APG, 2022)

Rising electricity prices can severely affect the economic performance of on-site renewable hydrogen production evaluated in Chapter 5. Under the Austrian spot market price of 2019, with an average of 40 €/MWh, electrolysis with direct feed-in from variable renewable electricity (evaluated with an LCOE of 26 €/MWh for PV and 36 €/MWh for wind power) was not competitive due to highly variable operation and respective capacity needs and efficiency losses. However, the almost 5-fold market price increase could change this situation, as outlined in Section 5.4.3. While the cost for grid-connected hydrogen production accounted for about 109 €/MWh with price levels of 2019, an average price of 150 €/MWh would increase the cost to 267 €/MWh, almost making wind power feed-in competitive. With a 250 €/MWh market price, even highly variable Spanish solar PV feed-in could compete. Direct renewable feed-in at the LCOE would therefore be an economically attractive approach from the perspective of conversion plants such as electrolysers.

E-mobility, another new electricity demand source, could increasingly benefit from the distributed renewable energy supply with increasing market prices. On-site electricity production from rooftop PV for single-family buildings or in energy communities is a promising alternative to escape the market uncertainty and instead rely on locally produced renewable energy. Apart from the strategies described in Section 4.3.4, an appropriate load management approach could optimise BEV charging with solar PV generation. In that case, vehicle-to-grid can also be an interesting consideration for optimising such locally controlled distributed energy systems or micro-grids (Marnay & Lai, 2012; Wang et al., 2018).

However, rising electricity market prices also lead to a higher market value of renewable electricity. As a result, own consumption of cheaper on-site electricity competes with the remuneration for grid feed-in (Hartner, 2016). For distributed energy production, this could also be in favour of a relatively large PV system installation for more feed-in remuneration. Concerning the profit optimisation of the renewable power plant, grid feed-in at market prices will, therefore, also be more economical than the supply to conversion plants at a lower price. The economic performance of renewable power generation plants is boosted, providing money for further investments (Hartner, 2016). Renewable energy providers will prosper under these conditions and can grow significantly. Electrolysers, however, will mainly rely on electricity from the grid and energy consumption costs will increase noticeably unless long-term price agreements have been made upfront. These dynamics could impose further challenges on the economic performance of enabling technologies for SC, such as P2H and P2G. Another trade-off in this upswing in renewable electricity from rising market prices is the social perspective and exposure of many households to extremely rising costs without any ability to change their energy source. These contrary situations may provide room for compensation between a prospering renewable energy sector and disadvantaged households.

The substantial dependence of many countries on natural gas causes severe uncertainty concerning the security of supply, mainly for residential heating and the industry, currently amplified by bottlenecks and consequently high prices. This situation triggers investments into decentral energy generation and district heating connections, especially to substitute individual gas boilers for residential heating. For example in Austria, the high share of natural gas connections needs to decrease and be substituted by local renewable sources to reduce dependency on energy imports, as well as the natural gas share in district heating. The latter comprised around 35 % in the whole country in 2021 and even 40-70 % in many Austrian capital cities, as illustrated in Figure 99 (BMK, 2021; GLOBAL 2000, 2022). Therefore, the timely correlation between renewable energy sources and heating and cooling demand, as indicated in Chapter 3, becomes even more valuable. Additionally, the political debate around short-term security of supply focuses on extended toleration or claimed amplified dependence of several countries on coal, natural gas or nuclear energy, which represents a considerable setback to the efforts around climate change mitigation and environmental protection. The European Commission has even suggested including nuclear energy and natural gas in the EU Taxonomy list of environmentally sustainable economic activities, which was accepted in a vote by the Members of the European Parliament in July 2022 (EC, 2022; EP, 2022).

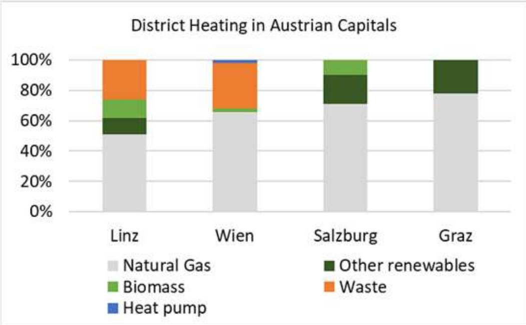

Figure 99 Energy carrier shares for district heating in Austrian capitals (GLOBAL 2000, 2022)

The burden toward the installation and successful integration of renewable energy in the short term seems too high and the response too slow compared to reactivating or extending the use of known, fossil-fuel-based processes. The risk and long-term environmental impact associated with nuclear power and related waste handling seem to be assessed as justifiable. The required energy transition through the integration of much higher renewable shares still is subject to uncertainty. It requires immediate guidance to quickly and successfully implement research and development findings. The mere installation of renewable capacities is not the solution yet. Answering current supply and market uncertainties with renewable systems requires comprehensive support by renewable storage options, digital interfaces for integrating all energy producing and consuming sectors, appropriate grid capacity, easy market entry of new actors in energy markets, and new business models.

6.4. Highlights

The following highlights compress the main takeaways of this thesis:

- Historical market frameworks need to adjust to support enabling SC technologies
- The correlation between solar irradiance and heating and cooling degree days is promising
- Off-peak charging avoids an extension of electricity demand peaks
- Grid-connected renewable H_2 production enables maximum electrolyser optimisation
- Rising electricity prices may harm economic feasibility of conversion technologies

7. Conclusions & outlook

The SC concept represents one part of the solution for successful VRE integration in the energy transition. The opportunities and requirements for SC differ widely with the implemented technologies and related processes. This thesis critically reviews the SC concept and evaluates its implementation in three different end-consumption sectors, each with an individual methodology. This work provides valuable recommendations for the role of SC in the energy transition and highlights opportunities and risks in different end-consumption sectors. The review on the state of the art of SC reveals that the interpretation of the concept is multiplied. However, the literature agrees that the renewable energy system relies on large-scale electricity sources such as wind and solar power. Even if the intermittency of renewable energy from wind and sun causes new challenges to the energy system, the direct use of electricity is usually the most efficient form of use. Furthermore, the ongoing electrification in all end-consumption sectors creates new demand sources for the electricity system. Therefore, the energy transition increases energy system complexity on both the demand and supply sides and must be handled successfully.

The interrelationship between VRE and temperature patterns can also be a chance to cover heating and cooling needs. The first contribution in this thesis represents a statistical analysis of weather variables and temperature-dependent heating and cooling needs. The results can serve to understand the value of using the natural interdependencies between wind speed and solar irradiance with temperatures to achieve SC with heating and cooling demand. The conclusions presented in this thesis specifically highlight the strong, time-based correlation between solar irradiance and an increase in temperature causing cooling demand. The conclusions presented in this thesis specifically prove the strong correlation between hourly solar irradiance patterns and cooling degree hours. In some locations in Spain, the correlation reaches a strong coefficient of 0.8 on daily time intervals and above 0.6 in three Austrian locations throughout the season. Solar irradiance patterns even correlate moderately with heating degree hours after accounting for the time lag between the solar irradiance peak at noon and the lowest temperature in the mornings in Spain and Austria, with correlations between 0.40-0.59. This would resemble balancing needs of 12 hours. Nevertheless, the correlation between wind speed profiles and heating degree hours only achieves moderate results with monthly data aggregation—matching monthly total wind speed with total heating degree hours. This monthly simultaneity is also strong between CDH and solar irradiance in Austria and Spain. The considered weather variables will develop dynamically along with climate change and lead to different circumstances and requirements. For example, Madrid is expected to experience the strongest mean temperature increase (almost 10 %) towards 2100, accompanied by growing solar irradiance. At the same time, energy demand needs to be minimised. By avoiding demand where possible and investing in building insulation and shading, capacity requirements for renewable electricity can be reduced, and materials and occupied land can be saved.

In order to offer relief to the electricity system, the gas infrastructure will also play a major role in enabling flexible long-term storage of renewable energy and providing an energy source for many processes, e.g. in industry. However, the efficiency and investment cost of conversion technologies such as from power to gas via electrolysis still harms economic feasibility. On-site renewable hydrogen production, therefore, has been detected as a robust, low-risk option to increase the scale and reduce cost. The third analysis presented in this thesis compares different on-site renewable hydrogen production strategies. The results are of great value in understanding the economic relationships of different operation strategies concerning investment and energy cost. The results prove that only the PEM electrolyser is feasible for variable operation due to better performance at lower loads. In contrast, the cost advantage of the more mature ALK electrolyser enfolds with continuous H_2 generation. Based on the Austrian electricity market price of 2019, grid-connected H_2 production for constant demand resulted in the lowest overall LCOH&S, providing electrolyser capacity optimisation with 8,600 full load hours. Direct RES feed-in from wind power causes 2.5 and from PV power up to 5-fold higher hydrogen production cost than the grid-connected scenario. The RES profiles influence hydrogen production cost more than the hydrogen demand profile. With increasing electricity market prices, direct connection to a RES plant may also become competitive and avoids the occupation of limited grid capacities and additional access cost. Upscaling the electricity price profile to an average of 207 €/MWh (the Austrian market price by May 2022) would make Spanish PV power feed-in, characterised by higher availability, almost competitive to grid connection. Nevertheless, the level of electrolyser market participation and system integration depends on the type of operation and may become important with increasing installed capacities. Such market frameworks must be discussed and clearly defined to promote further development.

Another important end-consumption sector facing increasing electrification is individual passenger transport. The second contribution on load management for BEV charging in multi-unit apartments reveals that intelligent load-management can successfully distribute charging processes to avoid additional electricity demand peaks—and consequent distribution grid or power connection expansion—up to a large share of electrification. The optimisation applied distributes charging processes according to specific parameters, e.g. avoiding existing household electricity demand peaks, where potential backup electricity capacities are already in use. The results show that uncontrolled charging promotes the correlation between BEV electricity demand and not only HH load peaks but also fossil fuel based electricity generation (investigated for Austria). Controlled charging reduces the required building power connection by about 63 % compared to uncontrolled charging. Under full information, for 100 % BEV diffusion, an off-peak time of use (ToU) approach can reduce the building's maximum electricity demand by up to 40 % compared to uncontrolled charging. Instead of requiring on average 3.5 kW/charging point of power connection, controlled charging in the field test and in a more realistic daily rolling optimisation only used 1.3kW. Furthermore, the results show the remaining optimisation potential by the difference in the minimum power connection calculated with a yearly model optimisation based on full information of 0.44 kW/CP. Increasing information on user behaviour and charging demand, vehicle standardisation, knowledge of the battery state of charge and plug-in discipline can further improve LM efficiency. The results emphasise the need to promote controlled charging solutions to exploit the pooling effect and provide a reliable service for a large amount of BEVs. While the ToU approach avoids more extreme electricity demand peaks at noon and the evening and represents the most favourable strategy from a grid perspective, the missing availability of renewable solar power to cover demand shifted into night times could be a downside. From an environmental perspective, charging all available vehicles at noon to exploit the solar electricity generation peak could be a desirable strategy. More investigation on the optimal coordination of VRE availability and charging LM is recommended in the future, also on a regional level, e.g. in energy communities with local renewable electricity generation.

The increasing use of renewable energy to substitute fossil fuels also has various benefits concerning local creation of value and expertise and independence from the import of fossil fuels. The vast dependence on very few countries for the supply of, for example, natural gas, is currently causing severe market uncertainty. The former fear usually associated to the intermittent availability of variable renewables is presently existing even more with respect to uncertain natural gas supply. Renewable energy can be produced locally and sustainably and reduce this dependence, while at the same time reducing emissions, creating national value, jobs and expertise. Nevertheless, rising electricity market prices may harm the economic performance of conversion technologies such as P2G.

With its one-way view from power-to-X, the SC concept offers a simplified scope that enables the analysis of specific use cases without considering the whole system complexity. Eventually, the energy transition depends on an extensive installation of renewable energy capacities. At the same time, it is essential to avoid energy consumption where possible, shift to more sustainable processes or technologies and improve the process to prevent a waste of resources. Environmental effects must be internalised into market frameworks to promote relatively new renewable technologies instead of the known conventional approaches. Clear regulatory guidelines must be developed to prevent uncertainty in a highly dynamic area of new renewable technologies from slowing down decision-making in several sectors.

Above all, the energy transition relies on a paradigm shift towards integrated grids and systems. Digital interfaces are essential to communicate between formerly isolated energy grids and guarantee informed decisions and a certain amount of automation. New market structures need to consider multiple energy carriers across different end-consumption sectors to provide flexibility to a renewable system. This may also cause shifts in the importance and roles of the electricity, gas and heat infrastructure. Under the aim to fulfil end-consumer demands emission-free, a new fully integrated framework could be developed from scratch to levy synergies.

References

Abdul Quader, M., Ahmed, S., Dawal, S. Z., & Nukman, Y. (2016). Present needs, recent progress and future trends of energy-efficient Ultra-Low Carbon Dioxide Steelmaking (ULCOS) program. *Renewable and Sustainable Energy Reviews*, *55*, 537–549. https://doi.org/10.1016/j.rser.2015.10.101

Abeysekera, M. (2016). *Combined analysis of coupled energy networks* [Phd, Cardiff University]. https://orca.cardiff.ac.uk/id/eprint/97879/

Agora Energiewende, AFRY Management, & AFRY Management Consulting. (2021). *No-regret hydrogen: Charting early steps for H_2 infrastructure in Europe*. https://www.agora-energiewende.de/en/publications/no-regret-hydrogen/

Aguilar-Dominguez, D., Dunbar, A., & Brown, S. (2020). The electricity demand of an EV providing power via vehicle-to-home and its potential impact on the grid with different electricity price tariffs. *Energy Reports*, *6*, 132–141. https://doi.org/10.1016/j.egyr.2020.03.007

Ahmed, T., Muttaqi, K. M., & Agalgaonkar, A. P. (2012). Climate change impacts on electricity demand in the State of New South Wales, Australia. *Applied Energy*, *98*, 376–383. https://doi.org/10.1016/j.apenergy.2012.03.059

Alstom Group. (2020a). *Towards clean and future-oriented mobility*. Coradia ILint – the World's 1st Hydrogen Powered Train. https://www.alstom.com/our-solutions/rolling-stock/coradia-ilint-worlds-1st-hydrogen-powered-train

Alstom Group. (2020b, March 6). *Alstom's hydrogen train Coradia iLint completes successful tests in the Netherlands*. Alstom. https://www.alstom.com/press-releases-news/2020/3/alstoms-hydrogen-train-coradia-ilint-completes-successful-tests

Al-Zayer, J., & Al-Ibrahim, A. A. (1996). Modelling the impact of temperature on electricity consumption in the Eastern Province of Saudi Arabia. *Journal of Forecasting*, *15*(2), 97–106. https://doi.org/10.1002/(SICI)1099-131X(199603)15:2<97::AID-FOR608>3.0.CO;2-L

American Automobile Association Inc. (AAA). (2019). *AAA electric vehicle range testing*. https://www.aaa.com/AAA/common/AAR/files/AAA-Electric-Vehicle-Range-Testing-Report.pdf

APG. (2022a). *Day-Ahead: EXAA-Spotmarkt*. https://markttransparenz.apg.at/de/markt/Markttransparenz/Uebertragung/EXAA%20Spotmarkt

APG. (2022b). *Day-Ahead Preise: EXAA-Spotmarkt*. https://www.apg.at/de/markt/Markttransparenz/Uebertragung/EXAA-Spotmarkt

Arabzadeh, V., Mikkola, J., Jasiūnas, J., & Lund, P. D. (2020). Deep decarbonization of urban energy systems through renewable energy and sector-coupling flexibility strategies. *Journal of Environmental Management*, *260*, 110090. https://doi.org/10.1016/j.jenvman.2020.110090

Arent, D. J., Bragg-Sitton, S. M., Miller, D. C., Tarka, T. J., Engel-Cox, J. A., Boardman, R. D., Balash, P. C., Ruth, M. F., Cox, J., & Garfield, D. J. (2021). Multi-input, Multi-output Hybrid Energy Systems. *Joule*, *5*(1), 47–58. https://doi.org/10.1016/j.joule.2020.11.004

Arnold, K., & Janssen, T. (2016). *Demand side management in industry – necessary for a sustainable energy system or a backward step in terms of improving efficiency?*

Ausfelder, F., Drake, F.-D., Erlach, B., Fischedick, M., Henning, H. M., Kost, C. P., Münch, W., Pittel, K., Rehtanz, C., Sauer, J., Schätzler, K., Stephanos, C., Themann, M., Umbach, E., Wagemann, K., Wagner, H.-J., & Wagner, U. (2017). *'Sektorkopplung'—Untersuchungen und Überlegungen zur Entwicklung eines integrierten Energiesystems*.

Ausfelder, F., & Dura, H. E. (2018). *Optionen für ein nachhaltiges Energiesystem mit Power-to-X Technologien*.

BAFA. (2022). *BAFA - Erdgasstatistik*. https://www.bafa.de/DE/Energie/Rohstoffe/Erdgasstatistik/erdgas_node.html

Balmin, J., Bonett, G., & Kirkeby, M. (2012). *Increasing Electric Vehicle Charging Access in Multi-Unit Dwellings in Los Angeles*.

Bell, W. P., Wild, P., Foster, J., & Hewson, M. (2015). Wind speed and electricity demand correlation analysis in the Australian National Electricity Market: Determining wind turbine generators' ability to meet electricity demand without energy storage. *Economic Analysis and Policy*, *48*, 182–191. https://doi.org/10.1016/j.eap.2015.11.009

Bellocchi, S., Manno, M., Noussan, M., Prina, M. G., & Vellini, M. (2020). Electrification of transport and residential heating sectors in support of renewable penetration: Scenarios for the Italian energy system. *Energy*, *196*, 117062. https://doi.org/10.1016/j.energy.2020.117062

Belyaev, L. S., Kaganovich, B. M., Krutov, A. N., Filippov, S. P., Martinsen, D., Müller, M., Wagner, H. J., & Walbeck, M. (1987). *Ways of transition to clean energy use: Two methodological approaches*. IIASA.

Bernath, C., Deac, G., & Sensfuß, F. (2019). Influence of heat pumps on renewable electricity integration: Germany in a European context. *Energy Strategy Reviews*, *26*, 100389. https://doi.org/10.1016/j.esr.2019.100389

Bertuccioli, L., Chan, A., Hart, D., Lehner, F., Madden, B., & Standen, E. (2014). *Study on development of water electrolysis in the EU*.

Bessec, M., & Fouquau, J. (2008). The non-linear link between electricity consumption and temperature in Europe: A threshold panel approach. *Energy Economics*, *30*(5), 2705–2721. https://doi.org/10.1016/j.eneco.2008.02.003

Bett, P. E., & Thornton, H. E. (2016). The climatological relationships between wind and solar energy supply in Britain. *Renewable Energy*, *87*, 96–110. https://doi.org/10.1016/j.renene.2015.10.006

Bhandari, R., & Shah, R. R. (2021). Hydrogen as energy carrier: Techno-economic assessment of decentralized hydrogen production in Germany. *Renewable Energy*, *177*, 915–931. https://doi.org/10.1016/j.renene.2021.05.149

Bitar, E., & Xu, Y. (2016). *Deadline Differentiated Pricing of Deferrable Electric Loads*. http://arxiv.org/abs/1407.1601

Bloess, A. (2019). Impacts of heat sector transformation on Germany's power system through increased use of power-to-heat. *Applied Energy*, *239*, 560–580. https://doi.org/10.1016/j.apenergy.2019.01.101

Bloess, A., Schill, W.-P., & Zerrahn, A. (2018). Power-to-heat for renewable energy integration: A review of technologies, modeling approaches, and flexibility potentials. *Applied Energy*, *212*, 1611–1626. https://doi.org/10.1016/j.apenergy.2017.12.073

BMK. (2021). *Energie in Österreich 2021: Zahlen-Daten-Fakten*. https://www.bmk.gv.at/themen/energie/publikationen/zahlen.html

BMNT. (2018). *#MISSION2030—Austrian climate and energy strategy*. Bundesministerium für Nachhaltigkeit und Tourismus.

Bourasseau, C., & Guinot, B. (2015). Hydrogen: A storage means for renewable energies. In *Hydrogen Production by Electrolysis* (1st ed., pp. 311–382). John Wiley & Sons, Ltd. https://doi.org/10.1002/9783527676507

Brändle, G., Schönfisch, M., & Schulte, S. (2020). *Estimating Long-Term Global Supply Costs for Low-Carbon Hydrogen* (EWI Working Paper No 20/04).

Bremen, L. V. (2010). Large-Scale Variability of Weather Dependent Renewable Energy Sources. In A. Troccoli (Ed.), *Management of Weather and Climate Risk in the Energy Industry* (pp. 189–206). Springer Netherlands. https://doi.org/10.1007/978-90-481-3692-6_13

Breslow, P. B., & Sailor, D. J. (2002). Vulnerability of wind power resources to climate change in the continental United States. *Renewable Energy*, *27*(4), 585–598. https://doi.org/10.1016/S0960-1481(01)00110-0

Brinkel, N. B. G., Schram, W. L., AlSkaif, T. A., Lampropoulos, I., & van Sark, W. G. J. H. M. (2020). Should we reinforce the grid? Cost and emission optimization of electric vehicle charging under different transformer limits. *Applied Energy*, *276*, 115285. https://doi.org/10.1016/j.apenergy.2020.115285

Bristowe, G., & Smallbone, A. (2021). The Key Techno-Economic and Manufacturing Drivers for Reducing the Cost of Power-to-Gas and a Hydrogen-Enabled Energy System. *Hydrogen*, *2*(3), 273–300. https://doi.org/10.3390/hydrogen2030015

Brown, T., Schlachtberger, D., Kies, A., Schramm, S., & Greiner, M. (2018). Synergies of sector coupling and transmission reinforcement in a cost-optimised, highly renewable European energy system. *Energy*, *160*, 720–739. https://doi.org/10.1016/j.energy.2018.06.222

Brynolf, S., Taljegard, M., Grahn, M., & Hansson, J. (2018). Electrofuels for the transport sector: A review of production costs. *Renewable and Sustainable Energy Reviews*, *81*, 1887–1905. https://doi.org/10.1016/j.rser.2017.05.288

Buffa, S., Cozzini, M., D'Antoni, M., Baratieri, M., & Fedrizzi, R. (2019). 5th generation district heating and cooling systems: A review of existing cases in Europe. *Renewable and Sustainable Energy Reviews*, *104*, 504–522. https://doi.org/10.1016/j.rser.2018.12.059

Bundesministerium für Verkehr, Innovation und Technologie (BMVIT). (2016). *Österreich unterwegs 2013/2014*.

Bundesministerium für Wirtschaft und Energie (BMWi). (2016). *Green paper on energy efficiency: Discussion paper of the Federal Ministry for Economic Affairs and Energy*.

Bundesministeriums für Umwelt, Naturschutz, Bau und Reaktorsicherheit (BMUB). (2016a). *Climate Action Plan 2050 – Principles and goals of the German government's climate policy*.

Bundesministeriums für Umwelt, Naturschutz, Bau und Reaktorsicherheit (BMUB). (2016b). *Klimaschutzplan 2050—Klimaschutzpolitische Grundsätze und Ziele der Bundesregierung*.

Bundesverband der Energie-und Wasserwirtschaft e.V. (BDEW). (2017). *Positionspapier: 10 Thesen zur Sektorkopplung*. http://www.bdew.de/service/stellungnahmen/10-thesen-sektorkopplung/

Burandt, T., Xiong, B., Konstantin Löffler, & Pao-Yu Oei. (2019). Decarbonizing China's energy system – Modeling the transformation of the electricity, transportation, heat, and industrial sectors. *Applied Energy*, *255*, 113820. https://doi.org/10.1016/j.apenergy.2019.113820

Buttler, A., & Spliethoff, H. (2018). Current status of water electrolysis for energy storage, grid balancing and sector coupling via power-to-gas and power-to-liquids: A review. *Renewable and Sustainable Energy Reviews*, *82*, 2440–2454. https://doi.org/10.1016/j.rser.2017.09.003

Cabello, M., & Orza, J. A. G. (2010). Wind speed analysis in the province of Alicante, Spain. Potential for small-scale wind turbines. *Renewable and Sustainable Energy Reviews*, *14*(9), 3185–3191. https://doi.org/10.1016/j.rser.2010.07.002

Cambini, C., Congiu, R., Jamasb, T., Llorca, M., & Soroush, G. (2020). Energy systems integration: Implications for public policy. *Energy Policy*, *143*, 111609. https://doi.org/10.1016/j.enpol.2020.111609

Caparrós Mancera, J., Fernández, F. J., Segura, F., & Andujar Marquez, J. (2019). *Optimized Balance of Plant for a medium-size PEM electrolyzer. Design, Modelling and Control*.

Castillejo-Cuberos, A., & Escobar, R. (2020). Understanding solar resource variability: An in-depth analysis, using Chile as a case of study. *Renewable and Sustainable Energy Reviews*, *120*, 109664. https://doi.org/10.1016/j.rser.2019.109664

Castro, P. M., Sun, L., & Harjunkoski, I. (2013). Resource–Task Network Formulations for Industrial Demand Side Management of a Steel Plant. *Industrial & Engineering Chemistry Research*, *52*(36), 13046–13058. https://doi.org/10.1021/ie401044q

Chen, C., Zarazua de Rubens, G., Noel, L., Kester, J., & Sovacool, B. K. (2020). Assessing the socio-demographic, technical, economic and behavioral factors of Nordic electric vehicle adoption and the influence of vehicle-to-grid preferences. *Renewable and Sustainable Energy Reviews*, *121*, 109692. https://doi.org/10.1016/j.rser.2019.109692

Chen, S., Gong, F., Zhang, M., & Yuan, J. (2021). Planning and Scheduling for Industrial Demand-Side Management: State of the Art, Opportunities and Challenges under Integration of Energy Internet and Industrial Internet. *Sustainability*, *13*.

CleanTechnica. (2018, January 12). *Crowd Charging—New Pilot Project In Denmark*. CleanTechnica. https://cleantechnica.com/2018/01/12/crowd-charging-new-pilot-project-denmark/

Coker, P., Barlow, J., Cockerill, T., & Shipworth, D. (2013). Measuring significant variability characteristics: An assessment of three UK renewables. *Renewable Energy*, *53*, 111–120. https://doi.org/10.1016/j.renene.2012.11.013

Connolly, D., Lund, H., & Mathiesen, B. V. (2016). Smart energy Europe: The technical and economic impact of one potential 100% renewable energy scenario for the European Union. *Renewable and Sustainable Energy Reviews*, *60*, 1634–1653. https://doi.org/10.1016/j.rser.2016.02.025

Coughlin, K., & Eto, J. H. (2010). *Analysis of Wind Power and Load Data at Multiple Time Scales* (LBNL-4147E, 1004166; p. LBNL-4147E, 1004166). https://doi.org/10.2172/1004166

Coughlin, K., Murthi, A., & Eto, J. (2014). Multi-scale analysis of wind power and load time series data. *Renewable Energy*, *68*, 494–504. https://doi.org/10.1016/j.renene.2014.02.011

Crozier, C., Morstyn, T., & McCulloch, M. (2020). The opportunity for smart charging to mitigate the impact of electric vehicles on transmission and distribution systems. *Applied Energy*, *268*, 114973. https://doi.org/10.1016/j.apenergy.2020.114973

Cutforth, H. W., & Judiesch, D. (2007). Long-term changes to incoming solar energy on the Canadian Prairie. *Agricultural and Forest Meteorology*, *145*(3), 167–175. https://doi.org/10.1016/j.agrformet.2007.04.011

Dai, A., & Deser, C. (1999). Diurnal and semidiurnal variations in global surface wind and divergence fields. *Journal of Geophysical Research: Atmospheres*, *104*(D24), 31109–31125. https://doi.org/10.1029/1999JD900927

Danish Energy Agency (DEA). (2016). *Technology data for electricity, district heating, energy storage and energy conversion*. https://ens.dk/sites/ens.dk/files/Statistik/technology_data_catalogue_for_el_and_dh_-_0009.pdf

Danish Energy Agency (DEA). (2017). *Regulation and planning of district heating in Denmark*.

Das, H. S., Rahman, M. M., Li, S., & Tan, C. W. (2020). Electric vehicles standards, charging infrastructure, and impact on grid integration: A technological review. *Renewable and Sustainable Energy Reviews*, *120*, 109618. https://doi.org/10.1016/j.rser.2019.109618

Deutsche Energie-Agentur (Dena). (2017). *dena-Leitstudie: Integrierte Energiewende*.

Dixon, J., Bukhsh, W., Edmunds, C., & Bell, K. (2020). Scheduling electric vehicle charging to minimise carbon emissions and wind curtailment. *Renewable Energy*, S0960148120310934. https://doi.org/10.1016/j.renene.2020.07.017

DVGW. (2020, March 5). *Sektorenkopplung*. Sektorenkopplung – Synergien sinnvoll nutzen. https://www.dvgw.de/themen/energiewende/sektorenkopplung/

DVGW & VDE. (2016). *Eckpunkte zur Begriffsdefinition Sektorenkopplung*.

El-Emam, R. S., & Özcan, H. (2019). Comprehensive review on the techno-economics of sustainable large-scale clean hydrogen production. *Journal of Cleaner Production*, *220*, 593–609. https://doi.org/10.1016/j.jclepro.2019.01.309

EMD International. (2020). *Skagen Varmeværk*. Energyweb. http://www.energyweb.dk/skagen/?english&history

Emeis, S. (2018). *Wind Energy Meteorology: Atmospheric Physics for Wind Power Generation*. Springer.

Emonts, B., Reuß, M., Stenzel, P., Welder, L., Knicker, F., Grube, T., Görner, K., Robinius, M., & Stolten, D. (2019). Flexible sector coupling with hydrogen: A climate-friendly fuel supply for road transport. *International Journal of Hydrogen Energy*, *44*(26), 12918–12930. https://doi.org/10.1016/j.ijhydene.2019.03.183

Engeland, K., Borga, M., Creutin, J.-D., François, B., Ramos, M.-H., & Vidal, J.-P. (2017). Space-time variability of climate variables and intermittent renewable electricity production – A review. *Renewable and Sustainable Energy Reviews*, *79*, 600–617. https://doi.org/10.1016/j.rser.2017.05.046

ENTSO-E. (2022). *ENTSO-E Transparency Platform*. https://transparency.entsoe.eu/

Eto, J. H. (1988). On using degree-days to account for the effects of weather on annual energy use in office buildings. *Energy and Buildings*, *12*(2), 113–127. https://doi.org/10.1016/0378-7788(88)90073-4

European Commission DG-ENER. (2021). *Resource efficient cities implementing advanced smart city solutions—READY*. http://www.smartcity-ready.eu/wp-content/uploads/2021/02/Final-Publishable-Summary-Report-READY_v2.pdf

European Commission (EC). (2020, July 27). *Hydrogen generation in Europe: Overview of costs and key benefits.* [Website]. Publications Office of the European Union.

http://op.europa.eu/en/publication-detail/-/publication/7e4afa7d-d077-11ea-adf7-01aa75ed71a1/language-en

European Commission (EC). (2021a). *CMIP5 daily data on single levels*. https://cds.climate.copernicus.eu/cdsapp#!/dataset/projections-cmip5-daily-single-levels?tab=form

European Commission (EC). (2021b). *EU transport in figures: Statistical pocketbook 2021*. Publications Office of the European Union. https://data.europa.eu/doi/10.2832/27610

European Commission (EC). (2022). *EU taxonomy for sustainable activities*. European Commission - European Commission. https://ec.europa.eu/info/business-economy-euro/banking-and-finance/sustainable-finance/eu-taxonomy-sustainable-activities_en

European Parliament (EP). (2018). *Sector coupling: How can it be enhanced in the EU to foster grid stability and decarbonise?*

European Parliament (EP) & European Commission (EC). (2019). *REGULATION (EU) 2019/ 631 OF THE EUROPEAN PARLIAMENT AND OF THE COUNCIL - setting CO2 emission performance standards for new passenger cars and for new light commercial vehicles, and repealing Regulations (EC) No 443 / 2009 and (EU) No 510 / 2011*.

eurostat. (2020). *Energy statistics—Cooling and heating degree days*. https://ec.europa.eu/eurostat/cache/metadata/en/nrg_chdd_esms.htm

Evans, J. D. (1996). *Straightforward statistics for the behavioral sciences*. Brooks/Cole Pub. Co.

Fan, J.-L., Hu, J.-W., & Zhang, X. (2019). Impacts of climate change on electricity demand in China: An empirical estimation based on panel data. *Energy*, *170*, 880–888. https://doi.org/10.1016/j.energy.2018.12.044

Felten, B. (2020). An integrated model of coupled heat and power sectors for large-scale energy system analyses. *Applied Energy*, *266*, 114521. https://doi.org/10.1016/j.apenergy.2020.114521

Fischedick, M., Marzinkowski, J., Winzer, P., & Weigel, M. (2014). Techno-economic evaluation of innovative steel production technologies. *Journal of Cleaner Production*, *84*, 563–580. https://doi.org/10.1016/j.jclepro.2014.05.063

Foresight Climate & Energy. (2019, May 3). *Hydrogen: The Northern Netherlands is ready*. https://foresightdk.com/hydrogen-northern-netherlands-is-ready/

Foy, J. H., & Schlereth, T. J. (1994). *Foy, J: American Home Life 1880-1930* (1st ed.). University of Tennessee Press.

Fragiacomo, P., & Genovese, M. (2020). Technical-economic analysis of a hydrogen production facility for power-to-gas and hydrogen mobility under different renewable sources in Southern Italy. *Energy Conversion and Management*, *223*, 113332. https://doi.org/10.1016/j.enconman.2020.113332

Frank, L., Jacob, K., & Quitzow, R. (2020). Transforming or tinkering at the margins? Assessing policy strategies for heating decarbonisation in Germany and the United Kingdom. *Energy Research & Social Science*, *67*, 101513. https://doi.org/10.1016/j.erss.2020.101513

Fraunhofer ISE. (2021). *Studie: Stromgestehungskosten erneuerbare Energien*. Fraunhofer-Institut für Solare Energiesysteme ISE. https://www.ise.fraunhofer.de/de/veroeffentlichungen/studien/studie-stromgestehungskosten-erneuerbare-energien.html

Frischmuth, F., & Härtel, P. (2022). Hydrogen sourcing strategies and cross-sectoral flexibility trade-offs in net-neutral energy scenarios for Europe. *Energy*, *238*, 121598. https://doi.org/10.1016/j.energy.2021.121598

Gahleitner, G. (2013). Hydrogen from renewable electricity: An international review of power-to-gas pilot plants for stationary applications. *International Journal of Hydrogen Energy*, *38*(5), 2039–2061. https://doi.org/10.1016/j.ijhydene.2012.12.010

Geidl, M., Koeppel, G., Favre-Perrod, P., Klöckl, B., Andersson, G., & Fröhlich, K. (2007). *The energy hub: A powerful concept for future energy systems*. https://www.research-collection.ethz.ch/handle/20.500.11850/3133

Gerres, T., Ávila, J. P. C., & Llamas, P. L. (2019). *The transformation of the Spanish basic materials sector towards a low carbon economy*.

GLOBAL 2000. (2022). *Klimareport: So heizen die Landeshauptstädte*. GLOBAL 2000. https://www.global2000.at/publikationen/klimareport-so-heizen-die-landeshauptstaedte

Global Solar Atlas. (2020). https://globalsolaratlas.info/map

Global Wind Atlas. (2020). Global Wind Atlas. https://globalwindatlas.info

Gorre, J., Ruoss, F., Karjunen, H., Schaffert, J., & Tynjälä, T. (2020). Cost benefits of optimizing hydrogen storage and methanation capacities for Power-to-Gas plants in dynamic operation. *Applied Energy*, *257*, 113967. https://doi.org/10.1016/j.apenergy.2019.113967

Gough, R., Dickerson, C., Rowley, P., & Walsh, C. (2017). Vehicle-to-grid feasibility: A techno-economic analysis of EV-based energy storage. *Applied Energy*, *192*, 12–23. https://doi.org/10.1016/j.apenergy.2017.01.102

Haas, R., Ajanovic, A., Ramsebner, J., Perger, T., Knápek, J., & Bleyl, J. W. (2021). Financing the future infrastructure of sustainable energy systems. *Green Finance*, *3*(1), 90–118. https://doi.org/10.3934/GF.2021006

Haas, R., Ajanovic, A., Ramsebner, J., Perger, T., Knápek, J., Bleyl, J. W., Haas, R., Ajanovic, A., Ramsebner, J., Perger, T., Knápek, J., & Bleyl, J. W. (2021). Financing the future infrastructure of sustainable energy systems. *Green Finance*, *3*(1), 90–118. https://doi.org/10.3934/GF.2021006

Habib, S., Kamran, M., & Rashid, U. (2015). Impact analysis of vehicle-to-grid technology and charging strategies of electric vehicles on distribution networks – A review. *Journal of Power Sources*, *277*, 205–214. https://doi.org/10.1016/j.jpowsour.2014.12.020

Häfele, W., & Nebojsa, N. (1983). The contribution of oil and gas for the transition to long range novel energy systems. *World Demand for and Supply of Oil and Gas*, *9*(3).

Hall, D., & Lutsey, N. (2017). *Emerging best practices for electric vehicle charging infrastructure*.

Hariri, A.-M., Hejazi, M. A., & Hashemi-Dezaki, H. (2019). Reliability optimization of smart grid based on optimal allocation of protective devices, distributed energy resources, and electric vehicle/plug-in hybrid electric vehicle charging stations. *Journal of Power Sources*, *436*, 226824. https://doi.org/10.1016/j.jpowsour.2019.226824

Hart, M., & de Dear, R. (2004). Weather sensitivity in household appliance energy end-use. *Energy and Buildings*, *36*(2), 161–174. https://doi.org/10.1016/j.enbuild.2003.10.009

Hartner, M. (2016). *Economic aspects of photovoltaic from a strategic, end user and electricity system perspective* [Thesis, Wien]. https://repositum.tuwien.at/handle/20.500.12708/4762

Hekkenberg, M., Benders, R. M. J., Moll, H. C., & Schoot Uiterkamp, A. J. M. (2009). Indications for a changing electricity demand pattern: The temperature dependence of electricity demand in the Netherlands. *Energy Policy*, *37*(4), 1542–1551. https://doi.org/10.1016/j.enpol.2008.12.030

Herrmann, C., Schmidt, C., Kurle, D., Blume, S., & Thiede, S. (2014). Sustainability in manufacturing and factories of the future. *International Journal of Precision Engineering and Manufacturing-Green Technology*, *1*(4), 283–292. https://doi.org/10.1007/s40684-014-0034-z

Hidalgo, D., & Martín-Marroquín, J. M. (2020). Power-to-methane, coupling CO2 capture with fuel production: An overview. *Renewable and Sustainable Energy Reviews*, *132*, 110057. https://doi.org/10.1016/j.rser.2020.110057

Hiesl, A., Ramsebner, J., & Haas, R. (2021). Modelling stochastic electricity demand of EVs based on traffic surveys—The case of Austria. *Energies*, *13*.

Holttinen, H. (2005). Hourly wind power variations in the Nordic countries. *Wind Energy*, *8*(2), 173–195. https://doi.org/10.1002/we.144

Holttinen, H., Rissanen, S., Larsén, X. G., & Løvholm, A. L. (2013). *Wind and load variability in the Nordic countries*. VTT Technical Research Centre of Finland. https://orbit.dtu.dk/en/publications/wind-and-load-variability-in-the-nordic-countries

Hörsch, J., & Brown, T. (2017). The role of spatial scale in joint optimisations of generation and transmission for European highly renewable scenarios. *2017 14th International Conference on the European Energy Market (EEM)*, 1–7. https://doi.org/10.1109/EEM.2017.7982024

Hu, Z., Zhan, K., Zhang, H., & Song, Y. (2016). Pricing mechanisms design for guiding electric vehicle charging to fill load valley. *Applied Energy*, *178*, 155–163. https://doi.org/10.1016/j.apenergy.2016.06.025

IEA. (2020). *Projected Costs of Generating Electricity 2020*. IEA. https://www.iea.org/reports/projected-costs-of-generating-electricity-2020

IEA. (2022). *Evolution of natural gas spot market prices, 2014-2019 – Charts – Data & Statistics*. IEA. https://www.iea.org/data-and-statistics/charts/evolution-of-natural-gas-spot-market-prices-2014-2019

IEA/Nordic Energy Research. (2018). *Nordic EV Outlook 2018*. OECD/IEA.

International Energy Agency (IEA). (2019). *The future of hydrogen* [Report prepared by the IEA for the G20, Japan].

International Renewable Energy Agency (IRENA). (2018). *Hydrogen from renewable power: Technology outlook for the energy transition*.

Iqbal, M. (2012). *An Introduction to Solar Radiation*. Elsevier.

IRENA. (2015). *Renewable Energy Options for Shipping*.

IRENA. (2019). *Electric-Vehicle Smart Charging – Innovation Landscape Brief*. International Renewable Energy Agency. https://www.irena.org/-/media/Files/IRENA/Agency/Publication/2019/Sep/IRENA_EV_Smart_Charging_2019.pdf?la=en&hash=E77FAB7422226D29931E8469698C709EFC13EDB2

IRENA. (2021). *Renewable Power Generation Costs in 2020*. /Publications/2021/Jun/Renewable-Power-Costs-in-2020. https://www.irena.org/publications/2021/Jun/Renewable-Power-Costs-in-2020

IRENA. (2022). *Energy Transition*. Energy Transition. https://www.irena.org/energytransition

IRENA, IEA, & REN21. (2018). *Renewable energy policies in a time of transition*.

Jambagi, A., Kramer, M., & Cheng, V. (2015). Electricity and heat sector coupling for domestic energy systems: Benefits of integrated energy system modelling. *2015 International Conference on Smart Cities and Green ICT Systems (SMARTGREENS)*, 1–6.

Jang, H. S., Bae, K. Y., Jung, B. C., & Sung, D. K. (2020). Apartment-level electric vehicle charging coordination: Peak load reduction and charging payment minimization. *Energy and Buildings*, *223*, 110155. https://doi.org/10.1016/j.enbuild.2020.110155

Jerez, S., Trigo, R. M., Sarsa, A., Lorente-Plazas, R., Pozo-Vázquez, D., & Montávez, J. P. (2013). Spatio-temporal Complementarity between Solar and Wind Power in the Iberian Peninsula. *Energy Procedia*, *40*, 48–57. https://doi.org/10.1016/j.egypro.2013.08.007

Jimenez-Navarro, J.-P., Kavvadias, K., Filippidou, F., Pavičević, M., & Quoilin, S. (2020). Coupling the heating and power sectors: The role of centralised combined heat and power plants and district heat in a European decarbonised power system. *Applied Energy*, *270*, 115134. https://doi.org/10.1016/j.apenergy.2020.115134

Joas, F., Witecka, W., Lenck, T., & Peter, F. (2019). *Klimaneutrale Industrie: Schlüsseltechnologien und Politikoptionen für Stahl, Chemie und Zement*.

Jovanović, S., Savić, S., Bojić, M., Djordjević, Z., & Nikolić, D. (2015). The impact of the mean daily air temperature change on electricity consumption. *Energy*, *88*, 604–609. https://doi.org/10.1016/j.energy.2015.06.001

JRC Photovoltaic Geographical Information System (PVGIS)—European Commission. (2020). https://re.jrc.ec.europa.eu/pvg_tools/en/tools.html#TMY

Kempton, W., & Tomić, J. (2005). Vehicle-to-grid power fundamentals: Calculating capacity and net revenue. *Journal of Power Sources*, *144*(1), 268–279. https://doi.org/10.1016/j.jpowsour.2004.12.025

Khalid, M. R., Alam, M. S., Sarwar, A., & Jamil Asghar, M. S. (2019). A Comprehensive review on electric vehicles charging infrastructures and their impacts on power-quality of the utility grid. *ETransportation*, *1*, 100006. https://doi.org/10.1016/j.etran.2019.100006

Khalkhali, H., & Hosseinian, S. H. (2020). Multi-class EV charging and performance-based regulation service in a residential smart parking lot. *Sustainable Energy, Grids and Networks*, *22*, 100354. https://doi.org/10.1016/j.segan.2020.100354

Kim, J. D. (2019). Insights into residential EV charging behavior using energy meter data. *Energy Policy*, *129*, 610–618. https://doi.org/10.1016/j.enpol.2019.02.049

Kiviluoma, J., Holttinen, H., Weir, D., Scharff, R., Söder, L., Menemenlis, N., Cutululis, N. A., Lopez, I. D., Lannoye, E., Estanqueiro, A., Gomez-Lazaro, E., Zhang, Q., Bai, J., Wan, Y.-H., & Milligan, M. (2016). Variability in large-scale wind power generation. *Wind Energy*, *19*(9), 1649–1665. https://doi.org/10.1002/we.1942

Klima- und Energiefonds. (2022). *URCHARGE*. https://www.klimafonds.gv.at/unsere-themen/mobilitaetswende/leuchttuerme-der-elektromobilitaet/urcharge/

Kopp, M., Coleman, D., Stiller, C., Scheffer, K., Aichinger, J., & Scheppat, B. (2017). Energiepark Mainz: Technical and economic analysis of the worldwide largest Power-to-Gas plant with PEM electrolysis. *International Journal of Hydrogen Energy*, *42*(19), 13311–13320. https://doi.org/10.1016/j.ijhydene.2016.12.145

Lam, J. C. (1998). Climatic and economic influences on residential electricity consumption. *Energy Conversion and Management*, *39*(7), 623–629. https://doi.org/10.1016/S0196-8904(97)10008-5

Lam, J. C., Tang, H. L., & Li, D. H. W. (2008). Seasonal variations in residential and commercial sector electricity consumption in Hong Kong. *Energy*, *33*(3), 513–523. https://doi.org/10.1016/j.energy.2007.10.002

Lamb, H. H. (1950). Types and spells of weather around the year in the British Isles: Annual trends, seasonal structure of the year, singularities. *Quarterly Journal of the Royal Meteorological Society*, *76*(330), 393–429. https://doi.org/10.1002/qj.49707633005

Larscheid, P., Lück, L., & Moser, A. (2018). Potential of new business models for grid integrated water electrolysis. *Renewable Energy*, *125*, 599–608. https://doi.org/10.1016/j.renene.2018.02.074

Larsen, M. A. D., Petrović, S., Radoszynski, A. M., McKenna, R., & Balyk, O. (2020). Climate change impacts on trends and extremes in future heating and cooling demands over Europe. *Energy and Buildings*, *226*, 110397. https://doi.org/10.1016/j.enbuild.2020.110397

Le Comte, D. M., & Warren, H. E. (1981). Modeling the Impact of Summer Temperatures on National Electricity Consumption. *Journal of Applied Meteorology (1962-1982)*, *20*(12), 1415–1419.

Leahy, P. G., & Foley, A. M. (2012). Wind generation output during cold weather-driven electricity demand peaks in Ireland. *Energy*, *39*(1), 48–53. https://doi.org/10.1016/j.energy.2011.07.013

Leitner, B., Widl, E., Gawlik, W., & Hofmann, R. (2019). A method for technical assessment of power-to-heat use cases to couple local district heating and electrical distribution grids. *Energy*, *182*, 729–738. https://doi.org/10.1016/j.energy.2019.06.016

Lester, M. S., Bramstoft, R., & Münster, M. (2020). Analysis on Electrofuels in Future Energy Systems: A 2050 Case Study. *Energy*, *199*, 117408. https://doi.org/10.1016/j.energy.2020.117408

Lewandowska-Bernat, A., & Desideri, U. (2018). Opportunities of power-to-gas technology in different energy systems architectures. *Applied Energy*, *228*, 57–67. https://doi.org/10.1016/j.apenergy.2018.06.001

Limmer, S., & Rodemann, T. (2019). Peak load reduction through dynamic pricing for electric vehicle charging. *International Journal of Electrical Power & Energy Systems*, *113*, 117–128. https://doi.org/10.1016/j.ijepes.2019.05.031

Linares, P., Santos, F. J., & Ventosa, M. (2008). Coordination of carbon reduction and renewable energy support policies. *Climate Policy*, *8*(4), 377–394. https://doi.org/10.3763/cpol.2007.0361

LINZ AG. (2021). *Urcharge—Ein Projekt für zukunftsfitte E-Mobilität*. LINZ AG. https://www.linzag.at/portal/de/ueber_die_linzag/projekte/urcharge

Lopez-Behar, D., Tran, M., Froese, T., Mayaud, J. R., Herrera, O. E., & Merida, W. (2019). Charging infrastructure for electric vehicles in Multi-Unit Residential Buildings: Mapping feedbacks and policy recommendations. *Energy Policy*, *126*, 444–451. https://doi.org/10.1016/j.enpol.2018.10.030

Lund, H., Andersen, A. N., Østergaard, P. A., Mathiesen, B. V., & Connolly, D. (2012). From electricity smart grids to smart energy systems – A market operation based approach and understanding. *Energy*, *42*(1), 96–102. https://doi.org/10.1016/j.energy.2012.04.003

Lund H., Mathiesen B.V., Connolly D., & Ostergaard P.A. (2014). Renewable energy systems—A smart energy systems approach to the choice and modelling of 100 % renewable solutions. *Chemical Engineering Transactions*, *39*, 1–6. https://doi.org/10.3303/CET1439001

Lund, H., Østergaard, P. A., Connolly, D., & Mathiesen, B. V. (2017). Smart energy and smart energy systems. *Energy*, *137*, 556–565. https://doi.org/10.1016/j.energy.2017.05.123

Lund, H., Werner, S., Wiltshire, R., Svendsen, S., Thorsen, J. E., Hvelplund, F., & Mathiesen, B. V. (2014). 4th generation district heating (4GDH). *Energy*, *68*, 1–11. https://doi.org/10.1016/j.energy.2014.02.089

Luo, X. J., Oyedele, L. O., Akinade, O. O., & Ajayi, A. O. (2020). Two-stage capacity optimization approach of multi-energy system considering its optimal operation. *Energy and AI*, *1*, 100005. https://doi.org/10.1016/j.egyai.2020.100005

Luo, Y., Zhu, T., Wan, S., Zhang, S., & Li, K. (2016). Optimal charging scheduling for large-scale EV (electric vehicle) deployment based on the interaction of the smart-grid and intelligent-transport systems. *Energy*, *97*, 359–368. https://doi.org/10.1016/j.energy.2015.12.140

Ma, T., Wu, J., Hao, L., Lee, W.-J., Yan, H., & Li, D. (2018). The optimal structure planning and energy management strategies of smart multi energy systems. *Energy*, *160*, 122–141. https://doi.org/10.1016/j.energy.2018.06.198

Machhammer, O., Bode, A., & Hormuth, W. (2016). Financial and Ecological Evaluation of Hydrogen Production Processes on Large Scale. *Chemical Engineering & Technology*, *39*(6), 1185–1193. https://doi.org/10.1002/ceat.201600023

Mancarella, P. (2014). MES (multi-energy systems): An overview of concepts and evaluation models. *Energy*, *65*, 1–17. https://doi.org/10.1016/j.energy.2013.10.041

Mansilla, C., Avril, S., Imbach, J., & Le Duigou, A. (2012). CO2-free hydrogen as a substitute to fossil fuels: What are the targets? Prospective assessment of the hydrogen market attractiveness. *International Journal of Hydrogen Energy*, *37*(12), 9451–9458. https://doi.org/10.1016/j.ijhydene.2012.03.149

Marnay, C., & Lai, J. (2012). Serving electricity and heat requirements efficiently and with appropriate energy quality via microgrids. *The Electricity Journal*, *25*(8), 7–15. https://doi.org/10.1016/j.tej.2012.09.017

Masera, M., Bompard, E. F., Profumo, F., & Hadjsaid, N. (2018). Smart (Electricity) Grids for Smart Cities: Assessing Roles and Societal Impacts. *Proceedings of the IEEE*, *106*(4), 613–625. https://doi.org/10.1109/JPROC.2018.2812212

Mathiesen, B. V., & Lund, H. (2009). Comparative analyses of seven technologies to facilitate the integration of fluctuating renewable energy sources. *IET Renewable Power Generation*, *3*(2), 190–204. https://doi.org/10.1049/iet-rpg:20080049

Mathiesen, B. V., Lund, H., Connolly, D., Wenzel, H., Østergaard, P. A., Möller, B., Nielsen, S., Ridjan, I., Karnøe, P., Sperling, K., & Hvelplund, F. K. (2015). Smart energy systems for coherent 100% renewable energy and transport solutions. *Applied Energy*, *145*, 139–154. https://doi.org/10.1016/j.apenergy.2015.01.075

Matthes, F. Chr. (2018). *Energy transformation in Germany: Progress, shortfalls and prospects*.

Matute, G., Yusta, J. M., & Correas, L. C. (2019). Techno-economic modelling of water electrolysers in the range of several MW to provide grid services while generating hydrogen for different applications: A case study in Spain applied to mobility with FCEVs. *International Journal of Hydrogen Energy*, *44*(33), 17431–17442. https://doi.org/10.1016/j.ijhydene.2019.05.092

McKenna, R. C., Bchini, Q., Weinand, J. M., Michaelis, J., König, S., Köppel, W., & Fichtner, W. (2018). The future role of Power-to-Gas in the energy transition: Regional and local techno-economic analyses in Baden-Württemberg. *Applied Energy*, *212*, 386–400. https://doi.org/10.1016/j.apenergy.2017.12.017

Mohammadi, A., & Mehrpooya, M. (2018). A comprehensive review on coupling different types of electrolyzer to renewable energy sources. *Energy*, *158*, 632–655. https://doi.org/10.1016/j.energy.2018.06.073

Mohanpurkar, M., Luo, Y., Terlip, D., Dias, F., Harrison, K., Eichman, J., Hovsapian, R., & Kurtz, J. (2017). Electrolyzers Enhancing Flexibility in Electric Grids. *Energies*, *10*(11), 1836. https://doi.org/10.3390/en10111836

Monteiro, V., Pinto, J. G., & Afonso, J. L. (2019). Improved vehicle-for-grid (iV4G) mode: Novel operation mode for EVs battery chargers in smart grids. *International Journal of Electrical Power & Energy Systems*, *110*, 579–587. https://doi.org/10.1016/j.ijepes.2019.03.049

Moss, R. H., Edmonds, J. A., Hibbard, K. A., Manning, M. R., Rose, S. K., van Vuuren, D. P., Carter, T. R., Emori, S., Kainuma, M., Kram, T., Meehl, G. A., Mitchell, J. F. B., Nakicenovic, N., Riahi, K., Smith, S. J., Stouffer, R. J., Thomson, A. M., Weyant, J. P., & Wilbanks, T. J. (2010). The next generation of scenarios for climate change research and assessment. *Nature*, *463*(7282), 747–756. https://doi.org/10.1038/nature08823

Mullan, J., Harries, D., Bräunl, T., & Whitely, S. (2012). The technical, economic and commercial viability of the vehicle-to-grid concept. *Energy Policy*, *48*, 394–406. https://doi.org/10.1016/j.enpol.2012.05.042

Netze BW GmbH. (2019). *DIE E-MOBILITYALLEE*. https://assets.ctfassets.net/xytfb1vrn7of/6gXs8wiRSF0E2SqkwSq406/fc1c9430ba88b81c31e399242b09b17e/20191217_BroschuereE-Mobility_210x275mm_100Ansicht.pdf

Netze BW GmbH. (2021). *NETZlabor E-Mobility-Carré—Netze BW GmbH*. NETZlabor E-Mobility-Carré - Netze BW GmbH. https://www.netze-bw.de/unsernetz/netzinnovationen/netzintegration-elektromobilitaet/e-mobility-carre

Neuhoff, K., Chiapinelli, O., & Gerres, T. (2019). *Building blocks for a climateneutral European industrial sector*.

Neuhoff, K., Chiapinelli, O., & Richtstein, J. (2021). *Closing the Green Deal for Industry*.

Neuhoff, K., Lettow, F., Chiappinelli, O., Gerres, T., Joltreau, E., Linares, P., & Śniegocki, A. (2020). *Investments in climate-friendly materials to strengthen the recovery package* (Investments in Climate-Friendly Materials to Strengthen the Recovery Package). Climate Strategies. https://www.jstor.org/stable/resrep24973.1

Nguyen, T., Abdin, Z., Holm, T., & Mérida, W. (2019). Grid-connected hydrogen production via large-scale water electrolysis. *Energy Conversion and Management*, *200*, 112108. https://doi.org/10.1016/j.enconman.2019.112108

Nielsen, M. G., Morales, J. M., Zugno, M., Pedersen, T. E., & Madsen, H. (2016). Economic valuation of heat pumps and electric boilers in the Danish energy system. *Applied Energy*, *167*, 189–200. https://doi.org/10.1016/j.apenergy.2015.08.115

Noel, L., Zarazua de Rubens, G., Kester, J., & Sovacool, B. K. (2020). Understanding the socio-technical nexus of Nordic electric vehicle (EV) barriers: A qualitative discussion of range, price, charging and knowledge. *Energy Policy*, *138*, 111292. https://doi.org/10.1016/j.enpol.2020.111292

Noussan, M. (2018). Performance based approach for electricity generation in smart grids. *Applied Energy*, *220*, 231–241. https://doi.org/10.1016/j.apenergy.2018.03.092

Novak, P. (2017). Exergy as measure of sustainability of energy system. *International Journal of Earth & Environmental Sciences*, *2*(2). https://doi.org/10.15344/2456-351X/2017/139

Oesterreichs Energie. (2019). *Daten & Fakten zur Stromerzeugung*. https://oesterreichsenergie.at/daten-fakten-zur-stromerzeugung.html

O'Hare, G., & Sweeney, J. (1993). Lamb's Circulation Types and British Weather: An Evaluation. *Geography*, *78*(1), 43–60.

Olczak, M., & Piebalgs, A. (2018). *Sector coupling: The new EU climate and energy paradigm?*

Ornetzeder, M., & Sinozic, T. (2020). Sector coupling of renewable energy in an experimental setting: *TATuP - Zeitschrift Für Technikfolgenabschätzung in Theorie Und Praxis*, *29*(2), 38–44. https://doi.org/10.14512/tatup.29.2.38

Otto, A., Robinius, M., Grube, T., Schiebahn, S., Praktiknjo, A., & Stolten, D. (2017). Power-to-Steel: Reducing CO2 through the Integration of Renewable Energy and Hydrogen into the German Steel Industry. *Energies*, *10*(4), 451. https://doi.org/10.3390/en10040451

Pardo, A., Meneu, V., & Valor, E. (2002). Temperature and seasonality influences on Spanish electricity load. *Energy Economics*, *24*(1), 55–70. https://doi.org/10.1016/S0140-9883(01)00082-2

Parkinson, B., Balcombe, P., Speirs, J. F., Hawkes, A. D., & Hellgardt, K. (2019). Levelized cost of CO2 mitigation from hydrogen production routes. *Energy & Environmental Science*, *12*(1), 19–40. https://doi.org/10.1039/C8EE02079E

Parsons, G. R., Hidrue, M. K., Kempton, W., & Gardner, M. P. (2014). Willingness to pay for vehicle-to-grid (V2G) electric vehicles and their contract terms. *Energy Economics*, *42*, 313–324. https://doi.org/10.1016/j.eneco.2013.12.018

Pascuzzi, S., Anifantis, A., Blanco, I., & Scarascia Mugnozza, G. (2016a). Electrolyzer Performance Analysis of an Integrated Hydrogen Power System for Greenhouse Heating. A Case Study. *Sustainability*, *8*(7), 629. https://doi.org/10.3390/su8070629

Pascuzzi, S., Anifantis, A., Blanco, I., & Scarascia Mugnozza, G. (2016b). Electrolyzer Performance Analysis of an Integrated Hydrogen Power System for Greenhouse Heating. A Case Study. *Sustainability*, *8*(7), 629. https://doi.org/10.3390/su8070629

Pašičko, R., Branković, Č., & Šimić, Z. (2012). Assessment of climate change impacts on energy generation from renewable sources in Croatia. *Renewable Energy*, *46*, 224–231. https://doi.org/10.1016/j.renene.2012.03.029

Paulus, M., & Borggrefe, F. (2011). The potential of demand-side management in energy-intensive industries for electricity markets in Germany. *Applied Energy*, *88*(2), 432–441.

Pavičević, M., Mangipinto, A., Nijs, W., Lombardi, F., Kavvadias, K., Jiménez Navarro, J. P., Colombo, E., & Quoilin, S. (2020). The potential of sector coupling in future European energy systems: Soft linking between the Dispa-SET and JRC-EU-TIMES models. *Applied Energy*, *267*, 115100. https://doi.org/10.1016/j.apenergy.2020.115100

Peter, Bach Andersen, Seyedmostafa, Hashemi Toghroljerdi, Thomas, Meier Sørensen, Bjørn, Eske Christensen, Jens Christian, Morell Lodberg Høj, & Antonio, Zecchino. (2019). *The Parker Project: Final Report*. Energy Technology Development and Demonstration Program (EUDP). https://parker-project.com/wp-content/uploads/2019/03/Parker_Final-report_v1.1_2019.pdf

Pfeiffer, C., Puchegger, M., Maier, C., Tomaschitz, I. V., Kremsner, T. P., & Gnam, L. (2021). A Case Study of Socially-Accepted Potentials for the Use of End User Flexibility by Home Energy Management Systems. *Sustainability*, *13*(1), 132. https://doi.org/10.3390/su13010132

Posdziech, O., Schwarze, K., & Brabandt, J. (2019). Efficient hydrogen production for industry and electricity storage via high-temperature electrolysis. *International Journal of Hydrogen Energy*, *44*(35), 19089–19101. https://doi.org/10.1016/j.ijhydene.2018.05.169

Pryor, S. C., & Barthelmie, R. J. (2010). Climate change impacts on wind energy: A review. *Renewable and Sustainable Energy Reviews*, *14*(1), 430–437. https://doi.org/10.1016/j.rser.2009.07.028

Quaschning, V. (2016). *Sektorkopplung durch die Energiewende*.

Quayle, R. G., & Diaz, H. F. (1980). Heating Degree Day Data Applied to Residential Heating Energy Consumption. *Journal of Applied Meteorology (1962-1982)*, *19*(3), 241–246.

Ramsebner, J., Haas, R., Ajanovic, A., & Wietschel, M. (2021). The sector coupling concept: A critical review. *WIREs Energy and Environment*, *10*(4). https://doi.org/10.1002/wene.396

Ramsebner, J., Haas, R., Auer, H., Ajanovic, A., Gawlik, W., Maier, C., Nemec-Begluk, S., Nacht, T., & Puchegger, M. (2021). *From single to multi-energy and hybrid grids: Historic growth and future vision*. https://doi.org/10.1016/J.RSER.2021.111520

Ramsebner, J., Hiesl, A., & Haas, R. (2020). Efficient Load Management for BEV Charging Infrastructure in Multi-Apartment Buildings. *Energies*, *13*(22), 1–23.

Ramsebner, J., Linares, P., & Haas, R. (2021a). Estimating storage needs for renewables in Europe: The correlation between renewable energy sources and heating and cooling demand. *Smart Energy*, 100038. https://doi.org/10.1016/j.segy.2021.100038

Ramsebner, J., Linares, P., & Haas, R. (2021b). Estimating storage needs for renewables in Europe: The correlation between renewable energy sources and heating and cooling demand. *Smart Energy*, 100038. https://doi.org/10.1016/j.segy.2021.100038

Ramsebner, J., Linares, P., Hiesl, A., & Haas, R. (2022). Economic evaluation of renewable hydrogen generation strategies for the industrial sector. *Energy Economics*, *Mimeo-under review*.

Raux-Defossez, P., Wegerer, N., Pétillon, D., Bialecki, A., Bailey, A., & Belhomme, R. (2018). Grid Services Provided By The Interactions Of Energy Sectors In Multi-Energy Systems: Three International Case Studies. *Energy Procedia*, *155*, 209–227. https://doi.org/10.1016/j.egypro.2018.11.055

Rezania, R. (2013). *Integration of electric vehicles in the Austrian electricity system* [Doctoral Thesis, TU Wien]. https://repositum.tuwien.at/handle/20.500.12708/13244

Richts, C., Jansen, M., & Siefert, M. (2015). Determining the economic value of offshore wind power plants in the changing energy system. *Energy Procedia*, *80*, 422–432. https://doi.org/10.1016/j.egypro.2015.11.446

Ridjan, I., Mathiesen, B. V., & Connolly, D. (2016). *Terminology used for renewable liquid and gaseous fuels based on the conversion of electricity: A review | Elsevier Enhanced Reader*. https://doi.org/10.1016/j.jclepro.2015.05.117

Rissman, J., Bataille, C., Masanet, E., Aden, N., Morrow, W. R., Zhou, N., Elliott, N., Dell, R., Heeren, N., Huckestein, B., Cresko, J., Miller, S. A., Roy, J., Fennell, P., Cremmins, B., Koch Blank, T., Hone, D., Williams, E. D., de la Rue du Can, S., … Helseth, J. (2020). Technologies and policies to decarbonize global industry: Review and assessment of mitigation drivers through 2070. *Applied Energy*, *266*, 114848. https://doi.org/10.1016/j.apenergy.2020.114848

Roach, M., & Meeus, L. (2020). The welfare and price effects of sector coupling with power-to-gas. *Energy Economics*, *86*, 104708. https://doi.org/10.1016/j.eneco.2020.104708

Robinius, M., Otto, A. D.-I., Heuser, P., Welder, L., Syranidis, K., Ryberg, D. S., Grube, T. J., Markewitz, P., Peters, R., & Stolten, D. (2017). *Linking the power and transport sectors—part 1: The principle of sector coupling*. https://doi.org/10.3390/EN10070956

Robinius, M., Otto, A., Syranidis, K., Ryberg, D. S., Heuser, P., Welder, L., Grube, T., Markewitz, P., Tietze, V., & Stolten, D. (2017). Linking the power and transport sectors—part 2: Modelling a sector coupling scenario for Germany. *Energies*, *10*(7), 957ff. https://doi.org/10.3390/en10070957

Robinius, M., Raje, T., Nykamp, S., Rott, T., Müller, M., Grube, T., Katzenbach, B., Küppers, S., & Stolten, D. (2018). Power-to-Gas: Electrolyzers as an alternative to network expansion – An example from a distribution system operator. *Applied Energy*, *210*, 182–197. https://doi.org/10.1016/j.apenergy.2017.10.117

Sailor, D. J. (2001). Relating residential and commercial sector electricity loads to climate—Evaluating state level sensitivities and vulnerabilities. *Energy*, *26*(7), 645–657. https://doi.org/10.1016/S0360-5442(01)00023-8

Sailor, D. J., & Muñoz, J. R. (1997). Sensitivity of electricity and natural gas consumption to climate in the U.S.A.—Methodology and results for eight states. *Energy*, *22*(10), 987–998. https://doi.org/10.1016/S0360-5442(97)00034-0

Sanchez-Lorenzo, A., Brunetti, M., Calbó, J., & Martin-Vide, J. (2007). Recent spatial and temporal variability and trends of sunshine duration over the Iberian Peninsula from homogenized dataset. *Journal of Geophysical Research*, *112*. https://doi.org/10.1029/2007JD008677

Sanchez-Lorenzo, A., Calbó, J., & Martin-Vide, J. (2008). Spatial and Temporal Trends in Sunshine Duration over Western Europe (1938-2004). *Journal of Climate - J CLIMATE*, *21*. https://doi.org/10.1175/2008JCLI2442.1

Sandag. (2019). *Multi-Unit Dwelling Electric Vehicle Charging*.

Santos, J. A., Rochinha, C., Liberato, M. L. R., Reyers, M., & Pinto, J. G. (2015). Projected changes in wind energy potentials over Iberia. *Renewable Energy*, *75*, 68–80. https://doi.org/10.1016/j.renene.2014.09.026

Schaber, K. (2013). *Integration of Variable Renewable Energies in the European power system: A model-based analysis of transmission grid extensions and energy sector coupling*. Technische Universität.

Schaber, K., Steinke, F., & Hamacher, T. (2013). *Managing temporary oversupply from renewables efficiently: Electricity storage versus energy sector coupling in Germany*. 22.

Schaeffer, R., Szklo, A. S., Pereira de Lucena, A. F., Moreira Cesar Borba, B. S., Pupo Nogueira, L. P., Fleming, F. P., Troccoli, A., Harrison, M., & Boulahya, M. S. (2012). Energy sector vulnerability to climate change: A review. *Energy*, *38*(1), 1–12. https://doi.org/10.1016/j.energy.2011.11.056

Schemme, S., Samsun, R. C., Peters, R., & Stolten, D. (2017). Power-to-fuel as a key to sustainable transport systems – An analysis of diesel fuels produced from CO 2 and renewable electricity. *Fuel*, *205*, 198–221. https://doi.org/10.1016/j.fuel.2017.05.061

Schiebahn, S., Grube, T., Robinius, M., Tietze, V., Kumar, B., & Stolten, D. (2015). Power to gas: Technological overview, systems analysis and economic assessment for a case study in Germany. *International Journal of Hydrogen Energy*, *40*(12), 4285–4294. https://doi.org/10.1016/j.ijhydene.2015.01.123

Schill, W.-P., & Zerrahn, A. (2020). Flexible electricity use for heating in markets with renewable energy. *Applied Energy*, *266*, 114571. https://doi.org/10.1016/j.apenergy.2020.114571

Schlund, D., & Theile, P. (2021). *The economic viability of grid-connected power-to-hydrogen conversion—Quantifying short- and long-term determinants*.

Schreiner, H., & Fleischhacker, N. (2018, June). *Zillertalbahn 2020+ Energieautonom mit Wasserstoff*. Eurailpress. https://www.zillertalbahn.at/data.cfm?vpath=ma-wartbare-inhalte/ma-downloadfiles/quelle-etr-juni-2018-nr-6-wwweureilpressde-etr

Scorza, S. A., Pfeiffer, J., Schmitt, A., & Weissbart, C. (2018). *Kurz zum Klima: »Sektorkopplung« – Ansätze und Implikationen der Dekarbonisierung des Energiesystems*. *71*(10), 49–53.

Silva, S., Soares, I., & Pinho, C. (2020). Climate change impacts on electricity demand: The case of a Southern European country. *Utilities Policy*, *67*, 101115. https://doi.org/10.1016/j.jup.2020.101115

Sinden, G. (2007). Characteristics of the UK wind resource: Long-term patterns and relationship to electricity demand. *Energy Policy*, *35*(1), 112–127. https://doi.org/10.1016/j.enpol.2005.10.003

Smart Columbus. (2018). *Case Study: Increasing EV Charging Access at Multi-Unit Dwellings*. Smart Columbus. https://smart.columbus.gov/playbook-assets/electric-vehicle-charging/case-study--increasing-ev-charging-access-at-multi-unit-dwellings

Sortomme, E., & El-Sharkawi, M. A. (2011). Optimal Charging Strategies for Unidirectional Vehicle-to-Grid. *IEEE Transactions on Smart Grid*, *2*(1), 131–138. https://doi.org/10.1109/TSG.2010.2090910

Spöttle, M., Jörling, K., Schimmel, M., Staats, M., Grizzel, L., Jerram, L., Drier, W., & Gartner, J. (2018). *Research for TRAN Committee—Charging infrastructure for electric road vehicles*.

Stadler, I., & Sterner, M. (2018). Urban energy storage and sector coupling. In *Urban Energy Transition: Renewable Strategies for Cities and Regions* (2nd ed., pp. 225–244). Elsevier.

Stanhill, G., & Cohen, S. (2001). Global dimming: A review of the evidence for a widespread and significant reduction in global radiation with discussion of its probable causes and possible agricultural consequences. *Agricultural and Forest Meteorology*, *107*(4), 255–278. https://doi.org/10.1016/S0168-1923(00)00241-0

Statistics Austria. (2019). *Stock of motor vehicles and trailers*. https://www.statistik.at/web_en/statistics/EnergyEnvironmentInnovationMobility/transport/road/stock_of_motor_vehicles_and_trailers/index.html

Sterchele, P., Kersten, K., Palzer, A., Hentschel, J., & Henning, H.-M. (2020). Assessment of flexible electric vehicle charging in a sector coupling energy system model – Modelling approach and case study. *Applied Energy*, *258*, 114101. https://doi.org/10.1016/j.apenergy.2019.114101

Suomalainen, K., Pritchard, G., Sharp, B., Yuan, Z., & Zakeri, G. (2015). Correlation analysis on wind and hydro resources with electricity demand and prices in New Zealand. *Applied Energy*, *137*, 445–462. https://doi.org/10.1016/j.apenergy.2014.10.015

Tan, K. M., Ramachandaramurthy, V. K., & Yong, J. Y. (2016). Integration of electric vehicles in smart grid: A review on vehicle to grid technologies and optimization techniques. *Renewable and Sustainable Energy Reviews*, *53*, 720–732. https://doi.org/10.1016/j.rser.2015.09.012

Tang, O., Rehme, J., Cerin, P., & Huisingh, D. (2021). Hydrogen production in the Swedish power sector: Considering operational volatilities and long-term uncertainties. *Energy Policy*, *148*, 111990. https://doi.org/10.1016/j.enpol.2020.111990

Thema, M., Bauer, F., & Sterner, M. (2019). Power-to-Gas: Electrolysis and methanation status review. *Renewable and Sustainable Energy Reviews*, *112*, 775–787. https://doi.org/10.1016/j.rser.2019.06.030

Tijani, A. S., & Rahim, A. H. A. (2016). Numerical Modeling the Effect of Operating Variables on Faraday Efficiency in PEM Electrolyzer. *Procedia Technology*, *26*, 419–427. https://doi.org/10.1016/j.protcy.2016.08.054

Timmerberg, S., Kaltschmitt, M., & Finkbeiner, M. (2020). Hydrogen and hydrogen-derived fuels through methane decomposition of natural gas – GHG emissions and costs. *Energy Conversion and Management: X*, *7*, 100043. https://doi.org/10.1016/j.ecmx.2020.100043

Tjarks, G., Mergel, J., & Stolten, D. (2016). Dynamic Operation of Electrolyzers—Systems Design and Operating Strategies. In Prof. Dr. D. Stolten & Dr. B. Emonts (Eds.), *Hydrogen Science and Engineering: Materials, Processes, Systems and Technology* (pp. 309–330). Wiley-VCH Verlag GmbH & Co. KGaA. https://doi.org/10.1002/9783527674268.ch14

Tlili, O., de Rivaz, S., & Lucchese, P. (2020). *POWER-TO-HYDROGEN AND HYDROGEN-TO-X: SYSTEM ANALYSIS OF THE TECHNO-ECONOMIC, LEGAL AND REGULATORY CONDITIONS*. CEA-Université-Paris-Saclay.

Tlili, O., Mansilla, C., Frimat, D., & Perez, Y. (2019). Hydrogen market penetration feasibility assessment: Mobility and natural gas markets in the US, Europe, China and Japan. *International Journal of Hydrogen Energy*, *44*(31), 16048–16068. https://doi.org/10.1016/j.ijhydene.2019.04.226

Tobin, I., Greuell, W., Jerez, S., Ludwig, F., Vautard, R., Vliet, M. T. H. van, & Bréon, F.-M. (2018). Vulnerabilities and resilience of European power generation to 1.5\hspace0.167em°C, 2\hspace0.167em°C and 3\hspace0.167em°C warming. *Environmental Research Letters*, *13*(4), 044024. https://doi.org/10.1088/1748-9326/aab211

Tobin, I., Vautard, R., Balog, I., Bréon, F.-M., Jerez, S., Ruti, P. M., Thais, F., Vrac, M., & Yiou, P. (2015). Assessing climate change impacts on European wind energy from ENSEMBLES high-resolution climate projections. *Climatic Change*, *128*(1), 99–112. https://doi.org/10.1007/s10584-014-1291-0

Tom Smolinka, Jürgen Garche, & Martin Günther. (2010). *Stand und Entwicklungspotenzial der Wasserelektrolyse zur Herstellung von Wasserstoff aus regenerativen Energien*.

Tomson, T., & Tamm, G. (2006). Short-term variability of solar radiation. *Solar Energy*, *80*(5), 600–606. https://doi.org/10.1016/j.solener.2005.03.009

Totschnig, G., Hirner, R., Müller, A., Kranzl, L., Hummel, M., Nachtnebel, H.-P., Stanzel, P., Schicker, I., & Formayer, H. (2017). Climate change impact and resilience in the electricity sector: The example of Austria and Germany. *Energy Policy*, *103*, 238–248. https://doi.org/10.1016/j.enpol.2017.01.019

Trotter, I. M., Bolkesjø, T. F., Féres, J. G., & Hollanda, L. (2016). Climate change and electricity demand in Brazil: A stochastic approach. *Energy*, *102*, 596–604. https://doi.org/10.1016/j.energy.2016.02.120

Tu, R., Gai, Y. (Jessie), Farooq, B., Posen, D., & Hatzopoulou, M. (2020). Electric vehicle charging optimization to minimize marginal greenhouse gas emissions from power generation. *Applied Energy*, *277*, 115517. https://doi.org/10.1016/j.apenergy.2020.115517

Ueckerdt, F., Brecha, R., & Luderer, G. (2015). Analyzing major challenges of wind and solar variability in power systems. *Renewable Energy*, *81*, 1–10. https://doi.org/10.1016/j.renene.2015.03.002

Umweltbundesamt (UBA). (2018). *Update: Ökobilanz alternativer Antriebe*. https://www.umweltbundesamt.at/fileadmin/site/publikationen/dp152.pdf

United Nations. (2015). *Paris Agreement*. https://unfccc.int/sites/default/files/english_paris_agreement.pdf

Usman, M., Knapen, L., Yasar, A.-U.-H., Vanrompay, Y., Bellemans, T., Janssens, D., & Wets, G. (2016). A coordinated Framework for Optimized Charging of EV Fleet in Smart Grid. *Procedia Computer Science*, *94*, 332–339. https://doi.org/10.1016/j.procs.2016.08.049

van Vliet, O., Brouwer, A. S., Kuramochi, T., van den Broek, M., & Faaij, A. (2011). Energy use, cost and CO2 emissions of electric cars. *Journal of Power Sources*, *196*(4), 2298–2310. https://doi.org/10.1016/j.jpowsour.2010.09.119

Verband der Bayerischen Energie- und Wasserwirtschaft e. V. (VBEW). (2019). *VBEW-Hinweis E-Mobilität: Netzanschluss und Netzverträglichkeit von Ladeeinrichtungen*.

Vindel, J. M., & Polo, J. (2014). Intermittency and variability of daily solar irradiation. *Atmospheric Research*, *143*, 313–327. https://doi.org/10.1016/j.atmosres.2014.03.001

voestalpine. (2020). *Voestalpine climate protection strategy*. https://www.voestalpine.com/group/en/group/environment/climate-protection-strategy/

Wang, A., van der Leun, K., Peters, D., & Buseman, M. (2020). *European Hydrogen Backbone: How a dedicated hydrogen infrastructure can be created*. https://gasforclimate2050.eu/sdm_downloads/european-hydrogen-backbone/

Wang, D., Gao, J., Li, P., Wang, B., Zhang, C., & Saxena, S. (2017). Modeling of plug-in electric vehicle travel patterns and charging load based on trip chain generation. *Journal of Power Sources*, *359*, 468–479. https://doi.org/10.1016/j.jpowsour.2017.05.036

Wang, Y., Yang, Y., Zhao, N., Liu, C., & Wang, Q. (2012). The magnitude of the effect of air pollution on sunshine hours in China. *Journal of Geophysical Research: Atmospheres*, *117*(D21). https://doi.org/10.1029/2011JD016753

Wangpattarapong, K., Maneewan, S., Ketjoy, N., & Rakwichian, W. (2008). The impacts of climatic and economic factors on residential electricity consumption of Bangkok Metropolis. *Energy and Buildings*, *40*(8), 1419–1425. https://doi.org/10.1016/j.enbuild.2008.01.006

Warner, J. T. (2015). *The handbook of lithium-ion battery pack design: Chemistry, components, types and terminology*. Elsevier Science.

Watson, S. (2014). Quantifying the variability of wind energy. *WIREs Energy and Environment*, *3*(4), 330–342. https://doi.org/10.1002/wene.95

Weidner, S., Faltenbacher, M., François, I., Thomas, D., Skùlason, J. B., & Maggi, C. (2018). Feasibility study of large scale hydrogen power-to-gas applications and cost of the systems evolving with scaling up in Germany, Belgium and Iceland. *International Journal of Hydrogen Energy*, *43*(33), 15625–15638. https://doi.org/10.1016/j.ijhydene.2018.06.167

Widén, J. (2011). Correlations Between Large-Scale Solar and Wind Power in a Future Scenario for Sweden. *IEEE Transactions on Sustainable Energy*, *2*(2), 177–184. https://doi.org/10.1109/TSTE.2010.2101620

Widén, J., Carpman, N., Castellucci, V., Lingfors, D., Olauson, J., Remouit, F., Bergkvist, M., Grabbe, M., & Waters, R. (2015). Variability assessment and forecasting of renewables: A review for solar, wind, wave and tidal resources. *Renewable and Sustainable Energy Reviews*, *44*, 356–375. https://doi.org/10.1016/j.rser.2014.12.019

Wietschel, M., Haendel, M., Schubert, G., Köppel, W., & Degünther, C. (2015). *Kurz- und mittelfristige Sektorkopplungspotentiale*.

Wietschel, M., Plötz, P., Pfluger, B., Klobasa, M., Eßer, A., Haendel, M., Müller-Kirchenbauer, J., Kochems, J., Hermann, L., Grosse, B., Nacken, L., Küster, M., Pacem, J., Naumann, D., Kost, C., Kohrs, R., Fahl, U., Schäfer-Stradowsky, S., Timmermann, D., & Albert, D. (2018). *Sektorkopplung – Definition, Chancen und Herausforderungen*.

Wilbanks, T., Bhatt, V., Bilello, D., Bull, S., Ekmann, J., Horak, W., Huang, Y. J., Levine, M. D., Sale, M. J., Schmalzer, D., & Scott, M. J. (2008). Effects of Climate Change on Energy Production and Use in the United States. *Climate Change*.

Wild, M. (2009). Global dimming and brightening: A review. *Journal of Geophysical Research: Atmospheres*, *114*(D10). https://doi.org/10.1029/2008JD011470

Wild, M., Folini, D., Henschel, F., Fischer, N., & Müller, B. (2015). Projections of long-term changes in solar radiation based on CMIP5 climate models and their influence on energy yields of photovoltaic systems. *Solar Energy*, *116*, 12–24. https://doi.org/10.1016/j.solener.2015.03.039

Wild, M., Gilgen, H., Roesch, A., Ohmura, A., Long, C. N., Dutton, E. G., Forgan, B., Kallis, A., Russak, V., & Tsvetkov, A. (2005). From dimming to brightening: Decadal changes in solar radiation at Earth's surface. *Science (New York, N.Y.)*, *308*(5723), 847–850. https://doi.org/10.1126/science.1103215

Wild, M., Trüssel, B., Ohmura, A., Long, C. N., König-Langlo, G., Dutton, E. G., & Tsvetkov, A. (2009). Global dimming and brightening: An update beyond 2000. *Journal of Geophysical Research: Atmospheres*, *114*(D10). https://doi.org/10.1029/2008JD011382

Witkowski, K., Haering, P., Seidelt, S., & Pini, N. (2020). Role of thermal technologies for enhancing flexibility in multi-energy systems through sector coupling: Technical suitability and expected developments. *IET Energy Systems Integration*, *2*(2), 69–79. https://doi.org/10.1049/iet-esi.2019.0061

Wooten, R. (2011). Statistical Analysis of the Relationship Between Wind Speed, Pressure and Temperature. *Journal of Applied Sciences*, *11*. https://doi.org/10.3923/jas.2011.2712.2722

Wulf, C., Linssen, J., & Zapp, P. (2018). Power-to-Gas—Concepts, Demonstration, and Prospects. In *Hydrogen Supply Chains* (pp. 309–345). Elsevier. https://doi.org/10.1016/B978-0-12-811197-0.00009-9

Yan, J., Zhang, J., Liu, Y., Lv, G., Han, S., & Alfonzo, I. E. G. (2020). EV charging load simulation and forecasting considering traffic jam and weather to support the integration of renewables and EVs. *Renewable Energy*, *159*, 623–641. https://doi.org/10.1016/j.renene.2020.03.175

Yi, Z., Scoffield, D., Smart, J., Meintz, A., Jun, M., Mohanpurkar, M., & Medam, A. (2020). A highly efficient control framework for centralized residential charging coordination of large electric vehicle populations. *International Journal of Electrical Power & Energy Systems*, *117*. https://doi.org/10.1016/j.ijepes.2019.105661

Yodwong, B., Guilbert, D., Phattanasak, M., Kaewmanee, W., Hinaje, M., & Vitale, G. (2020). Faraday's Efficiency Modeling of a Proton Exchange Membrane Electrolyzer Based on Experimental Data. *Energies*, *13*(18), 4792. https://doi.org/10.3390/en13184792

Zhong, X., Islam, M., Xiong, H., & Sun, Z. (2017). Design the capacity of onsite generation system with renewable sources for manufacturing plant. *Procedia Computer Science*, *114*, 433–440. https://doi.org/10.1016/j.procs.2017.09.008

Zhu, K., Victoria, M., Andresen, G. B., & Greiner, M. (2020). Impact of climatic, technical and economic uncertainties on the optimal design of a coupled fossil-free electricity, heating and cooling system in Europe. *Applied Energy*, *262*, 114500. https://doi.org/10.1016/j.apenergy.2020.114500

Zini, G., & Tartarini, P. (2009). Hybrid systems for solar hydrogen: A selection of case-studies. *Applied Thermal Engineering*, *29*(13), 2585–2595. https://doi.org/10.1016/j.applthermaleng.2008.12.029

Appendices

A. Sector coupling: literature review and categorisation

Table 15 Definitions of SC from broad to narrow scope

No.	*Author*	*Definition of SC*	*PR*
1	Dena (2017)	Does not regard SC as a sufficient strategy or approach because of its usually limited scope to one sub-system but prefers a more integrated approach of the whole energy system.	
2	Ausfelder et al. (2017)	Integrated optimisation of the whole energy system, merging the power, mobility and heat sector.	
3	Scorza et al. (2018)	SC may refer to the integration or coupling of all sectors. The central aspect would then cover substituting fossil energy carriers, including excess heat and other RES such as biomass.	
4	Wietschel et al. (2018)	The ongoing process of replacing fossil energy carriers with largely renewably generated power or other renewable energy carriers and sustainable forms of energy use. This also includes integration among consumption sectors, for example, using excess heat in new or known cross-sectoral applications.	
5	BDEW (2017)	The energy-technical and energy-economic integration of electricity, heat, mobility, and industrial processes, as well as their infrastructures with the aim of decarbonisation and simultaneous flexibilisation of energy use in industry, households, commerce/trade/services, and transport sector under the premises of economic efficiency, sustainability, and security of supply.	
6	IRENA et al. (2018)	The concept of SC encompasses co-production, combined use, conversion, and substitution of different energy supply and demand forms—electricity, heat, and fuels.	

7	Richts et al. (2015)	Coupling electricity, heat, and transportation for decarbonisation with technologies based on renewable electricity.	X
8	BMWi (2016)	Power from RESs helps to promote the energy transition in other than the power sector. They claim that if this “clean” power is applied to reduce the share of fossil fuels in other sectors, this strategy is called SC.	
9	Wietschel et al. (2018)	RESs replace fossil fuels in new processes or are used increasingly in known applications through either direct use of electricity or a transformation from power into other energy carriers (P2G, P2L, and P2H)	
10	Scorza et al. (2018)	Use of power in consumption sectors or applications in which it currently has little or no meaning.	
11	Olczak and Piebalgs (2018)	Use of surplus power from renewables and transformation into hydrogen (H_2) or methane (CH_4), liquid fuels or heat.	
12	Scorza et al. (2018)	Use of surplus power from VRE in consumption sectors or applications in which it still has little meaning.	
13	Noussan (2018)	SC includes different applications that have the common goal of transforming the power excess into other forms of energy, for example, power-to-heat, power-to-liquids or power-to-gas.	X
14	Schaber (2013)	SC is regarded an attractive solution for the use of temporary excess electricity from VRE for renewable heat and gas production.	

Table 16 Relevant literature on sector coupling

			Focus area					Sector				Technology				Geographical scope
No.	**Reference**	**PR**	**ECO**	**TEC**	**SYS**	**MOD**	**POL**	**T**	**R**	**I**	**C**	**DE**	**P2H**	**P2G**	**P2L**	
1	(Arabzadeh et al., 2020)	✓	X		X	X		X	X			X	X			Helsinki
2	(Bellocchi et al., 2020)	✓	X	X				X	X			X	X			Italy
3	(Cambini et al., 2020)	✓					X									Europe
4	(Felten, 2020)	✓	X			X			X				X			
5	(Frank et al., 2020)	✓					X									Europe, UK
6	(Hidalgo and Martín-Marroquín, 2020)	✓		X										X		
7	(Jimenez-Navarro et al., 2020)	✓	X	X					X		X		X			Europe
8	(Lester et al., 2020)	✓	X					X						X	X	Denmark, Germany
9	(Ornetzeder & Sinozic, 2020)	✓			X											Austria
10	(Pavičević et al., 2020)	✓			X	X		X	X	X		X	X			Europe

11	(Roach & Meeus, 2020)	✓	X											X		
12	(Schill & Zerrahn, 2020)	✓	X	X					X			X				Germany
13	(Sterchele et al., 2020)	✓	X					X				X				Germany
14	(Witkowski et al., 2020)	✓		X	X				X				X			
15	(Zhu et al., 2020)	✓	X						X		X		X			Europe
16	(Bernath et al., 2019)	✓			X				X				X			Germany, Europe
17	(Bloess, 2019)	✓			X				X				X			Germany
18	(Buffa et al., 2019)	✓		X					X				X			Europe
19	(Burandt et al., 2019)	✓			X	X		X	X	X						China
20	(Emonts et al., 2019)	✓						X						X		Germany
21	(Leitner et al., 2019)	✓			X				X				X			
22	(Posdziech et al., 2019)	✓		X						X				X		
23	(Thema et al., 2019)	✓	X	X										X		
24	(Bloess et al., 2018)	✓		X		X			X				X			
25	(Brown et al., 2018)	✓	X		X			X	X		X		X	X		Europe

26	(Buttler & Spliethoff, 2018)	✓	X	X										X	X	Global
27	(McKenna et al., 2018)	✓	X	X										X		North-west Germany
28	(Robinius et al., 2018)	✓	X											X		
29	(Scorza et al., 2018)		X		X											Germany
30	(Stadler & Sterner, 2018)	✓	X	X									X	X	X	
31	(Wietschel et al., 2018)		X	X	X											Europe, Germany
32	(Ausfelder et al., 2017)		X	X	X	X										Europe, Germany
33	(Robinius, Otto, Heuser, et al., 2017)	✓		X	X			X				X		X	X	
34	(Robinius, Otto, Syranidis, et al., 2017)	✓					X	X				X		X	X	Germany
35	(Schemme et al., 2017)	✓		X				X							X	Germany
36	(Quaschning, 2016)			X	X											Europe, Germany

37	(Jambagi et al., 2015)	✓					X		X				X			
38	(Richts et al., 2015)	✓	X	X	X							X	X	X		
39	(Schaber, 2013)		X		X	X							X	X		Europe
40	(Schaber et al., 2013)		X	X									X	X		Germany

Table 17 Categorisation of sector coupling applications into centralised (C)/decentralised (D) transformation (based on scale and proximity to the consumer) and direct/indirect electrification (adapted from Ausfelder and Dura (2018)).

Sectors and applications	**Traditional**	**Direct electrification**	**C/D**	**Indirect electrification (P2X)**	**C/D**	**Alternative options***
Transport						
Cars and small trucks	Gasoline and diesel Natural gas	Batteries	C, D	Hydrogen, methane Liquid electro-fuels	C	Biofuels, biogas, trucks: purified biogas
Large trucks	Diesel, natural gas	Overhead lines on highways Batteries	C	Hydrogen, methane Liquid electro-fuels	C	Biofuels, trucks: purified biogas
Railway	Electric drive, diesel	Electrification of non-electrified sections	C	Hydrogen, methane Liquid electro-fuels	C	Biodiesel
Air	Turbines (kerosene)	No solutions expected	-	Liquid electro-fuels (kerosene) Hydrogen	C	Bio-kerosene
Maritime	Heavy fuel oil, diesel LNG	No solutions expected	-	Hydrogen, methane, liquid electro-fuels (diesel/kerosene)	C	Biodiesel, purified biogas
Residential/Industry/Trade: Low temperature heat for households, industry and trade/services						

Low temperature heat	Oil or gas heating, DH	Heat pumps Resistance heating	C, D	Hydrogen/methane	C, D	Biomass, biogas
Industry						
Industrial process heat	Gas engine, steam	Electrode boiler, induction heating, plasma process, resistance heating	D	Liquid electro-fuels	C	Biomass, biogas
Iron (primary route)	Coke	Not applicable	-	Hydrogen	C	Biomass, biogas
Refinery	H_2 (side product and from natural gas)	Not applicable	-	Hydrogen	C	Biomass, biogas
Chemicals		Not applicable	-	Hydrogen, liquid electro-fuels	C	Biomass, biogas

C … Centralised, D… Decentralised, *not depending on electricity input

B. Load management: field test verification

Table 18 Differences between the modelled and the field test environment.

No.	*Topic*	*Model*	*Field test*
1	Information on energy consumption and BEV charging availability	Full information for LM optimisation (Section 4.4.3) Comparison between full and daily information for minimum charging capacity (Section 4.4.4)	No information
2	Battery state of charge	Known	Unknown
3	Ratio plugged in/time parked	100 %, always plugged in when parked	45 % of the time plugged in when parked
4	Ratio plugged in/charging	Charging takes place during 30 % of the plug-in time for uncontrolled and 47 % for ToU charging	Charging takes place during 50 % of the plug-in time
5	BEV share analysed	0–100 %	50 %
6	LM	Constraints according to charging strategies in Section 4.3.4. ToU based on HH electricity demand	Charging as a system totally separate from the HH load. However, the HH load should be guaranteed. If BEV charging exceeds the building's power connection, charging is stopped first.
7	Phase charging	Each charging point provides 3.7 kW for charging.	1 or 3 phase charging: 1 phase vehicles currently always block all 3 phases with 11 kW but only consume 3.7 (11/3) kW. The LM algorithm was further developed in this project to release the available 2 phases to other 1- or 2-phase BEVs. In the future, this will release a substantial amount of capacity.

C. Modelling renewable hydrogen production

Optimisation Model

The yearly cost for hydrogen production and storage is minimised. According to Matute et al. (2019), the annual cost for H_2 production or the levelised cost of hydrogen LCOH&S is defined as equipment cost (C_{EQ}) plus variable energy cost (C_E). In this study, the relative cost per MWh is based on hydrogen demand.

$$min \sum_{t=1}^{T} \frac{C_{EQ(a)} + \sum_{t=1}^{T} C_{E(t)}}{P_{con(t)}^{H_2}} \text{ [€/MWh]}$$

C_{EQ} .... *annual equipment cost [€]*
C_E .... *hourly variable cost [€]*
$P_{con}^{H_2}$ .... *H_2 demand [kW]*
t .... *time step [h]*
T .... *8760 hours of a year*
a .... *annual*

The annual C_{EQ} includes CAPEX and OPEX of the electrolyser (C_C^{Ely}, $C_{O\&M}^{Ely}$) and the storage tanks (C_C^{St}, $C_{O\&M}^{St}$) plus indirect other CAPEX (C_C^{OT}) for engineering works and land permits and their respective OPEX ($C_{O\&M}^{OT}$) (Matute et al., 2019).

$$C_{EQ(a)} = C_C^{Ely} + C_C^{St} + C_C^{OT} + C_{O\&M}^{Ely} + C_{O\&M}^{OT} + C_{O\&M}^{St}$$

C_C^{Ely} .... *CAPEX electrolyser [€]*
C_C^{St} .... *CAPEX storage [€]*
$C_{O\&M}^{Ely}$ .... *OPEX electrolyser [€]*
$C_{O\&M}^{St}$ .... *OPEX storage [€]*
C_C^{OT} .... *CAPEX other [€]*
$C_{O\&M}^{OT}$ .... *OPEX other [€]*

The annual C_C^{Ely} is calculated as the annuity from the initial investment cost for the electrolyser. To calculate the yearly investment cost Haas et al. (2021) describe the calculation of the annuity as a product of an annuity factor (α) and the initial investment cost ($C_{C(t=0)}^{Ely}$). The annuity factor (α) results from the expected rate of return (r) and the predicted depreciation period or lifetime (n)[3].

$$C_{C(a)}^{Ely} = \alpha\, C_{C(t=0)}^{Ely}$$

[3] The depreciation may vary on the time of use and influences the yearly investment cost annuity

$\alpha = \frac{i\,(1+i)^n}{(1+i)^n-1}$

$C^{Ely}_{C(t=0)}$ .... *initial investment cost [€]*

α .... *annuity factor*

n .... *lifetime [y]*

i .... *interest rate*

The variable energy cost (C_E) consists of the wholesale or spot market (C_{WM}) cost for electricity consumption, access tariff for electricity (C_{ATE}), electricity tax (C_{ET}), municipal tax (C_{MT}), retailer operational cost, operation costs for accessing energy markets (C_{OC}), financing fees (C_{FF}) and water cost (C_W). This cost largely depends on the hourly electricity consumption and, therefore, on the chosen supply strategy.

$$C_{E(t)} = \sum (C_{WM(t)} + C_{ATE(t)} + C_{ET(t)} + C_{MT(t)} + C_{OC(t)} + C_{FF(t)})\, P^{el}_{con(t)} + C_{W(t)}\ Water$$

C_{WM} .... *wholesale market price [€/kWh]*

C_{ATE} .... *access tariff for electricity [€/kWh]*

C_{ET} .... *electricity tax [€/kWh]*

C_{MT} .... *municipal tax [€/kWh]*

C_{OC} .... *operational cost [€/kWh]*

C_{FF} .... *financing fees [€/kWh]*

C_W .... *water cost [€/L]*

$Water$ .... *water consumption [L]*

Cost data

The levelised cost of hydrogen (LCOH) is based on the costs described in Table 19 derived from Matute et al. (2019). The data input is presented in Table 20.

Table 19 Cost parameters for the optimisation model

Variable cost	Electricity spot market price – Austria 2019	C_{WM}	€/kWh electricity	
	Access tariff	C_{ATE}	€/kWh electricity	0.0012
	Electricity tax	C_{ET}	€/kWh electricity	0.0031
	Municipal tax	C_{MT}	€/kWh electricity	0.0005
	Operation cost	C_{OC}	€/kWh electricity	0.0012
	Financial cost	C_{FF}	€/kWh electricity	0.0002

	Water consumption	*Water*	€/L	0.004
CAPEX	Electrolyser	C_C^{Ely}	€/kW	Scenarios
	Other CAPEX	C_C^{OT}	% of CAPEX	60
	Storage	C_C^{St}	€/kW	Scenarios
	Lifetime	n	Years	20
	WACC	i	%	5
OPEX	OPEX electrolyser	$C_{O\&M}^{Ely}$	% of CAPEX	3
	Other OPEX electrolyser	$C_{O\&M}^{OT}$	% of CAPEX	2.4
	OPEX Storage	$C_{O\&M}^{St}$	% of CAPEX	1

Table 20 Data input to the optimisation model

Type	***Source***	***Temporal resolution***	***Unit***
Electricity supply	Grid 2019	h	MW
H_2 Demand	Annual demand for H_2-based steel production process Austria 2050	y	MWh
H_2 Demand Profile	Spain: industrial gas demand profile (daily variability, weekly cycle) Austria: H_2-based steel production process (constant)	d	
LCOE PV power	Fraunhofer ISE (2021), IEA (2020) and IRENA (2021)	26	€/MWh
LCOE wind power	Fraunhofer ISE (2021), IEA (2020) and IRENA (2021)	36	€/MWh

Capacity modelling

In order to optimise the electrolyser capacity in the first modelling step, the levelised cost of hydrogen and storage are minimised, as described in Eq. (23).

$$min\ \sum_{t=1}^{T} \frac{C_{EQ(a)} + \sum_{t=1}^{T} C_{E(t)}}{P_{con(t)}^{H_2}}\ [€/MWh] \qquad (23)$$

Hydrogen demand ($P_{con}^{H_2}$) is fulfilled either through discharging the H_2 storage ($P_{DC(t)}^{H_2}$) or directly form the electrolyser ($P_{dir(t)}^{H_2}$) (see Eq. (24)).

$$P_{con}^{H_2} = P_{DC(t)}^{H_2} + P_{dir(t)}^{H_2} \tag{24}$$

Eq. (25) makes sure that hydrogen generation ($P_{gen}^{H_2}$) equals the gross H_2 storage input ($P_{Ch(t)}^{H_2}$) and the direct demand fulfilment. In every time step t, electricity consumption (P_{con}^{el}) equals hydrogen generation divided by the P2G efficiency (see Eq. (26)).

$$P_{gen}^{H_2} = P_{Ch(t)}^{H_2} + P_{dir(t)}^{H_2} \tag{25}$$

$$P_{con}^{el} = \frac{P_{gen}^{H_2}}{\eta_t^{P2G}} \tag{26}$$

η_t^{P2G} is assumed to be 0.60. This is below the maximum of 0.7-0.75 to account for the additional load-dependent efficiency losses. These detailed losses are the result of operational optimisation.

The hydrogen state of charge is defined in Eq. (27) by the storage level from t-1 plus the hydrogen storage input or charge ($P_{Ch(t)}^{H_2}$) minus hydrogen output or discharge ($P_{DC(t)}^{H_2}$) to fulfil demand. The storage input ($P_{Ch(t)}^{H_2}$) in Eq. (28) and output ($P_{DC(t)}^{H_2}$) in Eq. (29) are derived by the gross hydrogen amount adjusted by the storage efficiency (η_t^{stor}).

$$SOC_t^{H2} = SOC_{t-1}^{H2} + P_{Ch(t)}^{H_2} - P_{DC(t)}^{H_2} \tag{27}$$

$$P_{Ch(t)}^{H_2} = P_{Ch_{gross}(t-1)}^{H_2}\, \eta_t^{stor} \tag{28}$$

$$P_{DC(t)}^{H_2} = \frac{P_{DC_{gross}(t)}^{H_2}}{\eta_t^{stor}} \tag{29}$$

To achieve a storage balance throughout the year, the hydrogen state of charge in time step 1 needs to equal the SOC at the end of the time horizon (see Eq. (30)).

$$\mathrm{SOC}_1^{H2} = \mathrm{SOC}_{T+1}^{H2} \tag{30}$$

As stated in Eq. (31), electricity consumption may not exceed electricity supply (P_s^{el}), which can be grid supply (Eq. (32)) or from a dedicated RES plant defined by the renewable generation profile and the RES capacity (P_{RES}^{el}) as shown in Eq. (33).

$$P_{con(t)}^{el} \leq P_{s(t)}^{el} \tag{31}$$

Grid connected electrolyser:

$$P_{s(t)}^{el} = grid\ supply \tag{32}$$

RES connected electrolyser:

$$P_{s(t)}^{el} \leq Profile_{RES(t)}\, P_{RES}^{el} \tag{33}$$

According to Eq. (34), electricity consumption may also not exceed electrolyser capacity (P_{Ely}^{el}), which is the one result that is an input to the operational efficiency modelling in the next step.

$$P_{con(t)}^{el} \leq P_{Ely}^{el} \tag{34}$$

Variables:

SOC_t^{H2} .... *state of charge* H_2 *[kWh]*

$P_{Ch}^{H_2}$ .... *charge* H_2 *(*H_2 *storage input) [kW]*

$P_{DC}^{H_2}$ .... *discharge* H_2 *(*H_2 *storage output) [kW]*

$P_{dir}^{H_2}$ .... *direct* H_2 *supply [kW]*

$P_{Ch_{gross}}^{H_2}$ .... *gross* H_2 *charge (gross storage input) [kW]*

$P_{DC_{gross}}^{H_2}$ .... *gross* H_2 *discharge (gross storage output) [kW]*

P_{con}^{el} .... *electricity consumption [kW]*

$P_{gen}^{H_2}$ .... *net* H_2 *generation [kW]*

P_{Ely}^{el} .... *electrolyser capacity [kW]*

P_{RES}^{el} .... *optimal RES capacity [kW]*

Input Data:

$P_{con}^{H_2}$ .... H_2 *Demand [kWh]*

P_s^{el} .... *electricity supply [kW]*

$Profile_{RES}$ .... *RES generation profile (PV or wind) [0-1]*

Parameters:

η_t^{P2G} .... *electrolyser efficiency (static) [%]*

η_t^{stor} .... *storage efficiency [%]*

Operational efficiency modelling

This second step of operational modelling considers load and, therefore, electrolyser capacity-dependent efficiency losses according to Section 5.3.3. To avoid multiple interdependencies in the model, the electrolyser capacity (P_{Ely}^{el}) is no longer a decision variable but a fixed parameter resulting from the former capacity optimisation.

The Faraday efficiency curve differs between the more flexible PEM and the ALK electrolyser and needs to be replicated differently in the model.

a. PEM electrolyser

For the PEM electrolyser, the Faraday efficiency can be modelled with one single curve, which makes the setup easier and leads to a solid model performance (see Section 5.3.3.1).

Additional losses due to low loads are calculated based on the electricity consumption, which in relation to the fixed electrolyser capacity results in a certain utilisation rate. The function described in Figure 79 is implemented in the operational model as a linear function to consider losses at specific load factors.

In the following Eq. (37) and Eq. (36), the gradient (k) and the axial interception (d) are derived for the loss function. L^{ele} and P^{el}_{con} represent a certain relationship between additional efficiency losses and a certain electricity consumption or load factor.

The loss function in Eq. (37) defines the loss at a certain electricity consumption (Figure 78):

$$k = \frac{L_1^{ele} - L_2^{ele}}{Con_1^{ele} - Con_2^{ele}} \tag{35}$$

$$d = L_1^{ele} - \mathrm{P}^{\mathrm{el}}_{con_1} * k \tag{36}$$

$$L_t^{ele} \leq k\ \mathrm{P}^{\mathrm{el}}_{con(t)} + d \tag{37}$$

L_t^{ele} ....*efficiency loss at a certain load [kW]*

k ....*gradient*

d ....*axial interception*

Furthermore, the H_2 generation balance needs to be extended by this additional loss (Eq. (38)).

$$P^{\mathrm{el}}_{con(t)} = \frac{P^{\mathrm{H_2}}_{gen(t)} + L_t^{ele}}{\eta_t^{\mathrm{P2G}}} \tag{38}$$

b. ALK electrolyser

The function ALK2 described in Figure 83 is implemented in the operational model as a linear function for a load factor >0.36, while the function ALK1 is added as a manual input, to consider losses at specific load factors ≤0.36.

For the manual function ALK1 described in Eq. (39)– a matrix listing the load factor and corresponding absolute loss for the load factors 0-0.36 with 36 data points *(x)* - an integer decision variable *($INT_{t,x}^1$)* enables the model's choice of operation. The integer variable decides on the combination of loss ($L_{t,x}$) and utilisation ($U_{t,x}$). The utilisation depends on the electricity consumption ($P^{el}_{con(t)}$) at the given electrolyser capacity (see Eq. (40)).

$$LM_t^{ele} = \sum_{x=1}^{36} INT_{t,x}^1\ L_{t,x} \tag{39}$$

$$P^{el}_{con(t)} = \sum_{x=1}^{36} (INT_{t,x}^1\ U_{t,x})\ P^{el}_{Ely} \tag{40}$$

LM_t^{ele} .... *loss manual function [kW]*

$INT_{t,x}^1$ ....*integer decision variable 1 [0 1]*

x .... *data points in manual function [0-36]*

L .... *loss in manual function [kW]*

U .... *utilisation in manual function [%]*

If, however, the electricity consumption is above a load factor of 0.36, the model chooses the linear ALK2 function with another integer decision variable, as shown in Eq. (41).

$$0.36\ INT_t^2 \leq \frac{P_{con(t)}^{el}}{P_{Ely}^{el}} \leq\ 1\ INT_t^2 \tag{41}$$

$INT_{t,x}^2$ .... *integer decision variable 2 [0 1]*

For the linear function ALK2 (LL_t^{ele}), the same approach as for the PEM electrolyser can be used and k and d are derived for the loss function in Eq. (44) (Figure 81):

$$k = \frac{LL_1^{ele} - LL_2^{ele}}{Con_1^{ele} - Con_2^{ele}} \tag{42}$$

$$d = LL_1^{ele} - Con_t^{ele} * k \tag{43}$$

$$LL_t^{ele} \leq\ k\ Con_t^{ele} + d \tag{44}$$

LL_t^{ele} .... *loss linear function [kW]*

To force a decision for one point along both loss functions, in every time step only one integer decision variable may be one, the other zero (see Eq. (45)).

$$\sum_{x=1}^{36} INT_{t,x}^1\ + INT_t^2 \leq\ 1 \tag{45}$$

In addition, the H_2 generation balance needs to be extended by this additional loss from both functions according to Eq. (46).

$$Con_t^{ele} = \frac{Gen_t^{H2} + LL_t^{ele} + LM_t^{ele}}{\eta_t^{P2G}} \tag{46}$$